

## ABSTRACT

Title of Document: USE OF INORGANIC BY-PRODUCT AMENDED COMPOST/MANURE TO SEQUESTER METALS AND PHOSPHORUS FROM DIFFUSE SOURCE POLLUTION

Hunho Kim, Doctor of Philosophy, 2010

Directed By: Professor, Allen P. Davis, Department of Civil and Environmental Engineering.  
Research Scientist, Rufus L. Chaney, ARS, US Department of Agriculture.

Heavy metals and nutrients released from diffuse sources by urban and agricultural runoff are important pollutants causing aquatic toxicity and/or eutrophication in water bodies. Diffuse source pollution is difficult to address because of the dispersed and often dynamic nature of the flows, which often lead to economic impracticality of traditional approaches.

Beneficial use of industrial and agricultural byproducts as amendments or media/barriers to treat diffuse source pollution can provide cost-effective solutions over various ranges of pollutants and flows. Two applications of this concept were examined in this research study: 1) Immobilization of phosphorus using Fe/Mn inorganic materials and an anaerobic incubation process; (2) Heavy metal removal from roof/wall runoff using a Biomat barrier supplemented with compost and inorganic byproducts.

Through the first study, three different low cost Fe/Mn-rich materials (iron ore, steel slag and Mn tailings) were evaluated as amendments to decrease phosphorus mobility from manure. Anaerobic incubation of fresh dairy manure with the Fe/Mn rich materials was also evaluated.

Steel slag addition significantly decreased water soluble phosphorus by 93% and Mehlich III extracted phosphorus by 80%, compared to manure-only control. An anaerobic incubation of manure with Fe ore decreased 62% water extractable P compared to fresh manure and 76% compared to incubated manure, due to oxalate extractable Fe (considered as amorphous Fe) increase. This work suggests possible anaerobic incubation use for non-active crystalline byproducts to decrease P loss from manure.

Through the second study, the feasibility of Biomat use, a mixture of sand, compost and inorganic byproducts, was evaluated through column and bench-scale experiments to remove dissolved heavy metals. A 25% grass/food waste compost + steel slag + sand column was the best media, not only demonstrating excellent metal removals from diffuse sources but also exhibiting the immobility of sorbed metals on the media. Throughout bench scale experiments, hydraulic characteristics and heavy metal removal performance of the mat media were evaluated in perpendicular flow. After all bench scale experiments, metal extractions showed performed very limited metal mobility in the media. Design parameters, implementations, and recommendations for future full scale Biomat application in a field were established.

USE OF INORGANIC BYPRODUCT AMENDED COMPOST/MANURE TO  
SEQUESTER METALS AND PHOSPHORUS FROM DIFFUSE SOURCE  
POLLUTION

By

Hunho Kim

Dissertation submitted to the Faculty of the Graduate School of the  
University of Maryland, College Park, in partial fulfillment  
of the requirements for the degree of  
Doctor of Philosophy  
2010

Advisory Committee:

Professor Allen P. Davis, Chair/Advisor

Dr. Rufus L. Chaney, Advisor

Professor. Bruce R. James

Professor. Alba Torrents

Professor Eric A. Seagren

© Copyright by  
Hunho Kim  
2010

## Table of Contents

Table of Contents -----	ii
List of Tables -----	v
List of Figures -----	viii
 Chapter 1: Introduction -----	 1
1-1. Immobilization of phosphorus using Fe/Mn inorganic materials and an anaerobic incubation process -----	2
1-2. Heavy metal removal from roof/wall runoff using a Biomat with compost and inorganic byproducts-----	5
 Chapter 2: Objectives and Scope of Study-----	 8
2-1 Immobilization of phosphorus using Fe/Mn inorganic materials and an anaerobic incubation process-----	8
2-2. Heavy metal removal from roof/wall runoff using a Biomat with compost and inorganic byproducts-----	10
 Chapter 3: Backgrounds and Literature Review-----	 12
3-1. Phosphorus in agriculture and its environmental implications-----	12
3-1-1. Phosphorus in Soil-----	14
3-1-2. Phosphorus in Manure -----	19
3-2. Use of Fe, Al, and Ca compounds as amendment to immobilize P from manure and soil -----	23
3-3. Bacterial Fe/Mn reductive dissolution during anaerobic incubation -----	30
3-3-1. Factors for enhancing Fe(III) reductive dissolution-----	32
3-4. Heavy metals and other water quality parameters, and heavy metal sources in storm water runoff-----	34
3-4-1. Metal corrosion -----	40
3-4-1-1. Lead corrosion-----	41
3-4-1-2. Cu corrosion -----	43
3-4-1-3. Zn corrosion -----	44
3-5. Surface chemistry and adsorption- -----	45
3-5-1. Inorganic mineral surfaces -----	45
3-5-2. Organic surface functional groups and metal retention by organic surfaces -----	47
3-5-3. Heavy metal (Pb) sorption mechanism -----	49
3-5-4. Competitive adsorption of heavy metals on soil components (on inorganic and organic materials) -----	50
3-6. Organic and/or inorganic amendments to remove heavy metals from the aqueous phase-----	52
3-7. Organic and/or inorganic amendments to remove heavy metals from soil -----	55
 Chapter 4: Immobilization of phosphorus using Fe/Mn inorganic materials and an anaerobic incubation process -----	 59
4-1. Introduction -----	59
4-2. Methods and Materials -----	62

4-2-1. Characterization and preparation of Low cost Fe and Mn material-----	62
4-2-2. Fe/Mn material applications to manure and characterization of the Fe/Mn materials + manure mixture during anaerobic incubation -----	65
4-3. Results and Discussion -----	67
4-3-1. Evaluation of Fe/Mn materials as amendments in manure before digestion -----	67
4-3-2. Evaluation of manure anaerobic incubation to increase amorphous Fe/Mn and decrease P mobility-----	70
4-3-3. pH and Eh of Fe/Mn material treated manure during anaerobic incubation-----	76
4-3-4. Extractable Zn and Cu -----	79
4-4. Discussion on microbial Fe/Mn reductive dissolution during anaerobic incubation---	85
4-5. Summary and Conclusions-----	86

## Chapter 5. Characterizing roof/wall runoff and soil around the B-580

APHIS building -----	89
5-1. Introduction -----	89
5-2. Methods and Materials -----	90
5-2-1. Characterization of Rooftop Runoff – Phase 1 -----	90
5-2-2. Characterization of soil around the APHIS building – Phase 1 -----	91
5-3. Results and Discussion -----	93
5-3-1. Monitoring and characterizing roof/wall runoff from the building(Phase 1)-----	93
5-3-1-1. Estimation of Pb released by roof/wall runoff and corrosion rate from APHIS building-----	97
5-3-2. Characterizing soil around the APHIS building; Phase 1 -----	98
5-4. Summary and Conclusions -----	104

## Chapter 6. Column study of heavy metals removal using industrial

byproducts-----	106
6-1. Introduction -----	106
6-2. Methods and materials -----	107
6-2-1. Column design and setup, and media preparation – Phase 2 -----	107
6-2-2. Column Sorption Study – Phase 2 -----	113
6-2-3. Column Leaching (Desorption) Study – Phase 2 -----	115
6-3. Results and Discussion-----	115
6-3-1 Column sorption study for compost media selection and evaluation – Phase 2---	115
6-3-2. Water quality parameter change during initial column operation -----	128
6-3-3. Discussion on Zn desorption during simultaneous sorption of Pb and Cu during sorption study-----	137
6-3-4. Column leaching study for compost media selection and evaluation: Phase 2 -----	143
6-3-5. Metal removal capacity and life of the Biomat media -----	149
6-4. Summary and Conclusion-----	154

## Chapter 7. Evaluation of heavy metal loading and hydraulic conductivity of Biomat in perpendicular flow using Bench-scale experiments. -----

7-1. Introduction-----	157
7-2. Methods and Materials-----	158
7-2-1. Biomat media and box preparation for bench scale experiment – Phase 3-----	158
7-2-2. Bench Scale Experimental setup and operation – Phase 3 -----	161
7-2-3. Evaluating Hydraulic Conductivity for bench scale experiments: (Phase 3)-----	165
7-2-4. Media extraction and analysis after the bench scale experiments – Phase 3-----	166
7-3. Results-----	169
7-3-1. Bench Scale performance of Biomat with both dissolved and precipitated forms of metals (Experiment 1 and 2) -----	169
7-3-2. Bench Scale performance of Biomat with dissolved forms of metals only (Experiments 3 and 4)-----	175
7-3-3. Change of bench scale Biomat performance on influent water head (flow rate change) and hydraulic conductivity of media (Experiments 7 to 9).-----	179
7-3-4. Biomat performance for low influent concentration during bench scale (Experiment 10) -----	186
7-3-5. Metal leaching study in bench scale Experiments 5 and 11 -----	190
7-3-6. Other water quality parameters -----	194
7-3-7. Discussion on hydraulic conductivity and metal loading rate of Biomat media during the bench scale experiments-----	196
7-3-8. Biomat media total metal extraction-----	207
7-3-9. Other metal extractions from Biomat media-----	211
7-4. Heavy metal removal mechanisms by Biomat media used in Bench-scale Experiments -----	216
7-5. Summary and conclusions-----	219
 Chapter 8. Conclusions and Recommendations-----	 223
8-1. Conclusions and recommendations on immobilization of phosphorus using Fe/Mn inorganic materials and an anaerobic incubation process-----	224
8-2. Conclusions on Heavy metals removal using industrial byproducts-----	225
8-3. Discussion and recommendations on Biomat configuration, installation and operation. -----	226
8-4. Consequences of work: Strength and weakness of the study, and necessary future work. -----	232
 Appendix-----	 237
Appendix A Information for Chapter 4-----	237
Appendix B Information for Chapter 5-----	241
Appendix C Information for Chapter 6-----	247
Appendix D Information for Chapter 7-----	265
 References -----	 301

## List of Tables

3-1 Estimated total amount of livestock waste, biosolids, and municipal solid waste compost in the U.S. (adapted from Pierzynski et al., 2000 sourced from Logan et al., in proceedings of the 4th Joint WEF and AWWA conference on biosolids and residual management, WEF, Alexandria, VA 1995, 15-13 to 15-28).-----	13
3-2. Inorganic phosphorus containing compounds commonly found in soil (listed in order of increasing solubility in each group) (Stum and Morgan, 1996; Brady and Weil, 2002) - -----	17
3-3. Mean values of chemical properties of livestock manure (adapted from Kleinman et al., 2005) -----	22
3-4. Fractions of inorganic and organic P in manures and composts. (adapted from Harpley and Moyer, 2000) -----	22
3-5. Phosphorus immobilizing amendments -----	26
3-6. Water quality of urban, industrial site and roadway stormwater runoff -----	36
3-7a. Water quality of roof runoff (based on research monitoring) -----	37
3-7b. Water quality of roof runoff (based on literature surveys) -----	38
3-8. Metal (Pb, Cu, Cd, and Zn) concentrations, loadings, and estimated contributions from various sources in urban runoff (adapted from Davis et al., 2001)-----	39
3-9. Characteristics of possible corrosion products (adapted from Graedel, 1994).-----	42
3-10. Composition of lead corrosion film in the urban environment (adapted from Matthes et. al., 2002, originally cited from Tranter, 1976)-----	42
3-11. Atmospheric corrosion rates for lead (adapted from Graedel, 1994) -----	43
3-12. Point of zero charge (pHpzc) and intrinsic surface acidity constants (equilibrium constants of Eq.3-2 and Eq. 3-3, respectively) for soil menerals (adapted from Essington, 2004) -----	46
3-13. Common organic surface functional groups (adapted from Essington, 2004)-	48
3-14. Metal properties affecting divalent metal affinity (Elliot et al., 1986; Veeresh et al., 2003) -----	51
3-15. Heavy metal affinity series for soil components (adapted from Elliott et al, 1986) -- -----	52
3-16. Heavy metal removal from aqueous phase using organic and/or inorganic wastes/byproducts -----	57
3-17. Heavy metal removal from soil using organic and/or inorganic wastes/byproducts--- -----	58
4-1 . Chemical properties and total elemental composition of iron ore (IO), steel slag (SS), and manganese tailings (MT) as obtained -----	68
4-2 . Chemical properties and characteristics of manure and manure with iron ore (IO), steel slags (SS) and manganese tailings (MT) before anaerobic incubation-----	69



5-1. Characteristics of the roof/wall runoff of the APHIS building-----	96
5-2. Pb, Cu, and Zn Concentrations in soil around the APHIS building (collected on April 17th and May 1st 2008). (Refer to Figure 4-3 for site map)-----	101
5-3. Comparison of heavy metal concentrations between the A0 soil samples and the roof/wall runoff samples -----	102
5-4. Heavy metal guidance values in residential soils (adapted from Peterson et al., 2006). -----	102
6-1 . Chemical properties and total metal content of manure compost, grass+food waste compost, steel slag, and Hubcutter heavies. -----	112
6-2. Composition of packed media in columns used for column study -----	113
6-3 Characteristics of the synthetic runoff used in the column study-----	114
6-4. Cumulative treated flow at start of breakthrough for Zn, Pb, and Cu for each Biomat media column: 10% Manure compost + sand (MC10); 10% Grass/Food waste compost + sand (GF10); 25% Grass/Food waste compost + sand (GF25); 25% Grass/Food waste compost + Steel slag + sand (GFS25); and 25% Grass/Food waste compost + Hubcutter heavies + sand (GFH25) -----	118
6-5. Percent Zn released based on previously adsorbed Zn and percent Zn removed based on total Zn input from each column during adsorption study: Manure compost + sand (MC10); 10% Grass/Food waste compost + sand (GF10); 25% Grass/Food waste compost + sand (GF25); 25% Grass/Food waste compost + Steel slag + sand (GFS25); and 25% Grass/Food waste compost + Hubcutter heavies + sand (GFH25) -----	123
6-6. State of Maryland Toxic metal criteria for Ambient Surface Waters. (the Code of Maryland Regulations (COMAR) 26.08.02.03-2) -----	128
6-7. Mass balance of Pb throughout the column study. MC10 (10% Manure compost column), GF10 (10% Grass/food waste column), GF25 (25% Grass/food waste column), GFS25 (25% Grass/food compost + 5% steel slag), GFH 25 (25% Grass food waste compost + 5% Hubcutter Heavies) -----	148
6-8. Metal removal capacity for each Biomat media and the media life for each metal: MC10 (10% Manure compost column), GF10 (10% Grass/food waste column), GF25 (25% Grass/food waste column), GFS25 (25% Grass/food compost + 5% steel slag), GFH 25 (25% Grass food waste compost + 5% Hubcutter Heavies)-----	150
7-1. Chemical properties and total metal content of grass+food waste compost, and steel slag, -----	160
7-2. Mass to volume ratio (g/L) and mass (g) of mat media for column studies and bench scale experiment-----	161
7-3. Target characteristics of the synthetic runoff used in the column study -----	162
7-4. Time from first experiment for each bench scale experiment -----	163

7-5. Hydraulic conductivity of Biomat media for each experiment during bench scale study-----	186
7-6. (a) Point precipitation frequency estimates of Beltsville, MD From NOAA ATLAS 14 (adapted from <a href="http://hdsc.nws.noaa.gov/cgi-bin/hdsc/buildout.perl?type=idf&amp;units=us&amp;series=pd&amp;statename=MARYLAND&amp;stateabv=md&amp;study=orb&amp;season=All&amp;intype=1&amp;plat=&amp;plon=&amp;liststation=BELTSVILLE++++++MD+%2C+18-0700&amp;slat=lat&amp;slon=lon&amp;mlat=40.816&amp;mton=-76.150&amp;elev=1397">http://hdsc.nws.noaa.gov/cgi-bin/hdsc/buildout.perl?type=idf&amp;units=us&amp;series=pd&amp;statename=MARYLAND&amp;stateabv=md&amp;study=orb&amp;season=All&amp;intype=1&amp;plat=&amp;plon=&amp;liststation=BELTSVILLE++++++MD+%2C+18-0700&amp;slat=lat&amp;slon=lon&amp;mlat=40.816&amp;mton=-76.150&amp;elev=1397</a> ), (b) Flow rate to Biomat estimates. -----	206
7-7. Extracted metal concentrations in the Biomat media; Relative Bioavailability Leaching Procedure (RBALP), acid ammonium oxalate extraction in darkness, and $\text{Sr}(\text{NO}_3)_2$ (0.01M) extraction; numbers in parenthesis represents percent of total metal concentration-----	215

## List of Figures

1-1. B-580 APHIS building, BARC-East in Beltsville, MD -----	6
1-2. The corroded exterior wall of B-580 APHIS building which contains Pb and Cu----	7
2-1. Proposed mechanisms and processes involved in production of active amorphous Fe/Mn oxides from non active Fe/Mn waste and organic matter mixtures (partially adopted from Lovely, 2000) -----	9
3-1. The Phosphorus Cycle in Soils (Adapted from Pierzynski et al., 2000; Brady and Weil, 2002) -----	16
3-2. Phosphate ion removal reactions (adapted from Brady and Weil, 2002) -----	18
3-3. Typical inorganic phosphorus distribution at various soil pH (adapted from Brady and Weil, 2002) -----	19
3-4. Model for organic matter degradation metabolism under an anoxic environment by Fe and Mn reducing microorganisms (adapted from Lovely, 1991 and 2000)-----	31
4-1. Fe/Mn waste materials sieved to <0.5 mm (a) Iron ore, (b) Steel slag, (c) Mn tailings -----	63
4-2. Basic anaerobic incubation container design to convert waste Fe and Mn additives to highly-active amorphous Fe/Mn materials -----	66
4-3. Water extractable Phosphorus, Mehlich III Phosphorus, and Oxalate extractable Fe for Fe/Mn materials amended manure mixture during anaerobic incubation (error bars represent 1 standard deviation): (a) Water soluble P (high scale), (b) Water soluble P (low scale), (c) Mehlich III P, and (d) Oxalate extractable Fe. -----	72
4-4. Proposed mechanisms and processes involved in production of active amorphous Fe/Mn oxides from non active Fe/Mn materials and organic matter mixtures.-----	74
4-5. pH change during anaerobic incubation for Fe/Mn materials amended manure mixtures: (a) pH of wet samples, and (b) pH of dry samples-----	78
4-6. Sr(NO <sub>3</sub> ) <sub>2</sub> extraction results from anaerobic incubation for Fe/Mn materials amended manure mixtures (error bars represent 1 standard deviation): (a) Sr(NO <sub>3</sub> ) <sub>2</sub> extractable Zn, (b) Sr(NO <sub>3</sub> ) <sub>2</sub> extractable Cu, and (c) pH of Sr(NO <sub>3</sub> ) <sub>2</sub> solution after extraction-----	83
4-7. Oxalate extractable Zn and Cu during anaerobic incubation for Fe/Mn materials amended manure mixtures (error bars represent 1 standard deviation): (a) Oxalate extractable Zn, and (b) Oxalate extractable Cu. -----	84
5-1. Satellite view of the APHIS site and Soil sampling spots (Satellite image was adapted from <a href="http://www.bing.com/maps/">http://www.bing.com/maps/</a> ).-----	92
5-2. Gravel layer right next to the APHIS building-----	93

6-1. Column reacto design for column heavy metal adsorption study-----	108
6-2. Composts used in the column experiment: (a) Manure compost, and (b) Grass/Food waste compost -----	109
6-3. Scanning electron micrographs for Manure compost (MC) and Grass+Food waste compost (GC): (a) MC with 25 times magnification; (b) GC with 25 times magnification; (c) MC with 100 times magnification; (d) GC with 150 times magnification; (e) MC with 450 times magnification; (f) GC with 450 times magnification-----	110
6-4. Waste materials used in the column experiment; (a) Steel slag, and (b) Hubcutter heavies-----	111
6-5. Dissolved effluent metal concentration from different Biomat media column as a function of cumulative treated flow during column sorption study; Breakthrough curve for (a) Zn, (b) Pb and (c) Cu: 10% Manure compost + sand (MC10); 10% Grass/Food waste compost + sand (GF10); 25% Grass/Food waste compost + sand (GF25); 25% Grass/Food waste compost + Steel slag + sand (GFS25); and 25% Grass/Food waste compost + Hubcutter heavies + sand (GFH25),-----	117
6-6. Scanning electron micrographs for (a) Manure compost and (b) Grass/Food waste compost       120 -----	119
6-7. Effluent pH change for different media during sorption column study: 10% Manure compost + sand (MC10); 10% Grass/Food waste compost + sand (GF10); 25% Grass/Food waste compost + sand (GF25); 25% Grass/Food waste compost + Steel slag + sand (GFS25); and 25% Grass/Food waste compost + Hubcutter heavies + sand (GFH25) -----	120
6-8. Effluent metal concentration during initial column operation: (a) Dissolved Pb; (b) Total Pb; (c) Dissolved Cu; (d) Total Cu; (e) Dissolved Zn;. (f) Total Zn. Note differences in concentration scales for each metal. MC10 (10% Manure compost column+sand), GF10 (10% Grass/Food waste column+sand), GF25 (25% Grass/food waste column+sand), GFS25 (25% Grass/Food compost + 5% Steel slag+sand), GFH 25 (25% Grass food waste compost + 5% Hubcutter Heavies+sand).-----	131
6-9. Effluent concentration of (a) Total P, (b) Turbidity, and (c) Total Cr during intial column operation for MC10 (10% Manure compost column+sand), GF10 (10% Grass/Food waste column+sand), GF25 (25% Grass/food waste column+sand), GFS25 (25% Grass/Food compost + 5% Steel slag+sand), GFH 25 (25% Grass food waste compost + 5% Hubcutter Heavies+sand).-----	135
6-10. Effluent total phosphorus concentration throughout the adsorption study (low scale) for MC10 (10% Manure compost column), GF10 (10% Grass/food waste column), GF25 (25% Grass/food waste column), GFS25 (25% Grass/food compost + 5% steel slag), GFH 25 (25% Grass food waste compost + 5% Hubcutter Heavies).-----	136
6-11. Effluent of columns containing 25% grass/food waste during first 65-75 cm flow: (a) 25% Grass/food waste column (GF25); (b) 25% Grass/food waste + steel slag column (GFS25); and (c) 25% Grass/food waste+Hubcttler heavies (GFH25) -----	136

6-12. Heavy metal removal during the sorption study for MC10 column (10% Manure compost + sand): (a) Heavy metal removed in molar concentration during the sorption study; and (b) Heavy metal percent removed during the sorption study. Negative concentration or percent indicates the desorption of the metal. -----	141
6-13. Heavy metal removal during the sorption study for GF10 column (10% Grass/Food waste compost + sand): (a) Heavy metal removed in molar concentration during the sorption study; and (b) Heavy metal percent removed during the sorption study. Negative concentration or percent indicates the desorption of the metal-----	142
6-14. Dissolved effluent metal concentration by treated cumulative flow during adsorption and leaching study for (a) Zn, (b) Pb and (c) Cu.: Arrow indicates the start of leaching study after adsorption study-----	147
6-15. Effluent pH change during sorption and leaching study: MC10 (10% Manure compost column), GF10 (10% Grass/food waste column), GF25 (25% Grass/food waste column), GFS25 (25% Grass/food compost + 5% steel slag), GFH 25 (25% Grass food waste compost + 5% Hubcutter Heavies) -----	149
6-16. Linearity of total metal concentration removed on cumulative flow: (a) MC10 column (10% Manure compost + sand); and (b) GF10 column (10% Grass/Food waste compost + sand) -----	153
7-1. Bench scale Biomat box reactor design for bench scale experimen-----	159
7-2. Experimental setup of bench scale experiment-----	164
7-3. Bench scale experiment during a experiment-----	165
7-4. Parameters used in estimating hydraulic conductivity of Biomat media-----	166
7-5. Soil sampling profile from Biomat media after bench-scale experiment-----	168
7-6. Water quality parameters for Experiment 1 during bench scale experiments. (a) Pb concentrations, water head, and turbidity; (b) Cu concentrations, P concentrations, and effluent flow rate; (c) Zn concentrations and pH -----	172
7-7. Water quality parameters for Experiment 2 during bench scale experiments. (a) Pb concentrations, water head, and turbidity; (b) Cu concentrations, P concentrations, and effluent flow rate; (c) Zn concentrations and pH -----	173
7-8. Water quality parameters for Experiment 3 during bench scale experiments. (a) Pb concentrations, water head, and turbidity; (b) Cu concentrations, P concentrations, and effluent flow rate; (c) Zn concentrations and pH -----	177
7-9. Water quality parameters for Experiment 4during bench scale experiments. (a) Pb concentrations, water head, and turbidity; (b) Cu concentrations, P concentrations, and effluent flow rate; (c) Zn concentrations and pH -----	178
7-10. Water quality parameters for Experiment 7 during bench scale experiments. (a) Pb concentrations, water head, and turbidity; (b) Cu concentrations, P concentrations, and effluent flow rate; (c) Zn concentrations-----	183

7-11. Water quality parameters for Experiment 8 during bench scale experiments. (a) Pb concentrations, water head, and turbidity; (b) Cu concentrations, P concentrations, and effluent flow rate; (c) Zn concentrations-----	184
7-12. Water quality parameters for Experiment 9 during bench scale experiments. (a) Pb concentrations, water head, and turbidity; (b) Cu concentrations, P concentrations, and effluent flow rate; (c) Zn concentrations-----	185
7-13. Water quality parameters for Experiment 10 during bench scale experiments. (a) Pb concentrations, water head, and turbidity; (b) Cu concentrations, P concentrations, and effluent flow rate; (c) Zn concentrations -----	189
7-14. Water quality parameters for Experiment 5 during bench scale experiments. (a) Pb concentrations, water head, and turbidity; (b) Cu concentrations, P concentrations, and effluent flow rate; (c) Zn concentrations and pH-----	192
7-15. Water quality parameters for Experiment 11 during bench scale experiments. (a) Pb concentrations, water head, and turbidity; (b) Cu concentrations, P concentrations, and effluent flow rate; (c) Zn concentrations and pH-----	193
7-16. Effluent metal concentration based on influent loading rate of each metal (in mg/m <sup>3</sup> /min) for: (a) Pb, (b) Cu, and (c) Zn. Solid line is trend line. Solid arrows are indicating the loading rate at Maryland fresh water acute criteria for each metal. Dashed lines are indicating the loading rate at 5% of influent (95% removal) for each metal---	202
7-17. Effluent metal concentration based on influent loading rate of three metal combined (mmol/m <sup>3</sup> /min) for: (a) Pb, (b) Cu, and (c) Zn. Solid line is trend line. Solid arrows are indicating the loading rate at Maryland fresh water acute criteria for each metal. Dashed lines are indicating the loading rate at 5% of influent (95% removal) for each metal. --	203
7-18. Flow rate through Biomat based on an influent water head at different hydraulic conductivities of Biomat media (Biomat media length parallel to the flow=18 cm)-----	204
7-19. Total Metal (Pb, Cu, and Zn) concentrations extracted from Biomat media (see Figure 7-5 for dimensions) -----	209
8-1. Recommended field design for Biomat media installation.-----	229
8-2. Filter socks with different opening size-----	230
8.3. Biomat saturation pattern with two extreme case-----	231

## CHAPTER 1. INTRODUCTION

Heavy metals (e.g., Pb, Cu, and Zn) and nutrients (e.g., phosphorus and nitrogen) released from diffuse sources by both urban and agricultural runoff are important pollutants causing aquatic toxicity and/or eutrophication in water bodies. The many diffuse sources include (1) urban runoff from residential, commercial and industrial areas; (2) agricultural runoff from excessive land application and poor management of manure/biosolids, fertilizers, herbicides and insecticides; (3) runoff from construction sites; and (4) runoff and acid drainage from abandoned mine and smelting sites (Carpenter et al., 1998; Pierzynski et al., 2000). Diffuse source pollution is difficult to address because of the dispersed and often dynamic nature of the flows. Specifically, high volumes of runoff flows and difficulties in collecting flows from diffuse sources for treatment are significant obstacles and often lead to economic impracticality of traditional approaches, which attempt to collect and treat runoff/infiltration in centralized facilities. Therefore, inexpensive technologies that are highly efficient at reducing targeted pollutants must be developed in order to address environmental permit conditions or potential contamination issues by overcoming the obstacles of diffuse source pollutants.

Beneficial use of byproducts/waste materials from industrial or agricultural activities as amendments or media/barriers to treat pollutants from non-point sources can provide cost-effective solutions over various ranges of pollutants and flows. There are two different in-situ approaches in which byproducts/waste materials can be used to treat pollutants from non-point sources. Firstly, they can be applied directly to the diffuse sources as amendments to stabilize/capture the pollutants so that few pollutants are leached to runoff from the non-point source. This application can be chosen when

collecting and inducing runoff to a treating system is relatively difficult (or expensive) and/or the amount of infiltration is relatively greater than the runoff volume.

Additionally, direct application can be applied when the byproducts/waste materials can be easily mixed with diffuse sources to provide good contact with pollutants. Secondly, these materials can be used as media/barrier constituents or amendments in runoff treatment systems, which can remove pollutants leached from the diffuse source. This system can be applied when collecting and inducing runoff/infiltration to the system is relatively easy. Therefore, two research topics were studied for investigating two different in-situ approaches for beneficial use of byproduct/waste materials to decrease environmental risks of pollutant loss from non-point diffuse sources.

### **1-1. Immobilization of phosphorus using Fe/Mn inorganic materials and an anaerobic incubation process.**

Immobilization of phosphorus (P) in manure and biosolids has been studied as the first part of an application study using byproducts/waste materials, because of significant environmental concerns for phosphorus release from land application of manure/biosolids. Land application of manure and biosolids is limited in many areas by environmental concerns from highly soluble P species which can cause eutrophication of freshwater by agricultural runoff and leachate (Sharpley et al., 1994; Carpenter et al., 1998; Correll, 1998; Daniel et al., 1998; Sharpley et al., 2003). Excessive application of phosphorus to meet crop requirements for nitrogen can often lead to high contents of P in soil and increased P loss through surface runoff and infiltration to ground water (Sharpley et al., 1994).



Therefore, the control and reduction of P compounds leached by agricultural surface runoff/infiltration from manure land application can significantly minimize environmental concerns of P, especially in the state of Maryland where Atlantic coastal plain soils, coarse textured with low clay and sesquioxides content are predominant (Novak et al., 2000).

High concentrations or additions of Fe, Al, and Ca in soils, or organic soil amendments have been reported as important constituents for immobilizing P via adsorption and precipitation mechanisms (McLaughlin et al., 1981; Shreve et al., 1995; Kalbasi and Karthikeyan, 2004; Torbert et al., 2005). Different Fe, Al and Ca amendments have been widely used to immobilize phosphorus in soils, manures and biosolids. These include reagent or commercial grade Fe, Al, and Ca salts (e.g., alum, lime, limestone, ferric chloride and others) (Moore and Miller, 1994; Smith et al., 2001; Boruvka and Rechcigl, 2003) or industrial byproducts/wastes (e.g., gypsum, and fly ash) (Dao, 1999; Peacock and Rimmer, 2000; Dou et al., 2003), and municipal water treatment residues with high Al, Ca and Fe contents (Peters and Basta, 1996; Codling et al., 2000; Haustein et al., 2000; Dao et al., 2001; Elliott et al., 2002; Makris et al., 2004; Novak and Watts, 2004). Recently, beneficial uses of byproducts/waste materials containing high Fe, Al, and Ca from industrial/municipal activities have been studied due to their cost-effective and environmental advantages, reusing the byproducts/wastes in order to immobilize P from manure and soil (Codling et al., 2000; Peacock and Rimmer, 2000; Elliott et al., 2002; Dayton and Basta, 2005). Specifically, more amorphous and more readily available/active forms of Al, Ca and Fe amendments demonstrated much better P retention than crystalline ones (McLaughlin et al., 1981).

Therefore, it is beneficial not only to determine the better application candidates among high Fe/Mn byproducts/waste materials, but also to develop an inexpensive process to increase the active amorphous Fe and/or Mn content in manure from non-active crystalline Fe/Mn additives for immobilizing P in manure and biosolids. In addition, both beneficial advantages and environmentally safe applicability of the byproduct/waste materials must be considered because the inorganic byproduct/waste materials may also contain trace amounts of toxic compounds that can be leached to environment by their application and cause adverse effects on human health and the environment (Proctor et al., 2000).

Although addition of Fe oxides alone to manure or compost may be a useful method to reduce phosphate solubility, it may also induce Mn deficiency if the amended product is applied to low Mn Coastal Plain soils. Such soils are depleted of Fe and Mn during genesis, and liming or addition of Fe rich materials can reduce Mn phytoavailability and reduce yields of crops sensitive to Mn deficiency such as soybeans and wheat. Addition of Mn with the Fe amendment can prevent this Fe-induced Mn deficiency and generally improve fertility of such soils (Brown et al., 1997).

In spite of the importance of this topic, few studies have been completed using industrial Fe/Mn byproducts/wastes (e.g., steel slag and Mn tailings) or raw Fe/Mn materials (e.g., iron ore) for immobilizing P in manure. Additionally, no study has focused on developing economical processes to increase the active amorphous Fe and/or Mn content in manure and biosolids from non-active crystalline Fe/Mn additives to immobilize P.

These studies evaluated effectiveness of different Fe/Mn waste/raw materials as amendments to immobilize P from manure/biosolids. Furthermore, effectiveness on use of anaerobic incubation to increase active amorphous Fe/Mn from less amorphous Fe/Mn additives and subsequently decrease P mobilization in manure was investigated through these studies. Applicability of these simple processes using a typical simple digestion process with Fe/Mn amendments was discussed to produce better biosolids as fertilizer which release minimal P and trace metals, with low environmental concern, but still provide enough fertility for plant synthesis during long periods of time.

### **1-2. Heavy metal removal from roof/wall runoff using a Biomat with compost and inorganic byproducts.**

As the second application of byproducts for diffuse source pollution, a site with a diffuse source of heavy metals was studied. Building-580 (location of an Animal and Plant Health Inspection Service facility) is located at the Beltsville Agricultural Research Center-East (BARC-East) in Beltsville, MD (Figure 1-1). Its exterior wall and roof are mainly made of Cu and Pb and their surface has significant corrosion (Figure 1-2). Therefore, they were suspected as potential sources of heavy metal contamination of surface water and soil from the runoff from the building rooftop and walls. The rainfall runs off of the roof and wall as sheet flow and drains into a gravel strip adjacent to the building. It then runs off into the adjacent grass and into a drainage ditch.



Figure 1-1. B-580 APHIS building, BARC-East in Beltsville, MD.

The traditional approach has been to attempt to collect and treat stormwater runoff in centralized facilities. However, this approach is costly and can cause major disruptions to operations, especially for retrofits in large and complex operations such as the USDA APHIS facility.

Composts and mineral-amended composts have been widely used to remediate metal-contaminated soils (Brown et. al, 2003; van Herwijnen et. al, 2007). However, little work has been completed on heavy metal removal from aqueous runoff solutions using compost. A bioremediation mat (Biomat) was used in this research to remove heavy metals (lead, copper and zinc) from the storm water runoff from the studied site. The mat was an engineered mixture of sand/compost/waste byproduct sorption media to adsorb/precipitate dissolved pollutants and trap/filter out large particulates. Use of industrial inorganic byproducts as well as agricultural organic byproducts (compost) provided economic advantages in removing heavy metals from runoff from non-point sources.



Figure 1-2. The corroded exterior wall of B-580 APHIS building which contains Pb and Cu.

These studies investigated heavy metal removal capacity and design parameters for Biomat media. This work also evaluated the flexible feasibility of the Biomat for removing heavy metals leached from various non-point sources under variable conditions.

## CHAPTER 2. OBJECTIVES OF STUDY

The overall objective of the selected two research studies were to evaluate beneficial use of byproduct/waste materials in order to decrease environmental risks from heavy metals (e.g., Pb, Cu, and Zn) and nutrients (eg., phosphorus and nitrogen) released from non-point sources by urban or agricultural runoff . The specific objectives of two studies are described in the following sections.

### **2-1. Immobilization of phosphorus using Fe/Mn inorganic materials and an anaerobic incubation process.**

The overall goal of this research study was to evaluate three different Fe/Mn inorganic byproducts/raw materials as amendments: iron ore, steel slag and Mn tailings, in fresh manure, throughout an anaerobic incubation process designed to increase and synthesize active amorphous Fe/Mn from less-amorphous Fe/Mn additives to correspondingly decrease P mobilization in manure.

Proposed mechanisms and processes hypothesized in this study are presented in Figure 2-1. First, dissolution of crystalline Fe/Mn can be achieved chemically and/or biologically under anaerobic conditions. Enzymatic microbial reduction of Fe(III) has been reported as the process being responsible for most of the Fe(III) reduction in aquatic sediments compared to nonenzymatic chemical Fe(III) reduction (Lovely et al., 1991). Exploiting this bacterial Fe/Mn reductive dissolution, the anaerobic incubation process has been adopted for increasing active amorphous Fe/Mn oxides. The dissolved Fe(II)/Mn(II) species synthesized by bacterial reductive dissolution can be subsequently oxidized to Fe(III)/Mn(IV) by oxygen, producing high surface area, active, amorphous Fe/Mn oxyhydroxides. It was hypothesized that these freshly precipitated species will have high sorption capacities for P.

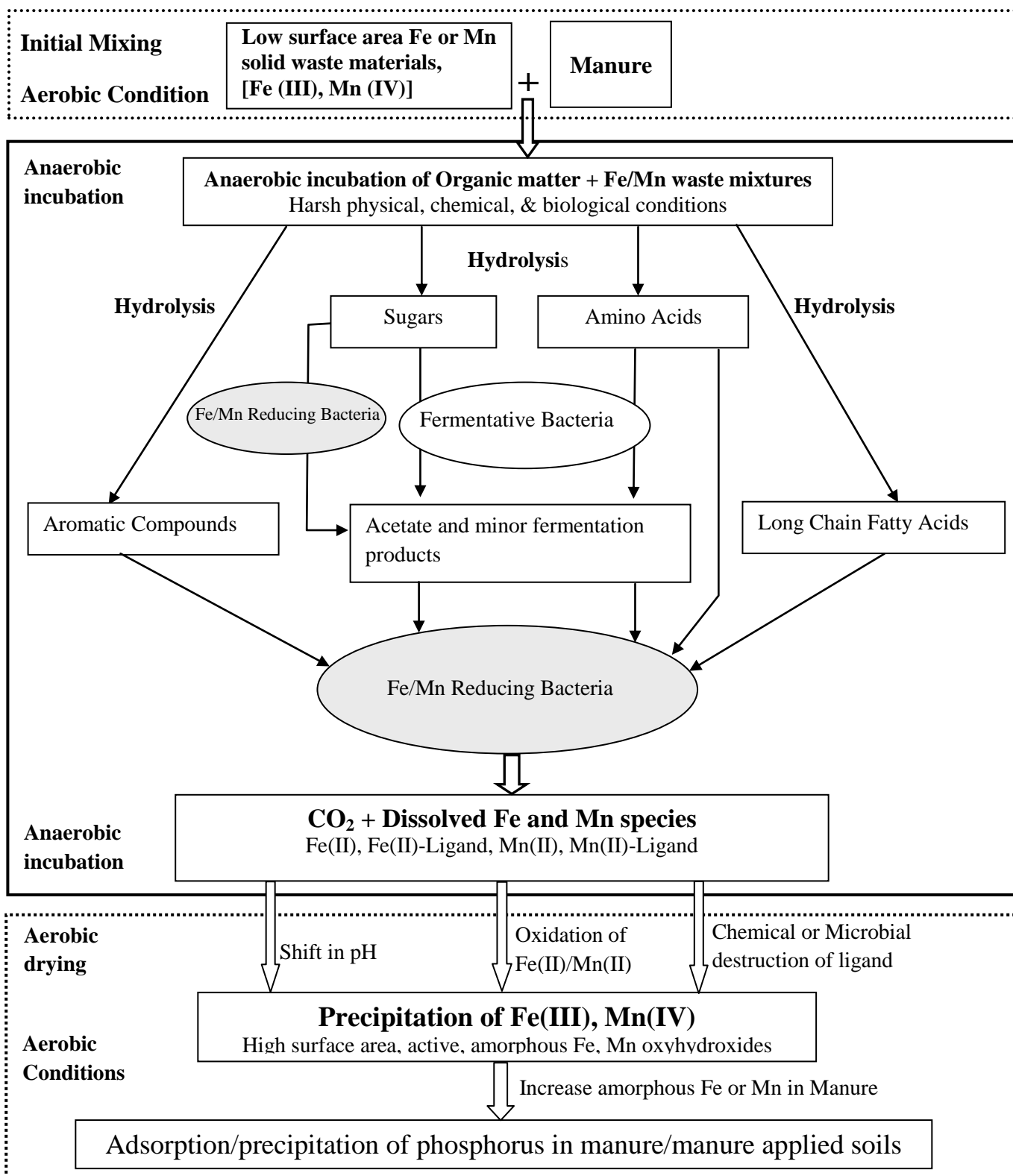


Figure 2-1. Proposed mechanisms and processes involved in production of active amorphous Fe/Mn oxides from non active Fe/Mn waste and organic matter mixtures (partially adopted from Lovely, 2000).

Three specific objectives in this research were: (1) evaluate three different Fe/Mn materials as amendments in manure by investigating the degree of P immobilization; (2) evaluate an anaerobic incubation process by investigating the relationship between change of oxalate- extractable Fe (considered as amorphous Fe) and P immobilization throughout the anaerobic incubation period; (3) evaluate environmental concerns from heavy metal release from the mixture of manure and Fe/Mn materials by investigating the change of heavy metal (Cu and Zn) extractability during the anaerobic incubation.

## **2-2. Heavy metal removal from roof/wall runoff using a Biomat with compost and inorganic byproducts.**

The overall goal of this research study was to evaluate the Biomat media mixture for its capacity and performance for heavy metal removal from the roof/wall runoff. Four specific experimental phases have been established to fulfill four specific objectives as follows: (1) monitoring and characterizing roof/wall runoff from the building; (2) screening, selecting and evaluating the mat media employing long-term column studies; (3) investigating hydraulic characteristics and demonstrating heavy metal removal capacity of the mat media with a bench-scale mat; and (4) establishing design parameters, implementations, and recommendations for future full scale Biomat application in a field.

Through the first phase investigation, the characteristics of the rooftop-wall runoff was studied. Two different types of compost, namely, manure compost and grass/food waste compost, and two different types of inorganic waste byproducts, steel slag and “hubcutter heavies”, an iron waste material from a train wheel manufacturer, were evaluated in column studies as the second phase investigation. Based on the column



adsorption and leaching studies, the media mixture that exhibited the highest capacity for removing heavy metals was selected as a candidate media for the mat and is evaluated in more detail in a bench scale experiment as the third phase of the investigation (Phase 3). Specifically, water quality performance and hydraulic characteristics of mat media will be investigated employing variable influent water head. Additionally, stability of adsorbed metals on the mat media will be studied by washing out the media by deionized water during the third phase bench-scale experiments.

As the last phase investigation (Phase 4), design parameters for a full scale Biomat was investigated and established based on previous research phases and implementations and recommendations for future application of full scale Biomats in the field was suggested.

## CHAPTER 3. BACKGROUNDS AND LITERATURE REVIEW

The goal of this chapter is to review the background information and basic theory pertinent to this research. The major topics reviewed in this chapter include: (1) Phosphorus in agriculture and its environmental implications; (2) Use of Fe, Al, and Ca compounds as amendment to immobilize P from manure and soil; (3) Bacterial Fe/Mn reductive dissolution during anaerobic incubation; (4) Heavy metals in runoff; (5) Surface chemistry and Adsorption; (6) Organic and/or inorganic amendments to remove heavy metals in aqueous phase; (7) Organic and/or inorganic amendments to remove heavy metals from soil; (8) Typical solid phase amendments for heavy metal immobilization in soil.

### **3-1. Phosphorus in agriculture and its environmental implications.**

Phosphorus (P), as an essential element for plant and animal growth, has been applied in agriculture to maintain profitable crops and animal production (Sharpley and Rekolainen, 1997). While a certain level of soil P needs to be maintained for economic crop production, part of the applied or accumulated soil P is lost from agricultural runoff, erosion and leaching (Sibbesen and Sharpley, 1997). Only approximately 30% of P input to farming systems has been estimated as output in crops and animal produce, and this excessive land application of manure phosphorus (often to meet crop requirements for nitrogen) can lead to high accumulations of P in soil and increased P loss to water bodies and ground water through surface runoff and leaching (Sharpley et al., 1994; 2003). The land application of animal manure and biosolids has been increased recently as waste production from the livestock industry and human activity has increased (Table 3-1).

Specifically, the estimated total amount of livestock waste (e.g., cattle and chicken manure) is large and therefore, the importance of efficient recycling of the nutrients from the manure wastes has increased as shown in Table 3-1 (Pierzynski et al., 2000).

Table 3-1. Estimated total amount of livestock waste, biosolids, and municipal solid waste compost in the U.S. (adapted from Pierzynski et al., 2000 sourced from Logan et al., 1995 in proceedings of the 4<sup>th</sup> Joint WEF and AWWA conference on biosolids and residual management, WEF, Alexandria, VA 1995, 15-13 to 15-28).

Source	Estimated amount produced (million Mg/year)
Biosolids	7.2
Municipal solid waste compost	0.13
Beef cattle	105
Dairy cattle	36
Swine	15
Chicken	121
Turkeys	5.4
Sheep	1.8

However, land application of manure and biosolids is limited in many areas by environmental concerns from soluble phosphorus (P) species, which can cause eutrophication of freshwater by agricultural runoff and leachate (Carpenter et al., 1998; Correll, 1998; Daniel et al., 1998; Sharpley et al., 2003). Phosphorus and nitrogen loss to surface waters from nonpoint sources occupies greater than 80% of total discharge in

the United States (Carpenter et al., 1998). P loss from nonpoint source is dominant in rural and agricultural areas. Locally, around 60% of total phosphorus entering the Chesapeake Bay was estimated to originate from diffuse sources and majority of the phosphorus (around 80% of the phosphorus from diffuse sources) was identified from agriculture (Boynton et al., 1995; Boesch et al, 2001). Therefore, it is important to decrease P loss from agricultural sources. Specifically, immobilizing phosphorus in livestock manure and manure-applied soil can decrease environmental risks caused by P loss. Characterization of P in manure, soil, and, aquatic systems is important to understand P movement and problems from manure and manure applied soil.

### **3-1-1. Phosphorus in Soil**

P in soil exists in inorganic and organic forms (Figure 3-1). Organic phosphorus forms are comprised of relatively labile forms such as phospholipids, nucleic acids, inositols and fulvic acids, and more resistant forms such as humic acids (Sharpley and Rekolainen, 1997). Organic P in soil can be mineralized through general decomposition of soil organic matter. Phosphorus exists in the pentavalent form in aquatic systems such as orthophosphate, pyrophosphate, longer-chain polyphosphates, organic phosphate esters and phosphodiester, and organic phosphonates (Corell, 1998). Inorganic phosphorus containing compounds commonly found in soils are shown in Table 3-2 and they are mostly stable and quite insoluble except mono- and di-calcium phosphates (i.e., commercial fertilizers) (Brady and Weil, 2002).

Hydrous sesquioxides and amorphous and crystalline Al and Fe, and less frequently, Mn compounds, are dominant inorganic P forms in acidic, non-calcareous

soils, while inorganic P forms are dominated by Ca compounds in alkaline, calcareous soils. This is because iron- and aluminum-containing phosphates (e.g.,  $\text{FePO}_4 \cdot 2\text{H}_2\text{O}$  and  $\text{AlPO}_4 \cdot 2\text{H}_2\text{O}$ ) are stable and insoluble in acidic soils while the calcium phosphates, especially the apatite minerals, are stable and extremely insoluble at high pH levels. Soil pH is the controlling factor in inorganic P fixations and reactions as illustrated in Figure 3-2 and 3-3. Under acidic conditions, inorganic fixation of phosphates in relatively unavailable forms occurs most with Al, Fe or Mn species (as dissolved ions, oxides or hydrous oxides) while moderate pH can cause phosphorus adsorption on edges of kaolinite or on the iron oxide coatings on kaolinite clays (Figure 3-2) (Brady and Weil, 2002).

The loss of soil P is largely caused by plant uptake, erosion of phosphorus carrying soil particles, phosphorus dissolved in surface runoff, and leaching to ground water (Brady and Weil, 2002).

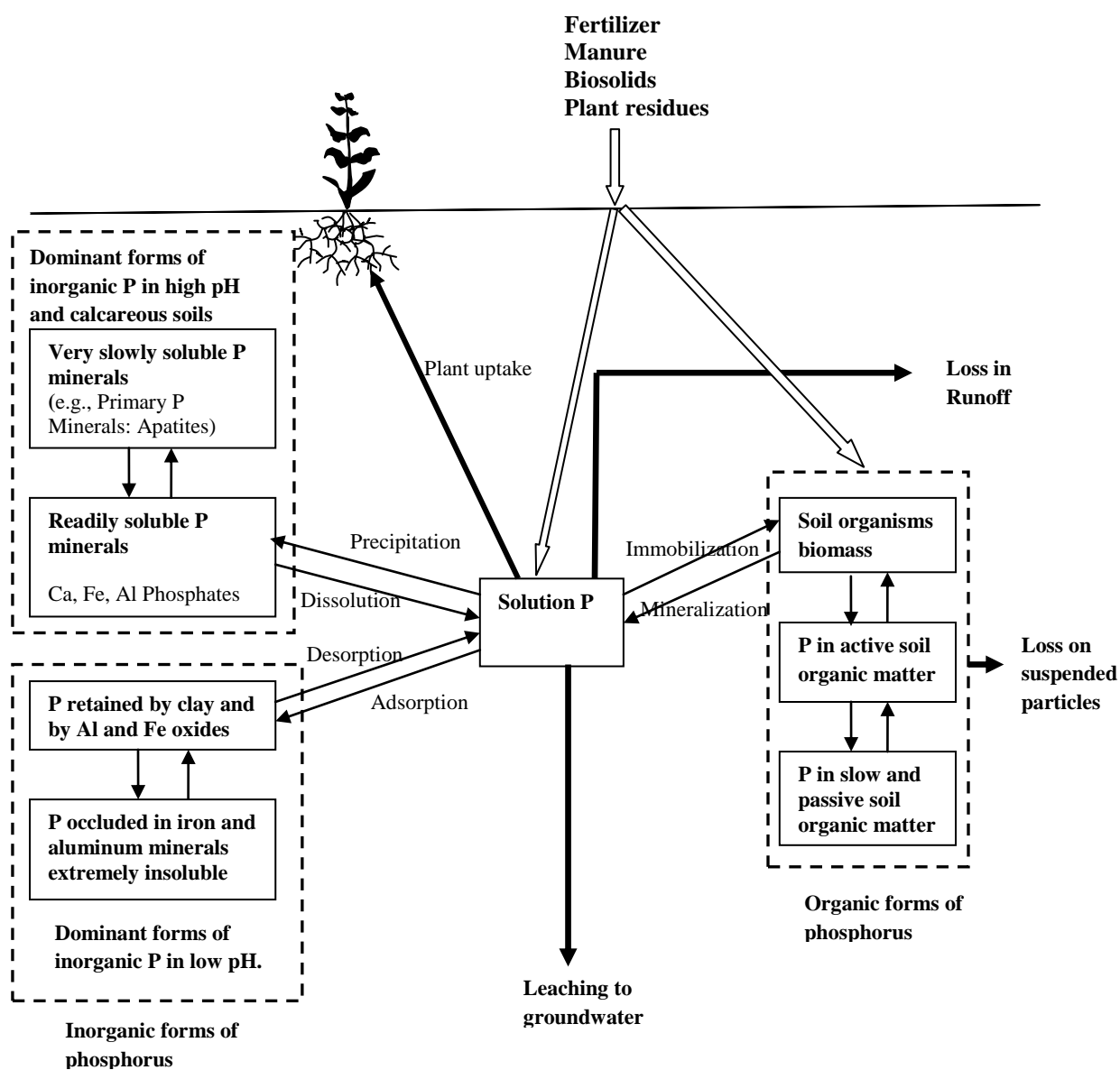
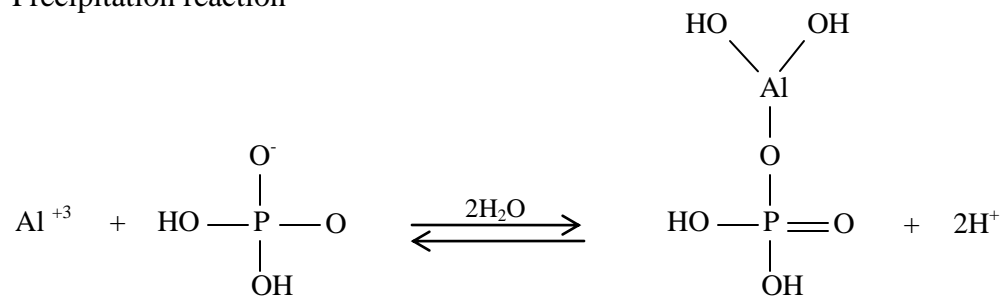


Figure 3-1. The Phosphorus Cycle in Soils (Adapted from Pierzynski et al., 2000; Brady and Weil, 2002).

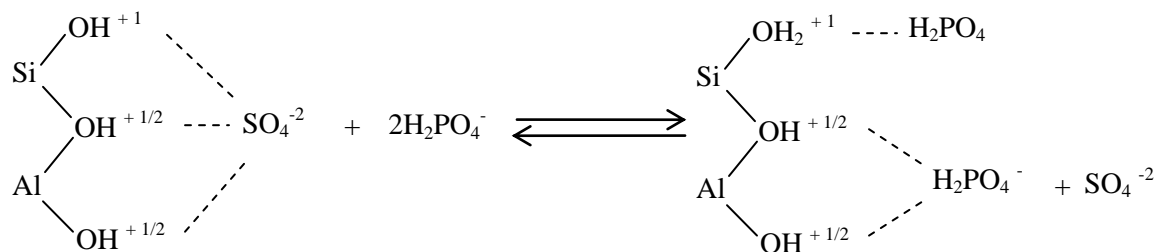
Table 3-2. Inorganic phosphorus containing compounds commonly found in soil (listed in order of increasing solubility in each group) (Stumm and Morgan, 1996; Brady and Weil, 2002).

Compound	Formula and solubility equilibrium	log K (25 °C, I=0)
<u>Iron and aluminum compounds</u>		
Strengite	$\text{FePO}_4 \cdot 2\text{H}_2\text{O}(\text{s}) = \text{Fe}^{+3} + \text{PO}_4^{-3} + 2\text{H}_2\text{O}$	-26
Variscite	$\text{AlPO}_4 \cdot 2\text{H}_2\text{O}(\text{s}) = \text{Al}^{+3} + \text{PO}_4^{-3} + 2\text{H}_2\text{O}$	-21
<u>Calcium compounds</u>		
Fluorapatite	$[\text{3Ca}_3(\text{PO}_4)_2] \cdot \text{CaF}_2(\text{s}) = 10\text{Ca}^{+2} + 6\text{PO}_4^{-3} + 2\text{F}^-$	-118
Carbonate apatite	$[\text{3Ca}_3(\text{PO}_4)_2] \cdot \text{CaCO}_3(\text{s}) = 10\text{Ca}^{+2} + 6\text{PO}_4^{-3} + 10\text{CaCO}_3^{-3}$	-
Hydroxy apatite	$[\text{3Ca}_3(\text{PO}_4)_2] \cdot \text{Ca}(\text{OH})_2(\text{s}) = 10\text{Ca}^{+2} + 6\text{PO}_4^{-3} + 2\text{OH}^-$	-114
	$[\text{3Ca}_3(\text{PO}_4)_2] \cdot \text{Ca}(\text{OH})_2(\text{s}) + 6 \text{H}_2\text{O} = 4[\text{Ca}_2(\text{HPO}_4)(\text{OH})_2] + 2\text{Ca}^{+2} + 2\text{HPO}_4^{2-}$	-17
Oxy apatite	$[\text{3Ca}_3(\text{PO}_4)_2] \cdot \text{CaO} = 10\text{Ca}^{+2} + 6\text{PO}_4^{-3} + \text{O}^{-2}$	-
Tricalcium phosphate	$\text{Ca}_3(\text{PO}_4)_2 = 3\text{Ca}^{+2} + 2\text{PO}_4^{-3}$	-
Octacalcium phosphate	$\text{Ca}_8\text{H}_2(\text{PO}_4)_6 \cdot 5\text{H}_2\text{O} = 8\text{Ca}^{+2} + 6\text{PO}_4^{-3} + 2\text{H}^+ + 5\text{H}_2\text{O}$	-
	$\text{Ca}_4\text{H}(\text{PO}_4)_3(\text{s}) = 4\text{Ca}^{+2} + 3\text{PO}_4^{-3} + \text{H}^+$	-46.9
Dicalcium phosphate (dihydrate)	$\text{CaHPO}_4 \cdot 2\text{H}_2\text{O} = \text{Ca}^{+2} + \text{HPO}_4^{-2} + 2\text{H}_2\text{O}$	-6.6
Monocalcium phosphate	$\text{Ca}(\text{H}_2\text{PO}_4)_2 \cdot \text{H}_2\text{O} = \text{Ca}^{+2} + 2\text{HPO}_4^- + \text{H}_2\text{O}$	

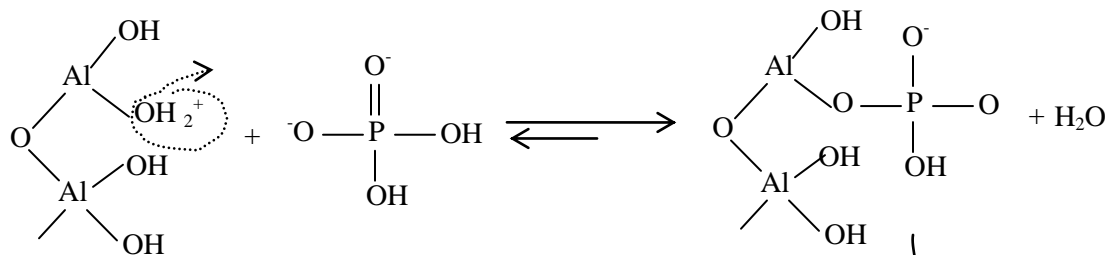
(a) Precipitation reaction



(b) Anion exchange reactions (Outer sphere)



(c) Reactions with Al or Fe oxides surfaces (Inner sphere)



(d) Formation of stable binuclear bridge (Inner sphere)

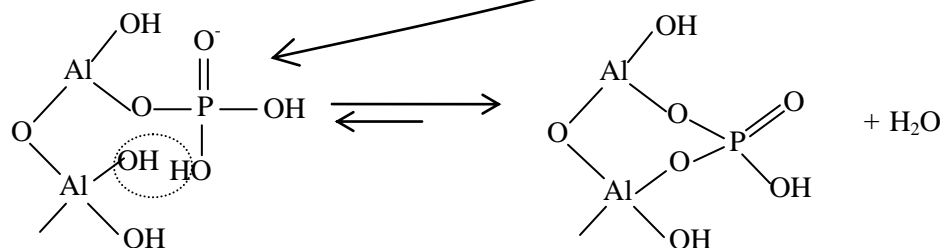


Figure 3-2. Phosphate ion removal reactions (adapted from Brady and Weil, 2002).



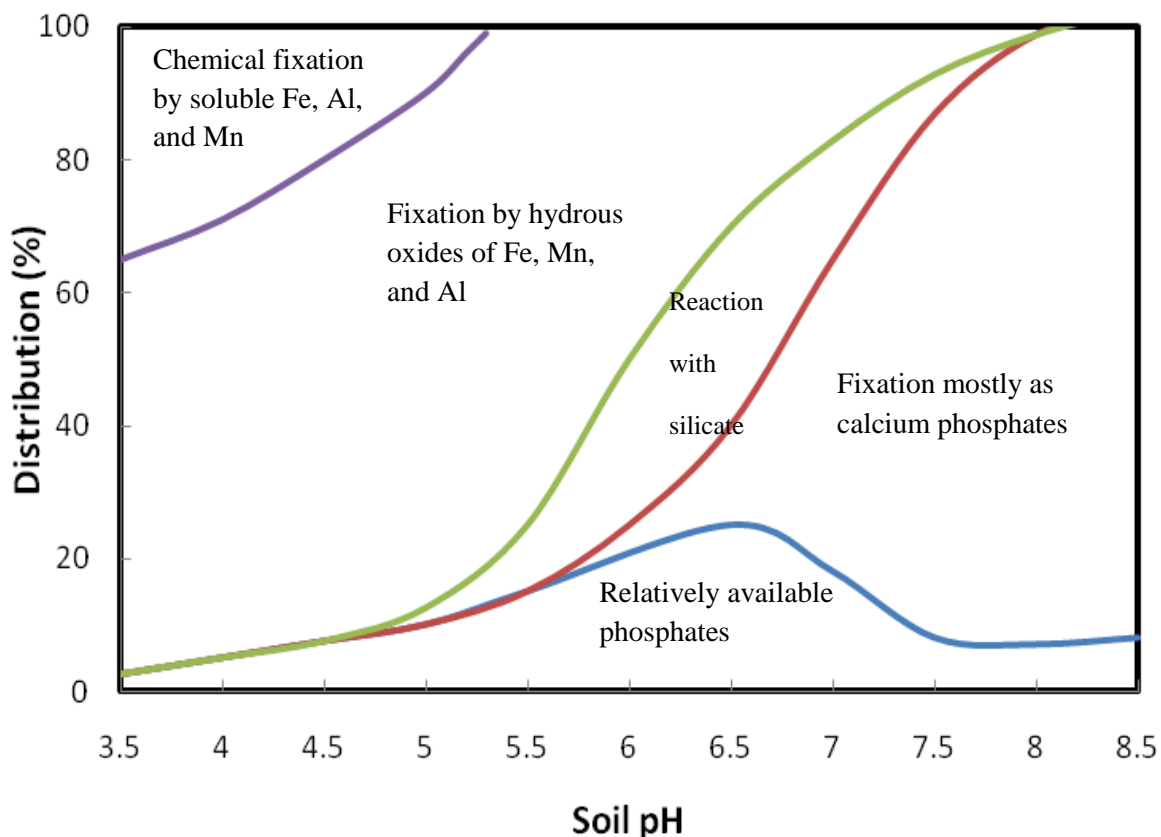


Figure 3-3. Typical inorganic phosphorus distribution at various soil pH (adapted from Brady and Weil, 2002).

### 3-1-2. Phosphorus in Manure

Properties of manure P are important to determine and predict its mobility and stability in soils. P speciation/distribution in manure allows the prediction of bioavailability and leachability of P in manure. Water extractable P (WEP) in manure has been widely studied and used to estimate manure P loss by agricultural runoff (Kleinman et al., 2002; Wolf et al., 2005; Vadas and Kleinman, 2006). Trends of variable WEP and other chemical properties based on manure types and storage were studied by Kleinman et al. (2002) using 140 livestock manures (Table 3-3). The survey

results suggested that manure WEP ranged wide from 0.2-16.8 g kg<sup>-1</sup>, indicating highest mean WEP from swine manure followed by turkey, layer chickens, dairy cattle, broiler chickens, and beef cattle. Significantly lower manure WEP was observed from dry manures than manures from liquid storage systems. High negative correlation between manure dry matter content and WEP was observed for dairy manure and liquid swine manure.

The distribution of inorganic and organic P fraction was studied by Sharpley and Moyer (2000) via sequential extractions with 24 manures and composts (Table 3-4). About 63 to 92 % of total P in manure existed as inorganic P. Most of the inorganic P in dairy manure was water extractable, while hydroxide extractable and acid extractable P made up the majority of inorganic P in swine slurry and poultry manure, respectively. This study also suggested the importance of water soluble P as an indicator of P loss estimation by leachate and surface runoff, demonstrating high correlation between water soluble inorganic and organic P and the amount of P leached by simulated rainfall events. Phosphorus distribution of dairy manure was studied by He et al. (2004) with 13 dairy manures. Inorganic and organic water soluble P occupied 12 to 44% (1400-6800 mg kg<sup>-1</sup>) and 2 to 23 % (130-1660 mg kg<sup>-1</sup>) of total manure P, respectively. The P extraction by sodium acetate buffer was suggested as an efficient evaluation of plant-available P in animal manure, showing it is equivalent to the sum of P by three extract fractions, water-, NaHCO<sub>3</sub>- and NaOH- extractable P, while more detailed P characterization can be obtained by the sequential extraction.

A study of poultry manure and manure amended soil by Sato et al. (2005) using phosphorus K-edge X-ray absorption near-edge structure spectroscopy, suggested that

free and weakly bound phosphate and soluble Calcium phosphate (CaP) species (relatively small proportions of soluble CaP species such as dibasic calcium phosphate (DCP) and amorphous calcium phosphate (ACP)) were the dominant P species in manure with no evidence of crystalline P minerals existence. It is also suggested that CaP compounds become dominant and possibly crystalline (e.g., relatively soluble CaP such as DCP and ACP to more crystalline CaP species such as tricalcium calcium phosphate), with continued soil applications of poultry manure, while Fe- and Al-P becomes negligible. However, crystalline CaP in heavily manured soil was not found in the study probably due to presence of organic acids, which can delay the crystallization and transformations of CaP minerals. Maintaining a high soil pH was suggested as a strategy to immobilizing P in manure amended soil by keeping DCP and CaP insoluble.

Table 3-3. Mean values of chemical properties of livestock manure (adapted from Kleinman et al., 2005)

Livestock	Dry matter %	Total P g kg <sup>-1</sup>	WEP g kg <sup>-1</sup>	WEP/TP	TN g kg <sup>-1</sup>	TN/TP	Total Al g kg <sup>-1</sup>	Total Ca g kg <sup>-1</sup>	Total Fe g kg <sup>-1</sup>	Total Mg g kg <sup>-1</sup>
Beef	37 (19*)	5.1 (1.82)	2.3 (1.9)	0.43 (0.29)	19.5 (6.9)	3.9 (1.0)	5.2 (7.9)	24.9 (29.9)	5.6 (6.7)	5.1 (3.4)
Dairy	15 (10)	6.9 (3.2)	4.0 (1.8)	0.6 (0.15)	37.3 (18.5)	5.6 (1.7)	1.8 (1.9)	20.9 (10.7)	2.3 (2.3)	7.9 (5.4)
Broilers	71 (8)	15.6 (5.7)	3.2 (1.4)	0.2 (0.06)	45.5 (10.8)	3.0 (0.8)	2.5 (2.8)	23.7 (8.6)	1.3 (1.0)	6.1 (2.9)
Layers	58 (22)	25.6 (6.2)	4.9 (1.8)	0.19 (0.05)	49.6 (25.7)	2.2 (1.4)	0.9 (0.5)	133.7 (36.4)	1.3 (0.4)	9.7 (2.8)
Swine	8 (9)	28.8 (10.4)	9.2 (3.7)	0.37 (0.20)	89.9 (56.9)	3.8 (3.4)	1.2 (0.7)	33.5 (12.6)	2.7 (1.3)	11.4 (6.1)
Turkey	75 (2)	23.8 (6.7)	6.3 (1.6)	0.34 (0.07)	43.9 (13.3)	2.0 (0.7)	2.4 (2.0)	37.6 (19.0)	2.6 (2.2)	6.6 (2.1)

\* Standard deviations in parentheses

Table 3-4. Fractions of inorganic and organic P in manures and composts. (adapted from Harpley and Moyer, 2000)

Manure/ Compost	Total P mg kg <sup>-1</sup>	<u>Inorganic P, mg kg<sup>-1</sup></u>					<u>Organic P, mg kg<sup>-1</sup></u>				Residual P mg kg <sup>-1</sup>
		Water	Bicarbonate	Hydroxide	Acid	Inorganic P total	Water	Bicarbonate	Hydroxide	Organic P total	
Dairy manure	<b>3987</b>	2030 (51%*)	360 (9%)	70 (2%)	60 (1%)	<b>2520</b> <b>(63%)</b>	470 (12%)	90 (2%)	420 (11%)	<b>980</b> <b>(25%)</b>	<b>487</b> <b>(12%)</b>
Dairy compost	<b>16531</b>	2410 (15%)	6000 (36%)	1320 (8%)	5520 (33%)	<b>15250</b> <b>(92%)</b>	260 (1%)	70 (1%)	520 (3%)	<b>850</b> <b>(5%)</b>	<b>431</b> <b>(3%)</b>
Poultry manure	<b>28652</b>	7430 (26%)	7180 (25%)	320 (1%)	9320 (32%)	<b>24250</b> <b>(84%)</b>	2360 (8%)	1100 (4%)	470 (2%)	<b>3930</b> <b>(14%)</b>	<b>472</b> <b>(2%)</b>
Poultry litter	<b>16320</b>	4026 (25%)	4983 (31%)	817 (5 %)	4776 (29%)	<b>14602</b> <b>(90%)</b>	508 (3%)	673 (4%)	294 (2%)	<b>1474</b> <b>(9%)</b>	<b>243</b> <b>(1%)</b>
Poultry compost	<b>9441</b>	2030 (21%)	2900 (31%)	810 (9%)	2520 (27%)	<b>8260</b> <b>(87%)</b>	60 (1%)	770 (8%)	250 (2%)	<b>1080</b> <b>(11%)</b>	<b>101</b> <b>(1%)</b>
Swine slurry	<b>32952</b>	6045 (18%)	4168 (13%)	16620 (50%)	3294 (10%)	<b>30127</b> <b>(91%)</b>	1526 (5%)	657 (2%)	281 (1%)	<b>2464</b> <b>(8%)</b>	<b>361</b> <b>(2%)</b>

\* Percent of total P in parentheses

### **3-2. Use of Fe, Al, and Ca compounds as amendment to immobilize P from manure and soil**

High concentrations or additions of Fe, Al, and Ca in soils/manure have been reported as important constituents for immobilizing phosphorus via adsorption and/or precipitation mechanisms (McLaughlin et al., 1981; Shreve et al., 1995; Kalbasi and Karthikeyan, 2004; Torbert et al., 2005). Therefore, various types and forms of Fe, Al and Ca amendments have been widely used to immobilize phosphorus in soils, manures and biosolids. These include reagent or commercial grade Fe, Al, and Ca salts (e.g., alum, sodium aluminate, quick lime, slaked lime, calcitic limestone, dolomitic limestone, gypsum, ferrous chloride, ferric chloride, ferrous sulfate, ferric sulfate) (Moore and Miller, 1994; Shreve et al., 1995; Smith et al., 2001; Boruvka and Rechcig, 2003), industrial byproducts/wastes (e.g., gypsum and fly ash) (Peters and Basta, 1996; Stout et al., 1998; Dao, 1999; Codling et al., 2000; Haustein et al., 2000; Peacock and Rimmer, 2000; Dou et al., 2003), and municipal water treatment residues with high Al, Ca and Fe contents (Peters and Basta, 1996; Gallimore et al., 1999; Codling et al., 2000; Haustein et al., 2000; Dao et al., 2001; Elliott et al., 2002; Makris et al., 2004; Novak and Watts, 2004, 2005; Dayton and Basta, 2005). Recently, beneficial use of byproducts/waste materials containing high Fe, Al, and Ca from industrial/municipal activities have been studied due to their cost-effective advantages and environmental friendly solutions by reusing the byproducts/wastes in order to immobilize P from manures and soils (Peters and Basta, 1996; Codling et al., 2000; Peacock and Rimmer, 2000). Specifically, more amorphous and more readily available/active forms of Al, Ca and Fe amendments demonstrated much better P retention than crystalline ones (McLaughlin et al., 1981).

Fe, Al and Ca compounds as soil/manure amendments to immobilize P are summarized in Table 3-5. Among Fe, Al, and Ca compounds studied by Moor and Miller (1994), calcitic and dolomitic limestone addition to poultry litter showed little effect on soluble reactive phosphorus (SRP) concentration. It was suggested that incubation time (1 week) was not enough for limestone to solubilize (around pH 7 to 8) and precipitate with phosphate while adsorption/chemisorptions of phosphate onto the calcitic or dolomitic limestone was inhibited by the high concentrations of soluble organic compounds such as fulvic and humic acids. SRP in poultry litter was moderately decreased by gypsum addition at the lowest application rate (around  $20 \text{ g Ca kg}^{-1}$ ), but increasing applications rate affect little on SRP reduction. This was because the lowest application rate of gypsum was high enough to exceed the solubility product of gypsum and adsorption of P by gypsum was not the dominant mechanism of P removal. Interestingly, alum or ferric Fe (as  $\text{Fe}_3(\text{SO}_4)_3 \cdot 2\text{H}_2\text{O}$  or  $\text{FeCl}_3$ ) addition decreased SRP significantly at the lower addition rates but the higher alum or ferric Fe addition rates ( $> \sim 35 \text{ g Al kg}^{-1}$ ,  $> \sim 70 \text{ g Fe kg}^{-1}$ ) increased SRP in litter without  $\text{CaCO}_3$  to buffer the pH. This was explained by the acidity created by the alum addition, which caused dissolution of inorganic Ca phosphates (highly soluble at this pH), acid hydrolysis of organic P, or dissolution of Al/Fe oxides and hydroxides, and therefore, resulted in P release. The pH of the litter treated by alum and Fe compounds at the highest rate was around 3.5 and 2, respectively, which are well below the optimum pH range for P removal by Al or Fe. Essentially, no SRP was detected in the litter with the alum as well as  $\text{CaCO}_3$  to buffer the pH (Moor and Miller, 1994). Ferrous compound (ferrous sulfate and chloride)

additions decreased SRP, significantly but  $\text{CaCO}_3$  addition did not significantly decrease SRP, suggesting that P removal by ferrous compounds is less pH dependent.

Shreve et al. (1995) evaluated alum and ferrous sulfate impact on P runoff from field-applied poultry litter and on total forage yield from the fields. They concluded that alum use as amendment to poultry litter shows considerable benefits for limiting P inputs to surface water bodies, while increasing forage yield and fertilizer value of litter. Alum and ferrous sulfate amendments also inhibit  $\text{NH}_3$  volatilization from the litter by lowering litter pH (which controls the  $\text{NH}_3/\text{NH}_4^+$  ratio) and, therefore, increased available N, which make treated litter more valuable as a fertilizer due to the high N/P ratio of litter). However, later study by Smith et al. (2000) showed no significant difference in fescue yields and N uptake by the fescue between plots fertilized with untreated swine manure only and swine manure amended with alum and aluminum chloride, although yields of plots fertilized with alum and aluminum chloride amended manure would be higher than the untreated manure as a result of reduced  $\text{NH}_3$  volatilization.

Cement kiln dust (a waste product rich in Ca and K oxides generated during production of cement), bauxite red mud (a waste product of the Al industry rich in Al and Fe oxides and Ca) and two drinking water treatment alum hydrosolids as amendments were evaluated by Peters and Basta (1996) to reduce excessive bioavailable P in soil. Two drinking water treatment alum hydrosolids showed greater soluble P reduction than bauxite red mud and cement kiln dust, which increased soil salinity in the amended soil at high rates.

Table 3-5. Phosphorus immobilizing amendments

Reference	Amendments	Amendments Type	*Application rate (g kg <sup>-1</sup> )	Target P
Moore and Miller (1994)	Al, Ca, Fe compounds: CaO, Ca(OH) <sub>2</sub> , CaCO <sub>3</sub> , CaMg(CO <sub>3</sub> ) <sub>2</sub> , CaSO <sub>4</sub> ·2H <sub>2</sub> O, Al <sub>2</sub> (SO <sub>4</sub> ) <sub>3</sub> ·18H <sub>2</sub> O, Na <sub>2</sub> AlSO <sub>4</sub> , Fe <sub>2</sub> (SO <sub>4</sub> ) <sub>3</sub> ·2H <sub>2</sub> O, FeCl <sub>3</sub> , FeSO <sub>4</sub> ·7H <sub>2</sub> O, FeCl <sub>2</sub> ·4H <sub>2</sub> O	Reagent Grade	30 - 500	Poultry litter
Shreve et al., (1995)	Alum (Al <sub>2</sub> (SO <sub>4</sub> ) <sub>3</sub> ·18H <sub>2</sub> O) Ferrous sulfate (FeSO <sub>4</sub> ·7H <sub>2</sub> O)	Reagent Grade	1:5 amendment/litter (w/w) ratio	Poultry litter
Peters and Basta (1996)	Drinking water treatment alum hydrosolids Cement kilin dust, Treated bauxite red mud	Waste from water treatment facility Waste from cement production Waste of Al industry	30 and 100	Soils amended with poultry litter or dairy manure
Dao (1999)	Alum Caliche Class C fly ash	Reagent grade Al <sub>2</sub> (SO <sub>4</sub> ) <sub>3</sub> ·18H <sub>2</sub> O Raw Ca minerals in calcic layers of soils Byproduct of the burning of coal	100, 250, 500	Stockpiled and composted cattle manure and manure treated soil
Codling et al., (2000)	Al-rich drinking water treatment residue Fe-rich residue	Waste from water treatment facility Byproduct of TiO <sub>2</sub> production	25-100 for litter 10-50 for soil	Poultry litter and litter amended soils
Dao et al., (2001)	Al-based drinking water treatment residuals Fe-rich titanium processing by product	Water treatment plants	590 200	Poultry manure
Smith et al., (2001)	Aluminum sulfate (Alum) Aluminum chloride	Reagent grade	215 and 430 mg Al per L manure	Swine manure
Elliott et al., (2002)	Aluminum sulfate coagulation residuals Ferric sulfate coagulation residuals Lime softening residual Fe <sub>2</sub> O <sub>3</sub> (Hematite)	Water treatment residuals Water treatment residuals Water treatment residuals Commercially available Fe <sub>2</sub> O <sub>3</sub>	0.1, 0.5, 1.0, 2.0, and 5.0 % by weight	Biosolids (digested activated sludge) Triple superphosphate (TSP)
Boruvka and Rechcigl (2003)	CaCO <sub>3</sub> Dolomite Gypsum CaCl <sub>2</sub>	Laboratory grade Commercially available dolomite to farmers Commercially available gypsum to farmers Laboratory grade	0.05 mmol Ca per 1g of soil: ~ 1t ha <sup>-1</sup> except gypsum (1.8t ha <sup>-1</sup> )	Soil (with added P) from Ap horizon of Immokalee fine sand on an intensive pasture of a cattle company
Dou et al., (2003)	Alum [ Al <sub>2</sub> (SO <sub>4</sub> ) <sub>3</sub> ·18H <sub>2</sub> O] Fluidized bed combustion fly ash Flue gas desulfurization byproduct Anthracite refuse fly ash	Technical grade Coal combustion power plant byproducts Coal combustion power plant byproducts Coal combustion power plant byproducts	25, 50, 100, 250 50, 100, 200, 400 50, 100, 150, 250 25, 50, 100, 250	Dairy Manure Swine manure Broiler litter
Torbert et al., (2005)	Gypsum (CaSO <sub>4</sub> ) Ferrous Sulfate (FeSO <sub>4</sub> ·7H <sub>2</sub> O) Lime (CaCO <sub>3</sub> )	Reagent grade	280 kg ha <sup>-1</sup> 400 kg ha <sup>-1</sup> 206 kg ha <sup>-1</sup>	Runoff from composted dairy manure applied sod

\* g kg<sup>-1</sup> unless stated



Among alum, caliche (a natural source of Ca found in calcic layer of soils in semiarid and arid regions), and class C fly ash (a byproduct of the burning of coal in electricity generation) amendments to stockpiled and composted cattle manures studied by Dao (1999), the fly ash decreased all extractable P (water soluble P, Bray-I P, Mehlich III-P) in the manures, while little Mehlich III-P was reduced by alum and caliche, probably due to redissolution of aluminum phosphates by the ammonium fluoride-strong acid solvent. The author concluded that application of nonhazardous municipal or industrial byproducts in manure as amendments can increase the N/P ratio in manure which is suitable for crop needs.

Two different drinking water treatment residues: Al-rich and Fe-rich drinking water treatment residues were evaluated by Codling et al. (2000) to decrease water soluble P and Bray and Kurtz no. 1-extractable P (BK1-P) in poultry litter and litter-amended soils. Fe rich drinking water treatment residues demonstrated more effective P reduction employing both water soluble P and BK1-P. Possible problems with early seeding establishment from the higher increases in soil electrical conductivity (EC) were suggested, caused by amendments of Fe-rich drinking water treatment residue.

Haustein et al. (2000) evaluated two Al-rich waste materials: water treatment residuals and HiClay alumina (a byproduct of commercial alum production process) to reduce dissolved P from high-P soil runoff, suggesting that P adsorption capacity for water treatment residuals was 20 times higher than HiClay alumina due to greater clay and Al (three times higher) content.

An aluminum water treatment residual and an iron-rich titanium processing byproduct were evaluated by Dao et al. (2001), investigating sequential extraction of

phosphorus in poultry manure. The results suggested that the Fe-rich byproduct reduced manure dissolved reactive phosphorus more effectively and enhanced the formation of NaOH-extractable P forms at the expense of  $\text{NH}_4\text{F}$ -extractable P than the Al-water treatment residual. Both byproducts increased the citrate-bicarbonate-dithionite extractable P fraction through composting, indicating the enhancement of P stabilization in treated manure.

The importance of reactive Fe- and Al- hydrous oxide contents were emphasized by Elliott et al. (2002) on evaluating P-fixing capacity of the sesquioxide-dominated materials (Al sulfate and ferric sulfate coagulation residuals, a lime softening residual, pure hematite) from soil amended with biosolids and triple superphosphate. Oxalate extraction (acid ammonium oxalate extraction) was suggested as an index for P-fixing capacity and amendment application rate of the Fe/Al materials as well as a risk indicator of soil-P loss (i.e., P saturation index:  $[\text{P}_{\text{ox}}]/[\text{Al}_{\text{ox}}+\text{Fe}_{\text{ox}}]$ ). Recent study by Dayton and Basta (2005) evaluated experimental conditions and method modifications of acid ammonium oxalate extraction of Al ( $\text{Al}_{\text{ox}}$ ) and Langmuir P adsorption maximum ( $\text{P}_{\text{max}}$ ) measurements in order to allow for comparisons to be made between WTR studies under standardized experimental conditions.

Phosphorus retention of an Ap horizon of a Spodosol with four different Ca compounds:  $\text{CaCO}_3$ , dolomite, gypsum, and  $\text{CaCl}_2$  was evaluated through batch P sorption experiments by Boruvka and Rechcigl (2003). All the amendments except  $\text{CaCl}_2$  increased P retention significantly compared with unamended soil.  $\text{CaCO}_3$  was more efficient in P retention than dolomite possibly due to the higher solubility of Mg phosphate than Ca phosphate, less Ca added, or different sorption site characteristics.

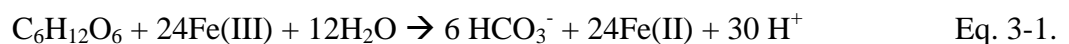
More efficient P retention was also observed by  $\text{CaCO}_3$  than by gypsum, because of the degree of pH increase. However, P sorption in gypsum-amended soil is faster than sorption in  $\text{CaCO}_3$ -amended soil, in terms of the kinetics. Little P retention by  $\text{CaCl}_2$  was explained by no adsorption sites by itself (due to application of soluble  $\text{CaCl}_2$  in solution form), no pH increase, and  $\text{Cl}^-$  ions which may compete with phosphate ions for sorption sites on soil particles. Therefore, the authors concluded that P retention in Ca-amended soil is mainly due to Ca ion addition, which must be accompanied by pH increase.

Tober et al. (2005) also used lime and gypsum as well as ferrous sulfate as soil amendments to reduce P loss from runoff in sod. The ferrous sulfate addition was very effective at reducing P from runoff, while lime and gypsum showed mediocre effectiveness.

Stabilizing P in manures (dairy, swine, and broiler) was studied by Dou et al. (2003) with alum and three different coal combustion byproducts (fluidized bed combustion fly ash, flue gas desulfurization byproduct, anthracite refuse fly ash). Flue gas desulfurization byproduct immobilized readily soluble P by 80% while fluidized bed combustion fly ash reduced it by 50-60% and anthracite refuse fly ash decreased P little. The results suggested that immobilizing readily soluble P is primarily related to inorganic phosphorus reduction with little change in organic P. The shift of manure P from water soluble P into a more stable fraction,  $\text{NaHCO}_3\text{-P}$ , by the combustion byproduct amendments was suggested by sequential extraction results while the alum amendment shifted the water soluble P into even more stable forms, mostly  $\text{NaOH-P}$ . However, the authors speculated that the shift of readily available P to more stable P would have little influenced on P availability for crops, while it would reduce P losses from manures.

### 3-3. Bacterial Fe/Mn reductive dissolution during anaerobic incubation

Bacterial reduction of Fe(III) and Mn (IV) oxides has been mostly studied to understand the biogeochemical cycles of carbon (Lovely and Phillips, 1986a, 1986b; Nealson and Myers, 1992), sulfur and trace metals (Brock and Gustafson, 1976; Bousserhine et al., 1999) as well as mobility of organic (e.g., petroleum in contaminated aquifer) (Lovely et al., 1996b) and inorganic contaminants (e.g., phosphate and heavy metals) (Francis et al., 1989; Francis and Dodge, 1990) in anaerobic aquifer/sediments and subsurface soils. Results by Lovely et al. (1991) indicated that enzymatic microbial reduction of Fe(III) is responsible for most of the Fe(III) reduction in aquatic sediments compared to nonenzymatic Fe(III) reduction, showing increase of HCl-extractable Fe(II) and CO<sub>2</sub> production by oxidation of organic compounds studied in Fe(III)-reducing aquifer sediments, but not in sterilized sediments. This dissimilatory microbial Fe(III) and Mn(IV) reduction can be defined as bacterial use of Fe(III) and Mn(IV) as an external electron acceptor in metabolism (Lovely, 2000). Fe(III) and Mn(IV) are reduced by a variety of fungi and bacteria to Fe(II) and Mn(II) as the end products under anaerobic condition. Microorganisms that primarily use fermentative metabolism were the first ones found to reduce Fe(III) and Mn(IV) while metabolizing fermentable sugars or amino acids, as shown by Eq 3-1. Sulfur-oxidizing, hydrogen-oxidizing, organic-acid-oxidizing (e.g., formate and lactate), aromatic-compound-oxidizing (e.g., benzoate, toluene, phenol, and p-cresol) Fe(III)/Mn(IV) reducers have been also identified and studied.



The prevalent model for organic matter metabolism by Fe and Mn reducing microorganism is well documented in two review papers by Lovely (1991, 2000) as shown in Figure 3-4.

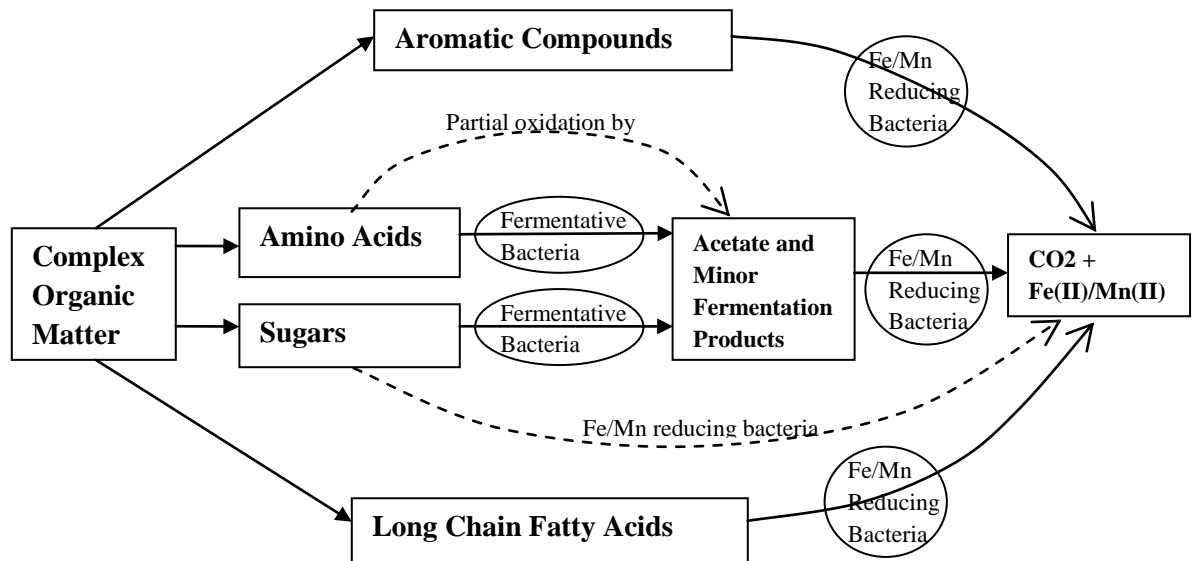


Figure 3-4. Model for organic matter degradation metabolism under an anoxic environment by Fe and Mn reducing microorganisms (adapted from Lovely, 1991 and 2000)

Microbial Fe/Mn reduction can cause the dissolution of Fe(III) and Mn(IV) oxides and minerals (Lovely, 2000). Possible bacterial reductive dissolution of crystalline/structural Fe oxides in aquifer sediments has been reported where the dominant forms of available Fe(III) for microbial reduction is crystalline Fe(III) oxides in anaerobic environments (Arnold et al., 1988; Kostaka and Nealson, 1995; Heron and Christensen, 1995; Roden and Zachara, 1996). Although bacterial reduction of crystalline Fe(III) oxides was found to be only a minor fraction of Fe(III) reduction in the aquifer sediments (Lovely and Phillips, 1986a, 1986b, 1987, 1988; Phillips et al, 1993), a study by Heron and

Christensen (1995) indicated substantial reductive dissolution of crystalline Fe(III) oxides in aquifer sediments polluted by landfill leachate. Also, laboratory studies by Roden and Zachara (1996) showed 8 to 18 % reduction of crystalline Fe(III) oxide content in various aquifer sediments after 30 days of incubation by a dissimilatory Fe(III) oxide-reducing bacterium (*Shewanella* strain BrY). These results indicate significant reduction of Fe(III) where the dominant forms of available Fe(III) for microbial reduction are crystalline Fe(III) oxides in anaerobic environments.

### **3-3-1. Factors for enhancing Fe(III) reductive dissolution**

The surface area of the crystalline oxide and the degree of Fe(II) surface phase absorbed or precipitated on Fe(III) oxides (and/or cells) have been suggested as factors controlling and limiting the rate and extent of microbial Fe(III) reductive dissolution (Roden and Zachara, 1996; Urrutia et al., 1998; Urrutia et al., 1999; Roden, 2003; Roden, 2004; Royer et al., 2004). Therefore, many recent studies have been focused on enhancing dissimilatory iron(III) reduction by three possible strategic mechanisms as described by Royer et al. (2002): eliminating the need for cell-oxide contact, alleviating Fe(II) inhibition, and making Fe(III) more bioavailable or bioreducible. The significant role of Fe(II) elimination by advective transport was suggested for enhancing the rate and extent of microbial dissimilatory Fe(III) oxide reduction (Roden and Urrutia, 1999; Roden et al., 2000; Royer et al., 2004). Specifically, the importance of well-mixed conditions for increasing diffusional flux (thermodynamic driving force) of Fe(II) to enhance Fe(III) reduction was noted in a recent study (Royer et al., 2004), demonstrating that higher mixing intensity increased hematite reduction. Therefore, mechanical mixing in typical manure

digester can enhance the synthesis of active amorphous Fe/Mn oxides from nonactive Fe/Mn materials.

Use of aqueous phase ligands/chelators such as NTA and EDTA (Arnold et al., 1988, Lovely et al., 1996a; Urrutia et al., 1999), methyliminodiacetic acid (Lovely et al., 1996b), ethanol diglycine (Lovely et al., 1996b), humic acids (Lovely et al., 1996b), natural organic matter (NOM) (Royer et al., 2002a, 2002b) phosphates (Lovely et al., 1996b), sodium acetate at pH 5 (Roden and Zachara, 1996), as well as solid phase materials (aluminum oxides and layer silicates) (Urrutia et al., 1999) have been also studied to enhance microbial reduction of crystalline iron(III) oxides by removing adsorbed or precipitated Fe(II) via forming Fe(II)-chelators/ligands complexes and binding Fe(II) on the solid materials, respectively. Specifically, stimulation of dissimilatory Fe(III) reduction by NOM (Royer et al., 2002a, 2002b) and humic substances (Lovely et al., 1996a) was achieved through two possible different mechanisms, initial electron shuttling between the humic/NOM-reducing microorganisms and Fe(III) oxides, and following Fe(II) complexation by alleviating the need for direct contact on Fe(III) oxides for Fe(III) reducing microorganisms and alleviating the inhibitory effect of Fe(II) accumulation.

### **3-4. Heavy metals and other water quality parameters, and heavy metal sources in storm water runoff**

Storm water runoff from various diffuse sources has been a major contributor to water pollution in the United States (Line et al., 1996). Over 90 percent of the assessed river pollution problems are associated with the various diffuse sources such as agricultural runoff, urban runoff, and mine drainage (Wu et al., 1998) and 64 percent of the lake pollution is caused by urban runoff (Voget, 1995). Therefore, characterizing stormwater runoff, indentifying diffuse sources and degree of pollution contribution are very important to address storm water runoff pollution.

Characterization of highway and urban stormwater runoff from previous literature data is summarized in Table 3-6. Various levels of heavy metals are noted in highway and urban runoff with typical levels of Zn, 20-500 µg/L; Cu and Pb, 5-200 µg/L; and Cd, <12 µg/L (Davis et al., 2001).

Specifically, heavy metal concentrations and other water pollutants leached by roof runoff, from previous literature is also summarized in Table 3-7a and 3-7b, due to their important contribution to urban runoff pollution. Gromaire et al. (1999) suggested that roof runoff contributed even greater amounts of trace elements than street runoff in their urban runoff characterization study. Boller (1997) reported average roof runoff metal concentrations of 90 µg/L Pb, 200 µg/L Cu, 400 µg/L Zn, and 0.6 µg/L Cd, based on his literature surveys. However, significantly different metal concentrations were observed from different roof material types (e.g., tile roof, polyester roof, and flat gravel roof) in various roof runoff studies (Tables 3-7a and 3-7b). Specifically, Zn was reported as the most important metal pollutant, which varies most significantly as affected by roofing materials, by Chang et al. (2004). In addition to roof material type,



roof catchment parameters (e.g., roof size, inclination, and exposure), precipitation events (e.g., precipitation intensity, duration and wind), local weather (e.g., season, antecedent dry periods), and chemical properties of pollutants were considered as factors that influence roof runoff water quality (Lye, 2009).

In the roof runoff infiltration study by Mason et al. (1999), mobility of heavy metals from roof runoff was investigated, demonstrating strong retention of Pb and Zn in the upper soil in the short term as opposed to the high mobility of Cu, Cd and Cr during infiltration due to their complexation by ligands in solution for Cu and Cu, and by dominant presence of Cr (VI) species for Cr. However, they also observed Zn and Pb mobility through the deeper soil layer of the unsaturated zone in the long term. Therefore, roof runoff can cause not only soil metal contamination, but also ground water contamination.

Pb, Cu, Cd, and Zn loadings from various urban sources were estimated by Davis et al. (2001) through controlled experimental runoff investigations as well as previous literature data (Table 3-8). The various diffuse urban sources in the study included siding, roofing, automobile brakes, tires and engine oils, and building siding for Pb, Cu, Zn, and Cd; vehicle brake emissions for Cu and tire wear for Zn were identified as important pollution sources.

Table 3-6. Water quality of urban, industrial site and roadway stormwater runoff

Reference	Wu et al. (1998) <sup>b</sup>	Barrett et al. (1998a) <sup>c</sup>	Barrett et al. (1998b) <sup>d</sup>	Barbosa & Hvitved-Jacobsen (1999) <sup>e</sup>	Kayhanian et al. (2007) <sup>f</sup>			Flint & Davis (2007) <sup>b</sup>	Gan et al., (2008) <sup>f</sup>		Legret & Pagotto (1999) <sup>f</sup>	Legret & Colandini (1999) <sup>b</sup>	Davis (2005) <sup>a</sup>		
Site location	North Carolina	Texas	Texas	North-east Portugal	California			Mound-Rainier, MD	Guangzhou China		Loire-Atlantique France	Loire-Atlantique France	-		
Runoff Type	Highway runoff	Highway runoff	Highway runoff	Highway runoff	Highway runoff			Highway runoff (Ultra Urban)	Highway runoff		Pavement Runoff	Pavement Runoff	Urban Stormwater Runoff		
					Non urban <sup>j</sup>	Urban Low <sup>k</sup>	Urban High <sup>j</sup>		Rural	Urban			Residential	Mixed	Commercial
	-	-	-	5.9-7.2	6.9	6.9	7.4	-	-	-	7.3	-			
<b>Metals</b>	µg/L														
Total Pb	<0.5 - 56	3-53	93, 138	<1 - 199.5	16.6 <sup>m</sup> , 3.2 <sup>n</sup>	23.5 <sup>m</sup> , 6.0 <sup>n</sup>	74.9 <sup>m</sup> , 12.4 <sup>n</sup>	15-1220	92.3	118.2	58	7.1 - 63.1	144	114	104
Total Cu	<0.5 - 51.5	7-37	-	<1 - 54.3	12.2 6.8	27.1 14.7	49.6 21.9	24-290	90	140	45	4.5 -44.1	33	27	29
Total Zn	-	24-222	129, 347	<50 - 1462	75.9 36.6	133.6 60.9	261.1 96.5	18-6030	700	1760	356	120 -226	135	154	226
Total Cr	<0.5 - 20.0	-	-	-	6.5 2.2	6.4 2.2	11.9 4.7	--	26.8	40.4	-	-	-	-	-
Total Cd	<0.5	-	-	-	0.4 -	0.6 0.2	0.9 0.3	13-93	1.5	1.6	1	0.33-2.93	-	-	-
Total As	-	-	-	-	2.0 -	2.7 0.7	2.6 1.3	-	-	-	-	-	-	-	-
Total Ni	-	-	-	-	11.3 4.6	7.8 3.7	13.0 6.0	-	13.4	22.6	-	-	-	-	-
	mg/L														
TDS	27 - 965	-	-	-	61.3	86.8	109.9	-	-	-	-	-	-	-	-
TSS	4-538	19 - 129	157, 190	<8 - 147	69.9	76.3	158.9	41-1600	111.1	415.7	71	5.0 - 86.1	101	67	69
BOD <sub>5</sub>	-	4 - 12	-	-	-	-	-	-	9	13	-	-	10	7.8	9.3
COD	4 - 177	37-130	94, 109	-	-	-	-	-	108	308	103	-	73	65	57
TP	0.04 - 1.54	0.10-0.33	0.24, 0.55	-	0.2	0.3	0.3	0.032-1.9	0.18	0.39	-	-	383	263	201
Soluble P	0.03 - 0.79 <sup>i</sup>	-	-	-	0.1 <sup>i</sup>	0.1 <sup>i</sup>	0.1 <sup>i</sup>	-	0.03 <sup>i</sup>	0.02 <sup>i</sup>	-	-	143	56	80
NO <sub>2</sub> <sup>-</sup> +NO <sub>3</sub> <sup>-</sup>	<0.01-13.37	0.37-1.07 <sup>g</sup>	0.91, 1.27 <sup>g</sup>	-	0.6 <sup>g</sup>	0.8 <sup>g</sup>	1.6 <sup>g</sup>	0.015-4.32	2.13 <sup>g</sup>	3.49 <sup>g</sup>	-	--	0.736	0.558	0.572
NH <sub>3</sub> -N	<0.01 - 1.74	-	-	-	-	-	-	-	-	-	-	-	-	-	-
TKN -N	0.26 - 2.45	-	2.17, 2.61	-	1.5	2.1	2.5	0.8-10	4.81 <sup>h</sup>	7.32 <sup>h</sup>	2.3	-	1.900	1.288	1.179

<sup>a</sup> Median event mean values cited from US.EPA (1999); <sup>b</sup> Range of EMC (Event Mean Concentration); <sup>c</sup> Range (three areas) of median EMC;

<sup>d</sup> Means of 34 events in two area; <sup>e</sup> Range of sample values (dissolved plus particulate values); <sup>f</sup> Means of EMC ; <sup>g</sup> Nitrate only;

<sup>h</sup> TN (Total Nitrogen.); <sup>i</sup> Orotho-P; <sup>j</sup> Annual average daily traffic (AADT) < 30,000 vehicles/day, <sup>k</sup> 30,300<AADT<100,000, <sup>l</sup> AADT>100,000; <sup>m</sup> Total, <sup>n</sup> dissolved;

Table 3-7a. Water quality of roof runoff (based on research monitoring)

Reference	Chang et al., (2004) <sup>f</sup>				Gromaire et al., (2001)	Athanasiadis et al. (2007)	Khan et al. (2006)	Boller (1997)			Mason et al. (1999) <sup>e</sup>		Schriewer et al. (2008)
Site location	Nacogdoches, TX				Paris, France	-	-	Duebendorf, Switzerland			Winterthur, Switzerland		Garching, Germany
Roof Type	Wood shingle	Composition Shingle	aluminum	Galvanized Iron	Eleven roofs with different materials of roof and gutters <sup>g</sup>	4 yr old copper roof	Copper arsenated treated wood	Tile roof	Polyester roof	Flat gravel roof	Gravel-covered flat roof (73%) Flat gravel roof with a humus layer (18%) Inclined plastic roof (9%)		14 yr old zinc roof
pH	5.07	6.69	6.20	6.59	-	7.1 <sup>a</sup> (6.6-8.0) <sup>b</sup>					First flush	After first	6.7 <sup>a</sup> (5.8-8.4) <sup>b</sup>
Heavy	µg/L												
Total Pb	45 <sup>a</sup> (25-700) <sup>b</sup>	38 <sup>a</sup> (25-203) <sup>b</sup>	37 <sup>a</sup> (25-134) <sup>b</sup>	49 <sup>a</sup> (25-255) <sup>b</sup>	392 <sup>c</sup> (76-2458) <sup>d</sup>		-	172	510	22	0.39 – 8.16	0.04 – 5.03	NA <DL – 31.0
Total Cu	29 (1-5410)	25 (1-126)	26 (1-248)	28 (1-224)	43 (14-240)	1623 <sup>a</sup> (200-21700) <sup>b</sup>	-	1950	6817	140	2.2 - 62.9	1.1 – 18.7	-
Total Zn	16,317 (39-109,700)	1372 (43-13,590)	3230 (514-16,600)	11,788 (124-)	2998 (582-12357)	-	-	360	2076	36	11.8 - 513	0.6 - 123	6,800 (300-30,000)
Total Cr	-	-	-	-	-	-	-				0.5 – 10.4	0.3 – 4.7	-
Total Cd	-	-	-	-	0.7 (0.2-4.5)	-	-	2.1	3.1	0.2	0.03-0.55	0.02 – 0.50	<DL –0.8
Total As	-	-	-	-		-	0.12-8400	-	-	-	-	-	-
	mg/L												
TSS	-	-	-	-	17 (6-74)	-	-	-	-	-	-	-	-
BOD <sub>5</sub>	-	-	-	-	4 (2-13)	-	-	-	-	-	-	-	-
COD	-	-	-	-	27 (12-73)	-	-	-	-	-	-	-	-
Ortho P	-	-	-	-	-	-	-	-	-	-	0.031-0.062	0.003-0.031	-
NO <sub>2</sub> <sup>-</sup> +NO <sub>3</sub> <sup>-</sup>	-	-	-	-	-	-	-	-	-	-	4.06 – 8.96 <sup>g</sup>	0.28-2.8 <sup>g</sup>	-
NH <sub>3</sub> -N	-	-	-	-	-	-	-	-	-	-	1.96-4.06	0.28-0.98	-
TKN -N	-	-	-	-	-	-	-	-	-	-	7.0-16.8 <sup>h</sup>	0.98 – 4.2 <sup>h</sup>	-

<sup>a</sup> Mean EMC; <sup>b</sup> Minimum – Maximum value; <sup>c</sup> Median EMC; <sup>d</sup> 10% EMC-90% EMC<sup>e</sup> roof covering materials: zinc sheet, slate, inter flat tiles a locking tiles, and roof gutters: zinc, copper, cast iron;<sup>f</sup> Based on runoff from 16 wooden structures with roofs (four commonly used materials) specially installed for the research; <sup>g</sup> Zinc sheet, slate, interlocking tiles, flat tiles for roof materials, and zinc, copper and cast irons for gutters.

Table 3-7b. Water quality of roof runoff (based on literature surveys)

Reference	Zimmermann et al. (2005); Gobel et al. (2007)					
Literature survey	Based on More than 300 citation providing about 1300 data					
Roof Type	Fiber cement, pantiles, concrete tiles and tar felt without Zn gutters	Fiber cement, pantiles, concrete tiles and tar felt with Zn gutters	Zinc sheets	Copper sheets	Aluminum sheets	Green roof
pH	5.7	5.7	5.7	5.7	5.7	7.5
EC $\mu\text{S}/\text{cm}$	141	141	141	141	141	71
Heavy Metals ( $\mu\text{g}/\text{L}$ )						
Total Lead	69 <sup>a</sup> (2-493) <sup>b</sup>	69 (11-493)	69 (4-302)	69 (2-493)	69	9 (2-76)
Total Copper	153 (6-3,416)	153 (34-2,733)	153 (11-950)	2,600 (2,200-2,600)	153	11 (1-355)
Total Zinc	370 (24-877)	1851 (280-4,880)	6000 (1731-43,674)	370 (24-877)	370	80 (5-235)
Total Cr	4	4	4	4	4	3
Total Cd	0.8	0.8	1.0	0.8	0.8	0.1
Total Ni	4	4	4	4	4	3
mg/L						
TSS	43	43	43	43	43	-
BOD <sub>5</sub>	12	12	12	12	12	-
COD	66	66	66	66	66	-
TP	0.22	0.22	0.22	0.22	0.22	-
NH <sub>3</sub>	3.39	3.39	3.39	3.39	3.39	1.30
NO <sub>3</sub> <sup>-</sup>	2.78	2.78	2.78	2.78	2.78	0.59
PAH	0.44	0.44	0.44	0.44	0.44	-
Cl <sup>-</sup>	7.74	7.74	7.74	7.74	7.74	-

<sup>a</sup> Mean EMC<sup>b</sup> Minimum – Maximum value

Table 3-8. Metal (Pb, Cu, Cd, and Zn) concentrations, loadings, and estimated contributions from various sources in urban runoff (adapted from Davis et al., 2001)

metals		Siding ( $\mu\text{g}/\text{m}^2$ )	Roofing ( $\mu\text{g}/\text{L}$ )			Automobile front brake area		Oil ( $\mu\text{g}/\text{L}$ - oil)	Tire	Wet Dep.	Dry Dep.	EMC* ( $\mu\text{g}/\text{L}$ )/
			Resid- ential	Com m- ercial	Institu- tional	Conc. ( $\mu\text{g}/\text{L}$ )	Estimated ( $\mu\text{g}/\text{km}$ - vehicle)					Total Loading (kg/ha-yr)
Pb	Range	<1-4500	-	-	-		3		-	-	-	7.7/  0.069
	Mean	270	1.5	62	64	11		1100	-	-	-	
	Median	50	2	12	64	7		400	-	-	-	
	Estimated % **	79%	1%			1%		<1%	1%	8%	10%	
Cu	Range	<1-320	-	-	-		75		-	-	-	4.2/  0.038
	Mean	51	7.5	200	5000	280		2100	-	-	-	
	Median	19	7	29	2100	26		1400	-	-	-	
	Estimated % **	22%	9%			47%		0.3%	0.6%	7%	14%	
Cd	Range	<0.1-15	-	-	-		0.5		-	-	-	0.2/  0.0012
	Mean	1.5	0.12	1.3	0.6	1.9		100	-	-	-	
	Median	0.4	0.1	0.7	0.4	0.2		20	-	-	-	
	Estimated % **	21%	5%			10%		0.4%	4%	41%	19%	
Zn	Range	24-23000	-	-	-		89		-	-	-	72/  0.646
	Mean	1900	100	1100	1100	330		$1.25\times 10^5$	-	-	-	
	Median	820	110	760	460	150		$1.6\times 10^5$	-	-	-	
	Estimated % **	58%	7%			3%		1%	25%	2%	3%	

\*Estimated Event mean concentration at 90 cm/yr total precipitation.

\*\* Estimated % contribution of various sources of metals in urban runoff.

### **3-4-1. Metal Corrosion**

As mentioned above in Table 3-8, the various diffuse urban metal sources, including siding, roofing, automobile brakes, tires and engine oils, building siding, vehicle brake emissions, and tire wear were studied by Davis et al. (2001) to investigate their contribution to urban runoff metal contamination. Specifically, corrosion of various metallic materials used as building construction components (e.g., building roofing and siding sheets) and automobile body and parts have been identified as one of the major processes releasing heavy metals to storm water runoff under various environmental conditions.

Therefore, understanding the corrosion process for important heavy metals in runoff is necessary to identify and evaluate heavy metal diffuse sources, and to address their environmental risks. Corrosion can be defined as the spontaneous deterioration caused by a flow of electricity for metal to another or to a recipient of some kind (i.e., anode and cathode) (Berger, 1984). An electrolyte, generally water (salt water), is needed for electron flow and various physicochemical environmental and metal characteristics and conditions including temperature, humidity, concentration of various species in the electrolyte, and pH are the parameters controlling the corrosion rate and intensity (Mattsson, 1984).

#### **3-4-1-1. Lead corrosion**

Lead was traditionally used in building and civil construction components such as roofing, siding, piping, sheet lining, and more recently used in batteries, radiation shields, and solders (Graedel, 1994). Atmospheric lead corrosion can be an environmental

concern due to its high toxicity through its release to the environment. Humidity is the major controlling parameter of Pb corrosion due to its significant role in producing a water layer on the surface of the metal, which can provide a medium for atmospheric gas deposition and the subsequent metal dissolution (Graedel, 1994).

Lead release to the environment by runoff depends on the Pb corrosion product solubility (the solubility of the Pb corrosion film on the metal surface through atmospheric corrosion). Litharge (PbO) has been identified as the first Pb corrosion product by atmospheric exposure (Graedel, 1994). Subsequently, hydrocerussite  $[\text{Pb}(\text{CO}_3)_2(\text{OH})_2]$ , anglesite ( $\text{PbSO}_4$ ), and cerussite ( $\text{PbCO}_3$ ) are the most common minerals detected on the metal surface corrosion film. Hydrocerussite, cotunnite ( $\text{PbCl}_2$ ), laurionite ( $\text{PbClOH}$ ), and a lead chloride carbonate  $[\text{Pb}_2\text{Cl}_2(\text{CO}_3)]$  can be detected in sea water environments. Table 3-9 presents characteristics of possible Pb corrosion products with their solubility product, suggesting that  $\text{SO}_2$ ,  $\text{CO}_2$ , and carboxylic acids are the primary atmospheric agents (precursor molecules) responsible for Pb degradation, forming corrosion products,  $\text{PbSO}_4$ ,  $\text{PbCO}_3$ , and  $\text{Pb}(\text{HCO}_2)_2$ .

As shown in Table 3-9, lead corrosion film study by Tranter (1976) suggested that lead oxide and lead hydroxyl carbonates were initially formed in the metal film. However, lead sulfate and lead sulfite, more soluble compounds, became dominant over 18 month exposure, suggesting lead is more readily solubilized in the runoff and are released to the environment with exposure time.

Table 3-11 presents lead corrosion rates in different environmental locations. Lead rate are greater than those for Cu and Al, but smaller than for Zn and steel (Graedel, 1994).

Table 3-9. Characteristics of possible corrosion products (adapted from Graedel, 1994).

Possible corrosion product	Precursor molecule	Precursor aqueous abundance	Corrosion product aqueous solubility ( $K_{sp}$ )	Relative detected abundance
PbO	O <sub>2</sub>	H	M ( $1.2 \times 10^{-15}$ )	M
PbS	H <sub>2</sub> S	L	VL ( $1 \times 10^{-28}$ )	ND
PbSO <sub>4</sub>	SO <sub>2</sub>	M	L ( $1.6 \times 10^{-8}$ )	M
PbCl <sub>2</sub>	HCl	L	M ( $1.5 \times 10^{-5}$ )	L
Pb(NO <sub>3</sub> ) <sub>2</sub>	NO <sub>2</sub>	L	H	ND
PbCO <sub>3</sub>	CO <sub>2</sub>	H	L ( $3.3 \times 10^{-14}$ )	M
Pb(HCO <sub>2</sub> ) <sub>2</sub>	HCOOH	M	H	M

Table 3-10. Composition of lead corrosion film in the urban environment (adapted from Matthes et. al., 2002, originally cited from Tranter, 1976)

compound	Percent composition (by weight) versus Exposure period			
	3 days	4 month	9 months	18 months
PbO	45	-	-	-
Pb <sub>x</sub> (OH) <sub>y</sub> (CO <sub>3</sub> ) <sub>z</sub>	45	-	-	-
PbCO <sub>3</sub>	tr	10	2	1
PbSO <sub>3</sub>	7	45	60	35
PbSO <sub>4</sub>	3	45	40	65



Table 3-11. Atmospheric corrosion rates for lead (adapted from Graedel, 1994).

Local	Corrosion rate ( $\mu\text{m}/\text{yr}$ )
Marine	0.1 to 2.2
Rural	0.4 to 1.9
Urban	0.5 to 0.7

### 3-4-1-2. Cu corrosion

Clean copper with no surface oxide shows salmon-pink color, but the color changes to brown and then black with further exposure and oxide growth. Cuprite ( $\text{Cu}_2\text{O}$ : +1 Cu oxidation state) causes these Cu color changes. Further atmospheric exposure and reaction leads to a green layer formation (green patina) on top of the cuprite oxide layer. Brochantite [ $\text{CuSO}_4 \cdot 3\text{Cu}(\text{OH})_2$ : the +2 oxidation state Cu] is the most common compound in the green layer with general atmospheric exposure. This is because the copper hydroxysulphate phases are much less soluble than chloride, carbonate and nitrate Cu compounds. Atacamite (or paratacamite) [ $\text{Cu}_2\text{Cl}(\text{OH})_3$ ] can be a major constituent in a Cu outer layer in marine exposure due to its high chloride level (FitzGerald et al., 2006). It is possible that trace amounts of Posnjakite [ $\text{Cu}_4\text{SO}_4(\text{OH})_6 \cdot 2\text{H}_2\text{O}$ ], a hydrated form of brochantite (only found in young Cu patinas) and antlerite [ $\text{CuSO}_4 \cdot 2\text{Cu}(\text{OH})_2$ ] can be detected in Cu patinas.

Based on a study by FitzGerald et al. (2005), decrease of Cu corrosion rate was observed with increasing atmospheric exposure time due to the protective nature of the cuprite layer. It is estimated that the steady state corrosion rate reaches  $0.18 \pm 0.08 \mu\text{m}$  Cu/yr after 70 years. An atmospheric Cu corrosion study at two different location also

found that copper corrosion rates decreases almost exponentially during the initial stages (Fonseca et al., 2003). They also suggested that the maritime atmospheric exposure resulted in a higher corrosion rate of  $70 \text{ g m}^{-2}\text{yr}^{-1}$  with generalized corrosion, compared to that of  $19 \text{ g m}^{-2}\text{yr}^{-1}$  with localized corrosion in the urban atmosphere for the identical period studied.

### **3-4-1-3. Zn corrosion**

Zn corrosion is particularly important due to its common use for galvanization (galvanized steel) to protect against steel corrosion. However, Zn can be easily corroded due to its negative standard redox potential ( $E^0 = -0.763 \text{ V}$ ) and lack of protective corrosion films in acidic environments (i.e., industrial areas). Zinc oxide (ZnO) or Zn hydroxide  $[\text{Zn}(\text{OH})_2]$  as the first corrosion products form first and various Zn compounds such as zinc hydroxycarbonate  $[\text{Zn}_5(\text{CO}_3)_2(\text{OH})_6]$  and hydroxychloride  $[\text{Zn}_5(\text{OH})_8\text{Cl}_2]$  form subsequently by reaction with surface contaminants, including carbonate, chloride, and sulfate ions originating from atmospheric gaseous species.

Specifically, in the presence of high carbon dioxide in humid air, zinc hydroxycarbonate  $[\text{Zn}_4\text{CO}_3(\text{OH})_6\cdot\text{H}_2\text{O}]$  and hydrozincite  $[\text{Zn}_5(\text{CO}_3)_2(\text{OH})_6]$  are the dominant corrosion products. Traces of  $\text{SO}_2$  lead to zinc hydroxycarbonate conversion to zinc hydroxysulfate  $[\text{Zn}_4\text{SO}_4(\text{OH})_6\cdot 4\text{H}_2\text{O}]$ .

Zn is released to environment by runoff through dissolution of the Zn corrosion products formed. Therefore, the Zn dissolution rate during the runoff depends on the solubility of the Zn corrosion products as well as the characteristics of the precipitation (e.g., pH, intensity, pollutants level, and frequency) (Veleva et al., 2009).

### 3-5. Surface chemistry and adsorption

The definition of adsorption is a surface process that results in the accumulation of a dissolved substance (an adsorbate) at the interface of a solid (the adsorbent).

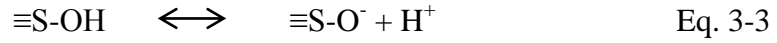
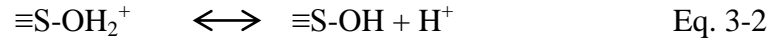
Surfaces of both mineral and organic soil particles have surface functional groups (charged or neutral), which are responsible for the retention of all ionic, nonionic, polar, nonpolar substances, controlled by types of mineral, functional group, R-group and specific surface areas.

#### 3-5-1. Inorganic mineral surfaces.

Charges on mineral surfaces can be classified by two basic types; permanent charges and pH dependent charges. Isomorphic substitution in the phyllosilicates generally causes the permanent net negative charge in minerals (e.g., isomorphic substitution of  $\text{Al}^{3+}$  for  $\text{Si}^{4+}$  in the tetrahedral layer or  $\text{Mg}^{2+}$  for  $\text{Al}^{3+}$  in the octahedral layer). However, net positive charge in a mineral is also possible by isomorphic substitution, such as  $\text{Fe}^{3+}$  substitution for  $\text{Mg}^{2+}$  in the octahedral layer. A pH dependent charge results from the protonation and deprotonation of surface hydroxyl groups ( $\equiv\text{SOH}$  groups on the surface), surface functional groups which can be commonly found on phyllosilicates, crystalline and amorphous metal oxides, hydroxides and oxyhydroxides as negative, positive, and neutral charges.

The protonation and deprotonation of inorganic surface functional groups can be expressed in a 2-pK approach as shown Eq. 3-2 and 3-3 as the surface dissociation reactions. Equilibrium constants of Eq. 3-2 and Eq. 3-3 are expressed as  $pK_{al}^{intb}$  and

$$pK_{a2}^{int}$$



The definition of the points of zero charge of a mineral surface is the pH values at which net surface charge is zero (Stumm and Morgan,1996). Points of zero charge of various minerals are shown in Table 3-7.

Table 3-12. Point of zero charge ( $\text{pH}_{\text{pzc}}$ ) and intrinsic surface acidity constants(  $pK_{al}^{\text{int}}$ ,  $pK_{a2}^{\text{int}}$ : equilibrium constants of Eq.3-2 and Eq. 3-3, respectively) for soil minerals (adapted from Essington, 2004).

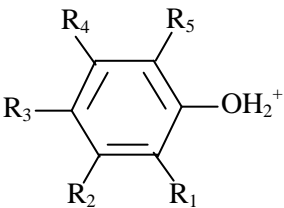
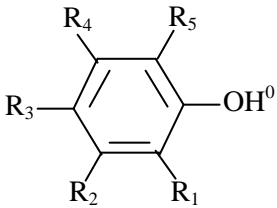
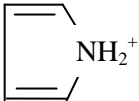
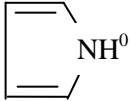
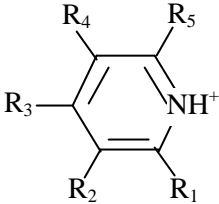
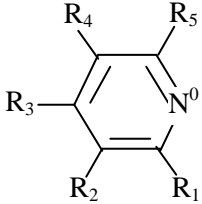
Mineral	$\text{pH}_{\text{pzc}}$	$pK_{al}^{\text{int}}$	$pK_{a2}^{\text{int}}$
Quartz [ $\alpha\text{-SiO}_2$ ]	2.9	-1.2	7.2
Amorphous Silica [ $\text{SiO}_2 \cdot 2\text{H}_2\text{O}$ ]	3.5	-0.7	7.7
Birnessite [ $\delta\text{-MnO}_2$ ]	3.76	0.16	7.36
Kaolinite [ $\text{Al}_2\text{SiO}_5(\text{OH}_4)$ ]	4.7		
Rutile [ $\text{TiO}_2$ ]	5.8	2.6	9.0
Anatase [ $\text{TiO}_2$ ]	6.0		
Magnetite [ $\text{Fe}_3\text{O}_4$ ]	6.9		
Muscovite [ $\text{KAl}_2(\text{Si}_3\text{Al})\text{O}_{10}(\text{OH})_2$ ]	7.5		
$\gamma$ -Alumina [ $\gamma\text{-Al}_2\text{O}_3$ ]	8.5		
Hematite [ $\alpha\text{-Fe}_2\text{O}_3$ ]	8.5	5.7	11.3
Gibbsite [ $\text{Al}(\text{OH})_3$ ]	8.9		
Corundum [ $\alpha\text{-Al}_2\text{O}_3$ ]	8.9	8.5	9.7
Goethite [ $\alpha\text{-FeOOH}$ ]	9.0	6.1	11.7

### **3-5-2. Organic surface functional groups and metal retention by organic surfaces.**

Various functional groups on organic matter compounds may cause the retention of cations or anions, based on solution pH. The important organic surface functional groups are shown in Table 3-8, which include the carboxyl, phenolic-OH, and carbonyl, amino, imide, sulfhydryl, and sulfonic groups (Essington, 2004). Their ionizing characteristics (i.e.,  $pK_a$ ) are related to not only to the functional groups themselves, but also the R-groups to which they are attached. Carboxyl and sulfonic groups are usually negatively charged in the soil pH ranges, and therefore, can retain cations, while amine, imide, phenolic-OH, and the sulfhydryl groups usually develops positive charge to retain anions. In spite of nonionization of carbonyl group, it may retain soluble species due to its polarization.

Humic substances in organic compounds in soil with a variety of functional groups can interact with metal ions in several ways, including ion exchange, complexation, adsorption and desorption, precipitation, and dissolution. This interaction between metal and organic compounds can affect the physical and chemical properties of metals including their oxidation state and chemical form, apparent solubility, phase distribution, and speciation, and thus influence free and labile metal concentrations, mobility and transport, immobilization and geoaccumulation, bioavailability and bioaccumulation, and toxicity to organisms in aqueous and soil environments (Chang Chien et al., 2006). Specifically, surfaces of solid phase humic substance, can retain metals in solution by adsorption.

Table 3-13. Common organic surface functional groups (adapted from Essington, 2004)

Functional group	Structure	
	Acid soil	Alkaline soil
Carboxyl	$\text{R}-\overset{\text{O}}{\parallel}{\text{C}}-\text{OH}$	$\text{R}-\overset{\text{O}}{\parallel}{\text{C}}-\text{O}^-$
Phenolic-OH		
Carbonyl	$\text{R}-\overset{\text{O}}{\parallel}{\text{C}}-\text{R}'$	$\text{R}-\overset{\text{O}}{\parallel}{\text{C}}-\text{R}'$
Sulfonic	$\text{R}-\overset{\text{O}}{\parallel}{\text{S}}(\text{O})-\text{O}^-$	$\text{R}-\overset{\text{O}}{\parallel}{\text{S}}(\text{O})-\text{O}^-$
Sulfhydryl	$\text{R}-\text{SH}_2^+$	$\text{R}-\text{SH}^0$
Amine	$\text{R}-\text{NH}_3^+$	$\text{R}-\text{NH}_2^0$
Imide		
Heterocyclic N		

### 3-5-3. Heavy metal (Pb) sorption mechanism

There are two different adsorption mechanisms called specific adsorption, and non-specific adsorption. Specific metal adsorption usually refers to chemisorbed inner-sphere complexes which are hardly reversible reactions. Non-specific adsorption is usually weak and less selective outer sphere complexes (Moreno et al., 2005). Another sorption mechanism is surface precipitation which mainly depends on pH and causes solid phase growth. Heavy metal can be also immobilized by forming less soluble precipitates through reaction with specific anions such as sulfide ( $S^{2-}$ ), phosphate ( $PO_4^{2-}$ ), carbonate ( $CO_3^{2-}$ ), sulfate ( $SO_4^{2-}$ ), and hydroxide ( $OH^-$ ) based on metal and anion species, concentration, and pH. Coprecipitation of heavy metals with iron or aluminum is also a possible metal retention mechanism specifically around neutral pH with relatively high heavy metal concentration in the presence of Fe/Al oxyhydroxides (Gibert et al., 2005; Martinez and McBride, 1998).

The pH of soil and water is a governing factor for adsorption and precipitation of heavy metals and, therefore, Pb in soil and water can be immobilized by pH increase (e.g., liming), which can enhance Pb retention. Specifically in soil, Pb can be immobilized through orthophosphate applications (through organic fertilizer application, hydroxyapatite  $Ca(PO_4)_3OH$ , monocalcium phosphate  $Ca(H_2PO_4)_2 \cdot 2H_2O$ , or  $Na_2HPO_4$ ) by forming the precipitation of low soluble lead phosphates, primarily pyromorphite  $[Pb_5(PO_4)_3X]$  (where X is OH [hydroxypyromorphite], Cl [chloropyromorphite], or F [fluoropyromorphite]) (Ryan et al., 2004; Ponizovsky and Tsadilas, 2003). It is also reported that lead adsorbed on goethite  $[Fe(OH)_3]$  and primary lead minerals (e.g.,

cerrusite [PbCO<sub>3</sub>], anglesite [PbSO<sub>4</sub>], litharge [PbO], massicot [PbO], and galena [PbS] was transformed to pyromorphite by apatite addition (Ryan et al., 2004).

Metal retention mechanism can be identified through analyzing other cation and anion concentration change, as well as metal concentration decrease through metal retention. For example, ion exchange, a Pb immobilization process, can be distinguished with Pb adsorption or Pb precipitation: (a) Pb retention through cation exchange caused the release of equal amount of cations displaced by Pb<sup>2+</sup>; while (b) Adsorption of Pb<sup>2+</sup> should not cause displacement of cations into solution or removal of anions from solution, but cause surface charge change on solid phase (i.e., soil particle).; and (c) precipitation of Pb<sup>2+</sup> cases equal amount of anion removal from solution and no cation is released by metal displacement (Ponizovsky, 2003).

#### **3-5-4. Competitive adsorption of heavy metals on soil components (on inorganic and organic materials).**

Possible metal properties affecting metal affinity sequences are shown in Table 3-10. Heavy metal affinity is generally reversely proportional to the unhydrated radii of each metal with following order: Pb<sup>2+</sup> (0.120 nm) > Cd<sup>2+</sup> (0.097 nm) > Zn<sup>2+</sup> (0.074 nm) > Cu<sup>2+</sup> (0.072 nm) > Ni (0.069 nm). Therefore, the Z<sup>2</sup>/r is proportion al to heavy metal affinity as shown in Table 3-10. It has been also noted that the metal affinity is strongly correlated to the first hydrolysis equilibrium constant, K<sub>1</sub> based on Equation 3-4 because the hydrolyzed metal ions (MOH<sup>+</sup>) adsorb more favorably than free divalent cations (M<sup>2+</sup>) (Veeresh et al., 2003; Elliot et al., 1986). The order of Log K<sub>a</sub> values for each heavy metals are : Pb (-6.2) > Cu (-8.0) > Zn (9.0) > Cd (-10.1). Based on the Irving and Williams series, order of the complex, the stability of the metal complexes with organic



ligands is Pb>Cu>Ni>Co>Zn>Cd>Fe>Mn>Mg (Essington, 2003). Based on competitive metal adsorption study by Veeresh et al (2003) using three soil type, poor agreement was noted between observed the observed metal affinity with the predicted metal affinity sequence based on ionic potential and metal softness.



Table 3-14. Metal properties affecting divalent metal affinity (Elliott et al., 1986; Veeresh et al., 2003)

Metal property	Metal affinity sequence
Ionic potential	Ni > Cu > Zn > Cd > Pb
$Z^2/r$	Ni > Cu > Zn > Cd > Pb
First hydrolysis constant ( $K_1$ )	Pb > Cu > Zn > Ni > Cd
Electro negativity	Cu > Ni > Pb > Cd > Zn
Softness	Pb > Cd > Cu > Ni > Zn

Soil constituents such as Fe and Al oxides, and organic matter are important constituents for adsorption, and, furthermore, their own metal sorbing properties can affect competitive adsorption of heavy metals on soils (Elliott et al., 1986). Elliot et al. summarized the relative affinity of heavy metals (Pb, Cu, Zn, and Cd) based on different soil constituents from previous studies as shown in Table 3-9.

Batch heavy metal adsorption study using garden waste compost by Seelsaen et al (2007) suggested that metal uptake affinity on compost in the order of  $Pb^{2+} > Cu^{2+} > Zn^{2+}$ , demonstrating 97, 93 and 88 % removal, respectively. Similarly, a batch metal adsorption study on mulch by Jang et al. (2005) also indicated that the order of both the

initial metal removal rate and metal sorption capacity on a molar basis is

$Pb^{2+} > Cu^{2+} > Zn^{2+}$ , which follows the Irving and Williams series, order of the stability of the metal complexes with organic ligands;  $Pb > Cu > Ni > Co > Zn > Cd > Fe > Mn > Mg$ .

However, stability constants of metal-humic acid complexes studied by Pandey et al (2000) demonstrated the order of  $Cu > Pb > Zn$ , which is consistent with our column study results.

Table 3-15. Heavy metal affinity series for soil components (adapted from Elliott et al., 1986).

Material	Relative affinity	Reference
Al oxides (amorphous)	$Cu > Pb > Zn > Cd$	Kinniburgh et al. (1976)
Goethite	$Cu > Pb > Zn > Cd$	Fobes et al. (1974)
Fe oxides (amorphous)	$Pb > Cu > Zn > Cd$	Kinniburgh et al (1976)
Mn oxides	$Cu > Zn$	Murray (1975)
Fulvic acid (pH 5.0)	$Cu > Pb > Zn$	Schnitzer and Skinner (1967); Schnitzer (1969)
Humic acid (pH 4-7)	$Zn > Cu > Pb$	Verloo and Cottenie (1972)
Humic acid (pH 4-6)	$Cu > Pb > Zn > Cd$	Stevenson (1977)

### 3-6. Organic and/or inorganic amendments to remove heavy metals from the aqueous phase.

Various organic waste/byproduct amendments have been evaluated and used in some research studies as sorbents for removing heavy metals from the aqueous phase, as presented in Table 3-9. A municipal compost and calcite mixture was evaluated in column experiments by Gibert et al. (2005) to remove metals from acid mine drainage. The results suggested that co-precipitation with Fe- and Al- (oxy)hydroxides (~60% of

Zn removal), and sorption onto the compost surface ( ~40% of Zn removal) are the major Zn removal mechanisms, whose hydroxide is not expected to precipitate at pH 6-7 before the saturation of compost sorption sites; precipitation as metal (oxy)hydroxides and carbonates is significant for Cu removal (Table 3-9).

Seelsaen et al. (2007) also evaluated use of garden-derived compost to remove dissolved heavy metals ( $\text{Cu}^{2+}$ ,  $\text{Pb}^{2+}$ ,  $\text{Zn}^{2+}$ ) via batch sorption study. The results suggested that  $\text{Pb}^{2+}$  showed the highest affinity on compost, followed by  $\text{Cu}^{2+}$  and  $\text{Zn}^{2+}$ , demonstrating 97% (uptake= 4.0 mg/g), 93% (3.2 mg/g) and 88% (3.2 mg/g) metal removal, respectively. Recent study by Kocasoy and Guvener (2009) also demonstrated compost as a promising sorbent for Cu, Zn, and Ni, but not for Cr.

Three types of mulch, cypress bark, hardwood bark, and pine bark nugget as sorbents were evaluated to remove heavy metals from urban runoff by Jang et al. (2005). The hardwood bark demonstrated the best performance with favorable physicochemical properties in heavy metal removal from runoff, demonstrating the greatest affinity for Pb followed by Cu and Zn. Aqueous Cu removal by adsorption on maple sawdust was studied by Yu et al. (2000). Ion exchange was suggested as one of the major adsorption mechanisms for binding heavy metal ions on the sawdust, which contained phenolic functional groups on its lignin, tannins or other phenolic compounds.

Heavy metal sorption on sewage sludge and paper mill waste (PMW) with/without composting was investigated. Sewage sludge demonstrated the most effective heavy metal sorption capacity (upto 39.3 mg/g). Composting the PMW increased the metal sorption capacity, demonstrating potential as low cost sorbents for metal removal.

Two types of zeolites, synthetic P-type zeolite with maximum aluminum content (MAP) and natural mordenite, were evaluated through batch experiments to test their heavy metal retention ability from simulated and spiked motorway stormwater (Pitcher et al., 2004). Synthetic zeolite MAP demonstrated better heavy metal removal (> 91%) than natural mordenite (42-89% removal for synthetic solution, 6-44% for motorway stormwater) although synthetic MAP increased sodium concentration (up to 295 mg/L), removed calcium and increased the solution pH to 8.5. Bentonite-sand liners were evaluated by Kaoser et al. (2005), suggesting that Pb was most retained by bentonite, followed by Cu and Cd.

As presented in Table 6-9, two sorption iso-therm equilibrium models, the Langmuir and the Freundlich isotherm equations have been widely used to describe iso-therm sorption of a solute in solution as described in Equation 3-4 and 3-5 (Bradl, 2004).

$$q_e = q_m \left( \frac{K_a C_e}{1 + K_a C_e} \right) \quad \text{Eq. 3-4.}$$

Where,  $q_e$  is the equilibrium sorption capacity (mg/kg);  $C_e$  is the equilibrium liquid phase concentration; and  $q_m$  is the  $q_e$  for a complete monolayer (mg/kg) and  $K_a$  the sorption equilibrium constant (L/mg).

$$q_e = K_F C_e^{1/n} \quad \text{Eq. 3-5.}$$

Where,  $q_e$  is the equilibrium sorption capacity (mg/kg);  $C_e$  the equilibrium liquid phase concentration; and  $K_F$  and  $1/n$  are empirical constants.

### **3-7. Organic and/or inorganic amendments to remove heavy metals from soil.**

Recent studies have demonstrated that heavy metal stabilizing techniques using byproduct/waste amendments in soils are promising, with simple and inexpensive advantages. Green waste compost and sewage sludge compost were evaluated by Herwijnen et al. (2007a) as amendments to immobilize heavy metals (Zn, Cd) from heavy metal contaminated soil via batch and column leaching studies (Table 3-10). Only green waste compost reduced the leachate concentration from 0.15 to 0.07 mg/L for Cd, and from 4.7 to 2.3 mg/L for Zn, while the use of sewage sludge compost increased Zn leachate concentration significantly, to 9.4 mg/L, indicating that the effect of compost amendment depends on the type of compost, the soil type, and related contamination levels. Interestingly, another similar study by Herwijnen et al. (2007b) showed similar results demonstrating doubled leachate Zn concentration with composted sewage sludge. However, plant concentrations of Cd, Cu, Pb or Zn from the same soil amended with composted sewage sludge was reduced by up to 80%. This suggests that the formation of complexes between the metals and organic matter governs the metal immobilization and bioavailability.

Li et al (2000) evaluated different amendments (NPK fertilizer, Limestone + NPK fertilizer, or composted iron-rich limed biosolids) on Zn phytotoxic soils for revegetation treatments. Biosolids compost showed effective remediation of Zn phytotoxicity showing that soluble Zn and Cd were reduced strongly and remarkable exclusion of Zn and Cd in vegetation. They suggested that the combination of calcareous soil pH and higher organic matter, Fe, and phosphate levels of biosolids-compost amended plots improved the overall success of vegetation establishment.

The approach used at the Palmerton superfund site in Pennsylvania (see Table 3-10) was to use fly ash, municipal sludge, limestone, and potash to create a synthetic soil that addressed all the soil problems, couples with an innovative application technique for steep slopes (Oyler, 1993). A combination of sewage sludge and fly ash were used due to two primary reasons: (a) in order to improve handling characteristics (i.e., sludge at 15 to 20% solids can be quite sloppy when used alone, and fly ash can be prone to dust generation); (2) in order to lighten the dark-colored sludge and the fly ash to be beneficial for use in an unincorporated setting as it would help lighten, thereby helping to prevent excessive temperatures from developing at or near the surface of the applied material. It was additionally postulated that the soil sized particles in the ash would help keep the sludge from crusting on the surface, and increase the overall porosity, infiltration, and percolation rates of the mixture.

Henry and Brown (1997) also evaluated biosolids mixed with a 1:1 blend of wood ash to restore zinc and lead contaminated soils at the Bunker Hill Superfund site. Their goal was to reestablish plant communities that will persist through the long term by providing alkalinity from the ash which protects against pH decline.

Table 3-16. Heavy metal removal from aqueous phase using organic and/or inorganic wastes/byproducts.

Reference	Organic amendments	Inorganic amendments	Target source and target metals	Type of study	pH	Model	Model constants
Gibert et al., (2005)	Municipal compost	calcite	Acid mine drainage/ Fe, Al, Zn, Cu	Column study >0.1 m d <sup>-1</sup> Batch study	Inf=3.0 Eff= ~6-7	Langmuir	$\Gamma_{\max}(\text{mg g}^{-1}) = 3.2$ for Zn, 12.1 for Cu $b(\text{L mg}^{-1}) = 0.024$ for Zn, 0.005 for Cu
McCauley et al., (2009)	Bark, Post Peel, Compost	Limestone, Mussel shells	Heavy metals from acid mine drainage	Bioreactor (continuous)	Inf = 4.5	-	-
Yu et al., (2000)	Sawdust	-	Aqueous solution/ Cu	Batch	Initial = 5	Frendlich	$K = 0.956 \text{ mg/g}$ $1/n = 0.601$
Jang et al., (2005)	Mulches Cypress bark Hardwood bark Pine bark nugget	-	Urban runoff/ Cu, Pb, Zn	Batch	Initial =5, 6	Langmuir	0.324 and 0.359 mmol/g for Cu 0.306 and 0.35 mmol/g for Pb 0.185 nad 0.187 mmol/g for Zn pH 5 and 6, respectively
Seelsaen et al., (2007)	Garden derived compost	-	Cu, Zn, Pb from wastewater or treating water for industries	Batch		Frendlich	$K = 0.56 - 1.24$ $1/n = 0.79 - 0.98$
Kocasoy and Guvener (2009)	Compost	-	Cu, Zn, Ni, Cr in industrial wastewater	Batch	Initial = 4.81 for Cu, 5.90 for Zn & 6.65 for Ni	-	-
Lister and Line	Sewage sludge Paper mill waste (PMV)	-	Cd, Cu, Pb and Zn ions from aqueous solution	Batch	-	-	39.3 mg Pb/g for sewage sludge 13.8 mg Cd/g, 19.3 mg Cu/g, 10.9 mg Zn/g 5.5 mg Cu/g for PMV 7.5 mg Cu/g fof composte PMV
Quek et al. (1998)	Sago waste	-	Heavy metals (Pb and Cu) from industrial waste water	Batch	2-5.5	Langmuir  Frendlich	$X_m(\text{mg/g}) = 46.64$ Pb, 12.42 for Cu $K(\text{L/mg}) = 0.246$ for Pb, 12.42 for Cu  $K_f(\text{mg/g}) = 16.84$ for pb, 4.22 for Cu $1/n = 0.235$ for Pb, 0.185 for Cu
Pitcher et al. (2004)	-	Zeolites; (synthetic MAP & natural mordenite)	Heavy metals (Zn, Cu, Pb, Cd) from Motorway strmwater	Batch	Initial = 3.2 for synthetic =7.1 for stormwater	-	-
Kaoser et al (2005)	-	5 % Bentonite & 95 % sand	Heavy metals (Cu, Pb, Cd)	Column study (continuous)			

\* g kg<sup>-1</sup> unless stated

Table 3-17. Heavy metal removal from soil using organic and/or inorganic wastes/byproducts.

Reference	Organic amendments	Inorganic amendments	Target source/ Target metals	Type of study	Amendment mixing ratio
Herxijnen et al. (2007a and 2007b)	Compost derived from green waste and sewage sludge	Clinoptilolite Bentonite	A silty-clay soil heavily contaminated with a range of heavy metals (Zn ,Cd) from Britannia Zinc, former zinc smelter near Avonmouth (since 1928)	Lab study: batch and column leaching study	4:1 soil:compost dry weight
Sauve et al. (2000)	Leaf compost	Pedogenic oxides Ferrihydrite	Free Pb <sup>2+</sup> in contaminated soils	Lab study	-
Brunori et al. (2005)	Compost	Red mud (byproduct of alumina production)	Heavy metal contaminated soil collected in the area of a mine dump (70 km north west of Rome, Italy)	Lab study: leaching batch test	4:1 soil: red mud 4:1 soil: compost 8:1:1 soil: red mud:compost
Li et al. (2000)	Composted iron-rich limed biosolids	- NPK fertilizer - Limestone + NPK fertilizer	~ 15000 mg/kg Zn and 158 mg.kg Cd From former zinc smelter in Palmerton, PA	Lab study	-
Oyler (1993)	Biosolids	fly ash with limestone and potash	As high as 30000 mg Zn/kg, 6500 Pb/kg, 1800 mg/kg Cd From former zinc smelter in Palmerton, PA	Field study	-
Henry and Brown (1997)	Biosolids + Wood fly ash (1:1)	Wood fly ash	1400 mg Zn/kg 10000 mg Zn/kg Mining and smelting of Zn, Bunker Hill, ID	Field study	-



## CHAPTER 4. IMMOBILIZATION OF PHOSPHORUS USING Fe/Mn INORGANIC MATERIALS AND AN ANAEROBIC INCUBATION PROCESS.

### 4-1. Introduction

Land application of manure and biosolids is limited in many areas by environmental concerns from soluble phosphorus (P) species, which can cause eutrophication of freshwater by agricultural runoff and leachate (Carpenter et al., 1998; Correll, 1998; Daniel et al., 1998). Only approximately 30% of P input to farming systems has been estimated as output in crops and animal produce, and this excessive land application of manure phosphorus (often to meet crop requirements for nitrogen) can lead to high accumulations of P in soil and increased P loss to water bodies and ground water through surface runoff and leaching (Sharpley et al., 1994; 2003).

P mobilization from manure land application has become of great concern in the state of Maryland because Atlantic Coastal Plain soils (coarse textured with low clay and sesquioxides content) are predominant and recent P inputs to the Chesapeake Bay watershed have increased significantly (Boynton et al., 1995; Novak et al., 2000). Furthermore, diffuse sources contribute approximately 60% of total P input to Chesapeake Bay water systems and agricultural runoff has been identified as the top contributor of P (approximately 49% of the total P input) among point and non-point sources (Boynton et al., 1995; Boesch, 2001).

Therefore, the control and reduction of P mobilization by agricultural surface runoff/leaching from manure land application can significantly minimize environmental concerns of P. High concentrations or addition of Fe, Al, and Ca in soils/manure have

been reported as important constituents for immobilizing phosphorus via adsorption and/or precipitation mechanisms (McLaughlin et al., 1981; Kalbasi and Karthikeyan, 2004; Torbert et al., 2005). Therefore, various types and forms of Fe, Al and Ca amendments have been widely used to immobilize phosphorus in soils, manures and biosolids. These include reagent or commercial grade Fe, Al, and Ca salts (e.g., alum, lime, limestone, ferric chloride and others) (Moore and Miller, 1994; Smith et al., 2001; Boruvka and Rechcigl, 2003) or industrial by-products/wastes (e.g., gypsum, and fly ash) (Dao, 1999; Peacock and Rimmer, 2000; Dou et al., 2003), and municipal water treatment residues with high Al, Ca and Fe contents (Peters and Basta, 1996; Codling et al., 2000; Haustein et al., 2000; Dao et al., 2001; Elliott et al., 2002; Makris et al., 2004; Novak and Watts, 2004). Recently, beneficial uses of by-products/waste materials containing high Fe, Al, and Ca from industrial/municipal activities have been studied due to their cost-effective and environmental advantages, reusing the by-products/wastes in order to immobilize P from manure and soil (Codling et al., 2000; Peacock and Rimmer, 2000; Elliott et al., 2002; Dayton and Basta, 2005). Specifically, more amorphous and more readily available/active forms of Al, Ca and Fe amendments demonstrated much better P retention than crystalline ones (McLaughlin et al., 1981).

Although addition of Fe oxides alone to manure or compost may be a useful method to reduce phosphate solubility, it may also induce Mn deficiency if the amended product is applied to low Mn Coastal Plain soils. Such soils are depleted of Fe and Mn during genesis, and liming or addition of Fe rich materials can reduce Mn phytoavailability and reduce yields of crops sensitive to Mn deficiency such as soybeans

and wheat. Addition of Mn with the Fe amendment can prevent this Fe-induced Mn deficiency and generally improve fertility of such soils (Brown et al., 1997a).

In spite of the importance of these topics, no study has focused on developing simple processes to increase the active amorphous Fe and/or Mn content of inexpensive byproducts in manure and biosolids from less-active crystalline Fe/Mn additives to immobilize P, which is therefore the overall goal of this study. Dissolution of crystalline Fe/Mn can be achieved chemically and/or biologically under anaerobic conditions; enzymatic microbial reduction has been reported as the process being responsible for most of the Fe(III) reduction in aquatic sediments compared to nonenzymatic chemical Fe(III) reduction (Lovely 1991; Lovely et al., 1991). Exploiting this bacterial Fe/Mn reductive dissolution, the anaerobic incubation process has been examined in this research for increasing active amorphous Fe/Mn oxides contents to immobilize phosphorus in manure.

Therefore, it is hypothesized that crystalline Fe(III)/Mn(IV) amendments in manure will dissolve as Fe(II)/Mn(II) species mainly by bacterial reductive dissolution during anaerobic incubation and the resulting dissolved Fe(II)/Mn(II) species can be subsequently oxidized to Fe(III)/Mn(IV) by oxygen under aerobic conditions. This simple procedure will produce high surface area, active, amorphous Fe/Mn oxyhydroxides and these freshly precipitated species will have high sorption capacities for phosphorus and be more available for plant Mn uptake.

In addition, both beneficial advantages and environmentally safe application of the amendments must be considered because the by-product/waste materials may also contain trace amounts of toxic compounds (Proctor et al., 2000). Extractability and

phytoavailability of trace metals in both manure and by-product amendments can be altered after mixing and incubation, and available heavy metals can be leached to the environment or taken up by vegetation after land application, possibly causing adverse effects on human health.

Three specific objectives in this research were: (1) evaluating P immobilization by three different low cost Fe/Mn materials: iron ore, steel slag, and Mn ore-waste tailings as amendments for dairy manure; (2) evaluating the effectiveness of the anaerobic incubation process in increasing the amount of oxalate Fe (considered as amorphous Fe) of the Fe/Mn materials; (3) evaluating environmental concerns of heavy metal release from the mixtures of manure and Fe/Mn materials by investigating the change of heavy metal extractability after the anaerobic incubation.

## **4-2. Methods and Materials**

Experimental materials and methods have been designed and prepared based on objectives of each research phase as described above

### **4-2-1. Characterization and preparation of Low cost Fe and Mn materials.**

Three different low cost Fe/Mn materials, iron ore (IO), waste steel slag (SS), and Mn waste tailings (MT) were evaluated as manure amendments (Figure 4-1). Industrial grade IO and waste SS were both obtained from a local steel manufacturer (Baltimore, MD). MT were obtained from a local company that processes Mn ore into various Mn chemical products. These Fe and Mn materials were air dried, sieved to <0.5 mm and the passed fraction was used as amendments. Fresh dairy manure was obtained from the U.S. Agricultural Research Facility, Beltsville, MD. The manure was well mixed in one large

container to increase homogeneity. The mixed dairy manure was sampled, air dried, ground to <2 mm using a stainless steel grinder, and stored in plastic bags.



Figure 4-1. Fe/Mn waste materials sieved to <0.5 mm (a) Iron ore, (b) Steel slag, (c) Mn tailings

The pH of Fe/Mn material was measured in 1:2 ratios (materials to deionized water, mass to volume) using a pH meter with a glass electrode (Mettler Toledo MA235 pH analyzer with pH probe Inlab 413, Columbus, OH) after 30 minutes (**McLean**, 1982). Electrical conductivity (EC) was determined using a YSI model 35 conductivity meter (Yellow Springs, OH) in 1:2 ratios by stirring samples vigorously and letting stand for 30 minutes. Manure pH and EC were measured in 1:6 ratios (dry manure to deionized water, mass to volume) as described above.

Water extractable phosphorus (WEP) for manure was determined according to the procedure of Sparks (1996) in which 2 g of sample in 20 mL of deionized water was shaken at 200 rpm on a platform oscillating shaker for 1 hr and subsequently filtered through Whatman no. 42 filter paper. Although recent studies more often use either 1:100 or 1:200 manure-to-water ratio for WEP rather than 1:10, the 1:10 ratio was used here for consistency with the WEP of manure+amendments mixtures, from which much lower P extractability was expected than from manure only.

As an agricultural soil P test in Maryland and other states, Mehlich III P (M3P) was determined according to the procedure of Wolf and Beegle (1995) in which 2 g of soil in 20 mL of Mehlich III extracting solution ( $0.2 \text{ N CH}_3\text{COOH} + 0.25 \text{ N NH}_4\text{NO}_3 + 0.015 \text{ N NH}_4\text{F} + 0.013 \text{ N HNO}_3 + 0.001 \text{ M EDTA}$ ) were shaken at 200 rpm on a platform oscillating shaker for 15 minutes and filtered through Whatman no. 42 filter paper.

Phosphorus concentration was determined using a modified ascorbic acid method by measuring absorbance of color developed via a Shimadzu (Kyoto, Japan) UV-120 spectrophotometer at a wavelength of 882 nm (Sparks, 1996). Total element content in Fe/Mn materials and manure was determined by aqua regia digestion (McGrath and Cunliffe, 1985), along with proper standard soils as controls. Chemically active amorphous forms of Fe and Mn oxides in Fe/Mn materials and manure were determined via acid ammonium oxalate extraction in darkness by shaking 500 mg of dry manure in 30 mL of  $0.175 \text{ M (NH}_4)_2\text{C}_2\text{O}_4 + 0.1 \text{ M H}_2\text{C}_2\text{O}_4$  solution (pH 3.0) for 2 h and centrifuging the extracted samples (Loeppert and Inskeep, 1996).

Heavy metal (Cu and Zn) extractability in Fe/Mn materials and manure was also evaluated. Firstly, the concentration of phytoavailable metals was determined by shaking 2 g of sample in 40 mL of  $0.01 \text{ M Sr(NO}_3)_2$  extracting solution for 1 hr (Madden, 1988). The extracted solution was filtered using Ahlstrom #513 fluted filter paper inside of a #40 Whatman filter paper, and a portion of the unfiltered slurry was used to measure pH of the mixture. Secondly, Cu and Zn in Fe/Mn materials and manure were also analyzed by acid ammonium oxalate extraction as described above to evaluate the extractability of heavy metals in manure. The filtered/centrifuged samples after the metal extractions were analyzed for metals using flame atomic absorption spectrophotometry.

#### **4-2-2. Fe/Mn material applications to manure and characterization of the Fe/Mn materials + manure mixture during anaerobic incubation**

Fe/Mn materials were added to fresh dairy manure and well mixed to produce approximately 50 g Fe kg<sup>-1</sup> (for IO and SS) or 10 g Mn kg<sup>-1</sup> (for MT) dry weight, based on Fe and Mn content information provided by the suppliers (data not shown), assuming that Fe and Mn contents in the raw manure are negligible compared to those in Fe/Mn materials. Actual Fe and Mn contents for the manure-amendment mixtures were later determined via aqua regia digestion and showed values of 46.5 g Fe kg<sup>-1</sup> for iron ore, 43.0 g Fe kg<sup>-1</sup> for steel slag, and 18.8 g Mn kg<sup>-1</sup> for Mn tailings. After mixing 6.0 kg of each manure mixture was immediately transferred to 7.6 L airtight containers with a gas outlet (Figure 4-2). A portion of each mixture was sampled, air-dried and ground <2 mm using a stainless steel grinder.

The containers were sealed air-tight and the gas outlet tube was filled with deionized water to maintain anaerobic conditions in the container and to release gas produced in the containers during the incubation. In total, ten containers for each mixture (IO + manure, SS + manure, and MT + manure) and five containers for control (manure only) were established. Two containers for each mixture and one control container (manure only) were sacrificed at days 3, 10, 33, 68 and 127. The contents in the containers for each mixture were mixed well before sampling. Samples were air dried at room temperature allowing for aerobic exposure of the mixture during the slow drying, ground <2 mm using a stainless steel grinder, and stored in plastic bags for later analyses. The room temperature throughout the incubation was kept at 26-27 °C during days 0 to 30 and 72 to 128, and 17-19 °C during days 30 to 72.

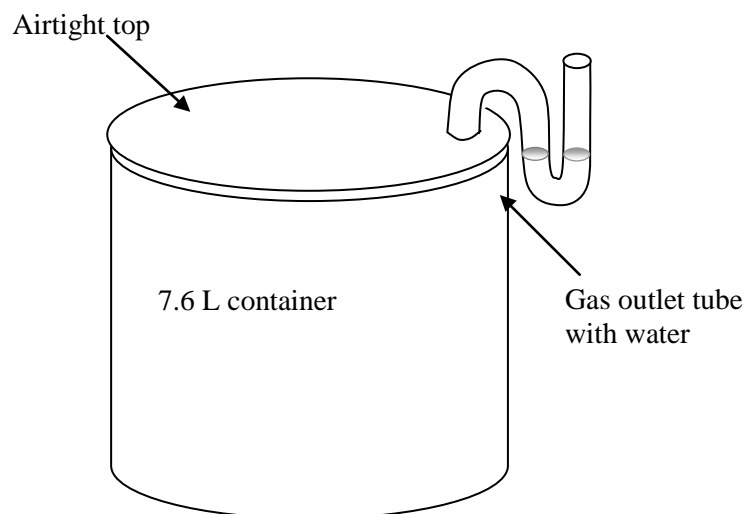


Figure 4-2. Basic anaerobic incubation container design to convert waste Fe and Mn additives to highly-active amorphous Fe/Mn materials.

Reduction potential during the anaerobic incubation was determined by measuring Eh using an Orion (Beverly, MA) model 96-78-00 Platinum redox electrode and a Mettler Toledo (Columbus, OH) model Pt 4805-DPAS-SC redox electrode with an Orion (Boston, MA) model 520A meter. The Eh was measured by sticking a redox electrode directly into the mixture through the gas outlet right before sacrificing the containers. The pH of mixtures was measured with fresh wet samples, and later, dry samples of the mixtures, representing anaerobic incubation and aerobic exposure, respectively. The pH of the fresh wet samples was measured immediately in 1:1 mixtures (wet sample to deionized water, mass to volume) as soon as the container was sacrificed. The dry sample pH and EC were determined in 1:6 suspensions as described above. WEP, M3P, and heavy metal (Cu and Zn) extractability of Fe/Mn materials/manure mixtures were measured as described above.



### **4-3. Results and Discussion**

#### **4-3-1. Evaluation of Fe/Mn materials as amendments in manure before digestion.**

Raw Fe/Mn materials as amendments to immobilize phosphorus in manure were evaluated by comparing chemical properties and characteristics of the manure and the Fe/Mn materials + manure mixtures before anaerobic incubation (Tables 4-1 and 4-2). No significant pH change resulted in the manures with IO and MT additions compared to the control (Table 4-2). However, the SS + manure demonstrated a significant increase of pH due to its high CaO content. Slight increase of EC was only observed for MT + manure ( $9.3 \text{ mS cm}^{-1}$ ) compared to the control ( $8.7 \text{ mS cm}^{-1}$ ) due to the higher EC value of MT ( $12.2 \text{ mS cm}^{-1}$ ) (Tables 4-1 and 4-2). Increased soil EC by land application of MT + manure may cause plant growth problems with early seeding establishments (Codling et al., 2000).

WEP for SS + manure was significantly decreased compared to the control, showing 93% reduction of WEP, while MT + manure demonstrated 28% WEP reduction (Table 4-2). Essentially, no change of WEP for IO + manure was observed compared to the control. The greatest reduction in M3P was also observed for SS + manure, showing 80% M3P reduction compared with control (Table 4-2). The great reduction of WEP and M3P of SS + manure can be explained by the high Fe and Ca contents, which can immobilize P in manure by adsorption and precipitation. Specifically, a high oxalate extractable Fe content in SS may play an important role in immobilizing P in manure, considering that little WEP and M3P was reduced for IO + manure, which contains slightly higher total Fe content ( $46.5 \text{ g kg}^{-1}$ ) than SS + manure ( $43.0 \text{ g kg}^{-1}$ ), but much lower oxalate extractable Fe ( $1.25 \text{ vis-à-vis } 17.6 \text{ g kg}^{-1}$ ). The moderate P reduction

demonstrated by WEP and M3P (22% reduction compared to control) in MT + manure can be attributed to the relatively higher oxalate extractable Mn content (6.2 g kg<sup>-1</sup>) resulting from the Mn tailings addition, in spite of low oxalate extractable Fe (1.63 g kg<sup>-1</sup>).

Table 4-1 . Chemical properties and total elemental composition of iron ore (IO), steel slag (SS), and manganese tailings (MT) as obtained.

Parameters	IO	SS	MT
pH	6.85	12.19	7.30
Electrical Conductivity, mS cm <sup>-1</sup>	0.123	5.19	12.2
Fe, g kg <sup>-1</sup>	610	182	19.8
Oxalate extractable Fe, g kg <sup>-1</sup>	0.627	39.5	2.36
Mn, g kg <sup>-1</sup>	1.97	27.6	426
Oxalate extractable Mn, g kg <sup>-1</sup>	1.12	2.32	38.4
Al, g kg <sup>-1</sup>	3.4	8.0	21.0
Ca, g kg <sup>-1</sup>	0.006	159	16.3
Zn, mg kg <sup>-1</sup>	20.2	113	615
Cu, mg kg <sup>-1</sup>	23.0	24.0	371
Pb, mg kg <sup>-1</sup>	12.7	35.8	38.7
Cr, mg kg <sup>-1</sup>	6.8	877	18.9
Cd, mg kg <sup>-1</sup>	0.87	2.54	3.06
Ni mg kg <sup>-1</sup>	23.7	32.7	468
P, g kg <sup>-1</sup>	0.36 <sup>a</sup>	4.60 <sup>a</sup>	-
S, g kg <sup>-1</sup>	0.06 <sup>a</sup>	0.65 <sup>a</sup>	1.4 <sup>a</sup>

<sup>a</sup> Total concentration data from material sources.

Table 4-2 . Chemical properties and characteristics of manure and manure with iron ore (IO), steel slags (SS) and manganese tailings (MT) before anaerobic incubation.

Parameters	Control (Manure only)	Manure with Fe/Mn amendments		
		IO + manure	SS + manure	MT + manure
Amendment application rate (g kg <sup>-1</sup> )	-	74.0	239	33.5
Moisture content (%)	81.6	80.7	75.8	81.3
pH	7.92	7.93	8.49	7.79
Electrical Conductivity mS cm <sup>-1</sup>	8.70	8.30	6.65	9.30
Total Fe, g kg <sup>-1</sup>	2.65 ± 0.20	46.5 ± 7.5†	43.0 ± 4.0	3.73 ± 0.19
Oxalate extractable Fe, g kg <sup>-1</sup>	1.34 ± 0.12	1.25 ± 0.04	17.6 ± 2.9	1.63 ± 0.10
Total Mn, g kg <sup>-1</sup>	0.282 ± 0.015	0.423 ± 0.052	7.11 ± 0.80	18.8 ± 1.4
Oxalate extractable Mn, g kg <sup>-1</sup>	0.190 ± 0.011	0.288 ± 0.020	3.35 ± 0.35	6.17 ± 0.37
Total P, g kg <sup>-1</sup>	4.21 ± 0.08	4.01 ± 0.12	3.80 ± 0.09	4.09 ± 0.20
Water-extractable P, g kg <sup>-1</sup>	0.300 ± 0.009	0.309 ± 0.016	0.0198 ± 0.002	0.217 ± 0.018
Mehlich III P, g kg <sup>-1</sup>	2.68 ± 0.05	2.46 ± 0.06	0.536 ± 0.062	2.09 ± 0.070
Total Zn, mg kg <sup>-1</sup>	330 ± 8	300 ± 10	258 ± 4	351 ± 20
Sr(NO <sub>3</sub> ) <sub>2</sub> extractable Zn, mg kg <sup>-1</sup>	9.12 ± 0.30	7.94 ± 0.28	2.54 ± 0.10	5.53 ± 0.24
Oxalate extractable Zn, mg kg <sup>-1</sup>	297 ± 10	263 ± 6	65.1 ± 12.7	224 ± 44
Total Cu, mg kg <sup>-1</sup>	307 ± 5	272 ± 7	208 ± 6	315 ± 20
Sr(NO <sub>3</sub> ) <sub>2</sub> extractable Cu mg kg <sup>-1</sup>	54.2 ± 0.8	48.9 ± 0.5	41.7 ± 2.3	46.5 ± 1.0
Oxalate extractable Cu, mg kg <sup>-1</sup>	293 ± 9	260 ± 4	177 ± 15	292 ± 9

† mean ± standard deviation.

Slight increases in total Zn and Cu were observed only in MT + manure compared to the control (Table 4-2). Both  $\text{Sr}(\text{NO}_3)_2$  extractable and oxalate extractable Zn and Cu in manure were decreased by all three Fe/Mn materials applications. SS + manure especially showed significant decrease of  $\text{Sr}(\text{NO}_3)_2$  and oxalate extractable Zn compared to the control, likely due to possible adsorption and precipitation of the metal caused by high pH and high amorphous Fe content.

#### **4-3-2. Evaluation of manure anaerobic incubation to increase amorphous Fe/Mn and decrease P mobility.**

During the first 33 days of the anaerobic incubation, an increasing trend of WEP for the control was observed (Figure 4-3a). This is expected because manure organic matter is hydrolyzed and decomposed by anaerobic and facultative microorganisms, converting bound phosphorus, organic phosphorus or poly phosphate in manure to more water soluble species (e.g., hydrolysis of phytate-P) (Wild et al., 1997; Correll, 1998). After exhibiting the highest water soluble P ( $910 \text{ mg kg}^{-1}$ ) at day 33, water soluble P for the control decreased gradually to  $470 \text{ mg kg}^{-1}$  at day 127. This decrease can be explained by decrease of orthophosphate with volatile solid reduction as found by Wild et al. (1997) and Sanchez et al. (2000). The increase of oxalate extractable Fe for the control (from 1340 to  $2080 \text{ mg kg}^{-1}$ ) during the anaerobic incubation can also decrease water soluble P in manure by adsorption and precipitation of WEP.

During the anaerobic incubation, WEP of IO amended manure (IOM) decreased constantly down to  $124 \text{ mg kg}^{-1}$  day 127 after exhibiting initial increase up to  $441 \text{ mg kg}^{-1}$  at day 3 (Figure 4-3a). Like the control, the initial increase of water soluble P during the first 3 days of incubation is likely due to the rapid release of water soluble P by

decomposition and hydrolysis of organic materials. However, unlike the control, water soluble P for IOM decreased constantly from day 3. This is likely due to increases of newly-synthesized amorphous Fe oxides during the anaerobic incubation (Figure 4-3d). The most significant decrease in WEP (by  $146 \text{ mg kg}^{-1}$ ) for IOM was observed in a relatively short time, from day 3 to day 10. This corresponds to the highest oxalate extractable Fe increase rate ( $202 \text{ mg kg}^{-1} \text{ day}^{-1}$ ) during the incubation period, providing enough adsorption sites to decrease WEP released during the same incubation period. During the 127 total days of anaerobic incubation, IOM showed 62% reduction of WEP compared to fresh manure (before digestion) and a 76% reduction compared to the control. Overall, the highest sequestration of WEP ( $581 \text{ mg kg}^{-1}$  reduction) was observed at day 33 compared to the control.

The most significant increase of oxalate extractable Fe throughout the 127 days of anaerobic incubation was observed in the IOM (Figure 4-3d), about  $4740 \text{ mg kg}^{-1}$  (from 1250 to  $5990 \text{ mg kg}^{-1}$ ), while the oxalate extractable Fe for the control increased by  $740 \text{ mg/kg}$ . Nonetheless, in spite of exhibiting the greatest increase of oxalate extractable Fe, it is estimated that only 9.2 % of the crystalline iron ore added was converted into active amorphous Fe during the 127 days of anaerobic incubation.

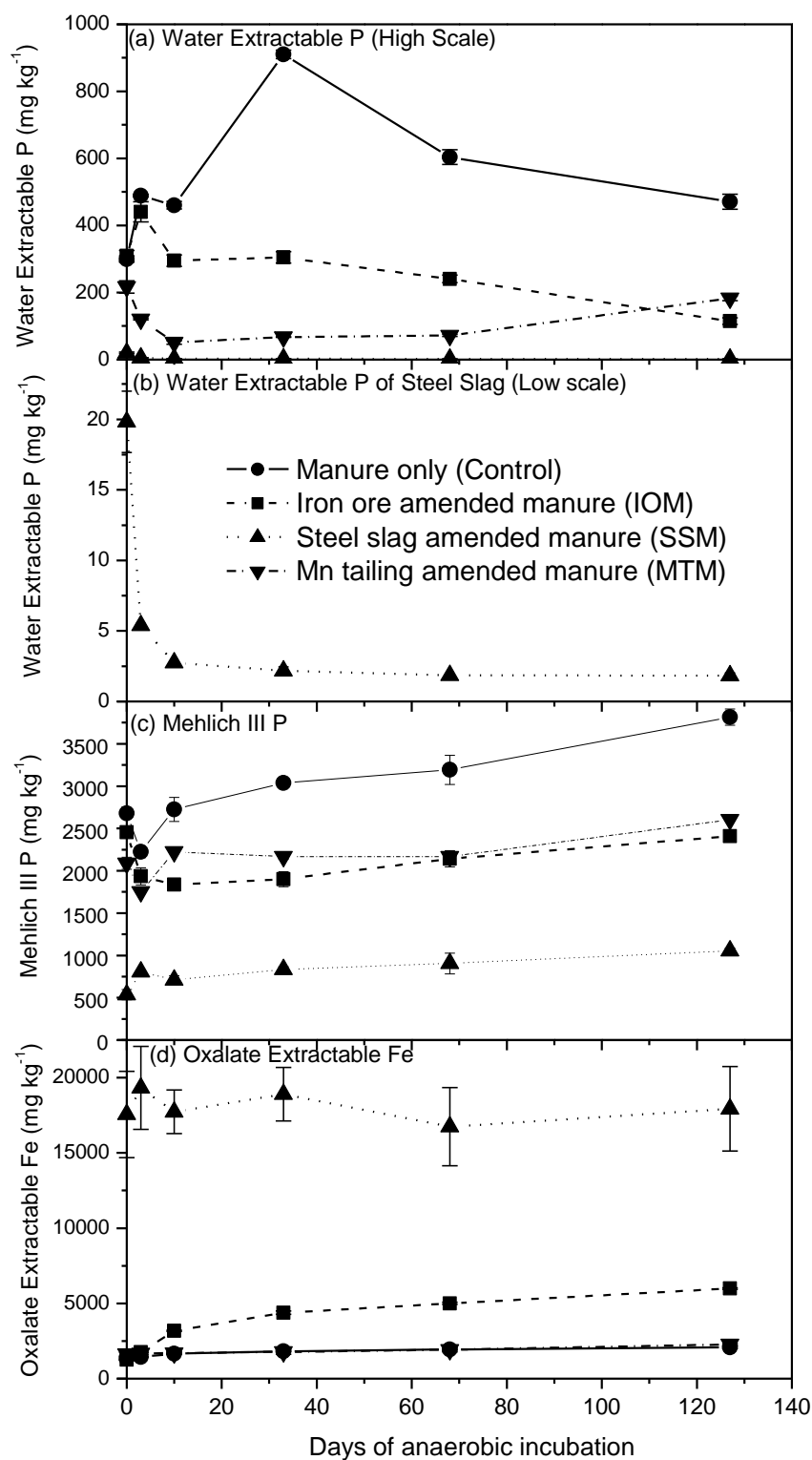


Figure 4-3. Water extractable Phosphorus, Mehlich III Phosphorus, and Oxalate extractable Fe for Fe/Mn materials amended manure mixture during anaerobic incubation (error bars represent  $\pm 1$  standard deviation): (a) Water soluble P (high scale), (b) Water soluble P (low scale), (c) Mehlich III P, and (d) Oxalate extractable Fe.

The increase of amorphous extractable Fe in IOM can be attributed to microbial reductive dissolution of crystalline Fe oxides during the anaerobic incubation. Proposed mechanisms and processes in this treatment consist of three parts; initial mixing, anaerobic incubation and aerobic drying as presented in Figure 4-4. The resulting dissolved Fe(II) from the microbial reductive dissolution can be rapidly oxidized to Fe(III) and precipitated as amorphous Fe(III) oxides during the aerobic drying procedure (Figure 4-4c).

Very low WEP was observed for SS amended manure (SSM) throughout all 127 days of the anaerobic period, showing >98 % reduction of water soluble P compared to both fresh manure and the incubated control. This is expected because of the high oxalate extractable Fe content in the raw steel slag. Oxalate extractable Fe in the SSM was consistently much higher than the other three mixtures, showing roughly 18000 mg Fe kg<sup>-1</sup> (Figure 5-1d). The high pH and relatively low water content (Table 4-2) in SSM likely inhibited microbial activity and, therefore little microbial-mediated dissolution of non-amorphous Fe was achieved (Stronach et al., 1986; Gerardi, 2003). Additionally, abundant readily-bioavailable amorphous (or poorly crystalline) Fe(III) oxides (oxalate extractable Fe) in steel slag could have been preferentially reduced to Fe(II) while crystalline Fe(III) oxides had less chance to become reduced via microbial dissimilatory reductive dissolution, and therefore remained unchanged, as demonstrated by Lovely and Philips (1986a and b), and Arnold et al. (1988). In spite of the minimal change of oxalate extractable Fe in SSM, WEP for SSM decreased with anaerobic digestion time (Figure 4-3b); the exact reason is uncertain but CaO in SS may be dissolved during anaerobic incubation and the dissolved Ca may react with phosphate and precipitate to decrease WEP.

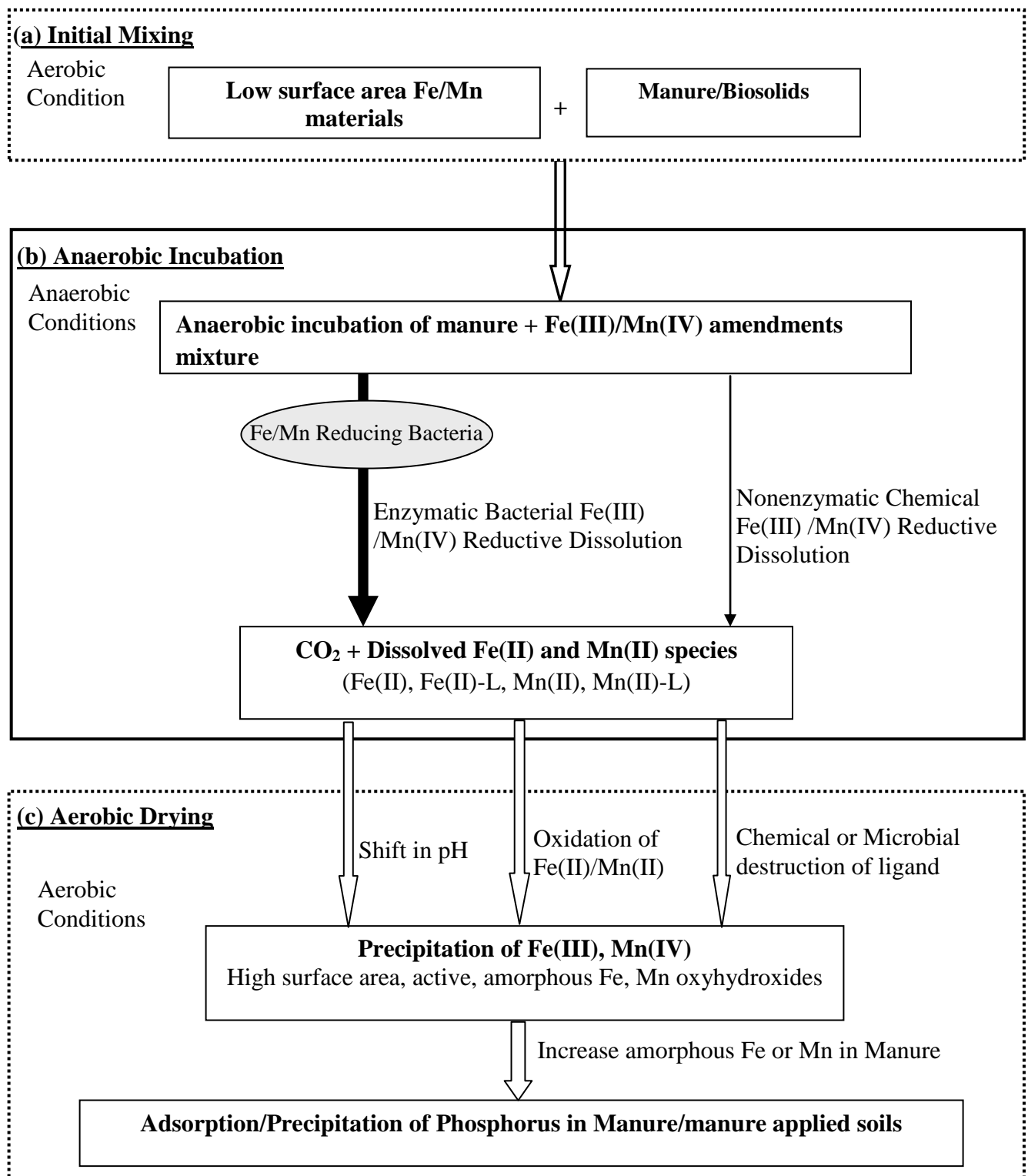


Figure 4-4. Proposed mechanisms and processes involved in production of active amorphous Fe/Mn oxides from non active Fe/Mn materials and organic matter mixtures.



Like SSM, WEP for MT amended manure (MTM) rapidly decreased during the first 10 days of incubation. This system subsequently showed relatively constant WEP levels up to day 68, demonstrating up to 93% P reduction at day 33 compared to the control (Figure 5-1a). However, unlike SSM, noticeable WEP increase was observed at the end of the incubation for MTM, which decreased percent P reduction to 61% at day 127 compared with the control. The initially-bound P on metal oxides or precipitated P with metals (i.e., high initial oxalate Mn content) during early stages of the incubation may be released as anaerobic incubation proceeded. This did not occur for IOM and SSM probably due to increase of oxalate extractable Fe or dissolved Ca during the incubation.

M3P exhibited different trends, with much higher extracted P levels as compared with WEP throughout the anaerobic incubation process for all manures (Figure 1c). Except for an initial drop at day 3, M3P for control constantly increased up to  $3820 \text{ mg kg}^{-1}$  throughout the anaerobic incubation, which is very close to the total P ( $4210 \text{ mg kg}^{-1}$ ). This suggests that most of total P in manure became Mehlich III extractable through manure decomposition during the 127 days of anaerobic incubation. The constant M3P increase for control throughout the incubation, in spite of WEP decrease during day 37 to 137, likely results from increase in partially mineralized organic phosphorus which is only extracted as M3P. Completely mineralized orthophosphate (which is extracted as WEP) decreased significantly with removal of volatile solids and increase of oxalate Fe in manure during anaerobic incubation.

Unlike WEP, the anaerobic incubation of SSM caused increase of M3P. However, SSM showed much lower M3P ( $709$  to  $1060 \text{ mg kg}^{-1}$ ) than the IOM ( $1840$  to  $2410 \text{ mg kg}^{-1}$ ), MTM ( $1750$  to  $2600 \text{ mg kg}^{-1}$ ) and control ( $2220$  to  $3820 \text{ mg kg}^{-1}$ ) throughout the

anaerobic incubation process, demonstrating 64 to 74% M3P reduction compared with control (Figure 4-3c).

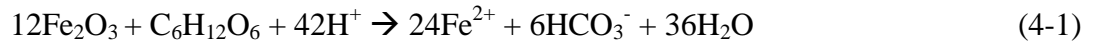
M3P for the IOM decreased initially to 1840 mg kg<sup>-1</sup> during the first 10 days of the incubation, and then demonstrated only slight increase during the rest of the anaerobic incubation, exhibiting M3P percent reduction from 33 to 38% compared to control. The MTM also demonstrated relatively constant M3P throughout the incubation, exhibiting 18 to 32 % M3P reduction compared with control.

No significant change of oxalate extractable Mn was observed in manures with all three Fe/Mn materials during the anaerobic incubation, including the control (data not shown), indicating no significant Mn reductive dissolution during the incubation. However, a significant increase of oxalate extractable Mn was observed when Mn tailings and steel slag were mixed with fresh manure before the incubation. The ratio of oxalate extractable Mn to total Mn significantly increased for SSM (from 0.084 for steel slag to 0.47 for SSM at day 0) and MTM (from 0.090 for Mn tailings to 0.33 for MTM at day 0) before the anaerobic incubation (Table 5-2). This is probably because chemical dissolution (ligand promoted) of crystalline Mn in steel slag and Mn tailings may be promoted through mixing of the manure and aerobic incubation during the drying process.

#### **4-3-3. pH and Eh of Fe/Mn material treated manure during anaerobic incubation**

During the anaerobic incubation, an initial pH drop was observed for the IOM, MTM, and control (Figure 4-5a). The lowest pH was noted at day 10 for IOM and at day 33 for MTM and control; subsequently, the pH increased during the rest of incubation. This initial pH drop is likely due to an increase of CO<sub>2</sub> concentration and the transient

production of fatty acids during hydrolysis, followed by acidogenesis in the anaerobic degradation of the organic matter. The pH increase later in the incubation probably resulted from the consumption of volatile fatty acids and CO<sub>2</sub>, as well as dissolution of metal oxides and oxyhydroxides during acetogenesis and methanogenesis (Dassonville and Renault, 2002). The IOM showed earlier increase of pH and higher pH than Mn tailings and the control beyond 10 days of the incubation (Figure 4-5a). Reductive dissolution of iron oxides in the IOM should consume acidity based on Fe(III) (hematite) reduction to Fe(II) with organic compounds such as glucose (Kostka and Nealson, 1995):



The SSM clearly showed the highest pH compared to the other mixtures throughout the incubation period because of the high CaO content in the steel slag. The pH of the SSM remained relatively constant up to day 68, ranging from 10.2 to 10.4 and dropping to 9.5 at the end of the incubation (Figure 4-5a).

As proposed in Figure 4-4, Fe(II) dissolved by bacterial reductive dissolution during the anaerobic incubation can be subsequently oxidized to Fe(III) by oxygen through aerobic incubation during the drying process, which will increase the pH. In contrast, Fe(III) hydroxide precipitation and NH<sub>3</sub> volatilization can act to decrease pH. Consequently, analyzing and evaluating pH of wet (anaerobic condition) and dry (aerobic condition) samples is complicated considering the nature of this complex biochemical system. Much lower pH values for dry SSM samples than wet samples were observed (Figure 4-5b), likely because of lost ammonia at high pH (Kirchmann and Witter, 1989).

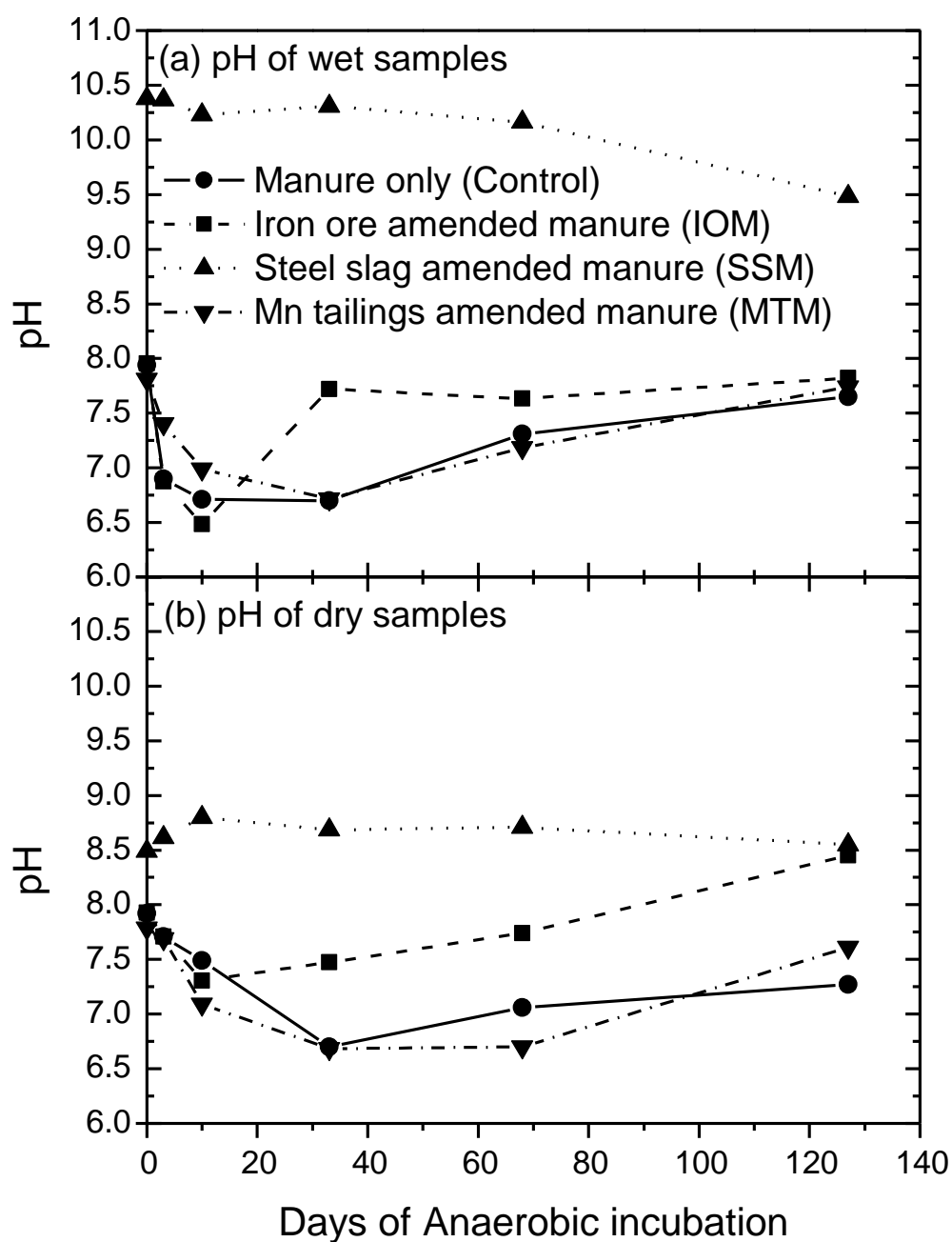


Figure 4-5. pH change during anaerobic incubation for Fe/Mn materials amended manure mixtures: (a) pH of wet samples, and (b) pH of dry samples

Eh values for SSM, MTM and the incubated control dropped to approximately -300 mV at day 3 and remained less than -300 mV throughout the 127 days of incubation. Eh

for IOM fell to about -200 mV at day 3 and remained less than -200 mV (-210 to -280 mV) for the rest of the incubation (data not shown). These values confirm strong reducing conditions and indicate that reduced Fe(II) and Mn(II) are the thermodynamically stable species (Dassonville and Renault, 2002).

#### **4-3-4. Extractable Zn and Cu**

Manure amended with inorganic by-product, before anaerobic digestion did not demonstrate any increase of metal (Cu and Zn) leachability compared to control (manure only), based on both  $\text{Sr}(\text{NO}_3)_2$  and oxalate extractions (Table 4-2, and Figures 4-6 and 4-7). In fact, significantly less metals (for both Cu and Zn) were leached from the SSM compared to control, suggesting decrease of metal (Cu and Zn) extractability and metal sequestration from SSM by steel slag. MTM also shows distinct decrease of Zn extractability for both  $\text{Sr}(\text{NO}_3)_2$  and oxalate extractions compared to control, while decrease of Cu extractability for MTM and both Cu and Zn extractability for IOM was relatively minimal. This decrease of metal extractability for SSM compared to control can be explained by increase of pH and oxalate Fe content by adding steel slag in manure. Extractable metals in manure may be sequestered by precipitation due to pH increase and adsorption on amorphous Fe through steel slag addition. The decrease of Zn extractability for MTM can be explained by high oxalate Mn content (considered as amorphous Mn) in Mn tailings, which can adsorb Zn in manure, while Cu in MTM is minimally sequestered by adsorption due to higher mobility through complexation with abundant organic ligands in manure (Hsu and Lo, 2000). For the same reason, more

significant sequestration of oxalate extracted Zn in SSM was observed compared to oxalate extracted Cu.

As the anaerobic incubation proceeded, SSM showed the highest  $\text{Sr}(\text{NO}_3)_2$  extractable Cu during the most of the incubation; the  $\text{Sr}(\text{NO}_3)_2$  extracted Cu concentration significantly decreased for IOM, MTM and control during the first 10 days of anaerobic incubation, while SSM showed relatively constant  $\text{Sr}(\text{NO}_3)_2$  extractable Cu until day 68. However, the  $\text{Sr}(\text{NO}_3)_2$  extractable Cu for SSM dropped at the end of the incubation, while the other mixtures showed relatively constant  $\text{Sr}(\text{NO}_3)_2$  extractable Cu (for MTM and Control) or consistent increase of  $\text{Sr}(\text{NO}_3)_2$  extractable Cu (for IOM) during the rest of the incubation. This  $\text{Sr}(\text{NO}_3)_2$  extractable Cu change during the anaerobic incubation can be explained by pH change of the manure mixtures during the incubation, which mainly controls Cu mobility with Cu complexes with organic ligands.

Comparing  $\text{Sr}(\text{NO}_3)_2$  extractable Cu (Figure 4-6b) and the pH of the extracting solution (Figure 4-6c), it is noted that  $\text{Sr}(\text{NO}_3)_2$  extractable Cu increased as pH increased and decreased as pH decreased in the high pH range ( $>7$ ). Specifically,  $\text{Sr}(\text{NO}_3)_2$  extractable Cu increased from day 10 for the IOM although oxalate extractable Fe increased (which can decrease Cu extractability by adsorption) as anaerobic incubation proceeded. Mixture pH appears as the controlling factor for  $\text{Sr}(\text{NO}_3)_2$  extractable Cu for all Fe/Mn materials amended manure mixtures in the high pH range because of high DOM (dissolved organic matter) contents. Cu-DOM complexes are formed, which decreases Cu sorption onto Fe/Mn oxides at high pH. Similar results were reported by Hsu and Lo using five (2000a) and eight (2000b) different swine manure composts. They suggested that extractability of Cu and Zn and dissolution of organic C were pH dependent. Their

results indicated that increase of dissolved Cu at high pH highly correlated to increased concentration of organic C ( $r=0.99$ ) due to large formation constants of Cu-organic complexes, showing that extractability of Cu and dissolution of organic C at  $\text{pH}>8$  increased significantly. The authors conversely suggested that the affinity of Zn for the same organic compounds was low, showing extractability of Zn remaining low at high pH. Similarly, high solubility of Cu from alkaline stabilized sludge due to high concentrations of dissolved organic matter was noted by McBride (1998), as well.

Interestingly, the SSM showed the highest  $\text{Sr}(\text{NO}_3)_2$  extractable Cu concentration (up to day 68) but the lowest  $\text{Sr}(\text{NO}_3)_2$  extractable Zn concentration compared to the other mixtures, throughout most of anaerobic incubation. This again is likely due to the slag producing the highest pH of the mixtures as well as highest amorphous Fe content.

The control and MTM showed decreasing trend of  $\text{Sr}(\text{NO}_3)_2$  extractable Zn throughout 127 days of the anaerobic incubation while Cu levels fell initially but exhibited relatively constant values after 10 days. This decrease of  $\text{Sr}(\text{NO}_3)_2$  extractable Zn for the control and MTM is probably due to amorphous Fe increase as anaerobic incubation proceeded. However,  $\text{Sr}(\text{NO}_3)_2$  extractable Zn for IOM increased during the rest of the incubation after demonstrating initial decrease up to day 33. It is speculated that reductive dissolution of iron ore during the anaerobic incubation released Zn to the mixture, which caused the increase of  $\text{Sr}(\text{NO}_3)_2$  extractable Zn for IOM.

Throughout the incubation, all the Fe/Mn + manure mixtures showed much lower  $\text{Sr}(\text{NO}_3)_2$  extractable Zn ( $< 10 \text{ mg/kg}$ ) than  $\text{Sr}(\text{NO}_3)_2$  extractable Cu (approximately, 20 – 55  $\text{mg/kg}$ ) (Figure 4-6) although total extraction indicated higher Zn than Cu (Table 4-2).

Cu forms strong complexes with low molecular weight dissolved organic matter, which can dissolve and exist as soluble negatively charged species at high pH (>7).

During the anaerobic incubation, oxalate extractable Zn and Cu exhibited different trends from  $\text{Sr}(\text{NO}_3)_2$  extracted metals, showing significantly higher ranges for both metals (Figure 4-7). Throughout the anaerobic incubation, little change of oxalate extractable Zn and Cu was observed for all mixtures compared to those before the incubation (except oxalate extracted Zn for MTM), suggesting little effect of anaerobic incubation on oxalate extracted metals. Therefore, all inorganic by-product amended manure mixtures showed lower or very similar oxalate extracted Zn and Cu compared to the control throughout the anaerobic incubation. SSM exhibited the lowest oxalate extractable metals for both Zn and Cu compared to the other three mixtures throughout the incubation while the IOM, MTM, and control showed similar trends; the MTM showed lower oxalate Zn than IOM and the control.



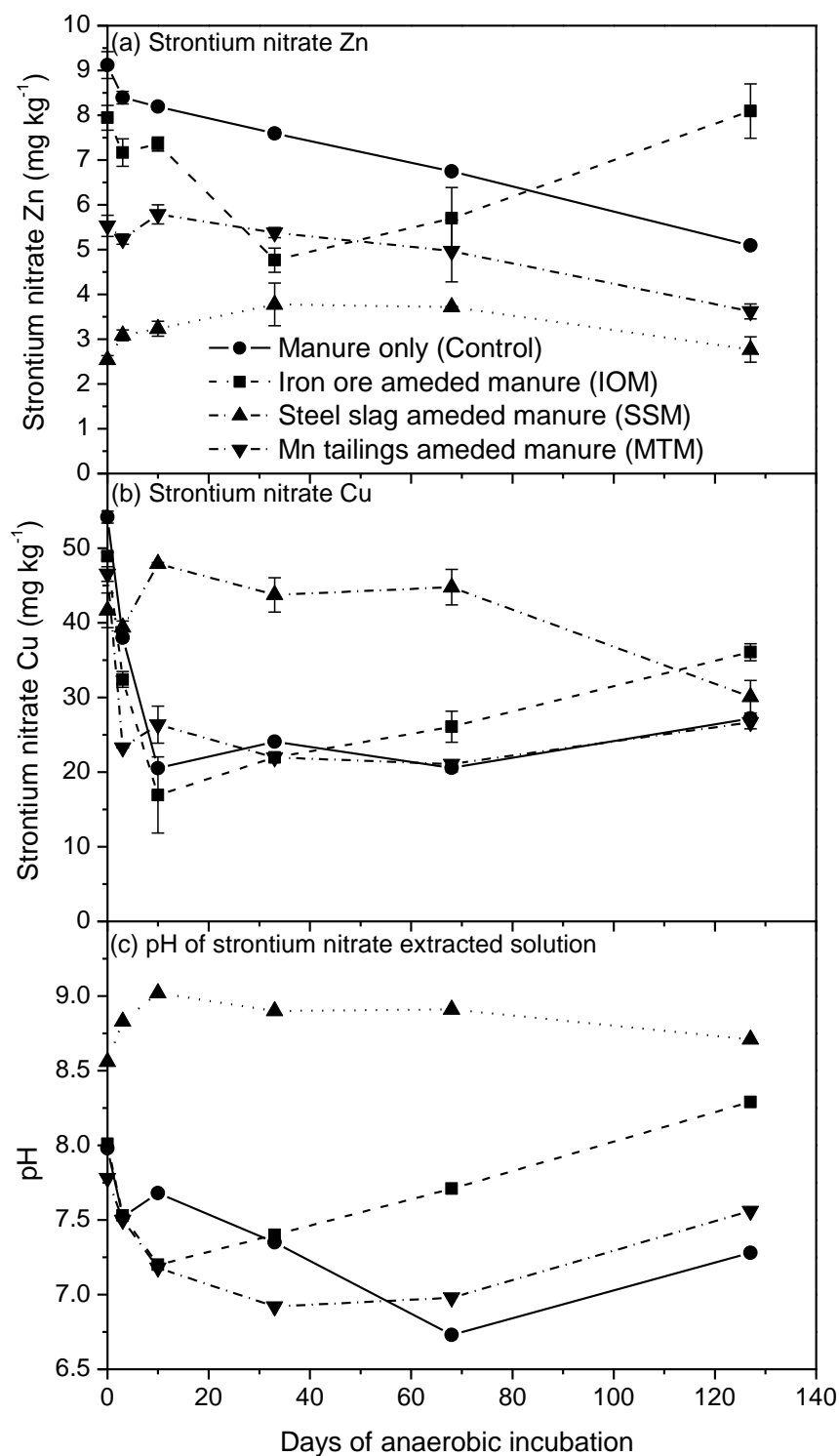


Figure 4-6.  $\text{Sr}(\text{NO}_3)_2$  extraction results from anaerobic incubation for Fe/Mn materials amended manure mixtures (error bars represent  $\pm 1$  standard deviation): (a)  $\text{Sr}(\text{NO}_3)_2$  extractable Zn, (b)  $\text{Sr}(\text{NO}_3)_2$  extractable Cu, and (c) pH of  $\text{Sr}(\text{NO}_3)_2$  solution after extraction

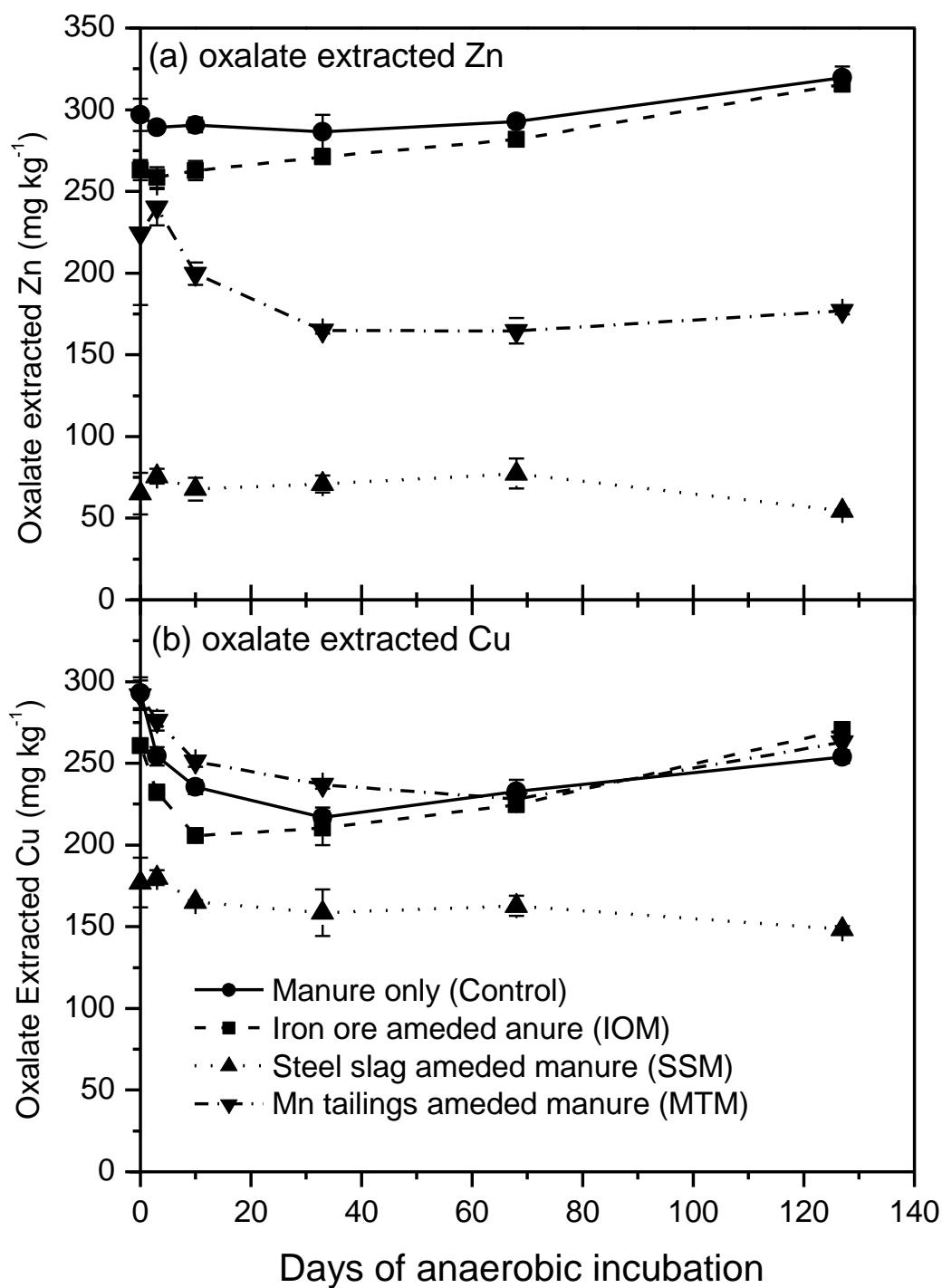


Figure 4-7. Oxalate extractable Zn and Cu during anaerobic incubation for Fe/Mn materials amended manure mixtures (error bars represent  $\pm 1$  standard deviation): (a) Oxalate extractable Zn, and (b) Oxalate extractable Cu.

#### **4-4. Discussion on microbial Fe/Mn reductive dissolution during anaerobic incubation**

Microbial reductive dissolution of Fe/Mn materials is proposed as a mechanism of increasing oxalate extractable Fe and Mn in Fe/Mn material amended manure in this research. Results by Lovely et al. (1991) indicated that enzymatic microbial reduction of Fe(III) is responsible for most of the Fe(III) reduction in aquatic sediments compared to nonenzymatic Fe(III) reduction. A study by Heron and Christensen (1995) indicated substantial reductive dissolution of crystalline Fe(III) oxides in aquifer sediments polluted by landfill leachate. Also, laboratory studies by Roden and Zachara (1996) showed 8 to 18 % reduction of crystalline Fe(III) oxide content in various aquifer sediments after 30 days of incubation by a dissimilatory Fe(III) oxide-reducing bacterium. These results indicate significant reduction of crystalline Fe(III) oxides in anaerobic environments.

In this work, the greatest increase of oxalate extractable Fe was observed in IOM, but it is estimated that only 9.2 % of the crystalline iron ore added was converted into active amorphous Fe during the 127 days of anaerobic incubation. However, any optimization or modification of anaerobic incubation to improve the synthesis of amorphous Fe was not attempted.

The surface area of the crystalline oxide and Fe(II) surface phase adsorbed or precipitated on Fe(III) oxides (and/or cells) have been suggested as factors controlling and limiting the rate and extent of microbial Fe(III) reductive dissolution (Roden and Zachara, 1996; Urruita et al., 1999; Roden, 2004; Royer et al., 2004). Specifically, the importance of well-mixed conditions for increasing diffusional flux (thermodynamic driving force) of Fe(II) to enhance Fe(III) reduction was noted in a recent study (Royer et al., 2004), demonstrating that higher mixing intensity increased hematite reduction. Therefore,

mechanical mixing in a typical manure digester should enhance the synthesis of active amorphous Fe/Mn oxides from nonactive Fe/Mn materials. Also high concentration of ligands/chelators can enhance microbial reduction of crystalline iron(III) oxides by removing adsorbed or precipitated Fe(II) via forming Fe(II)-chelators/ligands complexes and binding Fe(II) on the solid materials, respectively (Lovely et al., 1996a, 1996b; Royer et al., 2002a, 2002b ).

Exploiting the above information, further studies are needed to apply microbial Fe reductive dissolution to anaerobic manure incubation/digestion to produce stabilized organic amendments with high amorphous Fe content and low P mobility. Studies for optimization and modification of typical manure digesting processes may also be needed to enhance the bacterial Fe reductive dissolution and therefore increase the synthesis of amorphous Fe in manure if low cost iron ore byproducts are to be used to reduce phosphate risks from manures.

#### **4-5. Summary and Conclusions**

Fates of Fe and Mn, P, and Zn and Cu were measured in amended dairy manure during an anaerobic incubation process. Oxalate extractable Fe for SSM was much higher than for the other three mixtures (IOM, MTM and control); however, oxalate extractable Fe remained essentially constant throughout the anaerobic incubation. Oxalate extractable Fe for the IOM was increased by about 4740 mg/kg throughout the 127 days of anaerobic incubation, the most of any amendment, while the oxalate extractable iron for MTM and the incubated control increased less by 650 mg/kg and 740 mg/kg, respectively. This

increase can be attributed to bacterial reductive dissolution of crystalline Fe oxides during the anaerobic incubation.

During the incubation, manure with Fe ore showed 62% reduction of water soluble P compared to fresh manure and a 76% reduction compared to a incubated control. Very low WEP was observed for SSM addition throughout incubation period, showing 93% initial reduction (at day 0) and >98 % reduction compared to both fresh and incubated control manure. SSM showed much lower M3P than the IOM, MTM or control throughout the anaerobic incubation. M3P exhibited different trends, with much higher extracted P levels, as compared with WEP throughout the anaerobic incubation process. This extraction parameter exhibited much lower P percent reduction in Fe/Mn material amended manure compared to WEP, extracting stable and immobilized fractions of phosphorus. Therefore, M3P may not be the appropriate test to evaluate P immobility in manure because its high P extractability may not properly reflect P release from manure by runoff, and therefore underestimate reduction of P mobility by amendments.

Manure amended with inorganic by-product before anaerobic digestion did not demonstrate any increase of metal (Cu and Zn) leachability compared to control (manure only), based on both  $\text{Sr}(\text{NO}_3)_2$  and oxalate extractions (Table 4-2, Figures 4-6 and 4-7). In fact, significantly less metals (for both Cu and Zn) were leached from the SSM compared to control (manure only), suggesting metal sequestration from SSM by steel slag. Manure pH was the controlling factor for  $\text{Sr}(\text{NO}_3)_2$  extractable Cu for all Fe/Mn manure mixtures. In the high pH range, because of high DOM contents and therefore formation of Cu-DOM, Cu sorption on Fe/Mn oxides is decreased. The SSM showed the highest  $\text{Sr}(\text{NO}_3)_2$  extractable Cu concentration but the lowest Zn concentration compared to the other

mixtures throughout most of the anaerobic incubation due to the slag producing the highest pH of the mixtures. During the anaerobic incubation, oxalate extractable Zn and Cu exhibited different trends from  $\text{Sr}(\text{NO}_3)_2$  extracted metals, showing significantly higher ranges for both metals (Figure 4-7). Throughout the anaerobic incubation, little change of oxalate extractable Zn and Cu was observed for all mixtures compared to those before the incubation, except for oxalate extracted Zn for MTM, suggesting little effect of anaerobic incubation on oxalate extracted metals.

The use of Fe-rich by-products in a simple manure digestion process can provide a number of benefits by decreasing the environmental risk of high phosphorus release from manure and biosolids while concurrently improving the Fe and Mn fertility of Atlantic Coastal Plain soils. Some by-products contains amorphous Fe (e.g., steel slag) and, therefore, exposure to anaerobic condition may not be required to reduce P solubility of manure and biosolids. Anaerobically processed organic (manure or biosolids)/inorganic (Fe rich byproduct) mixtures have potential to sequester and decrease heavy metal contamination in soils by reducing the bioavailability and potential phytotoxicity of heavy metals from soils, with great merit for cost-effective in situ immobilization of heavy metals. This will use two existing waste byproducts, both inorganic Fe/Mn waste material and organic manure or biomass, with a beneficial outcome.

## CHAPTER 5. CHARACTERIZING ROOF/WALL RUNOFF AND SOIL AROUND THE B-580 APHIS (AN ANIMAL AND PLANT HEALTH INSPECTION SERVICE FACILITY) BUILDING

### 5-1. Introduction

Storm water runoff from various diffuse sources has been a major contributor to water pollution of lakes, rivers and estuaries in the United States (Line et al., 1996). Specifically, Gromaire et al. (1999) suggested that roof runoff contributed even greater amounts of trace elements than street runoff in their urban runoff characterization study. Boller (1997) reported average roof runoff metal concentrations of 90 µg/L Pb, 200 µg/L Cu, 400 µg/L Zn, and 0.6 µg/L Cd, based on his literature surveys. Furthermore, significantly different metal concentrations were observed from different roof material types in various roof runoff studies (Chang et al., 2004; Lye, 2009)

Identifying diffuse sources and characterizing runoff from the pollution sources, and investigating the degree of water pollution around the sources are, therefore, important to address risks from storm water runoff pollution. In addition to surface water pollution by diffuse source pollution, mobility of heavy metals through soils as well as soil pollution by the diffuse source is also important because roof runoff can cause both soil metal contamination and ground water contamination.

Building-580 (location of an Animal and Plant Health Inspection Service facility) is located at the Beltsville Agricultural Research Center-East (BARC-East) in Beltsville, MD. Its exterior wall and roof are mainly made of Cu and Pb and their surface has significant corrosion. Therefore, this exterior material was suspected as a potential

source of heavy metal contamination of surface water and soil from runoff originating from the building rooftop and walls.

Monitoring and characterizing roof/wall runoff from the B-580 was the first phase study to address risks of heavy metal contamination in water. The heavy metal concentration of soil around the building was also monitored to investigate the degree of heavy metal contamination of soil by roof/wall runoff and infiltration. If significant contamination is found, appropriate remedial measures will be evaluated.

## **5-2. Methods and Materials**

Experimental materials and methods were designed and prepared based on the objective of each research phase as: (1) monitoring and characterizing roof/wall runoff from B-580; (2) monitoring and characterizing soils around B-580 to evaluate the degree of heavy metal contamination of soils caused by the roof/wall runoff from the APHIS building.

### **5-2-1. Characterization of Rooftop Runoff – Phase 1**

Rooftop runoff samples were collected from four different locations around B-580 during four different storm events from August 9<sup>th</sup> to September 11<sup>th</sup>, 2007. Plastic rain gutters were installed on the side of the wall to collect the runoff from the rooftop with plastic liner attached on the wall for better collection. A portion of the collected runoff was transferred to sampling bottles through a hole in the rain gutter and the rest was bypassed to drainage. The sampling bottles and the gutter were covered by plastic liner to minimize input of direct rainfall during strong storm events. The samples from the



first three storm events were collected using 10 L glass bottles as composite samples and the samples from the last storm event were collected as grab samples in Nalgene 1 L plastic bottles.

All samples were prepared, analyzed, and stored following methods in *Standard methods for the examination of water and waste water* (APHA et al., 1995). Total suspended solids (TSS), Total dissolved solids (TDS), and pH of the samples were immediately analyzed as soon as the samples were collected (Standard Methods 2540C and 2540D). Dissolved heavy metal concentrations (Pb, Cu, and Zn) of the samples were measured using flame or graphite furnace atomic absorption spectrophotometry (Perkin Elmer 5100PC with Perkin Elmer Zeeman Furnace module 5100ZL) after filtering the samples through 0.2 µm pore size, 25 mm diameter membrane disk filters (Standard Method 3111, 3113). Total heavy metal concentrations (Pb, Cu, and Zn) of the samples were also measured as described above after nitric acid digestion of samples following Standard Method 3030 E (APHA et al., 1995).

#### **5-2-2. Characterization of soil around the APHIS building – Phase 1**

Soil samples were collected from various locations surrounding the APHIS building on April 17<sup>th</sup> and May 1<sup>st</sup>, 2008 to characterize the degree of heavy metal contamination of soil around the site (Figure 5-1). Six different soil sampling locations: back yard, front yard, side yard, swale 2, swale 1, and culvert/creek were chosen and designated as sites A, B, C, D, E, and F, respectively, with specific sampling spots labeled by numbers.

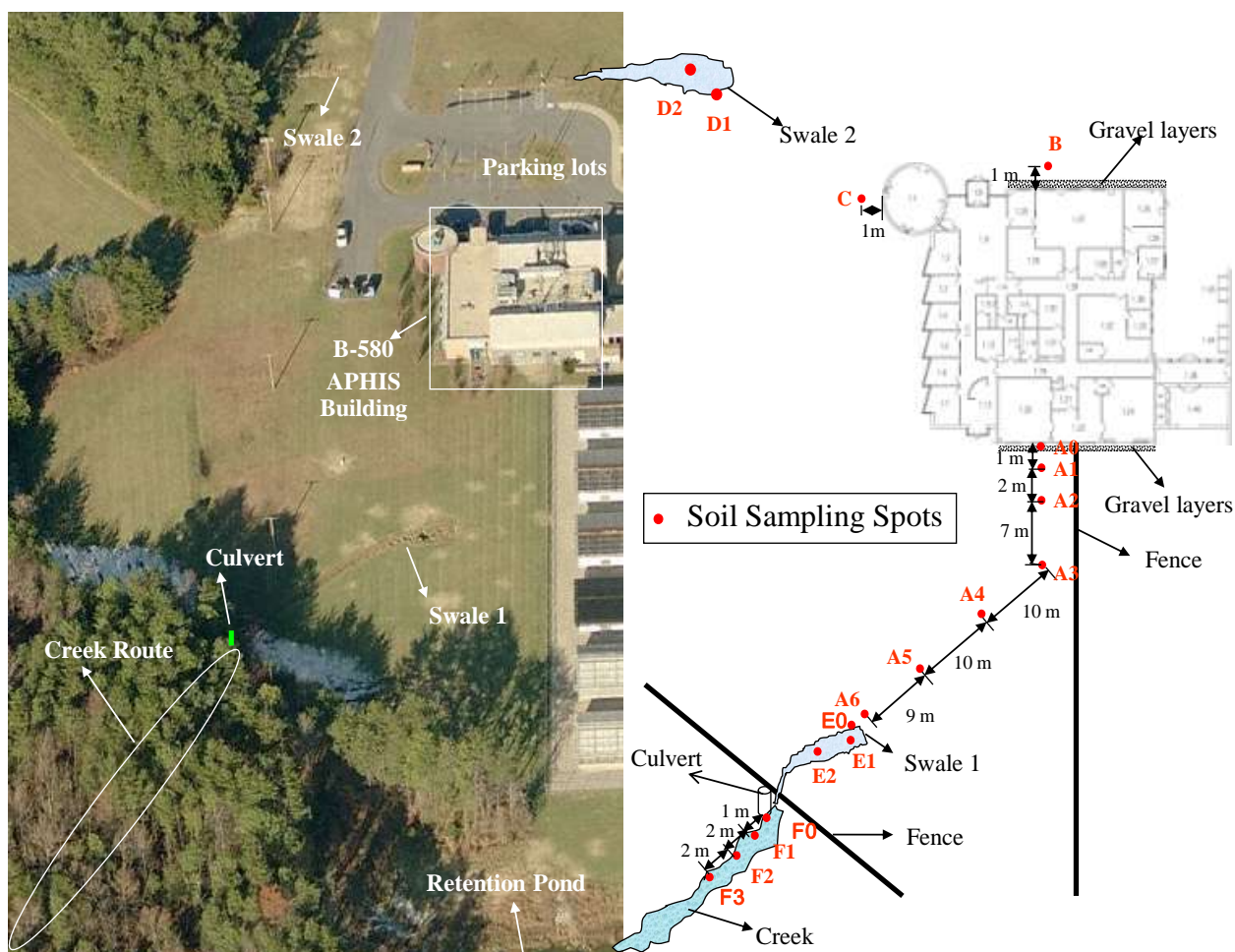


Figure 5-1. Satellite view of the APHIS site and Soil sampling spots (Satellite image was adapted from <http://www.bing.com/maps/>).

Triplicate soil samples were collected from a sampling location using a 2 cm diameter stainless steel soil probe sampler, which allowed the collection of soil samples from four different soil depths, except for sample A0. The A0 soil/organics sample was collected from a gravel layer right next to the building (Figure 5-2). The A0 soil/organics samples were taken using a small stainless steel shovel by gloved hand from various locations less than 30 cm depth.

The samples were air-dried and stored in soil sampling bags for later analysis. Total metal content in samples was determined by hot nitric acid digestion. The digested

and filtered samples were analyzed for Pb, Cu and Zn using flame atomic absorption spectrophotometry.



Figure 5-2. Gravel layer right next to the APHIS building.

### **5-3. Results and Discussion**

#### **5-3-1. Monitoring and characterizing roof/wall runoff from the building; Phase 1**

The characteristics of the roof/wall runoff are summarized in Table 5-1. The TSS concentration of the runoff was relatively low (average 10.5 mg/L) compared to the TDS (average 172 mg/L), as expected, considering that the rain hit and ran down the metal rooftop and wall only. For the same reason, the TSS levels for the roof/wall runoff were lower than typical highway runoff TSS levels reported in the literature, as summarized in Table 3-6. Mean event mean concentrations (EMC) of highway runoff TDS from three different sites (157, 88, and 216 mg/L) reported by Wu et al. (1999) were close to the TDS values of 172 mg/L from the roof/wall runoff.

As expected, due to the corroded nature of the roof and wall, the roof/wall runoff contained very high Pb and Cu concentrations. The Pb concentrations from the roof/wall runoff samples (4.10 – 11.29 mg/L as total) were much greater than typical Pb levels in

highway/urban runoff (5-200 µg/L) and roof runoff (~90 µg/L as average), summarized in Tables 3-6, 3-7a and 3-7b. The roof/wall runoff samples also showed higher Cu concentrations than that of typical highway (5-200 µg/L) and roof (~200 µg/L as average) runoff (Boller, 1997; Davis et al., 2001a). On the contrary, the Zn concentration of the roof/wall runoff (32-110 µg/L) was lower than that of typical highway (20-5000 µg) and roof (~400 as average) runoff; Zn is the usually highest among trace heavy metals in runoff likely because of the common use of galvanized steel and Zn rich tire debris.

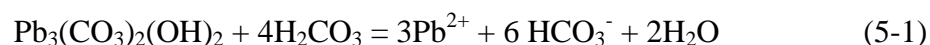
Significantly different metal concentrations were reported from different roof material types in various roof runoff studies (Tables 3-7a and 3-7b). Based on previous research, very high Zn concentrations (as high as 212 mg/L Zn by Zimmermann et al., 2005) were observed in the roof runoff from Zn or Zn-galvanized roofs. Similarly, roof runoff from Cu sheet roofs showed the highest Cu levels (as high as 21.7 mg/L) compared with other roofing materials monitored by Athanasiadis et al. (2007). As high as 2.5 mg/L Pb in roof runoff was reported by Gromaire et al. (2001) from roofs with different materials (zinc sheet, slate, interlocking tiles, and flat tiles). However, limited data regarding runoff monitoring from Pb-based roofs was found and the reported Pb levels from various roof materials were significantly lower than the Pb concentrations from the roof/wall runoff from B-580 which was studied.

Pb corrosion and leaching by precipitation water from a high purity lead sheet (>99% Pb with 0.184 m<sup>2</sup> of exposed skyward area) was studied in two different locations (rural and marine) by Matthes et al. (2002). In their study, Pb concentration in the precipitation runoff from the lead sheet was 2.1 mg/L for both locations with a range of 0.7-3.7 mg/L for the rural area and 1.4-3.4 mg/L for the marine area. Compared to the

above, Pb concentrations from the roof/wall runoff samples (4.10 – 11.29 mg/L as total) were greater, probably due to prolonged corrosion and longer runoff-flow retention times on the metal sheet (greater area of roof and wall metal sheet). Another possible explanation is that the metal sheet used for roofs and walls in APHIS building is alloyed with Cu and faster dissolution has been reported for lead-rich alloys than the pure metals under all aqueous conditions (Graedel, 1994). The results of lead concentrations from painted structures and building roofs studied by Davis and Burns (1999) showed concentrations as high as 28 mg/L Pb (from >10 yr old structure), although mean and median values were less than 0.81 mg/L and 88 µg/L, respectively; 70% or greater Pb was particulate Pb form.

Different from the study by Davis and Burns (1999), the total Pb and Cu concentrations from B-580 were essentially the same as the dissolved values. However, total Zn concentrations were distinctly higher than dissolved Zn concentrations, although both demonstrated much lower values compared to those of Pb and Cu.

The pH range (5.3-6.5) of the roof/wall runoff samples was higher than the annual average precipitation pH values of 4.12 to 4.37 across the Maryland region reported by Maxwell and Mahn (1987). They also reported that the lowest pH over the region was observed during the period of June through September, often showing monthly average pH value lower than 4.0, during which the roof/wall runoff monitoring study was also performed (August to September). Therefore, it is speculated that the pH of rainfall was increased by dissolution of the alkaline lead compounds [e.g., hydrocerrusite,  $\text{Pb}_3(\text{CO}_3)_2(\text{OH})_2$ ], which were formed as a surface film on roof/wall metal sheets through Pb corrosion during and between storm events, as shown in Eq. 5-1 (Matthes et al, 2002).



This was also observed by Mattes et al. (2002) in their Pb oxidation and leaching study by precipitation runoff using high purity lead (>99.9%); the runoff solution from the Pb sheet was one unit higher pH than the incident rainfall.

Table 5-1. Characteristics of the roof/wall runoff of the APHIS building.

Parameters	<u>Range</u>		<u>Mean ± Standard Deviation</u> <sup>a</sup>	
pH	5.3 – 6.5		5.7 <sup>b</sup>	
TSS (mg/L)	3.4 – 18.5		10.5 ± 4.54	
TDS (mg/L)	78.0 – 238.7		172 ± 50.1	
	<u>Dissolved Concentration</u>		<u>Total Concentration</u>	
Metals	<u>Range</u>	<u>Mean ± 1 Standard Deviation</u> <sup>a</sup>	<u>Range</u>	<u>Mean ± 1 Standard Deviation</u> <sup>a</sup>
Pb (mg/L)	3.98 – 10.94	7.58 ± 2.69	4.10 - 11.29	7.75 ± 2.78
Zn (mg/L)	0.027 – 0.088	0.042 ± 0.017	0.032 – 0.110	0.055 ± 0.022
Cu (mg/L)	0.27 – 2.10	0.78 ± 0.45	0.27 – 2.15	0.80 ± 0.47

<sup>a</sup> calculated based on total 15 samples collected from 4 different rainfall events.

<sup>b</sup> median value of total 15 samples

Lead release to environment by runoff depends on the Pb corrosion product solubility (the solubility of the Pb corrosion film on the metal surface through atmospheric corrosion). Litharge (PbO) has been identified as the first Pb corrosion product by atmospheric exposure (Graedel, 1994). However, through the deposition of atmospheric gases (SO<sub>2</sub>, CO<sub>2</sub>, and carboxylic acids) on the surface of the metal, anglesite (PbSO<sub>4</sub>), hydrocerrussite [Pb<sub>3</sub>(CO<sub>3</sub>)<sub>2</sub>(OH)<sub>2</sub>], and cerussite (PbCO<sub>3</sub>) become

dominant, are the most common minerals detected on metal surface corrosion films, and are responsible for Pb dissolution and release through runoff (Graedel, 1994; Matthes et al., 2002).

#### **5-3-1-1. Estimation of Pb released by roof/wall runoff and corrosion rate from B-580**

The amount of Pb released by roof/wall runoff from the APHIS building was estimated employing some assumptions listed below: (a) Maryland annual rainfall was assumed as 106 cm/yr (U.S. Geological Survey, 1999) and it was constant throughout the years of building age (as of November 2009) (b) Pb concentration of the roof/wall runoff was assumed to be constant throughout the years with the value equal to the average monitored Pb concentration (7.6 mg/L); (c) The building roof consist of two metal roofs in each side and one concrete roof between the two metal roofs. Actual roof area for each metal roof is 193 m<sup>2</sup> based on 10.06 m (33ft) width and 19.2 m (63ft) length. Therefore, actual total metal roof area is 386 m<sup>2</sup>. However, the concrete roof should be also included due to difficulty in separating two different roof runoff. Therefore, the roof perpendicular area is approximately 600 m<sup>2</sup> [19.2 m long × 31.1 m=597 m<sup>2</sup>]; (d) building age of 15 years (as of November 2009; built in November 1994). Based on the above assumptions and information, total mass of Pb leached to the environment can be calculated.

$$\begin{aligned}
 &= \left(106 \frac{cm}{yr}\right) \times (600 \text{ m}^2) \times (15 \text{ yr}) \times \left(7.6 \frac{mg}{L}\right) \times \left(\frac{1m}{100 \text{ cm}}\right) \times \left(\frac{1000L}{m^3}\right) \times \left(\frac{1kg}{1000000 \text{ mg}}\right) \\
 &= 72.5 \text{ kg Pb}
 \end{aligned}
 \tag{5-3}$$

Average Pb runoff rate was also estimated as below. In addition to the assumption above, the following assumption is made as well: (a) roof/wall area covered by the Pb/Cu

metal sheets were uniformly corroded throughout the whole area and time (total roof/wall area ~ 500 m<sup>2</sup> based on Building design: see Appendix B4 – B6)

The average Pb runoff rate:

$$= 72.5 \text{ kg Pb} \times \left( \frac{1}{500 \text{ m}^2} \right) \times \left( \frac{1}{15 \text{ yr}} \right) \times \left( \frac{1000 \text{ g}}{1 \text{ kg}} \right) = 9.67 \frac{\text{g}}{\text{m}^2 \cdot \text{yr}} \quad (5-4)$$

The atmospheric corrosion rate for roof/wall metal sheets was estimated based on the assumptions above and: (a) metal sheets used for roofs and walls of B-580 were assumed as pure Pb sheets in spite of high Cu content (density = 11.34 g/cm<sup>3</sup>); (b) All Pb corrosion products were leached by roof/wall runoff.

Pb corrosion rate:

$$\begin{aligned} &= 72.5 \text{ kg pb} \times \left( \frac{1}{500 \text{ m}^2} \right) \times \left( \frac{\text{cm}^3}{11.34 \text{ g}} \right) \times \left( \frac{1}{115 \text{ yr}} \right) \times \left( \frac{1000 \text{ g Pb}}{\text{kg Pb}} \right) \times \left( \frac{\text{m}^2}{10000 \text{ cm}^2} \right) \left( \frac{10000 \text{ } \mu\text{m}}{\text{cm}} \right) \\ &= 0.85 \text{ } \mu\text{m/yr} \end{aligned} \quad (5-4)$$

The estimated Pb corrosion rate (0.85  $\mu\text{m/yr}$ ) of the roof/wall metal sheets from the APHIS building is within or very close to the range of previously reported Pb corrosion rates as previously shown in Table 3-11 (0.4-1.9  $\mu\text{m/yr}$  for rural areas and 0.5-0.7  $\mu\text{m/yr}$  for urban areas) (Graedel, 1994).

### 5-3-2. Characterizing soil around the APHIS building; Phase 1

Most soil samples showed relatively low Pb concentrations, with the exception of surface samples A0, A1, B, and C (>100 mg/kg) which were taken from the locations



very close to the building (Figure 5-1). The A0 organics/soil sample collected from a gravel layer right next to the building showed a much higher Pb level (8800 mg/kg Pb) than the other samples (Table 5-2). Furthermore, the highest Cu concentration was also noted from A0 (665 mg/L), while most of the samples showed relatively low Cu levels. This suggests that most of roof/wall runoff drains and infiltrates into the gravel strip adjacent to the building with little flow/runoff farther from the wall to the soil/grass surface.

The Zn concentration of A0, however, was not significantly higher than other samples. This is probably because the Zn concentration of roof/wall runoff from the building is lower than the Pb and Cu concentrations (Table 5-2). Table 5-3 shows that the ratios of Pb, Cu, and Zn concentrations in the A0 soil/organics sample in the gravel layer compared to those of the roof/wall runoff samples were similar. This also suggests that heavy metals detected in the samples from the gravel layer originated from the roof/wall runoff.

The ratio of Cu concentrations in the A0 soil/organics sample in the gravel layer to that of the roof/wall runoff was somewhat lower than the ratio of Pb and Zn. Furthermore, the soil samples taken from the spots very close to the building (e.g., A0, A1, B and C) did not show higher Cu concentrations than the other soil samples (i.e., background soil Cu concentration). This suggests that less Cu is retained by the soil (or higher Cu mobility in soil) as compared to Pb and Zn. Similar results were also found by Mason et al. (1999) in their heavy metal behavior study during roof runoff infiltration, suggesting strong Pb and Zn retention in the upper soil layers but high Cu, Cd and Cr

mobility with limited retention in soil. The high mobility of Cu in soil was explained by complexation by ligands in solution, due to the high affinity with organic ligands.

Table 5-2. Pb, Cu, and Zn Concentrations in soil around the APHIS building (collected on April 17<sup>th</sup> and May 1<sup>st</sup> 2008). (Refer to Figure 4-3 for site map)

Sample Location	Soil ID	Pb conc. (mg/kg)				Cu conc. (mg/kg)				Zn Conc. (mg/kg)			
		Soil Depth (cm)				Soil Depth (cm)				Soil Depth (cm)			
		0-7.5	7.5-15	15-30	>30	0-7.5	7.5-15	15-30	>30	0-7.5	7.5-15	15-30	>30
Back yard	A0	8804 <sup>a</sup>				665 <sup>a</sup>				63 <sup>a</sup>			
	A1	119	51	19	7	13	16	10	8	38	26	19	12
	A2	21	12	7	6	13	20	22	30	39	47	33	31
	A3	18	19	8	-	12	13	14	-	41	41	26	-
	A4	8	8	6	5	12	12	14	10	35	25	11	14
	A5	25	17	8	5	13	12	9	23	44	40	13	12
	A6	19	19	7	8	11	14	9	10	41	43	14	14
Front yard	B	161	15	21	-	22	19	13	-	43	40	22	-
Side yard	C	102	18	7	7	17	18	16	16	40	42	22	25
Swale 2	D1	51	24	9	10	28	-	-	-	653	-	-	-
	D2	93				14	15	17	17	43	35	33	34
Swale 1	E0	15	8	6	5	12	10	9	10	36	16	11	14
	E1	60	-	-	--	20	-	-	--	56	-	-	--
	E2	11	-	-	--	21	-	-	-	57	-	-	-
Culvert/Creek	F0	5	-	-	-	7	-	-	-	25	-	-	-
	F1	4	4	7	8	5	6	9	13	19	20	30	25
	F2	7	6	9	7	5	6	8	12	16	20	29	23
	F3	7	-	-	-	8	-	-	-	44	-	-	-

<sup>a</sup> soil/organics samples from <30cm depth of the gravel layer.

Table 5-3. Comparison of heavy metal concentrations between the A0 soil samples and the roof/wall runoff samples.

	A0 Soil/Organics Samples from Gravel layer (A)	Runoff samples from Rooftop/wall (B)	Ratio of A to B
Pb	8804 mg/kg	7.75 mg/L	1136
Cu	665 mg/kg	0.80 mg/L	831
Zn	63 mg/kg	0.055 mg/L	1145

Regulatory heavy metal remediation guidance values in residential soils for 30 states in the U.S. was compiled by Petersen et al. (2006) and the values for the state of Maryland, and mean values and ranges of three heavy metal (Pb, Cu, and Zn) values from 30 states are presented in Table 5-4. The total Pb concentration (8804 mg/kg) in soil/organic samples from the A0 gravel layer significantly exceeded the Maryland Pb remediation guidance value (400 mg/kg), which suggests possible risks and remediation need for the soil/organic matter in the gravel layer around the APHIS building.

Table 5-4. Heavy metal guidance values in residential soils (adapted from Peterson et al., 2006).

	Pb (mg/kg)	Cu (mg/kg)	Zn (mg/kg)
Maryland (MDE 2001)	400	3,100	23,000
Average <sup>a</sup>	350	3,700	28,000
Range <sup>b</sup>	61-500	25-20,000	20-170,000

<sup>a</sup> Mean value and <sup>b</sup> minimum to maximum value of heavy regulatory guidance values from 30 states.

Interestingly, relatively high Zn (653 mg/kg) was detected from the D1 surface sample collected from the middle of Swale 2, which is probably due to high Zn levels in the stormwater runoff from the asphalt pavement area, including the parking lot and

driveway close to the swale (See Figure 5-1). Automobile tires have been identified as a major source of Zn in stormwater runoff because Zn is used as a vulcanizing agent in automobile tire manufacturing (Davis et al., 2001a). High extracted Zn (3400 g/kg as a mean value) from tire wear was observed through extraction using synthetic stormwater (pH 4.2-4.4) in the controlled study by Davis et al. (2001a), which estimated as high as 58% contribution of Zn in urban residential stormwater runoff by tire wear. However, much lower extracted Pb (17 mg/kg), Cu (5 mg/kg), and Cd (1 mg/kg) were reported from tire wear. This explains why Pb (51 mg/kg) and Cu (28 mg/kg) levels from the D1 surface sample collected from the middle of swale 2 are lower than the Zn (653 mg/kg) level, although they are somewhat higher than most of other soil samples (i.e., background level), except for surface samples taken from spots very close to the APHIS building.

Further study is needed to investigate the degree of heavy metal contamination of the soil under the gravel layer and heavy metal movement through the soil in order to address heavy metal contamination risks to surface and ground water as well as soils around B-580.

Soil at the suggested drainage pipe discharge from the French drain system was not rich in Pb suggesting that Pb was collected within the French drain and drainage system.

#### **5-4. Summary and Conclusions**

Identifying diffuse sources and characterizing runoff from the pollution sources, in addition to investigating the degree of water pollution around these sources, is very important to address risks from stormwater runoff. Monitoring and characterizing roof/wall runoff from the APHIS building was the first phase in a study to address risks of heavy metal contamination in nearby soils and waters. The heavy metal concentration of soil around the APHIS building was also monitored to investigate the degree of heavy metal contamination of soil by roof/wall runoff and infiltration.

Specifically, the roof/wall runoff for the APHIS building demonstrated very high Pb and Cu concentrations. The Pb concentrations from the roof/wall runoff samples (4.10 – 11.29 mg/L as total) were much greater than typical Pb levels in highway/urban runoff (5-200 µg/L) and roof runoff (~90 µg/L as average), summarized in Table 3-6, 3-7a and 3-7b. The roof/wall runoff samples also showed higher Cu concentrations than that of typical highway (5-200 µg/L) and roof (~200 µg/L as average) runoff (Boller, 1997; Davis et al., 2001a). However, the Zn concentration of the roof/wall runoff (32-110 µg/L) was lower than that of typical highway (20-5000 µg) and roof (~400 as average) runoff; Zn is usually present at the highest concentration among trace heavy metals in runoff.

Most of soil samples showed relatively low Pb concentrations, with the exception of surface samples A0, A1, B, and C (>100 mg/kg) which were taken from locations very close to the building (Figure 5-1). The A0 organics/soil sample collected from a gravel layer right next to the building showed a much higher Pb level (8800 mg/kg Pb) than the other samples (Table 5-2). Furthermore, the highest Cu concentration was also noted

from A0 (665 mg/L), while most of the samples showed relatively low Cu levels. This suggests that most of roof/wall runoff drains and infiltrates into the gravel strip adjacent to the building with little flow/runoff farther to the soil/grass surface. Additional study is needed to investigate the degree of heavy metal contamination of the soil under the gravel layer and heavy metal movement through the soil in order to address heavy metal contamination risks to surface and ground water, as well as the fate of runoff Pb in the drainage system and soils around the APHIS building.

## CHAPTER 6. COLUMN STUDY OF HEAVY METALS REMOVAL USING INDUSTRIAL BYPRODUCTS.

### 6-1. Introduction

Composts and mineral-amended composts have been widely used to remediate metal-contaminated soils (Brown et. al, 2003; van Herwijnen et. al, 2007). However, little work has been completed on heavy metal removal from aqueous runoff solutions using compost. A bioremediation mat is suggested in this research to remove heavy metals (lead, copper and zinc) from storm water runoff from a studied site. The mat is an engineered mixture of sand/compost/waste byproduct sorption media to adsorb and/or precipitate dissolved pollutants and trap and/or filter out large suspended particulates. Use of industrial inorganic by-products as well as agricultural organic by-products (compost) will provide economic advantages in removing heavy metals from runoff from non-point sources.

In this chapter, feasibility of varied Biomat media for removing three different heavy metals (Zn, Pb, and Cu) through simultaneous competitive sorption/desorption behavior was evaluated based metal sorption performance, desorption behavior, and other water quality parameters. Finally, the removal and life time capacity for each Biomat media type were estimated for each metal, based on the metal results and flow data at each metal breakthrough.

These studies investigated heavy metal removal capacity and design parameters for Biomat media. This work also evaluated the feasibility and flexibility of the Biomat for removing heavy metals leached from various non-point sources under variable conditions.



## **6-2. Methods and Materials.**

Experimental materials and methods were designed and prepared based on the objective of each research phase as described in the following: (1) heavy metal removal efficiency and capacity of different composts and inorganic by-product media as a Biomat media candidate, through column adsorption and leaching study; (2) monitoring other important water quality parameters (phosphorus, turbidity, and Cr) which can be discharged from the media during heavy metal removal; (3) investigating the feasibility of the various Biomat media based on extractability of previously adsorbed metals through column leaching study.

### **6-2-1. Column design and setup, and media preparation – Phase 2**

Five 12.7 cm-long  $\times$  2.54 cm i.d. Plexiglas columns were used for compost/waste by-product evaluation and selection study (Figure 6-1). The effluent port (top) of the column was sealed by a rubber stopper with an outlet connection installed. The influent port (bottom) was a Plexiglas plate with seventeen holes to promote even distribution of flow across the cross-sectional area of the column. This plate was connected by a 1 cm piece of Plexiglas column to a solid lower base plate, creating the reactor underdrain, which had an inlet connection installed in the side. The effluent and influent ports were separated from the packing media by stainless steel screens.

ASTM 20-30 underground silica sand (US Silica Company, Ottawa, IL) was used as the primary porous media in the columns. The relatively large and uniform particle size (97% of the sand is between 0.65 and 0.85 mm size) of the sand was expected as an appropriate primary media for high hydraulic conductivity (See Appendix 1 for more detailed sand information). The sand was washed using tap water until most of small fine

particles were removed and then rinsed well with deionized (DI) water. The rinsed sand was then soaked in DI water for more than 24 hours and the supernatant was analyzed for heavy metals. The rinsing procedure with DI water was repeated until the dissolved heavy metal concentration was less than 10 µg/L for Pb and Cu and 50 µg/L for Zn.

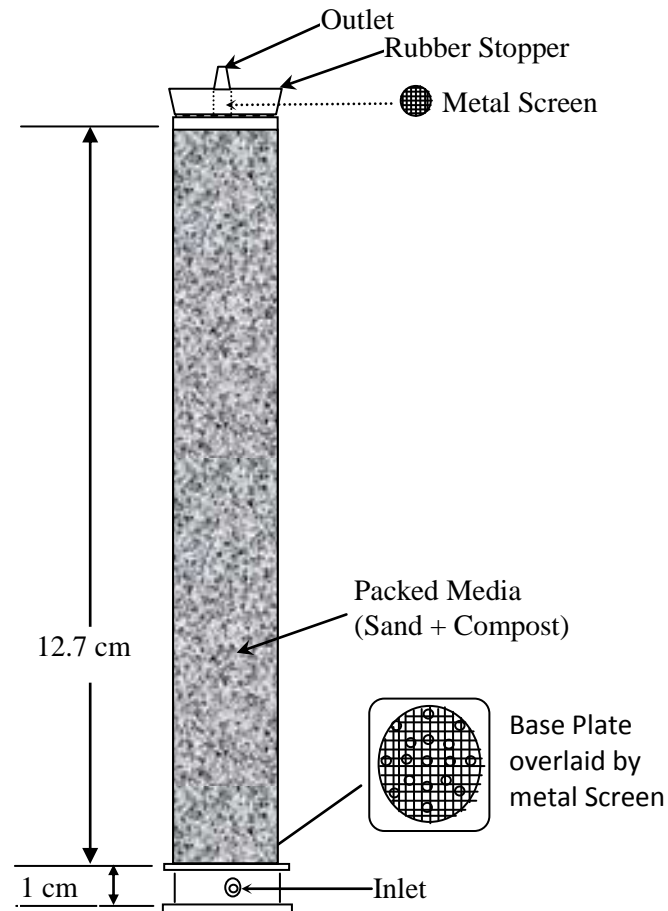


Figure 6-1. Column reactor design for column heavy metal sorption study.

Two different types of compost, manure compost and grass + food waste compost, were collected from the USDA-ARS Compost Research Facility site at the

Beltsville Agricultural Research Center in Beltsville, MD (Figure 6-2). The composts were prepared by sieving less than 2 mm (#10 US sieve size).

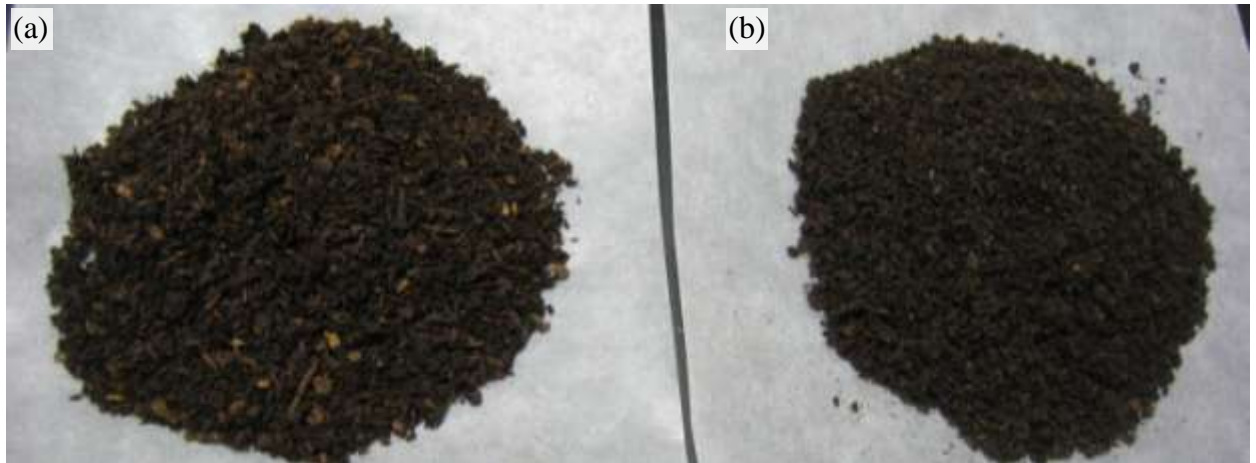


Figure 6-2. Composts used in the column experiment: (a) Manure compost, and (b) Grass/Food waste compost.

The microstructural surface images of the composts was investigated using Field Emission Scanning Electron Microscopy (SEM, JEOL JSM 6500F). Differently magnified SEM images in series are shown in Figure 6-3.

Two different types of inorganic waste by-products, steel slag and “Hubcutter heavies” were evaluated in the column study (Figure 6-4). Steel slag was obtained from a Baltimore steel manufacturer and Hubcutter heavies was obtained from a railroad wheel company (Griffin Wheel Company, Chicago, IL). The byproduct materials were prepared by air drying and sieving to  $<0.5$  mm (35 mesh).

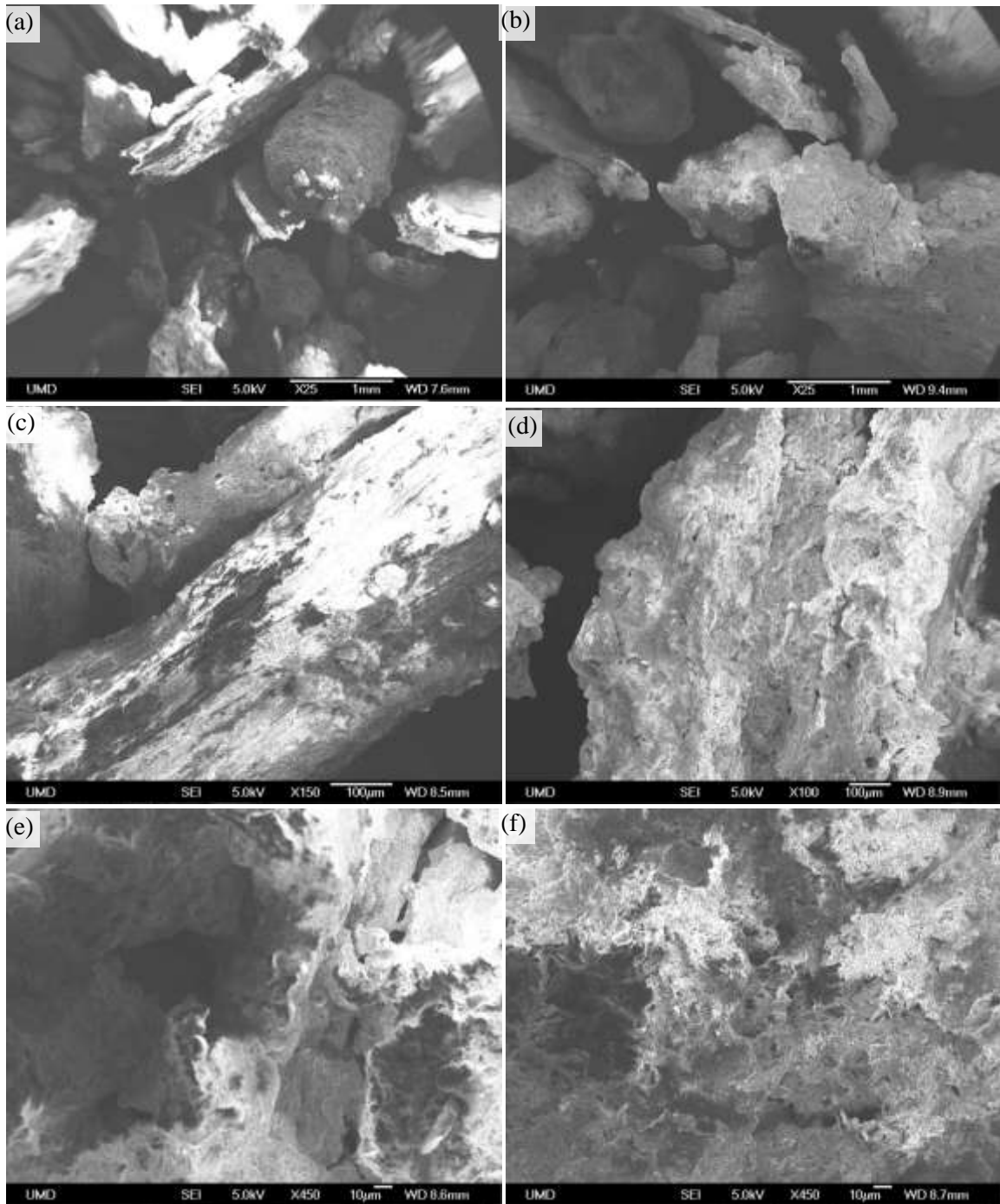


Figure 6-3. Scanning electron micrographs for manure compost (MC) and grass/food waste compost (GC): (a) MC with 25 times magnification; (b) GC with 25 times magnification; (c) MC with 100 times magnification; (d) GC with 150 times magnification; (e) MC with 450 times magnification; (f) GC with 450 times magnification

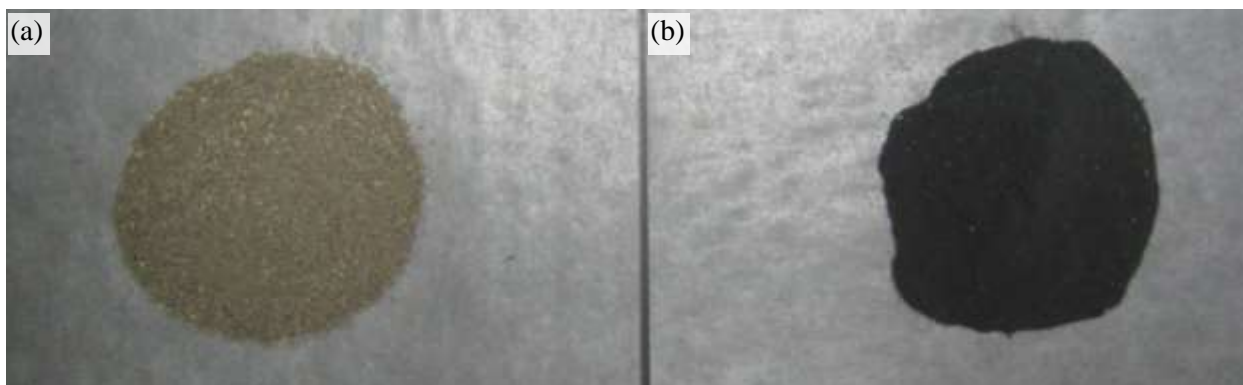


Figure 6-4. Byproduct materials used in the column experiment; (a) steel slag, and (b) hubcutter heavies

The chemical properties of the composts and waste byproduct materials are summarized in Table 6-1. The pH of composts was measured in 1:4 ratios (materials to deionized water, dry mass to volume) using a pH meter with a glass electrode after 30 minutes (McLean, 1982). Electrical conductivity (EC) was determined using a YSI model 35 conductivity meter (Yellow Springs, OH) in 1:2 ratios by stirring samples vigorously and letting stand for 30 minutes. The byproduct pH and EC were also measured in 1:2 ratios (dry mass to volume) as described above. Total metal content in the composts and byproduct materials was determined by aqua regia digestion (McGrath and Cunliffe, 1985), along with standard soils and controls.

Five columns, 10% manure compost + sand (MC10), 10% grass/food waste compost + sand (GF10), 25% grass/food waste compost + sand (GF25), 25% grass/food waste compost + sand + steel slag (GFS25), and 25% grass/food waste compost + sand + hubcutter heavies (GFH25) were set up to screen and evaluate potential composts and waste by-products to remove heavy metals from rooftop/wall runoff. The composition of packed media in the columns is summarized in Table 6-2. The measured mass of

compost, sand and byproduct sample to get the mass percent shown in Table 6-2 was uniformly mixed and packed in a column.

Table 6-1 . Chemical properties and total metal content of manure compost, grass/food waste compost, steel slag, and hubcutter heavies.

Parameters	Manure compost	Grass/Food waste compost	Steel Slag	Hubcutter heavies
pH	7.87	6.78	12.19	4.97
Electrical Conductivity, mS cm <sup>-1</sup>	7.58	7.98	5.19	0.11
Water Content (%)	44.0	46.3	2.32	<0.1
Loss on ignition (%) <sup>a</sup>	47.8	40.8	1.4	<0.1
Bulk density (g/cm <sup>3</sup> )	0.56 (wet)	0.68 (wet)	1.62 (dry)	-
Fe, g kg <sup>-1</sup>	9.16	10.16	182	862
Oxalate extractable Fe, g kg <sup>-1</sup>	1.22	1.96	39.5	192
Mn, g kg <sup>-1</sup>	0.48	0.74	27.6	4.45
Oxalate extractable Mn, g kg <sup>-1</sup>	0.16	0.38	2.32	0.69
Al, g kg <sup>-1</sup>	5.5	3.9	7.8	<0.1
Ca, g kg <sup>-1</sup>	11.4	13.8	159	0.0031
Zn, mg kg <sup>-1</sup>	172	140.0	113	9.3
Cu, mg kg <sup>-1</sup>	34.7	28.0	24.0	253
Pb, mg kg <sup>-1</sup>	12.6	15.3	35.8	4.9
Cr, mg kg <sup>-1</sup>	19.4	23.8	877	103
Cd, mg kg <sup>-1</sup>	0.76	0.71	2.54	1.04
Ni, mg kg <sup>-1</sup>	26.6	31.3	32.7	261
P, mg kg <sup>-1</sup>	5569	6096	-	-

<sup>a</sup> Loss on ignition at 550 °C and water content based on oven dry weight at 103-105 °C

Table 6-2. Composition of packed media in columns used for column study.

Column ID	Type of Compost	*Percent of compost	*Percent of sand	Type of byproduct	*Percent of byproduct
MC10	Manure	10% (9.70 g)	90% (87.30 g)	-	-
GF10	Grass + food waste	10% (9.70 g)	90% (87.30 g)	-	-
GF25	Grass + food waste	25% (19.7 g)	75% (59.10g)	-	-
GFS25	Grass + food waste	25% (19.7 g)	70% (55.16g)	Steel Slag	5% (3.94 g)
GFH25	Grass + food waste	25% (19.7 g)	70% (55.16g)	Hubcutter Heavies	5% (3.94 g)

\* Percent and mass of packed compost, sand, byproduct media are calculated based on dry weight.

The column study was more focused on evaluation of the grass/food waste compost media than manure compost media due to superior metal removal from grass/food waste compost, based on preliminary batch sorption results (data not shown). Therefore, more grass/food waste based columns with different media variation (4 columns) were set up, while a manure compost column was studied to clarify heavy metal removal performance employing a different manure type.

### 6-2-2. Column Sorption Study – Phase 2

Synthetic runoff was employed in the column experiments to provide controlled input conditions. The synthetic runoff was made using DI water with the source chemicals listed in Table 6-3. The water quality parameters and concentrations were selected based on previously monitored runoff characteristics (see Table 6-1). After normalization to room temperature, proper volumes of stock solutions of PbCl<sub>2</sub> (J.T. Baker, Phillipsburg, NJ), ZnSO<sub>4</sub>·7H<sub>2</sub>O (J.T. Baker, Phillipsburg, NJ), CuSO<sub>4</sub> (Fisher

Scientific, Fair Lawn, NJ), and  $\text{CaCl}_2 \cdot 2\text{H}_2\text{O}$  (Aldrich, Milwaukee, WI) were added to the DI water to produce the concentrations listed in Table 6-3.

Table 6-3. Characteristics of the synthetic runoff used in the column study

	Target value	Source chemical
pH	5.5-5.8	HCl or NaOH
Total Dissolved Solids (mg/L)	172	$\text{CaCl}_2$
Pb (mg/L)	10.0 <sup>a</sup>	$\text{PbCl}_2$
Zn (mg/L)	1.0 <sup>a</sup>	$\text{ZnSO}_4 \cdot 7\text{H}_2\text{O}$
Cu (mg/L)	1.0 <sup>a</sup>	$\text{CuSO}_4$

<sup>a</sup> Dissolved Concentration

All five columns were operated at room temperature ( $26 \pm 2$  °C). Synthetic stormwater runoff was introduced into each column in an upflow mode at a flow rate of 10 cm/hr (0.845 mL/min). This flow rate was based on a 1.5 cm total rainfall event over a 6-hour duration assuming a Biomat media sized at 2% of roof area and a rational method runoff coefficient of 0.8 (Davis et al., 2001b).

All samples were prepared, analyzed, and stored by following methods in *Standard methods for the examination of water and waste water* (APHA et. al, 1995). Dissolved heavy metal concentrations (Pb, Cu, and Zn) in the samples were measured using flame or graphite furnace atomic absorption spectrophotometry (Perkin Elmer 5100PC with Perkin Elmer Zeeman Furnace module 5100ZL) after filtering the samples through 0.2  $\mu\text{m}$  pore size, 25 mm diameter membrane disk filters (Standard Method 3111, 3113). Total heavy metal concentrations (Pb, Cu, Zn, and Cr) of the samples were



also monitored periodically as described above after nitric acid digestion of samples following Standard Method 3030 E (APHA et. al, 1995).

Total phosphorus concentration was determined via an ascorbic acid method (Standard Method 4500-P E) or stannous chloride method (Standard Method 4500-P D) by measuring absorbance of color developed via a spectrophotometer at a wavelength of 882 nm or 690 nm, respectively (APHA et. al, 1995).

### **6-2-3. Column Leaching (Desorption) Study – Phase 2**

After 28810 cm of synthetic roof/wall runoff was treated (simulating over 5 years of runoff at B-580 based on average Maryland precipitation of 106 cm/yr), a leaching study was started by introducing DI water containing only  $\text{CaCl}_2$  (to produce 172 mg/L total dissolved solids) with pH of 5.6. All five columns were operated at the same flow rate and conditions as with the previous adsorption study described above, until the study was terminated at 57115 cm of cumulative treated flow. All samples were analyzed as described above in Section 6-2-2.

## **6-3. Results and Discussion**

### **6-3-1 Column sorption study for compost media selection and evaluation: Phase 2**

Based on the column sorption study, as shown in Figure 6-5 and summarized in Table 6-4, the 10% grass/food waste compost (GF10) exhibited higher capacity of heavy metal removal than the 10% manure compost (MC10), which showed earlier breakthrough for all three heavy metals (Pb, Cu and Zn). This is probably due to the greater surface area of the grass/food waste compost as observed in the microstructural surface

images (Figure 6-2) by field emission SEM, and possibly greater humic substance content in the composted grass, with a variety of functional groups, compared to manure compost. It is stated by Smidt et al. (2008) that composting with yard/kitchen waste generally produces more humic substances than that with other materials possibly due to the higher content of aromatic compounds in plant materials. They also concluded through their co-composting study with different lignin sources that grass or leaves (i.e., lignified compost materials) are more readily converted to humic substances than wood in which lignin is bound to the wood wall ultrastructural matrix. Furthermore, more small pores ( $<10\text{ }\mu\text{m}$ ) on more variably shaped surface were observed in the grass/food waste compost (Figure 6-6b), compared to that of the manure compost (Figure 6-6a).

The initial effluent pH from MC10 was higher than that from GF10 (Figure 6-7) as expected due to the higher pH of manure compost than that of grass/food waste compost (Table 6-1). Nonetheless, consistently higher effluent pH from GF10 was observed since 3605 cm of accumulated treated flow, suggesting that grass/food waste compost has higher acid buffering capacity compared to the manure compost. This higher acid buffering capacity from GF10 also played a role in removing heavy metals through sorption and precipitation by keeping the water pH high. Adsorption of Pb and Cu displaces protons from the compost matrix.

As expected, the columns containing the higher ratio of the grass + food waste compost (25% of dry mass ratio, GF25) showed better metal removal capacity than the lower ratio (10% of dry mass ratio, GF10) for all the three metals. Specifically, GF25 demonstrated around 1.8-1.9 times higher removal compared to GF10 for each metal in terms of the accumulative treated flow at the start of breakthrough.

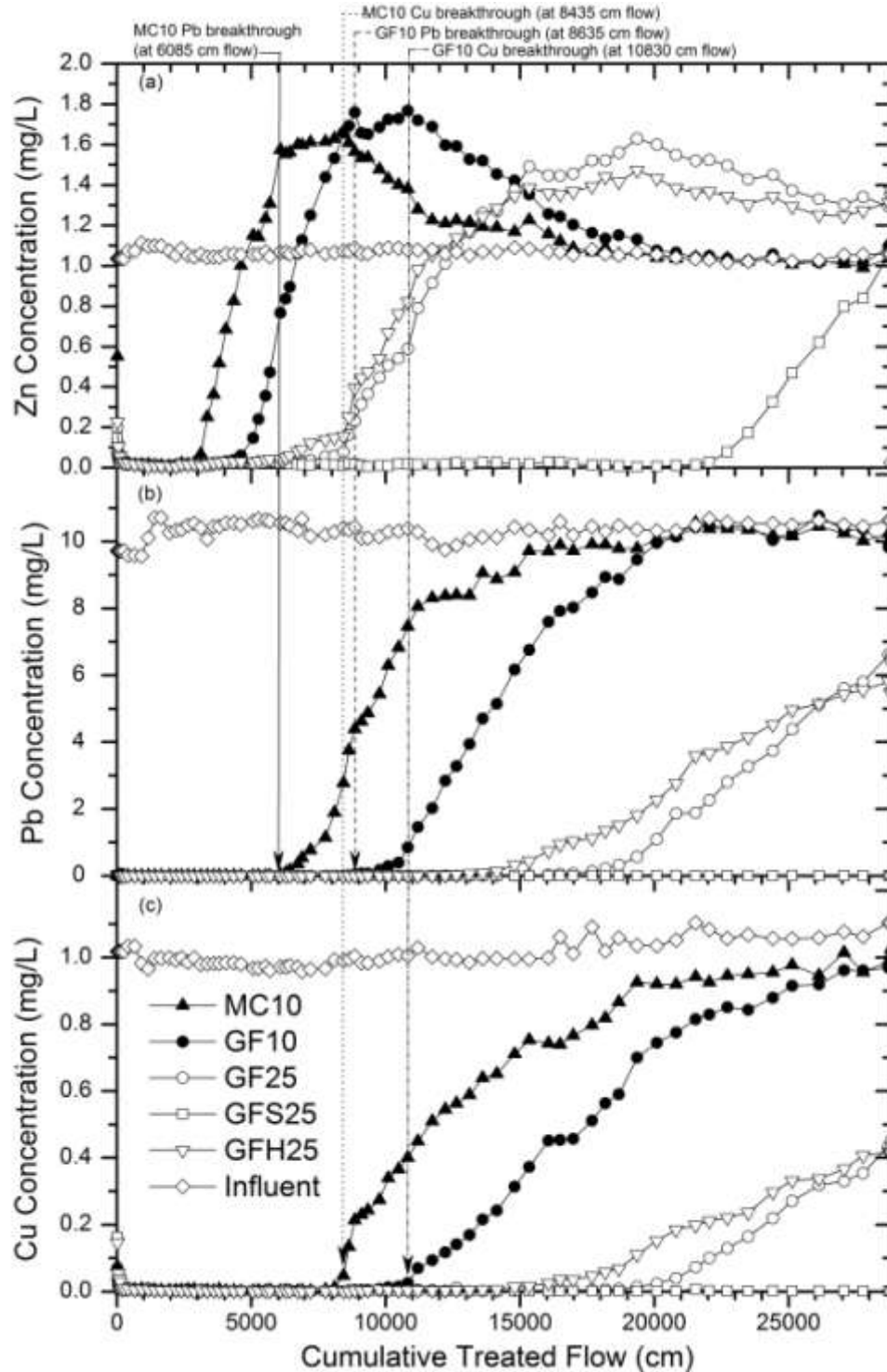


Figure 6-5. Dissolved effluent metal concentration from different Biomat media column as a function of cumulative treated flow during column sorption study; breakthrough curve for (a) Zn, (b) Pb and (c) Cu: 10% Manure compost + sand (MC10); 10% Grass/Food waste compost + sand (GF10); 25% Grass/Food waste compost + sand (GF25); 25% Grass/Food waste compost + Steel slag + sand (GFS25); and 25% Grass/Food waste compost + Hubcutter heavies + sand (GFH25).

Table 6-4. Cumulative treated flow at start of breakthrough for Zn, Pb, and Cu for each Biomat media column: 10% Manure compost + sand (MC10); 10% Grass/Food waste compost + sand (GF10); 25% Grass/Food waste compost + sand (GF25); 25% Grass/Food waste compost + Steel slag + sand (GFS25); and 25% Grass/Food waste compost + Hubcutter heavies + sand (GFH25).

<u>Cumulative treated flow and effluent pH at breakthrough start</u>						
<u>Columns</u>	<u>Zn<sup>a</sup></u>		<u>Pb<sup>b</sup></u>		<u>Cu<sup>b</sup></u>	
	Cumulative Flow (cm)	Effluent pH	Cumulative Flow (cm)	Effluent pH	Cumulative Flow (cm)	Effluent pH
MC10	3125	7.2	6085	6.8	8435	6.1
GF10	4615	7.0	8855	6.5	10830	6.2
GF25	8435	6.9	16065	6.5	20095	6.1
GFS25	22725	7.1	NR <sup>c</sup>	NR <sup>c</sup>	NR <sup>c</sup>	NR <sup>c</sup>
GFH25	6435	6.9	12640	6.6	16065	6.1

<sup>a</sup> Cumulative flow at concentration > 50 ppb (2× detection limit)

<sup>b</sup> Cumulative flow at concentration > 20 ppb (4× and 10× detection limit for Pb and Cu, respectively)

<sup>c</sup> Breakthrough not reached

Use of steel slag as an additive (GFS25) in the media increased the metal removal capacity significantly for all three metals. This significant enhancement of heavy metal sorption by steel slag addition can be explained by buffering against pH decrease due to high CaO and MgO content as well as heavy metal adsorption by high amorphous Fe minerals as represented by oxalate extractable Fe in steel slag (Table 6-1 and Figure 6-7).

Nonetheless, in spite of high amorphous Fe content in hubcutter heavies, GFH25 column did not demonstrate any heavy metal sorption enhancement but, rather, slight decrease of metal sorption capacity was observed in GFH25 compared to GF25. This is likely due to acidity produced by hubcutter heavies material and therefore, pH decrease, demonstrating the significance of pH on heavy metal sorption capacity of compost (Table 6-1 and Figure 6-7).

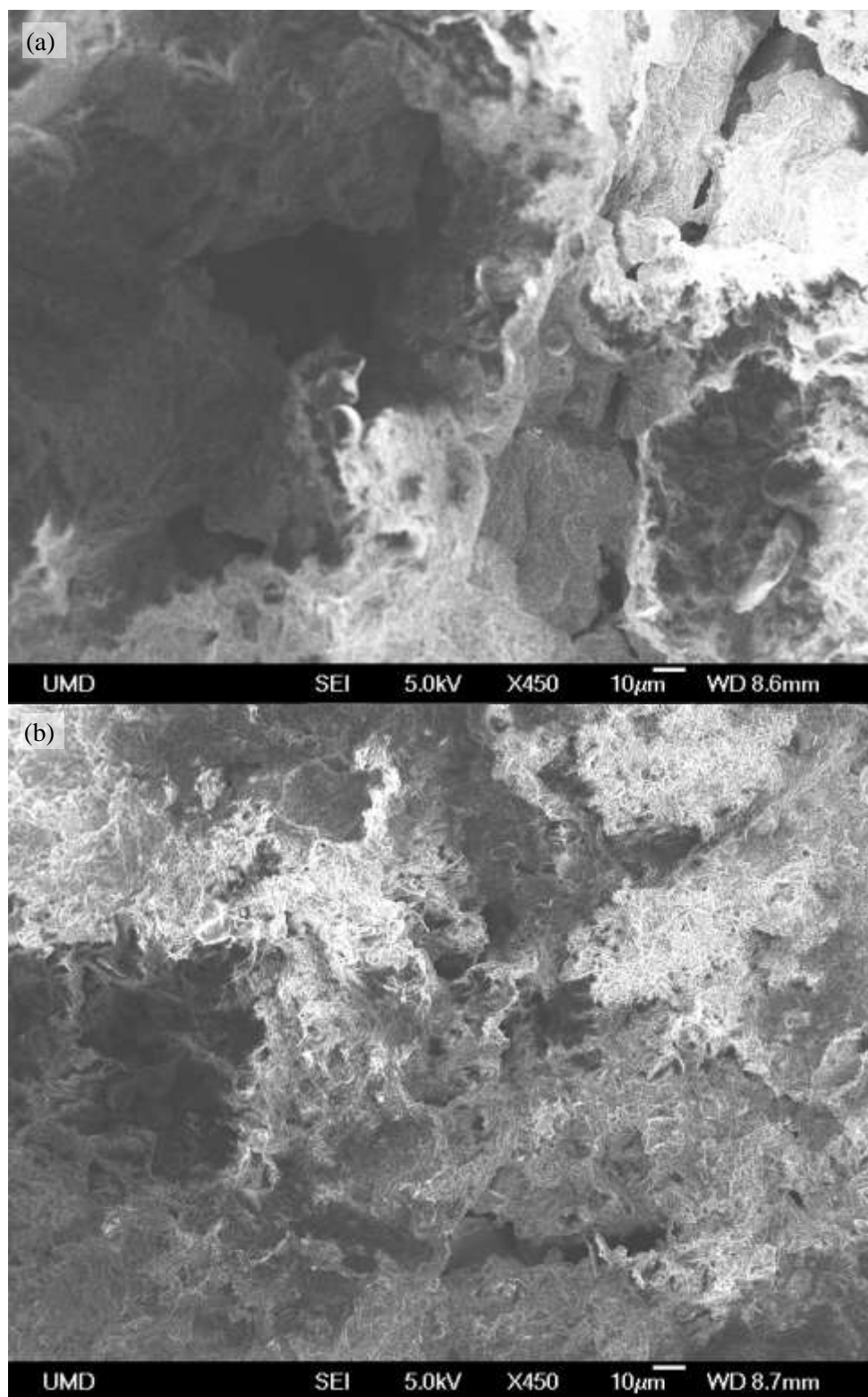


Figure 6-6. Scanning electron micrographs for (a) Manure compost and (b) Grass/Food waste compost.

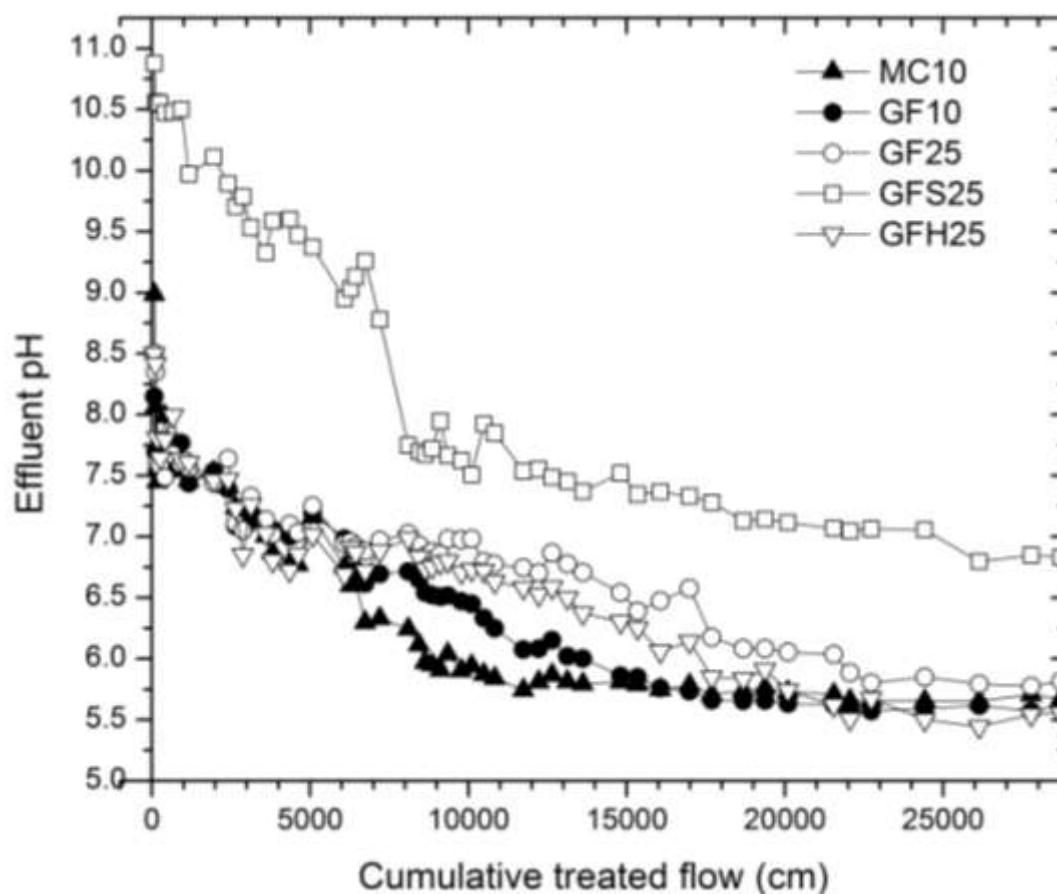


Figure 6-7. Effluent pH change for different media during sorption column study: 10% Manure compost + sand (MC10); 10% Grass/Food waste compost + sand (GF10); 25% Grass/Food waste compost + sand (GF25); 25% Grass/Food waste compost + Steel slag + sand (GFS25); and 25% Grass/Food waste compost + Hubcutter heavies + sand (GFH25).

As cumulative treated effluent volume increased, effluent pH of all media columns decreased relatively fast initially and decreased slowly down to 6.8 for GFS25, and around 5.6 to 5.8 for the other columns during the rest of sorption study (Figure 6-7). This pH decrease is likely due to the acidity of the influent as well as proton release from compost functional group displaced by heavy metals (Pb, Cu and Zn) through ion exchange. Yu et al. (2000), through their heavy metal sorption batch study using sawdust, proposed ion exchange as a possible mechanism for pH decrease, suggesting that heavy metal ions bind with hydroxylic and oxylic groups of the phenolic compounds,

including lignin and tannin, major components in sawdust and release two hydrogen ions into solution. They verified their hypothesis showing that the theoretical pH based on Cu concentration change through adsorption on sawdust is in good agreement with actual pH of the final solution. Earlier metal adsorption study on peat by Buzl et al. (1976) also suggested ion exchange as the adsorption mechanism, showing similar equivalent of metal uptake and hydrogen ion release.

As summarized in Table 6-4, effluent pH values at each metal breakthrough from all columns are relatively similar. Specifically, Zn breakthrough for all columns started at effluent pH around 7.0, while Pb and Cu demonstrated their breakthrough at around 6.5 and 6.1, respectively, although MC10 (the only manure compost based column) started its breakthrough at higher pH for Zn (7.2) and Pb (6.8) than the other columns. This may suggest that effluent pH measurement by simple onsite or offsite pH monitoring can be potentially used as prediction of compost treatment effectiveness longevity for specific metal saturation on each compost media used. Further study would be needed to evaluate effluent pH change on different Biomat operational conditions, such as flow rate at different precipitation intensity and duration, intermittent loading, dry periods between precipitation events and temperature.

After the Zn breakthrough for MC10 and GF10, the effluent Zn concentration increased until it surpassed the influent concentration (~1 mg/L) and demonstrated relatively constant maximum effluent Zn concentration at around 1.55-1.66 mg/L for MC10 and 1.65-1.77 mg/L for GF10. This is because Zn previously-adsorbed by the compost media was desorbed by preferable Pb and Cu adsorption and released to effluent at lower pH. As desorbable Zn was leached out, effluent dissolved Zn concentration

decreased to the influent Zn concentration (~ 1 mg/L) during the rest of the sorption study. A similar trend was also observed for GF25 and GFH25 although effluent Zn concentration did not decrease to influent Zn concentration until the end of the adsorption study, while the GFS25 column never reached breakthrough of Pb and Cu during the period of the adsorption study.

As shown in Table 6-5, a significant portion of Zn previously adsorbed on the media was released from MC10 (83%) and GF10 (80%) during the adsorption study. Consequently, minimal Zn was removed by the Biomat media during the sorption study, showing very low percent removal from the two columns (Table 6-5). Lower fractional Zn leaching from GF25 and GFH25 columns, and no desorption from GFS25 column during the adsorption study were noted simply because the experiments were ended before all the Zn desorbable by Pb and Cu in GF25, GFH25 and GFS25 was leached out. This Zn leaching from the Biomat compost media suggests that Pb and Cu not only outcompeted Zn for the available sorption sites, but also displaced the sorption sites on which Zn was sorbed. Furthermore, most of Zn was expected to adsorb on unspecific adsorption sites (outersphere adsorption) during the simultaneous competitive sorption with Pb and Cu, and therefore, significant portions of previously sorbed Zn were displaced by Pb and Cu (i.e., mainly through ion exchange) due to its weak binding on the media (Table 6-5).

The significant decrease of Zn adsorption capacity was also noted by Jang et al. (2005) through their batch adsorption study when Pb and/or Cu were simultaneously adsorbed on hardwood bark mulch. Nonetheless, approximately 17% and 20% of previously adsorbed Zn in MC10 and GF10, respectively, still remained in the column



media at the end of the adsorption study, suggesting possible inner sphere (specific) adsorption on inorganic constituents of the compost media or occlusion of the previously adsorbed Zn with organic constituents (Goto and Suyama, 2000). However, it was noted by Fontes et al. (2000) that Zn and Cd are more often immobilized by nonspecific sorption (i.e., electrostatic interactions with exchange sites), while Pb and Cu are more involved with specific sorption (i.e., covalent interactions) with minerals.

Table 6-5. Percent Zn released based on previously adsorbed Zn and percent Zn removed based on total Zn input from each column during adsorption study: Manure compost + sand (MC10); 10% Grass/Food waste compost + sand (GF10); 25% Grass/Food waste compost + sand (GF25); 25% Grass/Food waste compost + Steel slag + sand (GFS25); and 25% Grass/Food waste compost + Hubcutter heavies + sand (GFH25).

Column	MC10	GF10	GF25	GFS25	GFH25
Percent (%) Zn released (desorbed) based on previously adsorbed Zn	82.6	80.3	56.8	0	46.2
Percent (%) Zn removed based on total Zn input	2.7	4.1	15.2	87.7	17.6

Interestingly, Pb breakthrough for MC10 and GF10 columns started at the point at which the effluent Zn concentration stopped increasing (i.e., maximum Zn release) and showed relatively constant value, as shown with two arrows for MC10 (solid arrow) and GF10 (dashed arrow) in Figure 6-5. This suggests that Zn desorption (or Pb displacing adsorption) reached its maximum effect and, therefore, Pb started to leach. Furthermore, the effluent Zn concentration started to decrease (after showing relatively constant maximum Zn release) at the same time when Cu breakthrough for MC10 and GF10 columns started, as indicated by two arrows for MC10 (dotted arrows) and GF10 (dash dotted arrow) columns, respectively (Figure 6-5). This strongly suggests that Zn

desorption was directly related to Pb displacing Zn sorbed on the sites on which Zn once occupied. This were also observed in GF25 and GFH25 columns although the trend was not as clear as MC10 and GF10 columns, while GFS25 did not show this trend simply because neither Pb nor Cu breakthrough were reached during the period of the sorption study. This Zn desorption phenomenon during simultaneous competitive sorption/desorption with Zn and Pb will be discussed further in detail in Section 6-3.

For the influent metal concentrations and loading rate studied, Cu was most preferentially removed (sorbed) by all the Biomat media in terms of breakthrough in the order of  $\text{Cu}^{2+} > \text{Pb}^{2+} > \text{Zn}^{2+}$  (Figure 6-5 and Table 6-4). Furthermore, the Cu breakthrough demonstrated that the effluent Cu concentration increased slower than that of Pb, resulting in less steep Cu breakthrough curves than Pb. As a result, effluent Cu concentration reached to only 90% of influent concentration (around 1.0 mg/L effluent from 1.1 mg/L influent), suggesting that a portion of influent Cu was still being removed by the Biomat media at the end of the adsorption study. This also suggests that Cu is more strongly adsorbed than Pb on the compost media.

However, different influent molar concentrations used for Pb (~10 mg/L; 48  $\mu\text{mol/L}$ ) and Cu (~1 mg/L; 16  $\mu\text{mol/L}$ ) makes it difficult to make direct comparison of the adsorption affinity between Pb and Cu on the composts based on the column adsorption study (see Section 6-3-3 for further discussion). Furthermore, the effluent Pb concentration never exceeded the influent Pb concentration throughout the adsorption study for MS10 and GF10, while the effluent Cu concentration gradually increased and approached close to influent Cu concentration after the Pb breakthrough (Figure 6-5b and c), suggesting that no Pb desorption by Cu displacement occurred. Relatively smaller

cumulative flow difference between Pb and Cu breakthrough was also noted compared to that between Zn and Pb, suggesting that the adsorption affinity on the composts between Cu and Pb is relatively similar with order of  $\text{Cu}^{2+} > \sim \text{Pb}^{2+} \gg \text{Zn}^{2+}$  during the column study.

Batch heavy metal sorption studies using garden waste compost by Seelsaen et al (2007) suggested metal uptake affinity on compost in the order of  $\text{Pb}^{2+} > \text{Cu}^{2+} > \text{Zn}^{2+}$ , demonstrating 97% Pb, 93% Cu and 88 % Zn removal, respectively. Similarly, a batch metal adsorption study on hardwood bark mulch by Jang et al. (2005) also indicated that the order of both the initial metal removal rate and metal sorption capacity on a molar basis is  $\text{Pb}^{2+} > \text{Cu}^{2+} > \text{Zn}^{2+}$ , which follows the Irving and Williams series order of the stability of the metal complexes with organic ligands:  $\text{Pb}^{2+} > \text{Cu}^{2+} > \text{Ni}^{2+} > \text{Co}^{2+} > \text{Zn}^{2+} > \text{Cd}^{2+}$ . Heavy metal sorption study on tree fern by Ho et al. (2002) also noted favorable metal sorption in the order of  $\text{Pb}^{2+} > \text{Cu}^{2+} > \text{Zn}^{2+}$ . However, stability constants of metal-humic acid complexes studied by Pandey et al (2000) demonstrated the order of  $\text{Cu} > \text{Pb} > \text{Zn}$ , which is consistent with our column study results. Furthermore, electronegativity (see Table 3-10 in Chapter 3) may also influence the higher affinity of Cu on the Biomat media than the other two metals, as Pb showed higher affinity than Zn with the higher electronegativity (Antoniadis, et al., 2007).

It is important to note that metal removal capacity for a specific metal by the Biomat media depends on other metal concentrations in influent, which will be removed through competitive sorption processes. For example, Antoniadis et al. (2007) noted that  $K_d$  (effective distribution coefficient,  $\text{L kg}^{-1}$ : i.e., equilibrium partitioning of a metal between solid and liquid phase, measure of heavy metal mobility) of Zn and Ni when

alone were decreased by 2.3 and 2.6 times, respectively, when in competition with Cu, while Cu demonstrated only 18 and 17% decrease of its  $K_d$  when in competition with Zn and Ni, respectively. Therefore, considering that the sorption study was performed with three different metals (Zn, Pb, and Cu), the metal capacity estimated from the metal breakthrough curve (Figure 6-5) is most likely to be lower than that from the sorption with a single metal. In particular, Zn removal capacity when alone is expected to be much higher than it is estimated here based on the sorption study because retention capacity of the more mobile metals like Zn is much more affected by the less mobile metals like Pb and Cu (Jang et al., 2005; Antoniadis, 2007).

Effluent dissolved concentrations for all three metals from all columns before breakthrough were mostly less than their instrumentation detection limits (5  $\mu\text{g/L}$  for Pb, 2  $\mu\text{g/L}$  for Cu, and 25  $\mu\text{g/L}$  for Zn). This suggests that sorption rates of all three metals in the columns are fast enough not to limit the metal removal efficiencies (which are close to 100 %) for the metal loadings studied. In particular, Cu and Pb breakthrough for GFS25 were never observed during the adsorption study, suggesting that significant enhancement of metal removal capacity by steel slag addition was achieved by the GFS25 column due to high alkalinity/buffering as well as heavy metal adsorption by high amorphous Fe minerals as previously mentioned. Ion exchange has been mostly suggested as a major heavy metal removal mechanism for bio/cellulose/agricultural material and by-product sorbents including composts, sawdust, peat, mulches, and tree fern (Yu et al., 2000; Ho et al., 2002; Jang et al., 2004). However, in addition to ion exchange, pH-dependent specific/nonspecific metal adsorption on organic matter and Fe/Mn (oxy)hydroxides (Bradl, 2004), precipitation of metal oxy/hydroxides and metal

carbonates (Liu and Liu, 2003; Gibert et al., 2005), co-precipitation of heavy metals with Fe (oxy)hydroxides (Martinez and McBride, 1998; Gibert et al., 2005) may also be possible as a heavy metal removal mechanisms for GFS25 through steel slag addition. Consequently, significantly increased solution pH and high Fe contents in the media from steel slag addition are likely to increase heavy metal removal capacity for the GFS25 column.

The low heavy metal concentrations in treated effluent are important to minimize environmental risks. Specifically, the Federal action level for Pb in drinking water is 15  $\mu\text{g/L}$ , which is extremely low, compared to the action levels for Cu (1300  $\mu\text{g/L}$ ), and Zn (National secondary drinking water regulation standard of 5000  $\mu\text{g/L}$ ; no federal action level). The Cu concentration from the Maryland fresh water toxic metal criteria is very low due to its high toxicity to aquatic life such as fish, as shown in Table 6-6. Therefore, it is important to keep both Pb and Cu concentrations lower than both the Federal and local criteria in discharged water in order to minimize Pb and Cu input to drinking water sources as well as to minimize Pb and Cu toxicity to aquatic life. Zn also has a State aquatic toxicity limit (120  $\mu\text{g/L}$  for fresh water), which is relatively high compared to Pb and Cu, but much lower than the National secondary drinking water regulation standard (5000  $\mu\text{g/L}$ ).

Table 6-6. State of Maryland Toxic metal criteria for Ambient Surface Waters. (the Code of Maryland Regulations (COMAR) 26.08.02.03-2)

	<u>Aquatic Life (µg/L)</u>						<u>Human Health for Consumption of: (Risk Level = 10<sup>-5</sup>) (µg/L)</u>	
	<u>Fresh Water</u>		<u>Estuarine Water</u>		<u>Salt Water</u>		<u>Drinking Water + Organism</u>	<u>Organism Only</u>
	<u>Acute</u>	<u>Chronic</u>	<u>Acute</u>	<u>Chronic</u>	<u>Acute</u>	<u>Chronic</u>		
Arsenic <sup>1</sup>	340	150			69	36	10	41 <sup>a</sup>
Cadmium <sup>1, 2</sup>	2.0	0.25			40	8.8	5	
Chromium (total)							100	
Chromium III <sup>1</sup>	570	74						
Chromium VI	16	11			1100	50		
Copper <sup>1</sup>	13	9	6.1		4.8	3.1	1,300	
Lead <sup>1</sup>	65	2.5			210	8.1		
Mercury	1.4	0.77			1.8	0.94		
Nickel <sup>1</sup>	470	52			74	8.2	610	4,600
Selenium	20	5			290	71	170	4,200
Silver <sup>1</sup>	3.2				1.9			
Zinc <sup>1</sup>	120	120			90	81	7,400	26,000

<sup>1</sup>The toxicity of certain substances of this regulation is increased or decreased by hardness or pH. For these toxic substances

<sup>2</sup> The drinking water + organism criterion is the Safe Drinking Water Maximum Contaminant Level.

### 6-3-2. Water Quality Parameter Change during Initial Column Operation

The first flush sample (during the first 30 cm effluent flow) from all columns demonstrated relatively high Cu and Zn concentrations, while low effluent Pb was observed in the first flush sample (Figure 6-8). Specifically, MC10 exhibited the highest effluent Zn in the first flush, showing 990 µg/L total Zn with about a half of it (552 µg/L) in dissolved form (Figure 6-8e and f). GF25 and GFH25 columns demonstrated 200 µg/L and 226 µg/L dissolved Zn, and 380 µg/L and 392 µg/L total Zn from the first flush,

respectively. Lower first flush Zn concentration from GF10 was observed, showing 131 µg/L dissolved and 185 µg/L total Zn concentration, probably due to the lower compost content (10%) with less Zn release (i.e., relatively high Zn content in compost; see Table 6-1). Interestingly, GFS25 also showed low dissolved (148 µg/L) and total Zn (157 µg/L) concentration from the first flush, suggesting addition of steel slag in compost media decreased initial release of Zn from compost. Another mechanism for the first flush of metal release from compost media is the high soluble Ca causing a rise in exchanged metals, as well as the initial dissolved organic matter which can chelate metals and carry them into the effluent.

Significant initial decrease of dissolved Zn was observed for all columns (all down to  $\leq 100$  µg/L) including MC10 which decreased from 552 µg/L for the first flush (during the first 30 cm effluent flow) to 87 µg/L for the second flush (from 35 to 65 cm flow). This dissolved Zn concentration for all columns decreased further to  $\leq 30$  µg/L within about 175 cm treated flow. In spite of significant initial drop of dissolved Zn concentration from all columns, total effluent Zn concentration decreased only down to around 100 µg/L before Zn breakthrough started for all columns except GFS25, which showed less than 50 µg/L total Zn concentration before its Zn breakthrough.

The highest initial total Cu concentration of 261 µg/L was also detected from MC10, while GF10 demonstrated the lowest total Cu concentration of 99 µg/L. A little over 2 times higher dissolved Cu concentration was detected from the 25% compost columns (GF25, GFS25, and GFH25) showing 159, 162 and 146 µg/L Cu, respectively, than that of GF10 columns containing 10% compost (70 µg/L Cu), probably due to higher compost content leaching higher dissolved Cu. Interestingly, MC10 showed a

relatively low dissolved Cu concentration of 75 µg/L, suggesting high Cu release as solid form from manure compost in the first flush. The particulate Zn and Cu in the first flush from all columns are probably due to washing out fine compost particles containing Zn and Cu (Table 6-1) during the first flush. The dissolved first flush Zn and Cu can originate from leaching soluble metals, including soluble organic bound metals, as well as untreated influent Zn and Cu.

Relatively low total Pb was detected in the first flush from all the columns, showing the highest of 35 µg/L from MC10 and the lowest of 8 µg/L from GFS25. MC10 also showed the highest dissolved Pb concentration (23 µg/L), while GF10 demonstrated the lowest dissolved Pb of 4 µg/L (Figure 6-8a). The total and dissolved Pb concentration in the first flush decreased down to instrumentation detection limit (5 µg/L) immediately in the next 35 to 65 cm flow, except that from MC10, which later went below the detection limit during the next 65 to 95 cm flow. The dissolved and total Pb concentration remained less than or otherwise very close to detection limit for all columns during the rest of adsorption study before the start of breakthrough, except for an unusual high total Pb concentration of 14 µg/L from GF25 at 175 cm flow (Figure 6-4).



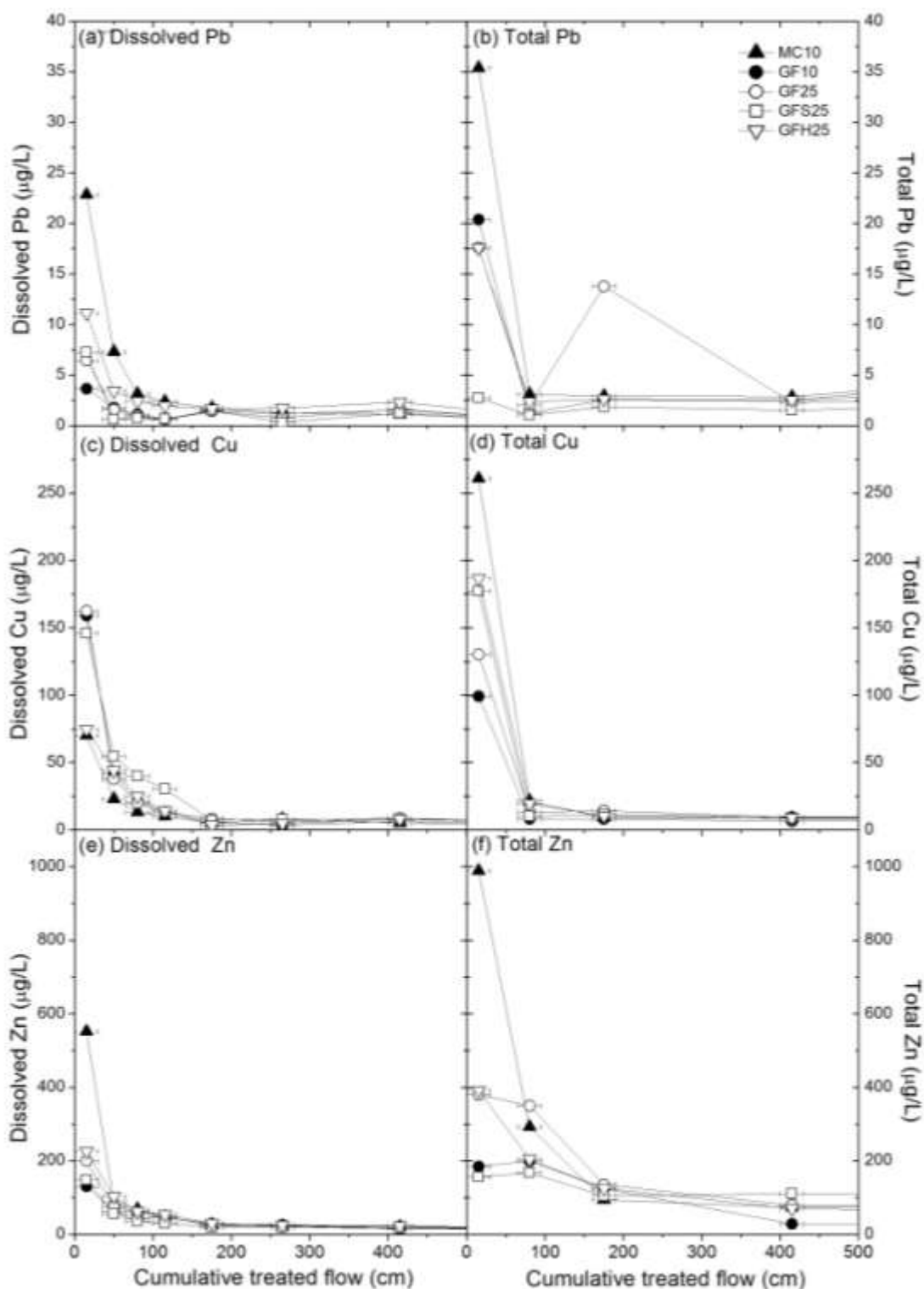


Figure 6-8. Effluent metal concentration during initial column operation: (a) Dissolved Pb; (b) Total Pb; (c) Dissolved Cu; (d) Total Cu; (e) Dissolved Zn; (f) Total Zn. Note differences in concentration scales for each metal. MC10 (10% Manure compost column+sand), GF10 (10% Grass/Food waste column+sand), GF25 (25% Grass/food waste column+sand), GFS25 (25% Grass/Food compost + 5% Steel slag+sand), GFH25 (25% Grass food waste compost + 5% Hubcutter Heavies+sand).

Dissolved effluent Cu concentration did not decrease below 10 µg/L until treated cumulative flow reached 175 cm (Figure 6-8b). The higher first flush dissolved Cu concentration as well as slow decrease of Cu concentration in treated effluent compared to those for Zn can be explained by the high level of dissolved organic compounds and the relatively high Cu content in compost during the initial Biomat operation. This Cu was leached by complexation with organic ligands in initial flows which contained high dissolved organic content (e.g., fulvic acid) in first flush and initial flows by leaching from compost organic materials (Hsu and Lo, 2000a and 2000b). Furthermore, copper sorption on compost can be also decreased by high dissolved organic matter (DOM) in solution, as suggested by Zhou and Wong (2001), showing that soil Cu sorption capacity significantly decreased with increase in DOM concentration due to formation of soluble DOM-Cu complexes.

High total phosphorus concentration in the first flush was detected from all columns except GFS25 (Figure 6-9a). Specifically, MC10 showed the highest total P of 79 mg/L in the first flush while GF10, GF25, and GFH25 showed total P of 33, 53 and 54 mg/L, respectively. This suggests higher P leaching by the first flush from manure compost than from grass/food waste compost. Significant initial decrease and subsequent gradual decrease of total P from the columns was observed. Therefore, little P (<0.05 mg/L) was released at the end of the adsorption study.

Unlike the other columns showing high total P in the first flush, much lower total P of 1.1 mg/L from the first flush was detected from GFS25 (Figure 6-9a). As demonstrated in Figure 6-10, drawn with a finer Y scale (P concentration) and extended X scale (accumulative treated flow), the GFS25 column showed relatively constant P

(ranges from 0.08 to 0.27) throughout the adsorption study after significant initial decrease during first 95 cm flow (Figure 6-10). This is likely due to a high oxalate Fe and Ca content, which significantly reduces initial phosphorus release from compost by adsorption and precipitation (Table 6-1) (Brady and Weil, 2002). The P from grass/food waste compost with steel slag released phosphorus relatively more uniformly throughout the adsorption study, resulting in consistently low effluent P concentration from the column. These results suggest that the effectiveness and advantage of steel slag use as an organic by-product amendment decreases phosphorus environmental risks through reducing initial high P release from organic by-product, while low uniform P release provides proper fertility to plants for long periods.

The lowest turbidity of 45 NTU in the first flush was observed from GFS 25, while the other columns showed much higher first flush turbidity ranging from 177 to 583 NTU (Figure 6-9b). During the first 130 cm, significant turbidity difference was also visually observed between GF25 and GFH25, and GFS25 as demonstrated in Figure 6-11 (during the first 100-130 cm flow sample), in spite of the same grass/food waste compost content (25 %). Unexpectedly, higher turbidity was detected from GF10 (280 NTU) than MC10 (177 NTU) suggesting that higher first flush turbidity was produced from glass/food waste compost than from the manure compost. In spite of high turbidity from the first flush, the effluent turbidity from all the columns subsequently decreased gradually down to about 0.1 NTU throughout the adsorption study (Figure 6-9b).

Cr was an environmental concern, especially for steel slag containing GFS25 due to high Cr content in the slag. However, GFS25 showed the lowest total Cr concentration of 5.5 µg/L in the first flush, while around 18 to 24 µg/L of Cr in the first flush was

observed for the other columns (Figure 6-9C). The total Cr for all columns decreased significantly and was less than instrumentation detection limit (0.5 µg/L) during most of the adsorption study. Except for the first flush for MC10, GF10, GF25, and GFH25, effluent Cr concentrations from all columns throughout the adsorption study were much lower than that for Maryland discharge criteria (Table 6-6). Specifically, low Cr effluent concentration from the GFS column in spite of relatively high Cr content (0.88 g/kg) in steel slag suggests low risk from Cr release from steel slag and environmentally safe use of the steel slag as a by-product amendment.

During heavy metal sorption study with various bio/cellulose/agricultural materials and by-product sorbents, it is important to evaluate not only the performance of the sorbent materials, but also the adverse impact of the materials as a expense of the target metal removal. In other words, it is needed to monitor not only target contaminants, but also other water quality parameters which can be potentially produced and/or released, and, therefore, cause adverse environmental impact.

Nonetheless, the majority of heavy metal sorption studies using these bio sorbents fail to examine the potential risk of various water quality parameters other than their target metal contaminants. Furthermore, most of the studies only evaluate dissolved metal concentrations by filtering samples without either evaluating possible total metal release to the environment or providing possible separation techniques of the sorbents slurries, including column and full scale studies (e.g., barrier/drainage filter media using the sorbent materials) as well as batch studies.

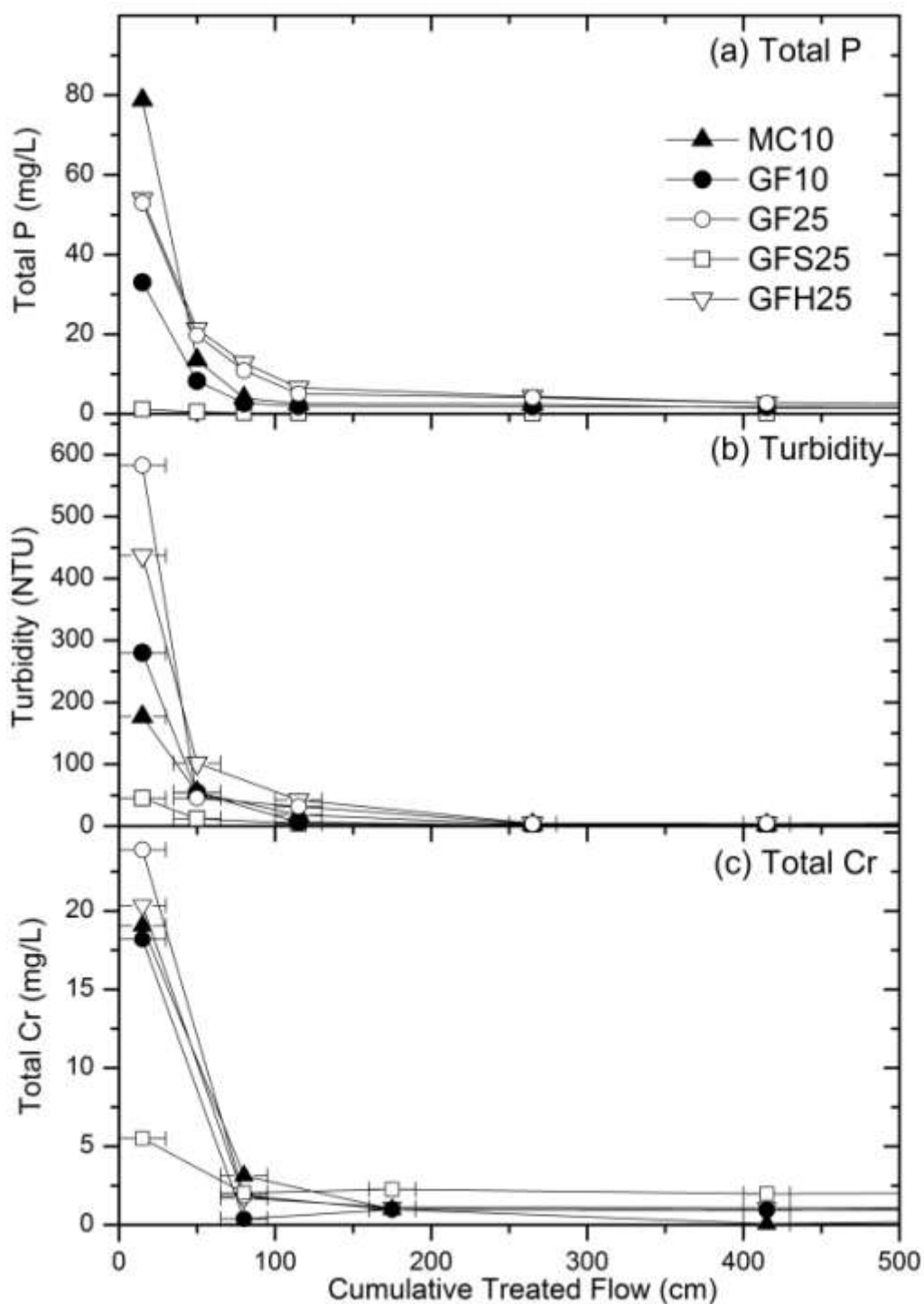


Figure 6-9. Effluent concentration of (a) Total P, (b) Turbidity, and (c) Total Cr during initial column operation for MC10 (10% Manure compost column+sand), GF10 (10% Grass/Food waste column+sand), GF25 (25% Grass/food waste column+sand), GFS25 (25% Grass/Food compost + 5% Steel slag+sand), GFH 25 (25% Grass food waste compost + 5% Hubcutter Heavies+sand).

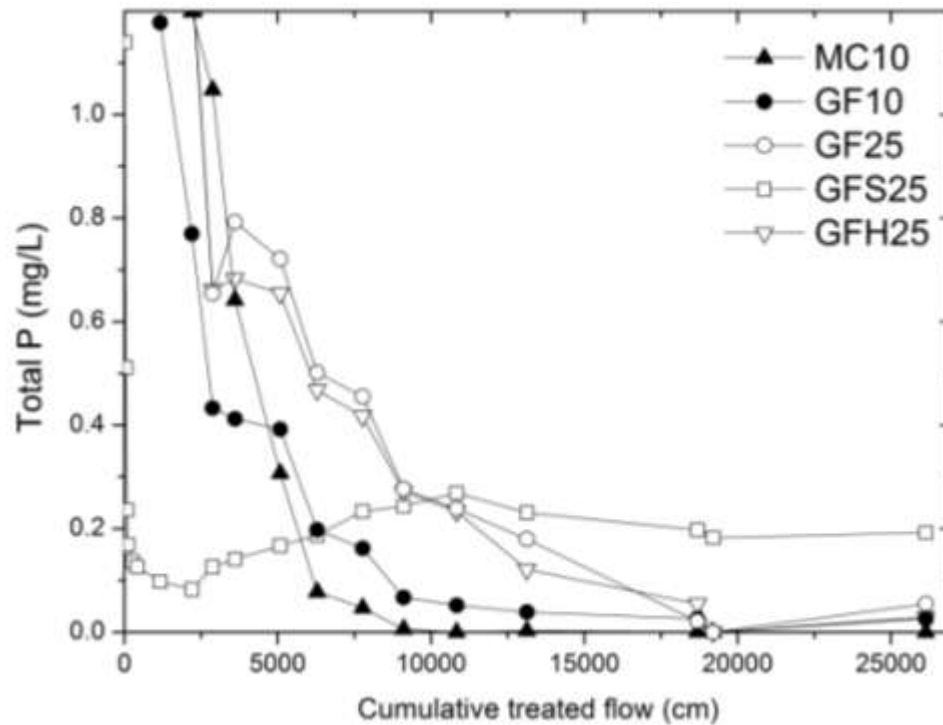


Figure 6-10. Effluent total phosphorus concentration throughout the adsorption study (low scale) for MC10 (10% Manure compost column), GF10 (10% Grass/food waste column), GF25 (25% Grass/food waste column), GFS25 (25% Grass/food compost + 5% steel slag), GFH25 (25% Grass/food waste compost + 5% Hubcutter Heavies).

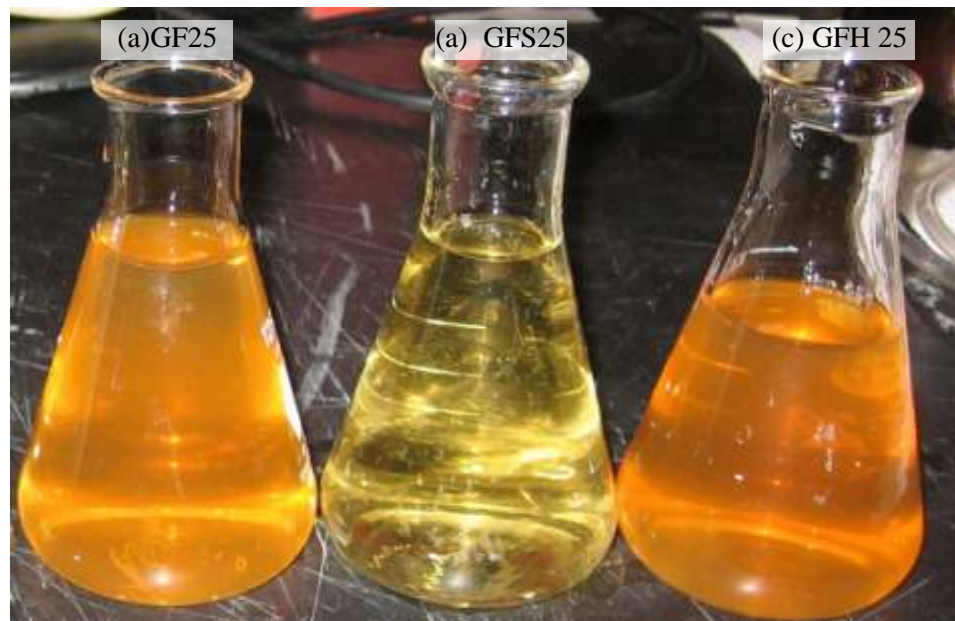


Figure 6-11. Effluent of columns containing 25% grass/food waste during first 65-75 cm flow: (a) 25% Grass/food waste column (GF25); (b) 25% Grass/food waste + steel slag column (GFS25); and (c) 25% Grass/food waste+Hubcutter heavies (GFH25).

### **6-3-3. Discussion on Zn desorption during simultaneous sorption of Pb and Cu during sorption study**

As briefly discussed in the previous Section 6-3-1, two interesting behaviors of Zn desorption were observed from MC10 and GF10 columns during the sorption study (see Figure 6-5): (i) Pb breakthrough for MC10 and GF10 columns started at the point which the effluent Zn concentration stopped increasing (i.e., maximum Zn release) (ii) the effluent Zn concentration started to decrease (after showing relatively constant maximum Zn release) at the same time when Cu breakthrough for MC10 and GF10 columns started (i.e., the Zn desorption started to decrease at the point when Cu breakthrough for MC10 and GF10 columns started).

To theoretically evaluate the above Zn desorption behaviors with simultaneous Pb and Cu sorption during the sorption study, Figure 6-12a was drawn showing total metal removed on a molar concentration basis for all three metals in the MC10 column during the sorption study. Obviously, Cu and Pb sorption did not only depend on Cu desorption, demonstrating Cu and Pb molar concentration removed were much greater than simultaneous Zn desorbed on a molar basis as Figure 6-12a clearly shows. In other words, a significant portion of Cu and Pb sorption during simultaneous Zn desorption occurred via sorption process other than displacing Zn.

Based on difference in Zn desorption behavior as well as Pb and Cu sorption behavior during the sorption study, the whole sorption experiments was divided into five different regions labeled from A to E with increasing cumulative treated flow, as shown in Figure 6-12a. Detailed discussion on Zn adsorption/desorption behavior with simultaneous Pb and Cu sorption during column study in MC10 column is as follows (Figure 6-12a):

**Region A:** In spite of competitive sorption among the metals (Zn, Pb, and Cu), all metals successfully find sites to be sorbed, showing that essentially, all metals are completely removed by the Biomat media during this period.

**Region B:** Zn, the most mobile metal among the three metals, is outcompeted by the other two metals for sorption on the media and, therefore, starts to be bled to effluent. However, a portion of influent Zn is still being sorbed by the media although the portion decreases with increasing cumulative flow.

**Region C:** Zn starts to be desorbed by sorption of the other two metals which displace the sorption sites of the Zn. The Zn desorption increases with increasing cumulative flow.

**Region D:** Zn desorption reaches to its maximum (i.e., maximum desorption rate) and shows the relatively constant desorption during the period. The stationary Zn desorption rate only limits the Pb metal sorption and therefore, Pb starts its breakthrough. Cu (which is sorbed more strongly than Zn) is still successfully sorbed, indicating that its sorption is not limited by the Zn desorption during Region D.

**Region E and F:** Cu finally starts to breakthrough as available sorption sites continue to decrease with increase of treated flow. As Cu sorption decreases, Zn desorption simultaneously decreases, suggesting that Zn desorption was mainly affected by Cu sorption for this region. In fact, the decreased rate of Zn desorption was reasonably close to the decreased rate of Cu sorption within Region F, demonstrating linear decrease of Zn desorption. The Zn and Cu data points within Region F were linearly regressed to calculate the rate of Zn desorption decrease (Zn desorption decrease per treated flow, mol/L/cm) and the rate of Cu sorption decrease (Cu sorption decrease per treated flow, mol/L/cm) as shown with a blue and a red line, respectively, with the trend line equations



in Figure 6-8a. The rate of Zn desorption decrease for the MC10 column was  $1.9 \times 10^{-9}$  mol/L/cm while the rate of Cu sorption decrease was  $1.8 \times 10^{-9}$  mol/L/cm (Figure 6-8a). This indicates that most of the Zn desorption (if not all) within the Region E is caused by Cu sorption. A portion of Cu sorption is attributed to mechanisms other than Zn desorption while most of Zn desorption (if not all) is caused by Cu displacing Zn sorption within the region E. In other words, Zn desorption behavior was mostly affected by Cu sorption E, while Pb sorption scarcely affected Zn desorption within the Region E.

Similar Zn desorption decrease rate ( $1.3 \times 10^{-9}$  mol/L/cm) to Cu sorption rate ( $1.4 \times 10^{-9}$  mol/L/cm) during Region E of GF10 column operation was also observed (Figure 6-13a). The same Zn desorption behavior with simultaneous Pb and Cu sorption, as well as superior Cu percent removal over Pb were also noted from the MC10, as presented in Figures 6-13a and b, respectively. Furthermore, GF25 and GFH25 columns also demonstrated similar metal sorption/desorption trends with the MC10 and GF10 columns, although their trends were not as clear as MC10 and GF25 (see Figure 6-5). The GFS 25 column never reached to the point that Zn desorption occurred during the sorption study.

In conclusion, both Pb and Cu sorption affect not only Zn release during Region B outcompeting Zn, but also Zn desorption during Region C by displacing Zn from sorption sites. However, the impact of Pb sorption on Zn desorption becomes limited during Region D when Zn desorption reached its maximum, while Cu (which is more favorably sorbed than Zn) is still completely sorbed and not limited by the Zn desorption rate. Finally, Zn sorption was mostly (if not all) affected by Cu sorption during Region E, when Cu started its breakthrough and its sorption decreased as much as Zn desorption

decreased. This Zn desorption behavior with simultaneous Pb and Cu sorption also indicates that Cu outcompetes Pb in sorption on the Biomat compost media, specifically during Region D and E where Cu displacing sorption for Zn sites significantly affected Zn desorption behavior, but Pb only showed limited or minimal impact on Zn desorption. Furthermore, preferential Cu sorption on the Biomat media over Zn and Pb can be also seen by Figure 6-12b for MC10 and 6-13b for GF10 which demonstrate better Cu percent removal than Pb and Zn throughout the sorption study.

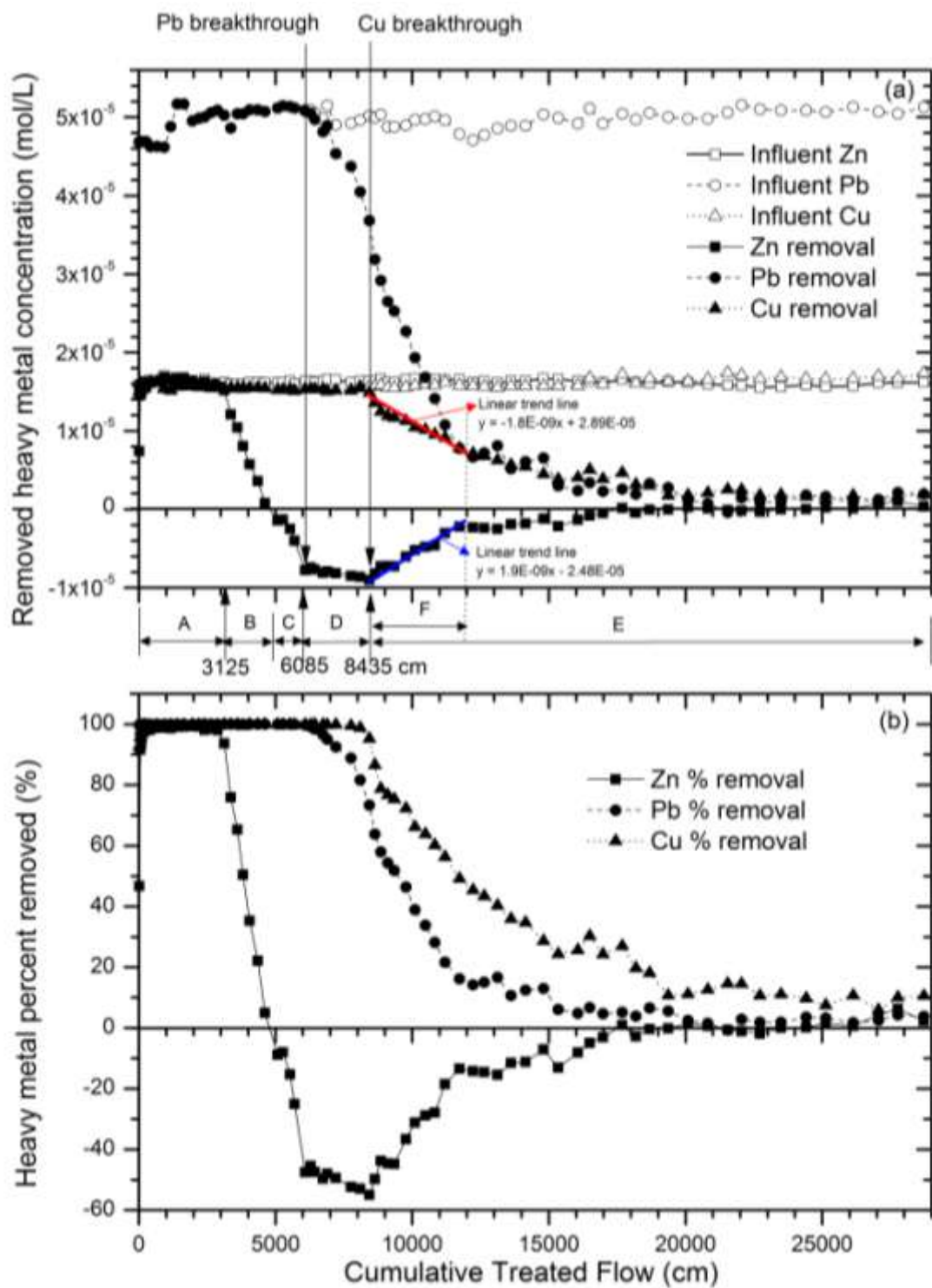


Figure 6-12. Heavy metal removal during the sorption study for the MC10 column (10% Manure compost + sand): (a) Heavy metal removed in molar concentration during the sorption study; and (b) Heavy metal percent removed during the sorption study.

\*Negative concentration or percent indicates desorption of the metal.

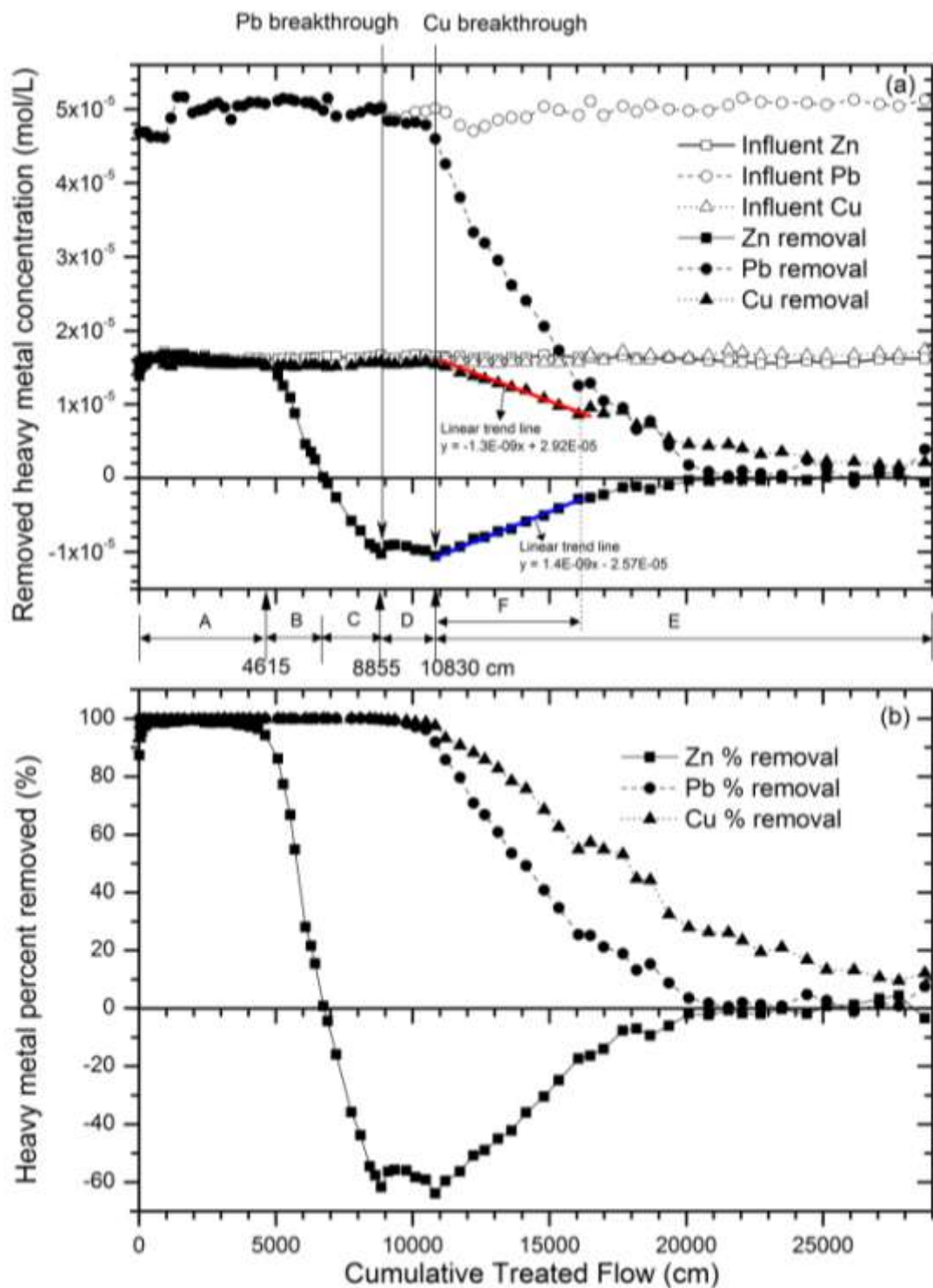


Figure 6-13. Heavy metal removal during the sorption study for the GF10 column (10% Grass/Food waste compost + sand): (a) Heavy metal removed in molar concentration during the sorption study; and (b) Heavy metal percent removed during the sorption study. \*Negative concentration or percent indicates desorption of the metal.

#### **6-3-4. Column leaching study for compost media selection and evaluation – Phase 2**

After 28810 cm accumulative treated flow for adsorption study, column leaching was performed (Figure 6-14). As soon as column leaching proceeded, effluent Zn concentration for MC10 and GF10 columns dropped to less than 25 µg/L (detection limit) suggesting essentially no Zn was leached from the media during the leaching study (Figure 6-12a). As discussed in the previous section (see Section 6-3-1), this is simply because all desorbable Zn on the MC10 and GF10 media was already displaced and leached out to solution by preferable Pb and Cu sorption during the previous sorption study and therefore, little desorbable Zn was left on the media. Specifically, a significant portions of Zn previously adsorbed on the media were released from MC10 (83%) and GF10 (80%) during the adsorption study (Table 6-5). Consequently, minimal Zn was removed by the Biomat media during the sorption study, showing very low percent removal from the two columns (2.7% and 4.1% for MC10 and GF10, respectively) (Table 6-5).

On the other hand, GF25 and GFH25 exhibited gradually consistent decrease of leached effluent Zn concentration during the leaching study and Zn concentration fell to the instrumentation detection limit (25 µg/L) at the end of the leaching study. This is due to the remaining desorbable Zn from GF25 and GFH25. Unlike the MC10 and GF10 columns, an effluent Zn concentration equal to 1.3 mg/L still leached from the GF25 and GFH25 columns at the end of the sorption study at around 1.06 mg/L influent Zn concentration, suggesting that significant desorbable Zn remained in the GF25 and GFH25 columns. In fact, 43.2% and 53.8% of previously sorbed Zn in GF25 and

GFH25, respectively, still remained in the columns at the end of the sorption study (Table 6-5).

The most Zn was leached from GFS25 during the desorption study and significant Zn (around 0.19 mg/L) was still leaching at the end of the experiment. This occurred because most of the Zn had remained in this media during the adsorption study unlike the other columns. The Zn remaining in the media was likely to be readily leachable because the GFS column already exhibited its Zn breakthrough before the leaching study started. Breakthrough for a metal (i.e., release of portion of influent metal) often occurred when the metal was outcompeted by other metals for the limited sorption sites, with unfavorable operation condition such as pH. Consequently sorbed metal on the media after the metal's breakthrough is often significantly more mobile than the sorbed metal before breakthrough on the same media.

Although Zn breakthrough for GFS25 column started at 22725 cm, before the desorption study, the effluent Zn concentration from GFS25 during the adsorption study never exceeded influent concentration, suggesting that no Zn was leached or exchanged during the previous adsorption study. Therefore, more Zn was leached from GFS25 than from the other columns during the desorption study because more desorbable Zn remained on the media.

Zn showed the highest percent leaching, followed by Pb and Cu. This was expected because Zn was noted as the most mobile metal (i.e., selectivity sequence) among the three metals studied (Zn, Pb, and Cu) in many studies with agricultural byproducts and soils (Bunzl et. al., 1976; Elliott et al., 1986; Veeresh et al., 2003; Jang et al., 2005; Seelsaen et al., 2007). Furthermore, Zn adsorption capacity is often

significantly decreased when it is simultaneously sorbed with other metals on specific media or soil (Jang et al., 2005). In addition, the weakly bound Zn on soil and other media was noted with competitive sorption with Pb and Cu. In fact, Zn is often expected to adsorb on outersphere adsorption sites during the simultaneous competitive sorption with Pb and Cu, while Pb and Cu are more involved with specific sorption with minerals and organic matter (Fontes et al., 2000).

Although the most Zn (in terms of absolute mass) was leached from GFS25 during the leaching study, the greatest mass of previously sorbed Zn (65% of previously sorbed Zn) still remained in this media at the end of the desorption study. Furthermore, GFS25 demonstrated both the least mass and percent leaching for both Pb and Cu by far compared to the other columns. In fact, unlike the other columns, little Pb and Cu was released from GFS25 during the leaching study, demonstrating that 99.8% of the Pb and 99.9 % of the Cu still remained in the media (Table 6-7). The GFS25 column produced very low Pb effluent concentrations (mostly less than 5 µg/L) throughout the leaching study before it started to release Pb at 43855 cm of cumulative treated flow, and increased up to 73 µg/L at the end of the experiment. Effluent pH from GFS25 was decreased during the leaching study as more flow went through the column (Figure 6-15). This pH decrease is likely due to acidity in influent. The pH at 43855 cm of cumulative treated flow (when Pb leaching starts) was 6.6 and the pH at the end of the leaching study was 6.5 at which most of the other columns started their Pb breakthrough and therefore, the pH sensitive sorbed Pb on GFS25 media started to leach.

Except for GFS25, effluent pH from all columns slightly increased throughout the leaching study (Figure 6-15). The effluent pHs at the beginning of the leaching study

from each column were 5.4 (MC10), 5.5 (GF10), 5.6 (GF25), 6.7 (GFS25), and 5.5 (GFH25), while they were 6.1 (MC10), 6.0 (GF10), 5.7 (GF25), 6.5 (GFS25), and 5.8 (GFH25) at the end of the experiment. This slight pH increase during the leaching study was mostly likely due to cation exchange between hydrogen ions in solution and heavy metal ions on the media.

Throughout the leaching study, all the columns except GFS25 showed constant decrease of leached effluent Pb and Cu after the rapid initial drop (Figure 6-14b and c). GFS25 did not leach any Cu during the leaching study while Pb was detected in the effluent from GFS25 at the end of the experiment; 72 µg/L dissolved Pb was detected at the end (56915 cm) of the leaching study since effluent Pb over 20 µg/L was observed at 46000 cm. Based on these column studies, the GFS25 media exhibited the best Pb removal throughout the adsorption study and showed the least amount of Pb leached during the leaching study. The MC10 column showed the worst performance of Pb removal and leaching (Table 6-6). More than 99% of the captured Pb for the GFS25 column during the adsorption study remained in the media after the leaching study. Therefore, the metal leaching study clearly indicated that the GFS25 column media is the best candidate for Biomat media, not only demonstrating the best metal removal from heavy metal contaminated water, but also exhibiting the immobility of sorbed metal on the media.



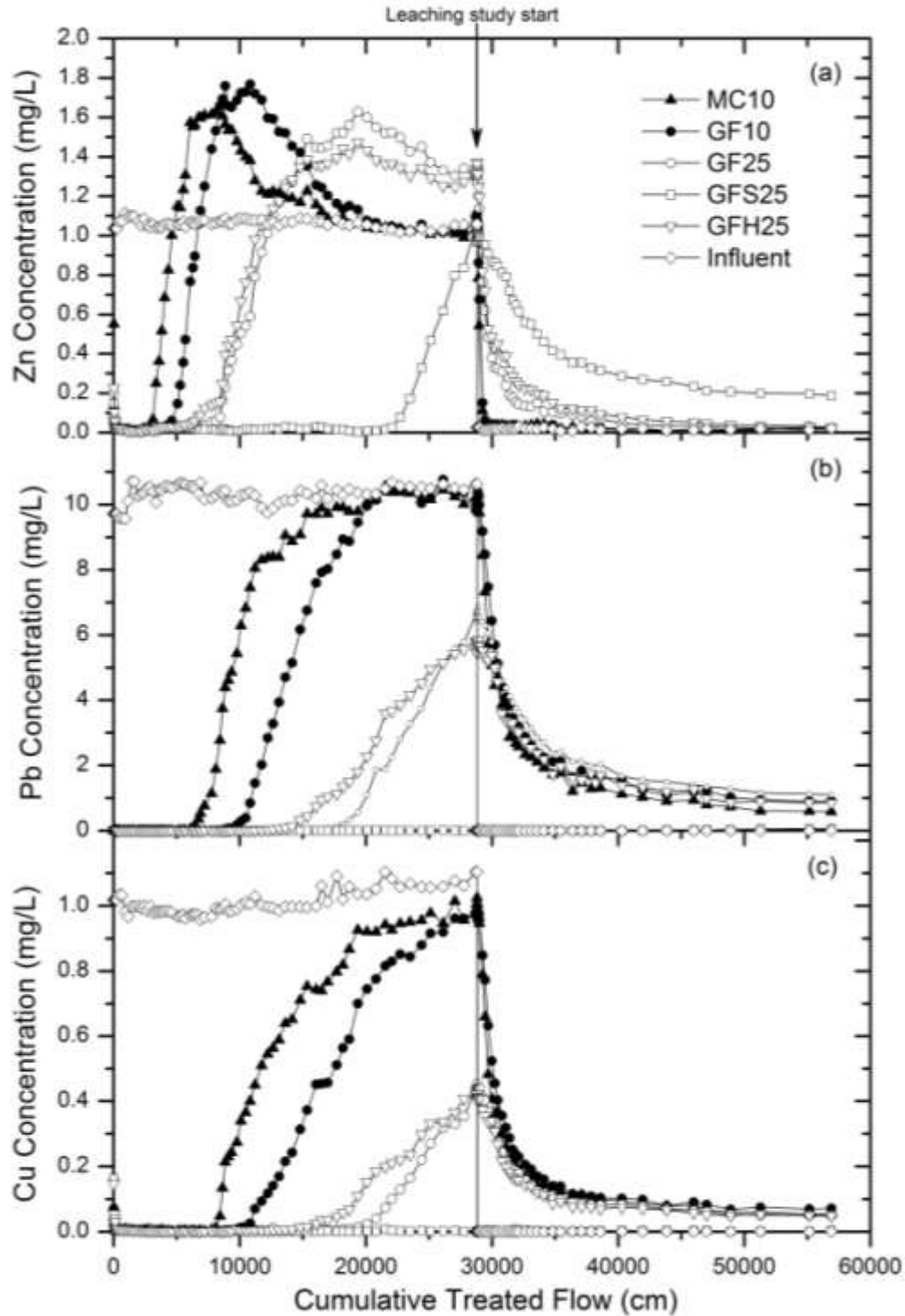


Figure 6-14. Dissolved effluent metal concentration by treated cumulative flow during adsorption and leaching study for (a) Zn, (b) Pb and (c) Cu.: Arrow indicates the start of leaching study: MC10 (10% Manure compost column), GF10 (10% Grass/food waste column), GF25 (25% Grass/food waste column), GFS25 (25% Grass/food compost + 5% steel slag), GFH 25 (25% Grass food waste compost + 5% Hubcutter Heavies).

Table 6-7. Mass balance of Pb throughout the column study: MC10 (10% Manure compost column), GF10 (10% Grass/food waste column), GF25 (25% Grass/food waste column), GFS25 (25% Grass/food compost + 5% steel slag), GFH 25 (25% Grass food waste compost + 5% Hubcutter Heavies).

Column ID	MC10	GF10	GF25	GFS25	GFH25	Input
Zn removed (mg) by media during adsorption study	4.2	6.3	23.5	135.5	27.2	154.5*
% Zn removed by media during adsorption study	2.7	4.1	15.2	87.7	17.6	-
Zn leached (mg) during the leaching study	1.9	1.8	11.6	47.0	16.6	
% of Zn remaining in the compost media after the leaching study	54	72	51	65	39	
Pb removed (mg) by media during adsorption study	547	759	1332	1510	1282	1511*
% Pb removed by media during adsorption study	36.2	50.3	88.2	100.0	84.8	
Pb leached (mg) during the leaching study	216	271	294	2.69	239	-
% of Pb remaining in the compost media after the leaching study	60.5	64.2	77.9	99.8	81.3	-
Cu removed (mg) by media during adsorption study	70.1	92.6	138.9	148.7	134.4	149.0*
% Cu removed by media during adsorption study	47.0	62.1	93.2	99.8	90.2	
Cu leached (mg) during the leaching study	17.8	20.4	14.0	0.15	13.0	
% of Cu remaining in the compost media after the leaching study	74.6	78.0	89.9	99.9	90.3	-

\* Total metal mass introduced to column media as influent throughout the sorption study.

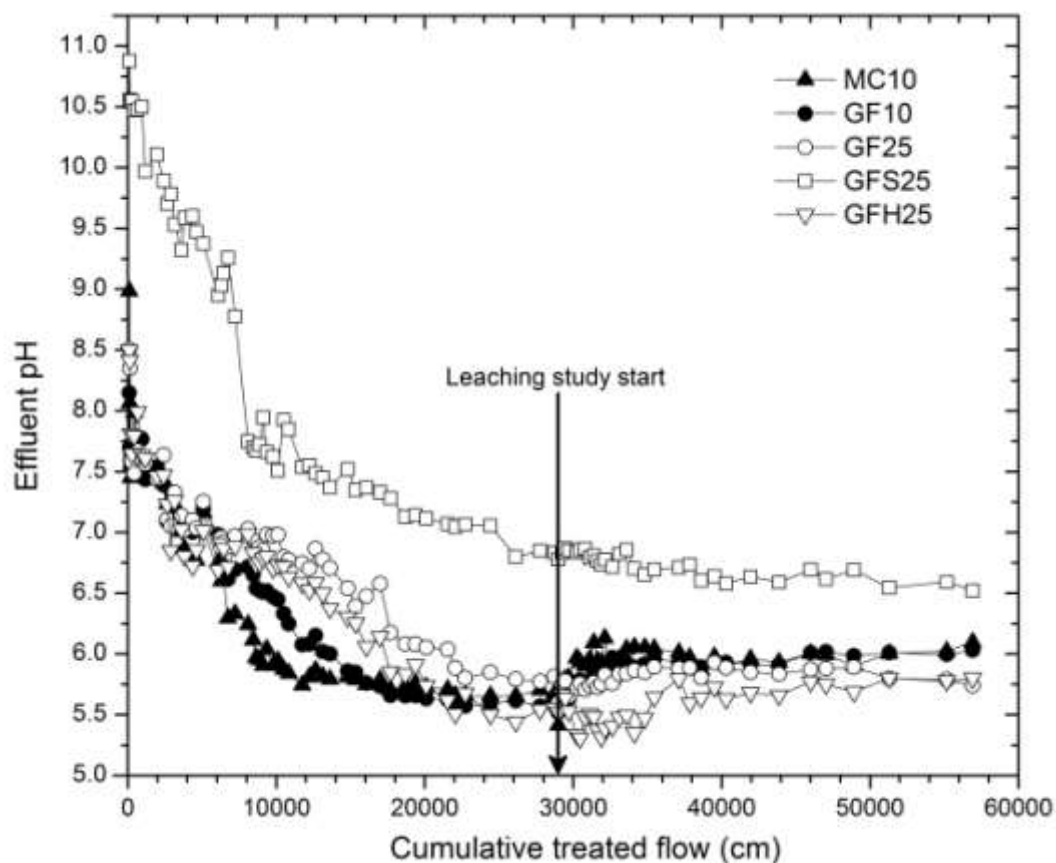


Figure 6-15. Effluent pH change during sorption and leaching study: MC10 (10% Manure compost column), GF10 (10% Grass/food waste column), GF25 (25% Grass/food waste column), GFS25 (25% Grass/food compost + 5% steel slag), GFH 25 (25% Grass food waste compost + 5% Hubcutter Heavies)

### 6-3-5. Metal removal capacity and life of the Biomat media

Based on the metal influent and effluent results (Figure 6-5) as well as accumulated flow data at each breakthrough from the sorption study presented in Section 6-3-1 (see Table 6-4), metal removal capacity for each Biomat media, as well as the expected media life for each metal and mat media were estimated and are presented in Table 6-8.

Table 6-8. Metal removal capacity for each Biomat media and the media life for each metal: MC10 (10% Manure compost column), GF10 (10% Grass/food waste column), GF25 (25% Grass/food waste column), GFS25 (25% Grass/food compost + 5% steel slag), GFH 25 (25% Grass food waste compost + 5% Hubcutter Heavies)

Estimate of metal removal capacity and life for each mat media				
Column media	Metal removal capacity ( <b>mg</b> metal / <b>g</b> media)	Expected media life <sup>a</sup> ( <b>yr</b> / <b>cm</b> media depth)	Expected media life ( <b>yr</b> ) <sup>a</sup> for media depth of	
			12.7 cm (5 inch)	25.4 cm (10 inch)
<u>Zn</u>				
MC10	0.171	0.046	0.59	1.18
GF10	0.251	0.068	0.87	1.74
GF25	0.563	0.125	1.59	3.18
GFS25	1.531	0.338	4.29	8.58
GFH25	0.429	0.096	1.21	2.43
<u>Pb</u>				
MC10	3.28	0.090	1.15	2.30
GF10	4.77	0.132	1.67	3.34
GF25	10.6	0.239	3.03	6.06
GFS25	> 19.2 <sup>a</sup>	0.427	> 5.42 <sup>b</sup>	>10.8 <sup>b</sup>
GFH25	8.34	0.188	2.38	4.78
<u>Cu</u>				
MC10	0.431	0.210	2.67	5.34
GF10	0.555	0.299	3.79	7.58
GF25	1.287	0.428	5.44	10.9
GFS25	>1.881 <sup>a</sup>	0.485	>6.16 <sup>b</sup>	>12.3 <sup>b</sup>
GFH25	1.017	0.413	5.24	10.5

<sup>a</sup> Estimated based on assumptions of: a) annual rainfall 106 cm/yr.; b) down-flow with a mat media top areal sized at 2% of roof wall area; (c) runoff coefficient of 1.0 (i.e., not runoff loss).

<sup>b</sup> value was calculated based on the total cumulative flow (cm) at the end of the sorption study

Each metal removal capacity was estimated based on removed metal mass by each mat media until the start of its breakthrough during the sorption study. Each mat media life was also estimated based on accumulated flow at the breakthrough of each metal. The assumptions made for these estimates include: (i) Maryland annual precipitation is 106 cm/yr (USGS, 1999), (ii) Mat media operates as a down flow with a mat media top areal sized at 2% of the drainage area and a rational method runoff coefficient of 1.0 (i.e., no runoff loss), (iii) Sorption and desorption behavior of metals with each mat media are not affected by the presence of other metals, (iv) Each metal removal capacity and life for each mat media increase proportionally with increase of media depth for the same media area. (v) The same media configuration used for the column sorption/desorption study is applied.

The sorption study here was performed employing simultaneous sorption with three different metals in a solution. As previously discussed in Section 6-3-1, the metal removal capacity for a media estimated here based on metal breakthrough capacity (Figure 6-5) is most likely to underestimate the individual metal removal capacity, compared to that from sorption study with a solely existing metal. Again, it has been noted that individual metal sorption capacity significantly decreased when it was sorbed with other metals through simultaneous competitive sorption (Jang et al., 2005; Antoniadis, 2007). In particular, Zn removal capacity when alone is expected to be much higher than it is estimated here based on the sorption study because retention capacity of the less strongly sorbed metal like Zn is much more affected by the more strongly sorbed metal like Pb and Cu (Jang et al., 2005; Antoniadis, 2007). Consequently, assumption (iii) is not valid and, therefore, the estimated individual metal capacity and life should be

carefully used with influent concentrations of the other metals (e.g., ~10 mg/L Pb, and 1 mg/L Cu and Zn: 10:1:1 concentration (mg/L) ratio in influent). Fortunately the metal capacity and life through competitive sorption underestimates, compared to individual metal sorption capacity and therefore, they can be used as conservative approach.

Because of the earliest breakthrough from Zn, life of the mat should be basically estimated based on Zn unless Zn is not a target metal for Biomat operation.

Based on Table 6-8, GFS media demonstrates by far the best removal capacity and life for all three metals. As a example, expected life of GFS25 media for Zn with 12.7 cm media depth is around 4.3 years when its influent concentration is around 1 mg/L with 1 mg/L Cu and 10 mg/L Pb.

As demonstrated in Figure 6-16 with two example media (MC10 and GF10), strong linearity in decrease of total heavy metal concentration removed on increasing cumulative treated flow was noted before it tapered off toward zero removal. The decrease in total metal concentration removed on total treated flow was calculated as  $7.8 \times 10^{-9}$  mol/L/cm for MC10 media and  $4.9 \times 10^{-9}$  mol/L/cm for GF10. This graph can be used to estimate the total molar effluent concentration (total metal input molar concentration – total metal concentration removed) at a specific cumulative flow, specifically when the Biomat is operated with extended period time after Zn breakthrough, which may be the case when influent concentration is low and therefore, leaching of portion of influent metal concentration is not environmentally risky.

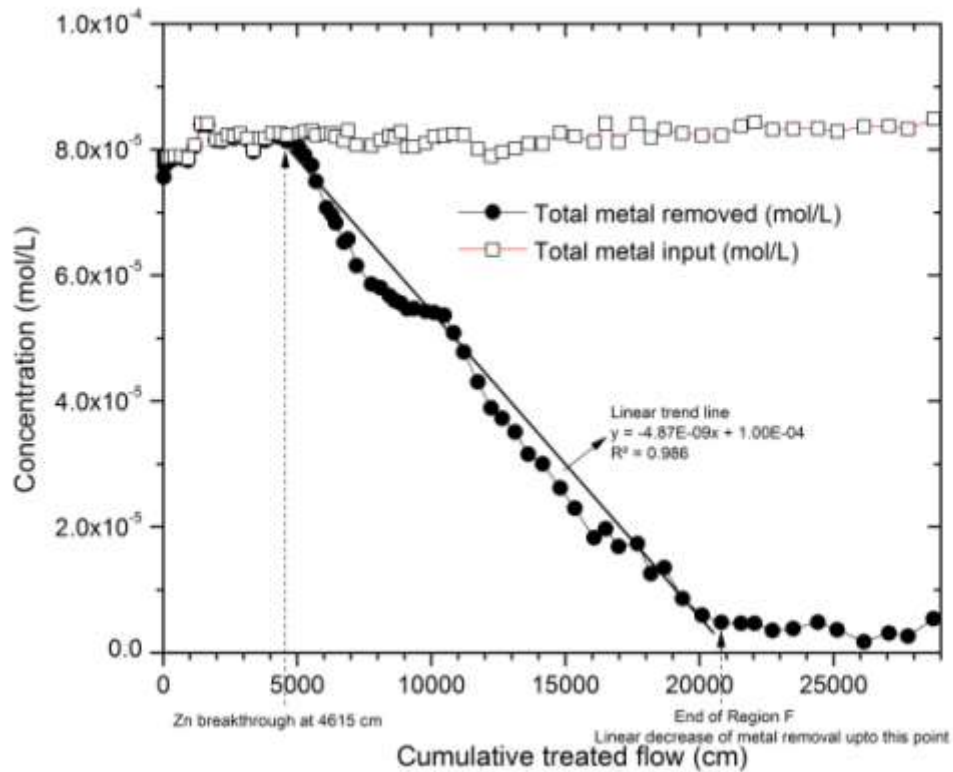
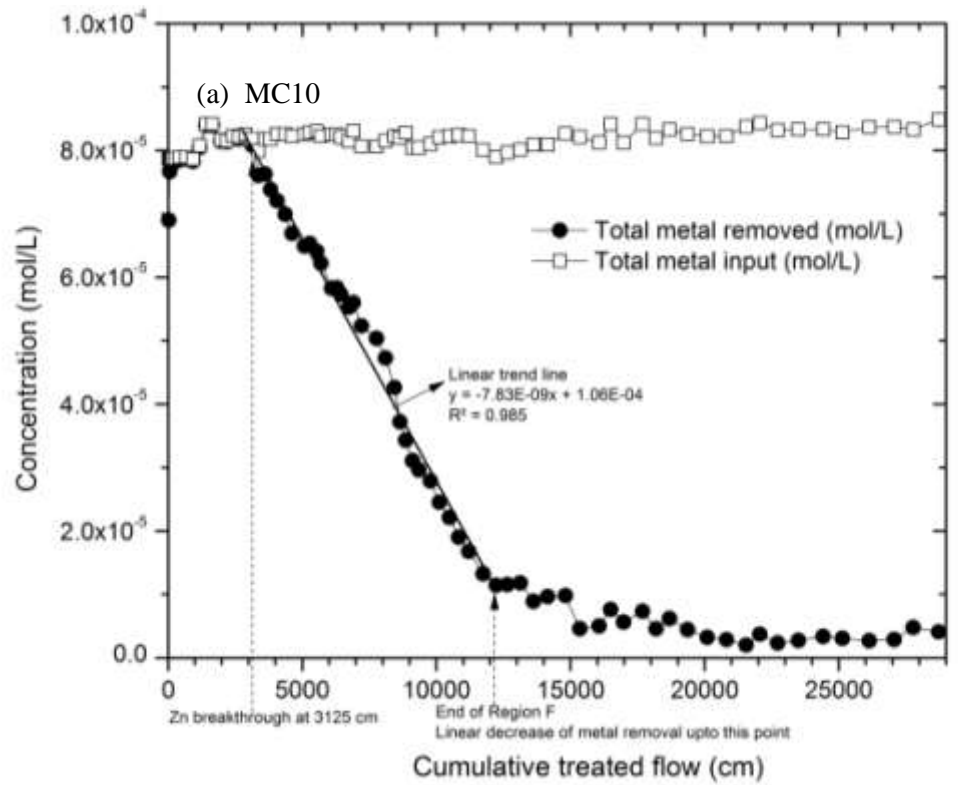


Figure 6-16. Linearity of total metal concentration removed (all three metal combined) as a function of cumulative flow: (a) MC10 column (10% Manure compost + sand); and (b) GF10 column (10% Grass/Food waste compost + sand)

#### **6-4. Summary and Conclusion**

. A bioremediation mat is suggested in this research to remove heavy metals (lead, copper and zinc) from the storm water runoff from the studied site. The mat will be an engineered mixture of sand/compost/byproduct sorption media to adsorb/precipitate dissolved pollutants and trap/filter out large particulates. Five columns, 10% manure compost + sand (MC10), 10% grass/food waste compost + sand (GF10), 25% grass/food waste compost + sand (GF25), 25% grass/food waste compost + 5% steel slag + sand (GFS25), and 25% grass/food waste compost + 5% hubcutter heavies + sand (GFH25) were set up to evaluate potential composts and by-products to remove heavy metals (10 mg/L Pb and 1 mg/L Cu and Zn) from synthetic rooftop/wall runoff.

The 10% grass/food waste compost (GF10) exhibited higher capacity of heavy metal removal than the 10% manure compost (MC10), which showed earlier breakthrough for all three heavy metals (Pb, Cu and Zn). This is probably due to the greater surface area of the grass/food waste compost as observed in the microstructural surface images (Figure 6-2) by field emission SEM, and possibly greater humic substance content in the composted grass, with a variety of functional groups, compared to manure compost. Furthermore, the columns containing the higher ratio of the grass + food waste compost (25% of dry mass ratio, GF25) showed better metal removal capacity than the lower ratio (10% of dry mass ratio, GF10) for all the three metals. Specifically, GF25 demonstrated around 1.8-1.9 times removal enhancement compared to GF10 for each metal in terms of the accumulative treated flow at the start of breakthrough.

Use of steel slag as an additive (GFS25) in the media increased the metal removal capacity significantly for all three metals probably due to pH buffering from the high



CaO and MgO content as well as heavy metal adsorption by high amorphous Fe minerals as represented by oxalate extractable Fe in steel slag. Nonetheless, in spite of high amorphous Fe content in hubcutter heavies, GFH25 column did not demonstrate any heavy metal sorption enhancement but, rather, slight decrease of metal sorption capacity was observed in GFH25 compared to GF25, probably due to acidity produced by the hubcutter heavies material and therefore, pH decrease, demonstrating the significance of pH in heavy metal sorption capacity.

For the influent metal concentrations and loading rate studied, Cu was most preferentially removed (sorbed) by all the Biomat media in terms of order of breakthrough in the order of  $\text{Cu}^{2+} > \text{Pb}^{2+} \gg \text{Zn}^{2+}$ . High stability constants of metal-humic acid complexes and electronegativity of Cu may also influence the higher affinity of Cu on the Biomat media than the other two metals.

Relatively high phosphorus, turbidity and total metals (particulate metals) were noted during the initial operation of all Biomat media column except GFS25. However, significant initial drop of these levels were noted, demonstrating decreased environmental risk.

Throughout the leaching study, all the columns except GFS25 showed constant decrease of leached effluent Pb and Cu after the rapid initial drop. Based on these column studies, the GFS25 media exhibited the best Pb removal throughout the adsorption study and showed the least amount of Pb leached during the leaching study.

To theoretically evaluate the Zn desorption behavior with simultaneous Pb and Cu sorption during the sorption study, total metal removed (molar concentration basis) for all three metals in the MC10 and GF10 columns during the sorption study was analyzed.

Based on difference in Zn desorption, as well as Pb and Cu sorption behavior, the whole sorption experiment was divided into five regions labeled from A to E with increasing cumulative treated flow (Figure 6-12a and 6-13a). Both Pb and Cu sorption affect not only Zn release during Region B by outcompeting Zn, but also Zn desorption during Region C through the sorption displacing Zn. However, impact of Pb sorption on Zn desorption becomes limited during Region D when Zn desorption reached its maximum, while Cu (which is sorbed more favorably than Zn) is still completely sorbed and not limited by the Zn desorption rate during Region D. Finally, Zn sorption was primarily affected by Cu sorption during Region E, when Cu started its breakthrough and its sorption decreased as much as Zn desorption decreased simultaneously.

The metal leaching study clearly indicates that the GFS25 column is the best candidate for Biomat media, not only demonstrating the best metal removal, but also exhibiting the immobility of sorbed metal on the media.

. Based on the metal influent and effluent results as well as accumulated flow data at each breakthrough, metal removal capacity for each Biomat media and the expected media life for each metal and mat media were estimated. Because of the earliest breakthrough from Zn, life time of the mat should be estimated based on Zn unless Zn is not a target metal for Biomat operation. Based on the estimations, GFS media demonstrates by far the best removal capacity and life for all three metals.

## CHAPTER 7. EVALUATION OF HEAVY METAL LOADING AND HYDRAULIC CONDUCTIVITY OF BIOMAT IN PERPENDICULAR FLOW USING BENCH-SCALE EXPERIMENTS: PHASES 3 AND 4.

### 7-1. Introduction

Based on the previous column sorption and leaching studies, the Grass/food waste compost + steel slag media mixture that exhibited the highest capacity for removing heavy metals and the best water quality effluent was selected as a test media for the Biomat and was evaluated in more detail in a bench scale experiment as the next of the investigation (Phase 3).

Understanding heavy metal removal efficiency of the Biomat for different loading rates, controlled by varying flow rate is important to the performance of Biomat media during an actual storm event due to variable storm characteristics. Furthermore, investigating hydraulic characteristic of the media is required because good hydraulic characteristics are essential to treat the variable storm intensity, including possible extreme events with high intensity. However, high hydraulic conductivity and contaminant removal efficiency are expected to be inversely proportional and optimization may be necessary for optimal metals removal for a wide range of storm treatment.

Therefore, water quality performance and hydraulic characteristics of mat media were investigated employing variable influent water head. Additionally, stability of adsorbed metals on the Biomat media is studied through metal leaching experiments during the bench scale experiments. Various metal extractions from the mat media after the bench

scale experiments were also performed to investigate the stability and risks of the adsorbed/precipitated metals on the media after the experiments.

A total of 11 bench-scale experiments were performed over a 13 month period and four different metal extractions for the Biomat media were performed based on five different experimental objectives: (1) evaluating Biomat performance with different water head (flow rate); (2) investigating Biomat hydraulic characteristics; (3) evaluating Biomat performance with lower influent metal concentrations; (4) investigating metal leachability during Biomat operation; (5) evaluating metal extractability and mobility of the media through media extraction.

Based on the Biomat media bench-scale experiments, design parameters, implementation conditions, and recommendations for future full scale Biomat application in the field will be recommended.

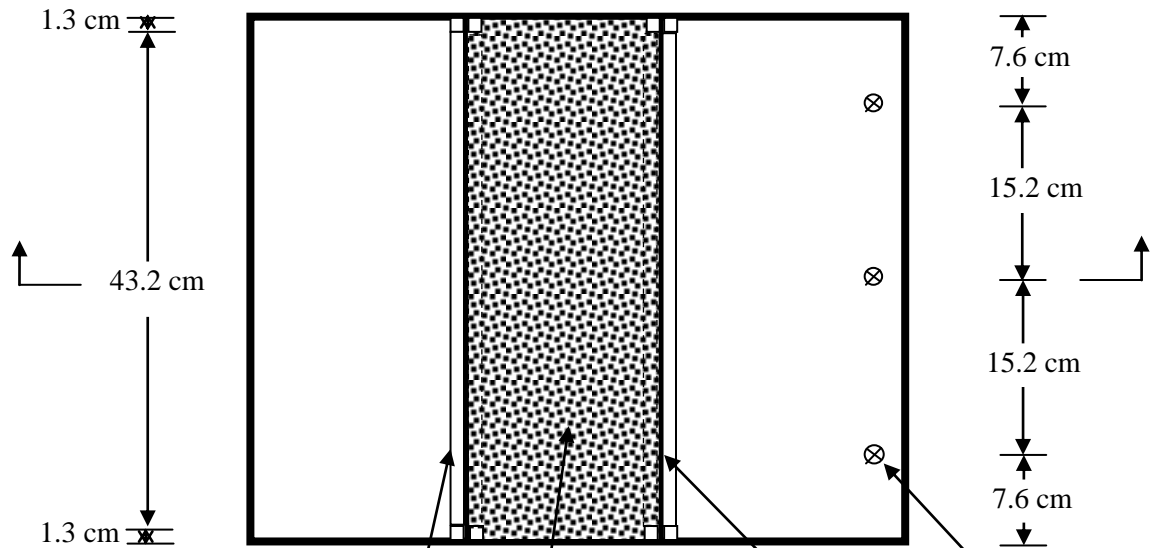
## **7-2. Methods and Materials.**

### **7-2-1. Biomat media and box preparation for bench scale experiment – Phase 3**

A 61 cm long × 45.7 cm wide × 45.7 cm high plastic box was constructed with two 45.7 cm wide and 22 cm high stainless steel screens in the middle of the box (Figure 4-7). Biomat media mixture was installed within a 18.0 cm long × 45.7 cm wide × 22 cm high volume between the stainless steel screens (40 mesh, 0.38 mm opening) in the middle of the box to simulate a perpendicular flow system (Figure 7-1). The media used was the steel slag mix (GFS25) as described in Section 6-2-1. However, larger sieves were used to produce <2.83 mm material for the compost and < 2.00 mm steel slag. Due to the use of different size media compared to the column study, media chemical

properties and total metal contents were measured again following the methods as described in the previous chapter (Table 7-1).

**a. Top View —**



**b. Cross sectional  
Side View of A-A'**

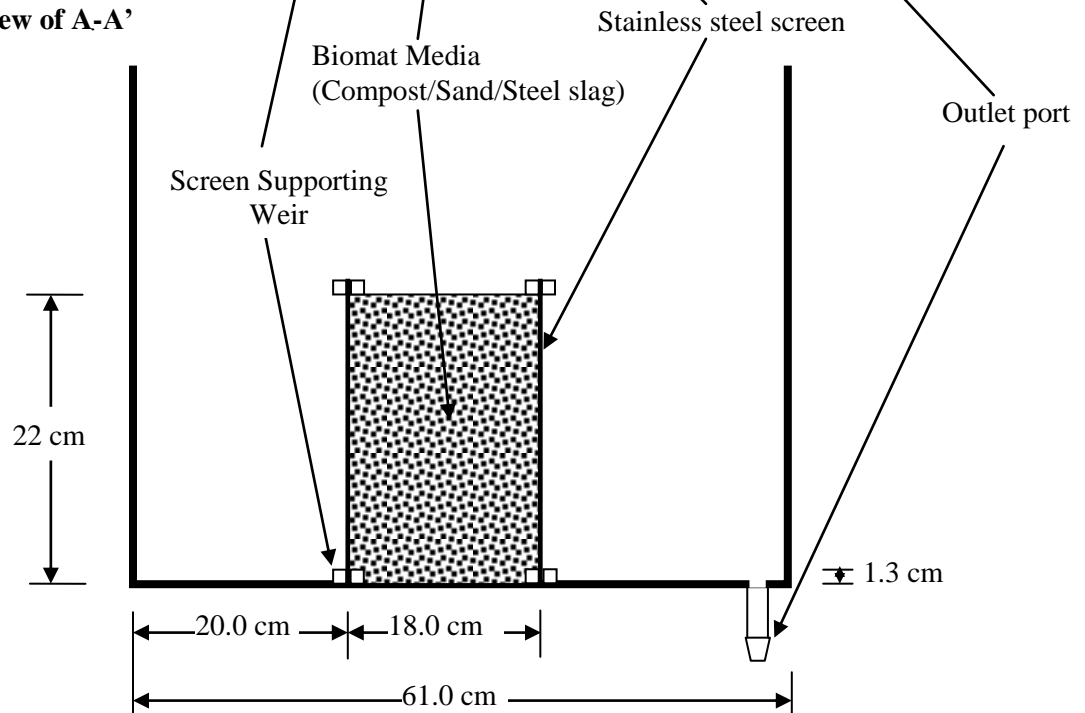


Figure 7-1. Bench scale Biomat box reactor design for bench scale experiment.

Table 7-1. Chemical properties and total metal content of grass/food waste compost, and steel slag after sieving to different size than in the earlier experiments,

Parameters	Grass/Food waste compost	Steel Slag
pH	6.95	11.8
Electrical Conductivity, mS cm <sup>-1</sup>	7.34	5.83
Water Content (%)	44.7	2.32
Bulk density (mg/cm <sup>3</sup> )	0.63 (wet)	1.73 (dry)
Loss on ignition (%) <sup>a</sup>	40.3	1.2
Fe, g kg <sup>-1</sup>	10.2	244
Oxalate extractable Fe, g kg <sup>-1</sup>	2.24	7.90
Mn, g kg <sup>-1</sup>	0.773	34.6
Oxalate extractable Mn, g kg <sup>-1</sup>	0.409	1.24
Al, g kg <sup>-1</sup>	6.1	10.8
Ca, g kg <sup>-1</sup>	15.2	143
Zn, mg kg <sup>-1</sup>	145	80.2
Cu, mg kg <sup>-1</sup>	28.7	48.9
Pb, mg kg <sup>-1</sup>	15.2	30.1
Cr, mg kg <sup>-1</sup>	25.5	734
Cd, mg kg <sup>-1</sup>	0.81	2.31
Ni mg kg <sup>-1</sup>	29.1	55.4
P, g kg <sup>-1</sup>	5.57	-

<sup>a</sup> Loss on ignition at 550 °C and % based on oven dry weight at 103 °C

The calculated mass of the compost, sand and steel slag was uniformly mixed as one batch and transferred to the box in order to produce 18.0 cm long × 45.7 cm wide × 22 cm high Biomat media between the screens. However, only 80% of the calculated mass was actually used because of lighter packing of the media and the larger particle size of the compost and steel slag (Table 7-2). After the media packing, DI water was

introduced to fill the box up to the mat height (22 cm) submerging both inlet and outlet sides and the mat media. After the water reached the mat height (22 cm), the outlet ports were opened and the water was discharged. This was performed to promote natural packing of the media and to wash out small particles from compost media.

Table 7-2. Mass to volume ratio (g/L) and mass (g) of mat media for column studies and bench scale experiment.

	Compost (g/L)	Sand (g/L)	Steel Slag (g/L)	Total (g/L)	Volume (L)
Column study	306 (19.70 g)	857 (55.16 g)	61.2 (3.94 g)	1225 (78.8 g)	0.0644
Calculated for Bench scale	306 (5543 g)	857 (15519 g)	61.2 (1109g)	1225 (22171 g)	18.1
Actually used for Bench scale	245 (4437 g)	686 (12423 g)	49.0 (887 g)	980 (17747 g)	18.1

\* Mass of compost, sand, steel slag media are calculated based on dry weight.

### 7-2-2. Bench Scale Experimental setup and operation – Phase 3

Synthetic runoff was employed in the bench scale experiments to provide controlled input conditions. A total of 11 bench-scale experiments were performed throughout a 13 month period (simulating over 5 month of runoff at B-580). The synthetic runoff (200 L except Experiment 6) was made using tap water for Experiments 1 and 2 and DI water for the rest of the experiments, with the water quality components listed in Table 7-3. The concentrations of the amendments were selected based on previously monitored runoff characteristics, except for Experiment 5, 10 and 11, during which no heavy metal amendments were added for leaching study (for Experiment 5 and 11) or evaluating a lower influent heavy metal concentration condition (for Experiment 10). Only half of the influent volume (100 L) was treated during Experiment 6 due to

Experimental incidents which caused missed flow rate and water head data. Therefore, results from Experiment 6 were not included in data analysis except for influent and effluent metal concentration data and partially acquired flow rate data to estimate the mass balance of the removed metal mass by the Biomat and to compare the results from the media metal extraction data after the experiments.

After normalization to room temperature, proper volumes of stock solutions of  $\text{PbCl}_2$ ,  $\text{ZnSO}_4 \cdot 7\text{H}_2\text{O}$ ,  $\text{CuSO}_4$ , and  $\text{CaCl}_2$  were added to the water to make 200 L of synthetic runoff. When tap water was used, the tap water was dechlorinated by  $\text{Na}_2\text{SO}_3$  addition, based on the stoichiometry of Equation 7-1.

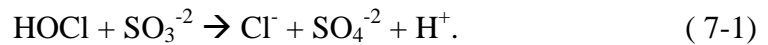


Table 7-3. Target characteristics of the synthetic runoff used in the column study

	Experiments with High metal concentrations		Experiments with low metal concentrations	Leaching study	Source chemical
Ex ID	Ex 1 and 2	Ex 3-4 & Ex 6-9	Ex 10	Ex 5 and 11	-
Water	Tap water	DI water			
pH	6.0 for Ex 1 5.7 for Ex 2	5.0-5.3			
TDS <sup>a</sup>	172 mg/L				CaCl <sub>2</sub>
Pb	10.0 mg/L	10.0 mg/L	200 µg/L	< 5µg/L <sup>b</sup>	PbCl <sub>2</sub>
Zn	1.0 mg/L	1.0 mg/L	200 µg/L	< 25 µg/L <sup>b</sup>	ZnSO <sub>4</sub> ·7H <sub>2</sub> O
Cu	1.0 mg/L	1.0 mg/L	200 µg/L	< 5µg/L <sup>b</sup>	CuSO <sub>4</sub>

<sup>a</sup>Total Dissolved Solids

<sup>b</sup>Chemical source is not added and the value is the instrumentation detection limit for the metals.



Table 7-4. Time from the first experiment for each bench scale experiment

Experimental ID	Days passed from the previous experiment	Days passed from 1 <sup>st</sup> Experiment	Influent total concentration	Experimental Condition
Experiment 1	0	0	Pb = 10 mg/L	Experiments with High metal concentrations
Experiment 2	10 days	10 days	Cu = 1 mg/L Zn = 1 mg/L	
Experiment 3	30 days	40 days	Pb = 10 mg/L	
Experiment 4	5 days	45 days	Cu = 1 mg/L Zn = 1 mg/L	Experiments with High metal concentrations
Experiment 5	28 days	73 days	Pb < 5 µg/L Cu < 5 µg/L Zn < 25 µg/L	Leaching study
Experiment 6	64 days	137 days	Pb = 10 mg/L Cu = 1 mg/L Zn = 1 mg/L	Experiments with High metal concentrations
Experiment 7	126 days	263 days		
Experiment 8	126 days	389 days		
Experiment 9	4 days	393 days		
Experiment 10	8 days	401 days	Pb = 200 µg/L Cu = 200 µg/L Zn = 200 µg/L	Experiments with low metal concentrations
Experiment 11	6 days	407 days	Pb < 5 µg/L Cu < 5 µg/L Zn < 25 µg/L	Leaching study

Two different pumps and pump heads were used to control various influent water heads and flow rates. A peristaltic pump (Cole Palmer Master flex model 7549-32) with an Easy-Load pump head (7529-00) and 9.5 mm inside diameter pump tubing (I/P Precision Pump tubing C-96410-73) was used for higher flow rates, and a L/S modular drive (07753-70) with I/P Easy-Load pump head (77601-00) and 6.4 mm inside diameter L/S precision pump tubing (C-06409-17) for lower flow rates (Figure 7-2). An overhead stirrer with a speed controller was used to mix the influent storage tank throughout experiments (Figure 7-2).

Various flow rates were studied in the experiments by controlling the influent water head. Target influent water heads were reached as fast as possible using the

highest flow rate of both pumps. When the target influent water head was reached, it was maintained by adjusting the flow rates of the pumps (Figure 7-3).

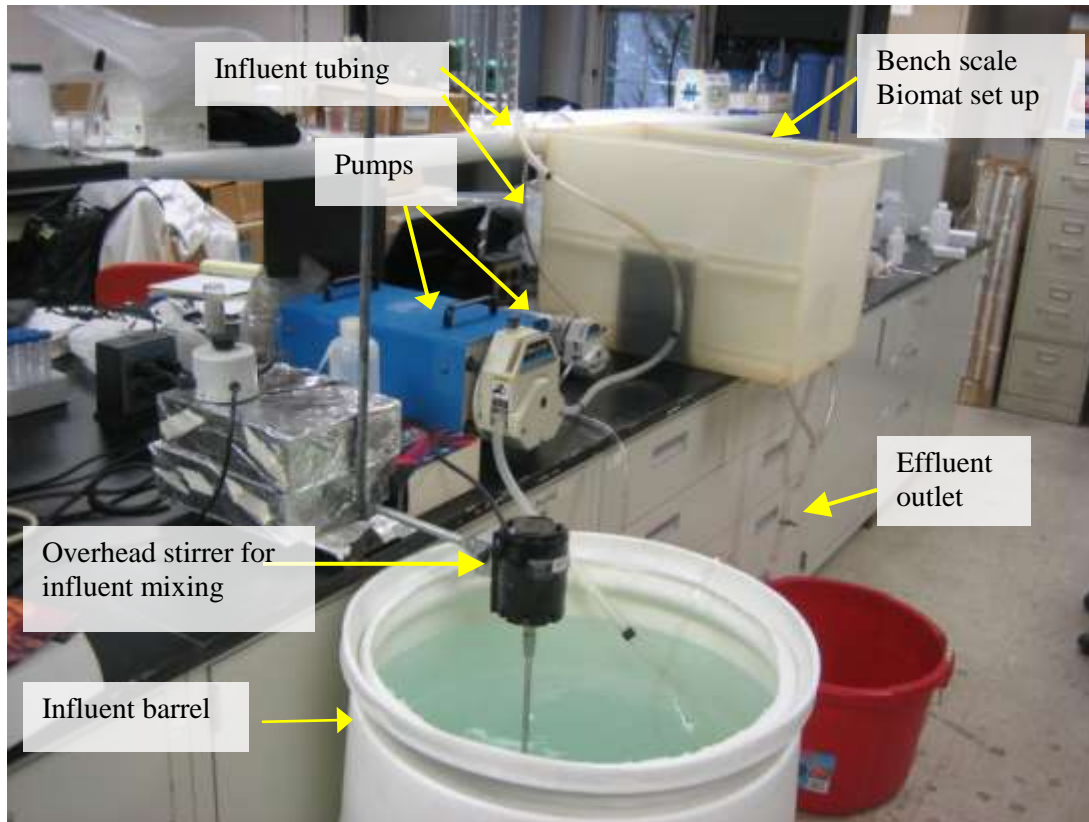


Figure 7-2. Experimental setup of bench scale experiment

Throughout all experiments, both effluent and influent samples were taken at various times from the start to investigate the performance of the Biomat media at various hydraulic loadings. Effluent flow rate as well as influent water head was measured during the experiments. Turbidity and pH were measured as soon as the samples were taken. Turbidity was measured using Standard Method, 2130 B, Nephelometric Method via a HACH 200N turbidity meter (APHA et al., 1995). Before turbidity measurement,

the sample was gently agitated and poured into the cell after air bubbles disappeared. Turbidity was read directly from the instrument display.

A portion of each sample was filtered through 0.2  $\mu\text{m}$  pore size, 25 mm diameter membrane disk filters, acidified using trace metal grade  $\text{HNO}_3$  and stored in a refrigerator for later analysis of dissolved elements. The remainder of unfiltered samples was also acidified and stored in a refrigerator for later digestion and analysis of total elements unless the samples were immediately analyzed. Dissolved and total heavy metal concentrations (Pb, Cu, Zn, and Cr) as well as total phosphorus in the samples were measured as described in Section 6-2-2.

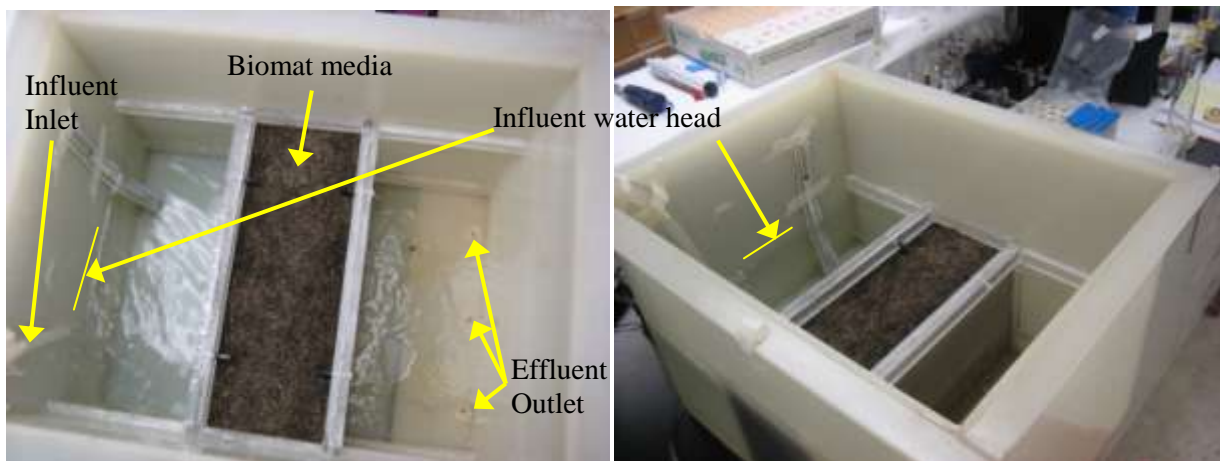


Figure 7-3. Bench scale experiment during a experiment.

### 7-2-3. Evaluating Hydraulic Conductivity for bench scale experiments – Phase 3

Hydraulic conductivity of the media was determined by measuring effluent flow rate and influent water head (Figure 7-4). Based on Darcy's law (where,  $k$  = hydraulic conductivity,  $Q$  = flow rate per unit width,  $h$  = water head,  $l$  = media length), hydraulic conductivity can be derived and calculated using the following equations

$$Q = -k \times h \frac{dh}{dl} \quad (7-1)$$

Integrating each side;

$$\int_0^L dl = \frac{-k}{Q} \int_0^H h \, dh \quad (7-2)$$

Therefore, hydraulic conductivity, k can be calculated as;

$$k = \frac{2Ql}{H^2} \quad (7-3)$$

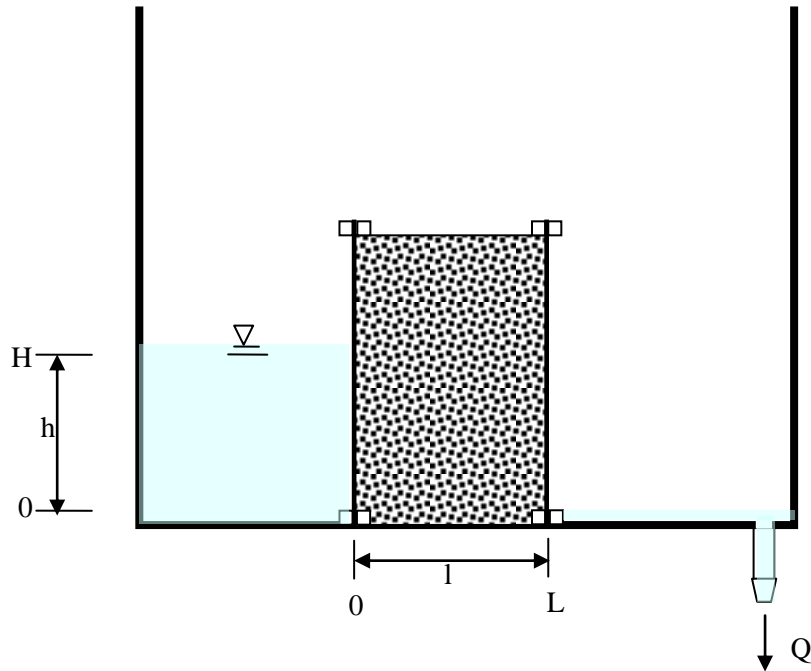


Figure 7-4. Parameters used in estimating hydraulic conductivity of Biomat media.

#### 7-2-4. Media extraction and analysis after the bench scale experiments – Phase 3.

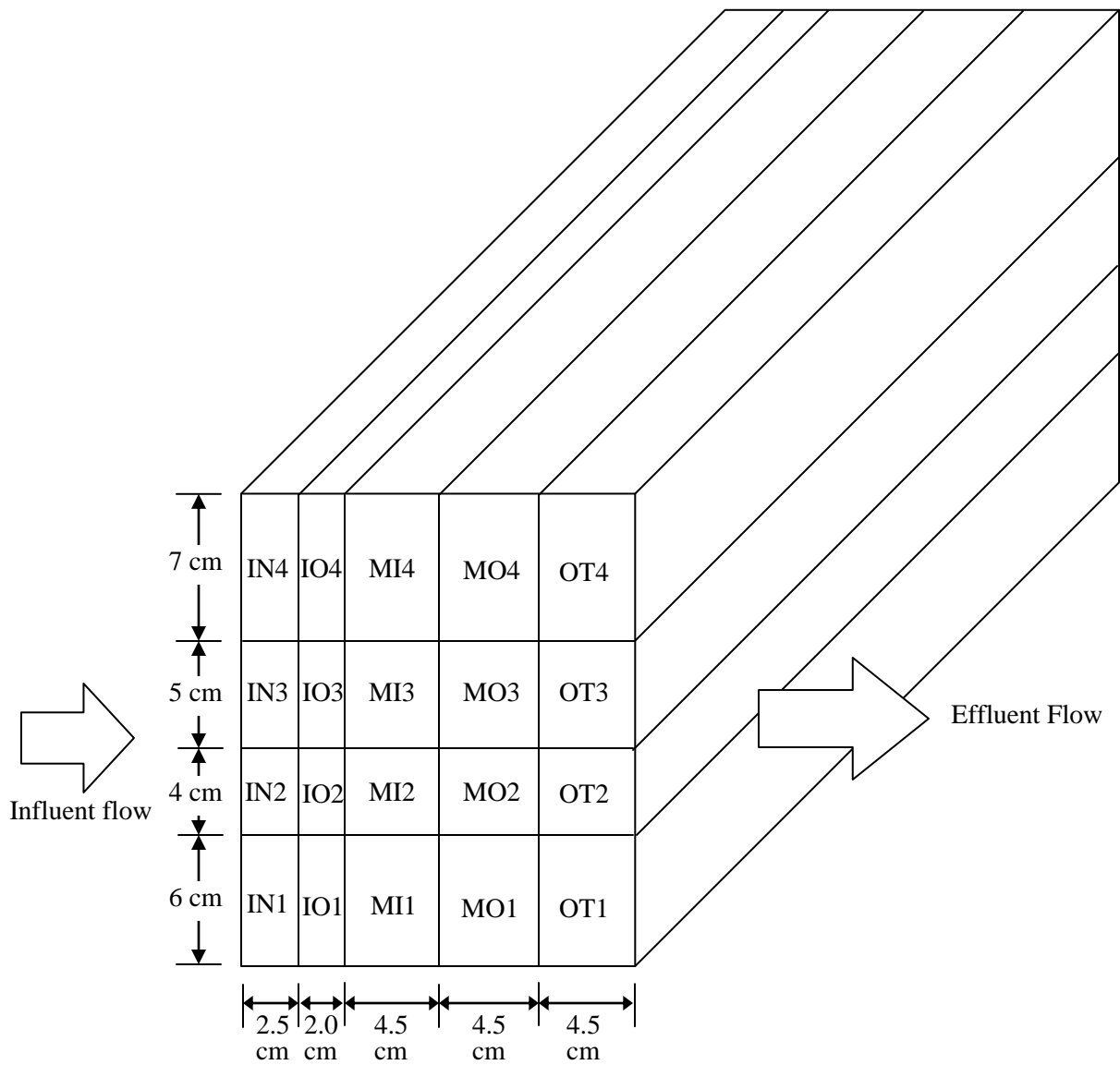
After all bench scale experiments, media samples were taken from the various media depths and lengths for metal extractions to characterize the metal lability in the media. The sampling profile from Biomat media and the media sample ID is shown in

Figure 7.5. First, the Biomat media was evenly divided into 4 layers (4.5 cm each) in terms of the media length parallel to the water flow using thin stainless steel sheets. The first 4.5 cm layer (the influent side) was again divided into 2 (2.5 cm and 2 cm) to make total 5 layers (Figure 7-5). Triplicate media samples were collected from a sampling profile using a soil probe sampler, which enabled one to take samples from four different media depths. The samples were air-dried and stored in soil sampling bags for later analysis.

Four different extractions were performed to characterize the metal extractability from the media after the bench scale experiments. Firstly, the concentration of phyto-available metals was determined by shaking 20 g of sample in 40 mL of 0.01 M  $\text{Sr}(\text{NO}_3)_2$  extracting solution for 1 hr (Madden, 1988). The extracted solution was filtered using a Ahlstrom #513 fluted filter paper inside of a #40 Whatman filter paper, and a portion of the unfiltered slurry was used to measure pH of the mixture.

Secondly, acid ammonium oxalate extraction in darkness was performed via the methods by Loeppert and Inskeep (1996) by shaking 500 mg of dry media in 30 mL of 0.175 M  $(\text{NH}_4)_2\text{C}_2\text{O}_4$  + 0.1 M  $\text{H}_2\text{C}_2\text{O}_4$  solution (pH 3.0) for 2 h, and centrifuging the extracted samples.

Thirdly, the bioaccessible fraction of heavy metals was determined employing the Relative Bioavailability Leaching Procedure (RBALP) in order to measure the fraction of metal solubilized from a media sample under simulated gastrointestinal conditions (at 37 °C and pH 1.5) using 0.4 M glycine solution (Drexler and Brattin, 2007). Finally an aqua regia procedure was performed to determine total metal content in the media (McGrath and Cunliffe, 1985).



**Figure 7-5. Soil sampling profile from Biomat media after bench-scale experiment.**

### 7-3. Results

#### 7-3-1. Bench Scale performance of Biomat with both dissolved and precipitated forms of metals (Experiment 1 and 2).

Dissolved metals only were expected in the influent for Pb, Cu, and Zn when the synthetic runoff for Experiments 1 and 2 was made using tap water by adding proper volumes of each stock solution. However, only 6.36 mg/L dissolved Pb out of 10.1 mg/L total Pb, and 6.33 mg/L dissolved Pb out of 10.5 mg/L total Pb were detected for Experiments 1 and 2, respectively (Figure 7-6a and 7-7a). This is probably because dissolved Pb in the influent reacts with some dissolved anions (e.g.,  $\text{CO}_3^{2-}$ ,  $\text{SO}_4^{2-}$ ,  $\text{HS}^-$ ) in tap water and precipitates (Patterson et al., 1977; Marani et al., 1995).

Various flow rates were studied for Experiment 1 and 2 by controlling four and five different target water heads, respectively, as shown in Figure 7-6a and 7-7b. The corresponding effluent flow rates at each target water head are shown in Figure 7-6b and 7-7b for Experiment 1 and 2, respectively. Approximately 92 to 96% total Pb removal throughout various Pb loadings rate was observed for Experiment 1, while Experiment 2 demonstrated similar results, but slightly lower percent removal, showing 89 to 92% total Pb removal. Total effluent Pb concentration ranged from 0.44 to 0.78 mg/L for Experiment 1 and 0.81 to 1.14 mg/L for Experiment 2 (Figure 7-6a and 7-7a). Interestingly, only 4.9 to 9.3% of total Pb for Experiment 1 and 2.0 to 7.7% for Experiment 2 was detected as dissolved Pb in the effluent, while dissolved influent Pb for Experiments 1 and 2 consisted of about 63% and 60% of total influent Pb, respectively. This suggests that most of the dissolved Pb was efficiently removed by the mat media from the influent during the experiments while some of the precipitated solids from the influent (i.e., small particle sizes) were not removed and became the majority form of Pb

in the effluent. It is speculated that the freshly precipitated solid Pb species in influent for Experiments 1 and 2 were mostly amorphous Pb precipitates and therefore, consisted of very fine particles. Relatively large and even particle sized sand was used in Biomat media (see Appendix D1, D4 and D5 for sand information) to enhance the hydraulic characteristics of the mat media (i.e., high hydraulic conductivity). Therefore, the Biomat media is not likely to trap/filter out extremely fine Pb precipitates efficiently, while dissolved metals were effectively removed by the media by adsorption/precipitation.

No significant increase of either effluent total or dissolved Pb was noted as influent water head increased throughout Experiments 1 and 2, demonstrating that the flow rate was not the important parameter controlling metal removal for the range of flow rates studied in the experiments. It is important to note that the flow rates plotted in Figures 7-6b and 7-7b are based on effluent flow rate per perpendicular unit length of Biomat media with  $\frac{mL}{min \cdot cm}$  units.

During the Experiments 1 and 2, precipitated Cu was also noted in the influent but much less compared to Pb, demonstrating that around 94% and 95% of total influent Cu consisted of dissolved form for Experiment 1 and 2, respectively (0.95 mg/L dissolved out of 1.01 mg/L total Cu for Experiment 1 and 0.97 mg/L dissolved out of 1.02 mg/L total Cu for Experiment 2) (Figure 7-6b and 7-7b). Higher total Cu % removal ( $\geq 98$  % except the first flush) was noted compared to Pb % removal throughout Experiments 1 and 2, demonstrating very low effluent total Cu concentration of 11 to 22  $\mu g/L$  for Experiment 1 and 13 to 17  $\mu g/L$  for Experiment 2, except for the first flush (Figures 7-6b and 7-7b). This higher Cu percent removal compared to that of Pb is due to



the higher percentage of dissolved species in the influent, which were more efficiently removed by Biomat media than solid species. However, relatively higher total effluent Cu concentration (134  $\mu\text{g/L}$  total) from the first flush for Experiment 2 (no first flush data are available from Experiment 1) was observed concomitant with low dissolved effluent Cu concentration (13  $\mu\text{g/L}$ ), suggesting that some fine media particles containing Cu were leached out in the first flush during these first two experiments

Unlike influent Pb and Cu, essentially no precipitated Zn was observed in influent for Experiment 1 and 2 and essentially all Zn was present as the dissolved forms (Figure 7-6c and 7-7c). In spite of no precipitated Zn in the influent, relatively high total Zn concentration (80 – 151  $\mu\text{g/L}$  for Experiment 1 and 85 - 136  $\mu\text{g/L}$  for Experiment 2) with very low dissolved Zn (all less than the instrumentation detection limit of 25  $\mu\text{g/L}$  for the both experiments) was observed in the effluent (Figures 7-6c and 7-7c). Therefore it is speculated that the high total Zn originated from the loss of precipitated Zn species produced through the infiltration of influent Zn or/and initial washing out of fine compost particles from the mat media which has a much higher Zn content than Pb and Cu (see Table 7-1). This high particulate Zn was also noted during the initial stages of the column study, as shown in Chapter 6.

As with Pb, no significant increase of either effluent total or dissolved Cu and Zn was observed as influent water head increased throughout Experiments 1 and 2, confirming that the flow rate was not the controlling parameter for the metal removal for the range of flow rates studied.

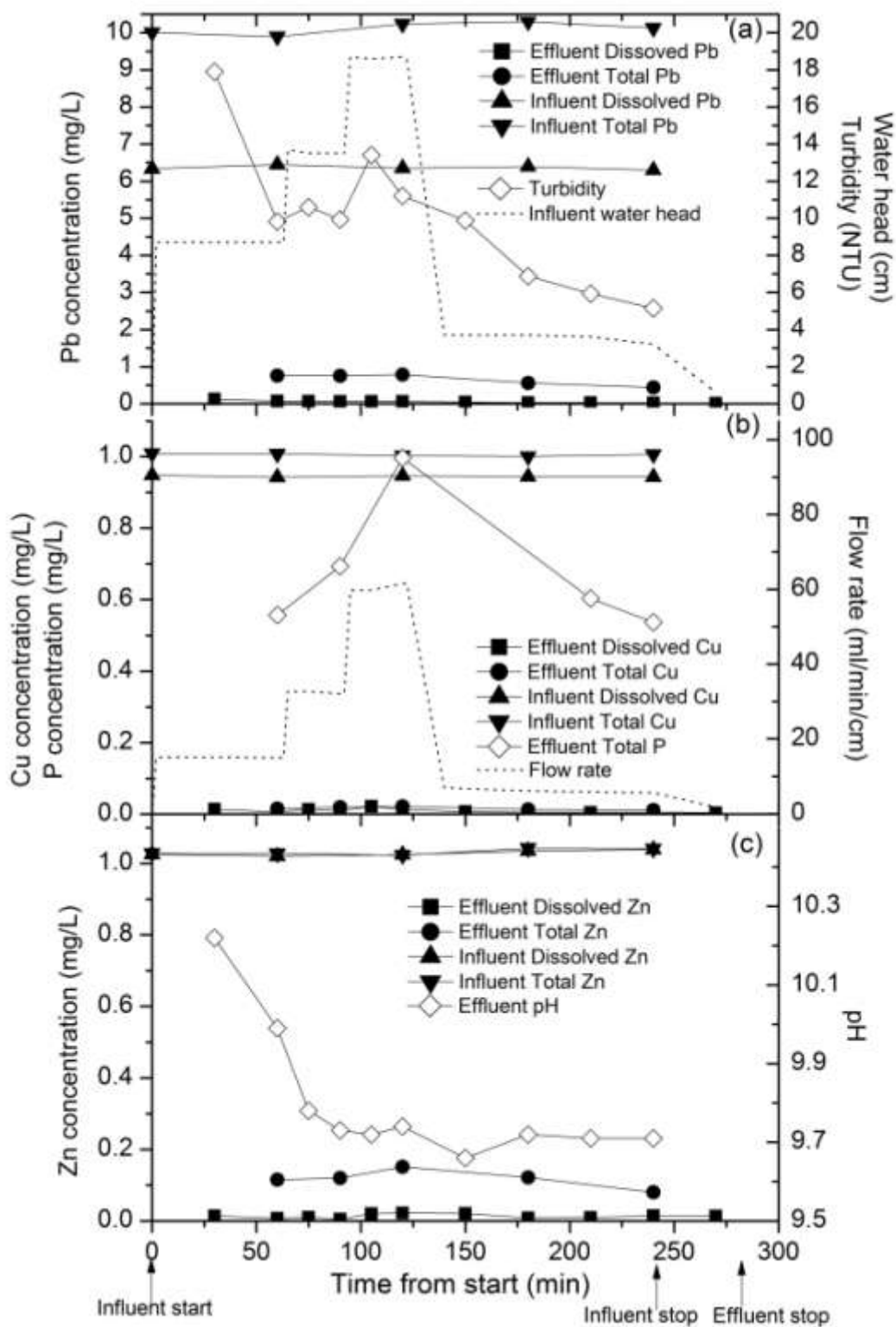


Figure 7-6. Water quality parameters for Experiment 1 during bench scale experiments. (a) Pb concentrations, water head, and turbidity; (b) Cu concentrations, P concentrations, and effluent flow rate; (c) Zn concentrations and pH.

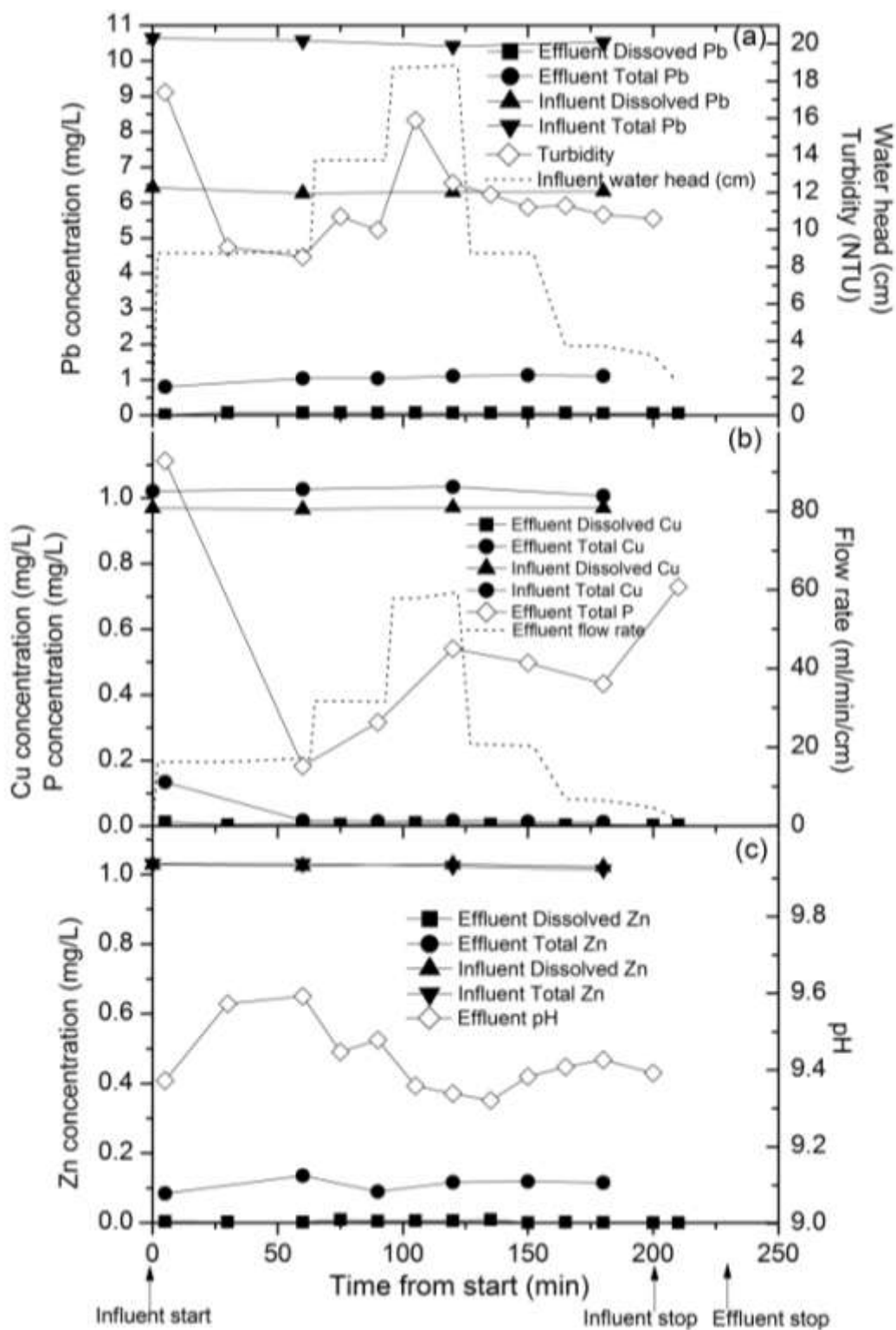


Figure 7-7. Water quality parameters for Experiment 2 during bench scale experiments. (a) Pb concentrations, water head, and turbidity; (b) Cu concentrations, P concentrations, and effluent flow rate; (c) Zn concentrations and pH.

Overall, moderate effluent turbidity during Experiments 1 and 2 (5.1-17.9 NTU for Experiment 1 and 8.5-17.4 NTU for Experiments 2) was noted with the highest value observed from the first samples of the experiments (Figures 7-6a and 7-7a). This was expected due to leaching of fine compost media particles and dissolution of organic matter from the media by flow during the initial stage of Biomat operation. For the same reason, high first flush total phosphorus (for Experiment 2; no first flush data for Experiment 1) was observed and significant initial drop was also observed as more flow was treated during the experiment (Figures 7-6b and 7-7b).

Interestingly, effluent turbidity and total phosphorus concentration demonstrated similar trends with the change of water head (effluent flow rate); they correspondingly increased and decreased as influent water head (effluent flow rate) increased and decreased (Figures 7-6 and 7-7). Again, this increased turbidity and phosphorus concentration in effluent at the higher flow rate can be explained by greater organic matter dissolution (color and phosphorus from dissolved organic species) from compost media and/or greater direct loss of fine compost media. The P loss from the media during the Biomat operation for metal removal can be one of the environmental drawbacks in using the compost media, especially during the initial stage of the Biomat media operation. It is, however, expected to decrease as more flow is treated through the Biomat media, based on the previous column study (Chapter 6).

### **7-3-2. Bench Scale performance of Biomat with dissolved forms of metals only (Experiments 3 and 4).**

For the rest of the bench scale experiments, DI water was used to make synthetic runoff. Therefore, no precipitation of the metals (Pb, Cu and Zn) was observed in the influent and essentially all the metals in the influent were detected as dissolved.

All dissolved effluent Pb concentrations for Experiment 3 were lower than the detection limit; 5 µg/L (Figure 7-8a). Experiment 4 also demonstrated that the effluent dissolved Pb concentrations were mostly lower than 5 µg/L except for the samples from the highest water head (up to 7.5 µg/L at 18.7 cm water head) (Figure 7-9a), demonstrating very efficient influent Pb removal and minimal release of dissolved Pb to effluent. Compared to Experiments 1 and 2, much lower effluent total Pb concentrations were observed for Experiment 3 (15-83 µg/L) and Experiment 4 (10 to 29 µg/L) mainly due to only dissolved Pb present in the influent, which can be more efficiently removed by Biomat media than fine particulate Pb.

Total Pb at 83 µg/L was detected initially, which decreased to 15 µg/L, demonstrating >99% of Pb removal throughout Experiment 3 (Figure 7-8a). This relatively high total Pb from the initial samples of Experiment 3 can originate from loss of compost organic matter with a highly sorbed Pb content and/or the precipitated Pb captured by mat media during previous Experiments 1 and 2, which was leached to the effluent during the subsequent Experiment. Therefore, this total Pb originating mostly from particulate Pb was related to effluent turbidity, which shows similar trends throughout Experiments 3 and 4 (Figure 7-8a and 7-9a). Compared to the initial total Pb (83 µg/L) in Experiment 3, effluent total Pb concentration from the first flush in

Experiment 4 was much lower (29 µg/L) and it decreased to 10 µg/L, with much greater than 99% total Pb removal throughout the experiment (Figure 7-9a).

No significant change in either dissolved or total Pb, Cu and Zn concentration was observed throughout Experiments 3 and 4, although somewhat notable increases in effluent Pb and Zn concentrations were observed during the highest water head. Again, this indicates the minimal impact of flow rate on effluent metal concentration for the flow rates studied. Overall, very low dissolved and total effluent Cu concentrations was noted at all influent water head studied during Experiment 3 and 4 (mostly lower than 10 µg/L total Cu except 13 µg/L at 13.8 cm influent water head during Experiment 4), suggesting very high total Cu removal through the Biomat media. However, relatively high total effluent Zn (86-121 µg/L for Experiment 3 and 97-192 µg/L for Experiment 4) was still noted, while dissolved Zn was very low (all less than the instrumentation detection limit of 25 µg/L) throughout the experiment as also observed in Experiments 1 and 2.

Like Experiments 1 and 2, the highest effluent turbidity was also observed from the first flush sample for both Experiments 3 and 4, and it significantly decreased in the following sample. However, influent water head change (i.e., effluent flow rate) during the both experiments did not significantly affect the effluent turbidity values, unlike with Experiments 1 and 2, demonstrating relatively consistent low turbidity with noticeable increase only at the highest water head. This indicates that the greatest portion of readily leachable fine compost media particles or readily dissolvable organic matter causing effluent turbidity were leached during the first two experiments and, therefore, higher flow rate rarely increased the effluent turbidity after the initial drop of the effluent turbidity.

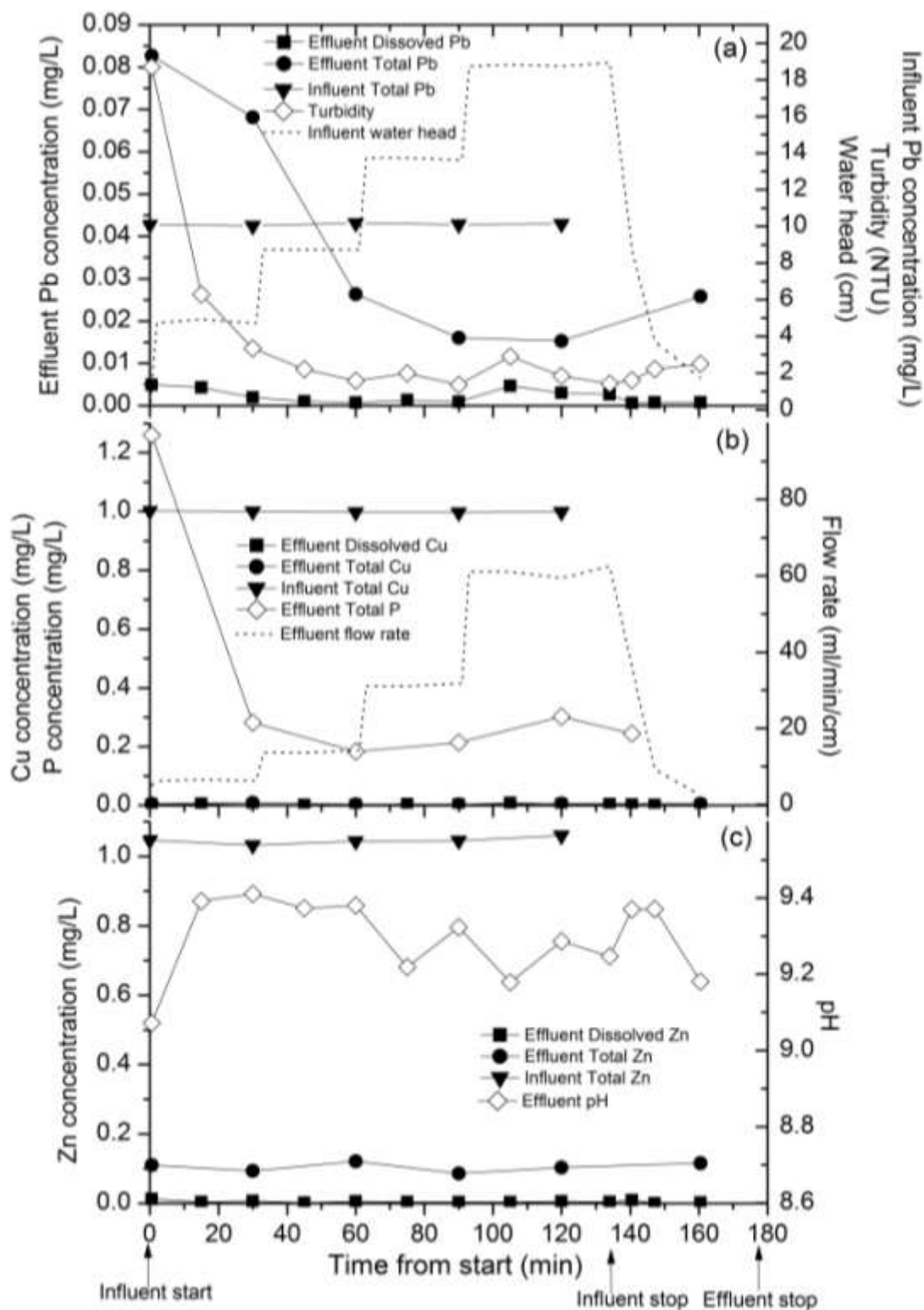


Figure 7-8. Water quality parameters for Experiment 3 during bench scale experiments. (a) Pb concentrations, water head, and turbidity; (b) Cu concentrations, P concentrations, and effluent flow rate; (c) Zn concentrations and pH.

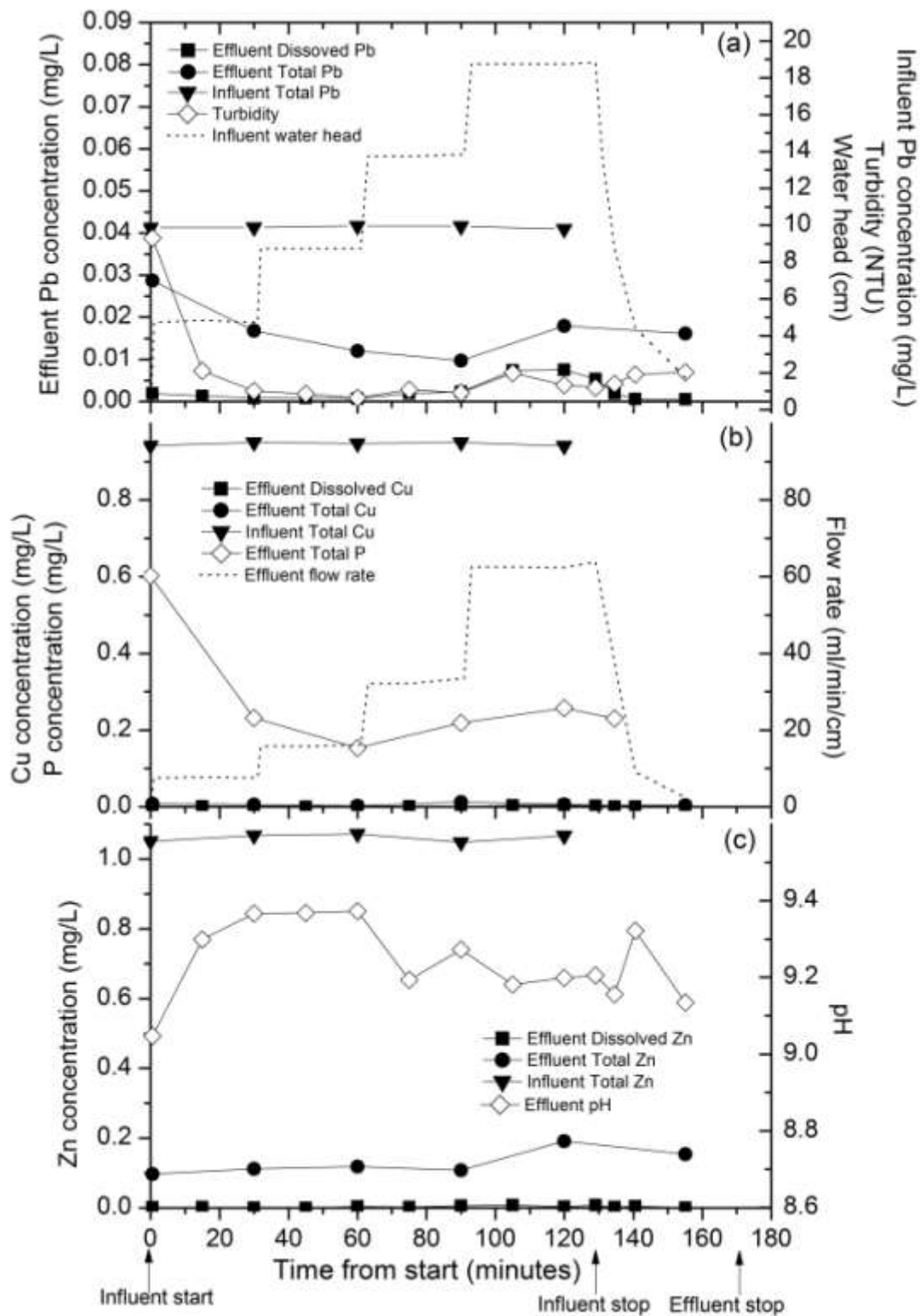


Figure 7-9. Water quality parameters for Experiment 4 during bench scale experiments. (a) Pb concentrations, water head, and turbidity; (b) Cu concentrations, P concentrations, and effluent flow rate; (c) Zn concentrations and pH.



### **7-3-3. Change of bench scale Biomat performance on influent water head (flow rate change) and hydraulic conductivity of media (Experiments 7 to 9).**

As discussed in the previous result section, significant Biomat performance change (i.e., effluent concentration increase) for heavy metal removal on influent water head increase (i.e., effluent flow rate increase) was not noted for all heavy metal loadings (by changing influent water head) studied during the first four bench scale experiments (Experiments 1 to 4). This suggests that the heavy metal removal rates by the mat media were fast enough that the heavy metal removal was not limited even at the highest water head studied.

However, effluent heavy metal concentration increase was observed as water head increased during Experiments 7 to 9 as presented through Figure 7-10, 7-11, and 7-12, respectively. This is because the hydraulic conductivity significantly increased from Experiments 1-5 (around 6.5 cm/min) to Experiments 7(11.5 cm/min) and further Experiments 8 to 9 (around 20 cm/min), which caused effluent flow rates to significantly increase. (Table 7-5 and Figures 7-10, 7-11, and 7-12). It should be noted that there was an extended time lag between Experiment 5 and 7 (64 days lag between Experiment 5 and 6 and 126 days lag between Experiment 6 and 7), which is relatively long compared to the time lag between any adjacent experiments from Experiment 1 to 5 (Table 7-4). Furthermore, there was also another long time lag (126 days) between Experiment 7 and 8, when significant hydraulic conductivity increase was also observed (Table 7-5). Therefore, it is speculated that structural change of media through physical, chemical and biological processes transpires during the extended lag time between two experiments (i.e., drying period between storm events). Hydraulic conductivity of Biomat media is further discussed in Section 7-3-7.

Due to hydraulic conductivity increase from Experiment 7 to Experiments 8 and 9 (Table 7-5), differences in Biomat heavy metal removal performance were noted. Experiment 7 demonstrated that effluent dissolved metal concentrations for heavy metals were not increased until influent water head increased to 13.7 cm, while effluent dissolved metal concentrations for Experiment 8 and 9 increased as influent water head increases from 4.7 cm to about 6.7 cm (Figures 7-10, 7-11, and 7-12). Furthermore, the highest effluent dissolved heavy metal concentrations were noted from Experiments 8 and 9, showing up to 428  $\mu\text{g/L}$  Pb for Experiment 8 and 523  $\mu\text{g/L}$  Pb for Experiment 9, compared to 190  $\mu\text{g/L}$  Pb for Experiment 7 at influent water head of about 18.7 cm (Figures 7-10a, 7-11a, and 7-12a). Again, this is due to hydraulic conductivity increase of the Biomat from 11.5 cm/min for Experiment 7 to about 20 cm/min during Experiments 8 and 9 (Table 7-5). This caused higher effluent flow rates (i.e., higher metal loading rates) for Experiments 8 and 9 (about 190 mL/cm/min) at the same influent water heads studied during Experiment 7 (about 115 mL/cm/min) (Figure 7-10b, 7-11b, and 7-12b).

Similar to effluent Pb, effluent Cu and Zn increases were also noted on water head increase during Experiments 7 to 9 (Figures 7-10, 7-11, and 7-12 b and c). During Experiments 7, 8 and 9, the effluent dissolved and total concentrations of Cu and Zn (mass based) were lower than those of Pb at the high water heads mainly due to higher Pb influent concentration ( $\sim 10$  mg/L) than Cu and Zn ( $\sim 1$  mg/L). At the high water head, lower effluent Cu concentrations (both mass and molar based) were also noted compared to that of Zn, suggesting that Cu affinity with the mat media is higher than that of Zn

(Figures 7-10, 7-11, and 7-12), which was also noted by Jang et al (2005) in their metal removal study from urban runoff using mulch.

Total effluent P concentration ranged from 0.28 to 0.43 mg/L for Experiment 7, 0.16-0.27 mg/L for Experiment 8, 0.17 – 0.31 mg/L for Experiment 9 except that from the first flush, which showed up to 1.4 mg/L P (Figures 7-10b, 7-11b, and 7-12b). As explained earlier, this high total P from the first flush of each experiment can be explained by leaching of both solid and dissolved organic compounds from compost materials in the media before the first flush. In these experiments, the first flush sample represents mostly less than 0.5 L taken during the first one minute from the first effluent start. The effluent P concentration decreased significantly as the subsequent flow was treated. Therefore, effluent P concentration is moderate throughout the experiments. Furthermore, the effluent P concentration is expected to decrease further as more flow is treated through Biomat based on the previous column results (refer to Chapter 7).

Nonetheless, the P release during the Biomat operation may be an adverse impact on environment as an expense of heavy metal removal, and therefore, should be minimized. It is speculated that the water remaining in the mat after each experiment (especially in the bottom of the mat due to poor drainage because there was no slope toward the effluent drainage) caused high residual moisture in the media. This promoted decomposition of compost and further hydrolysis of phosphorus between experiments. In a field application of the Biomat, a plastic liner with slight slope toward the effluent direction is recommended to be installed underneath the mat media to prevent flow downward through the media and to promote perpendicular water flow through the mat media. This will not only promote flow toward the effluent side, but also prevent water

from remaining in the media (better drainage) between storm water events. This modification may decrease the P release from the compost media by reducing the media materials organic matter decomposition and further hydrolysis of P materials.

As an approach to decrease effluent P concentration further, an extra layer of sand can be added after the Biomat mixture media to decrease discharge of particulate forms of P by filtering/trapping particulate organic matter better from the compost media. This might also help to separate particulate forms of heavy metals in the effluent and to decrease total effluent metal concentrations. Alternatively, further aggressive P reduction can be made using low cost by-product materials such as water treatment residuals (Al or Fe based) (Codling et al., 2000; Elliott et al., 2002; Gallimore et al., 1999; Haustein, 2000; Makris et al., 2004), gypsum (Peacock and Rimmer, 2000); or slags (Gruneberg and Kern, 2001), which are capable of P reduction from the effluent through application in the Biomat media mixture or the subsequent supporting sand media layer.

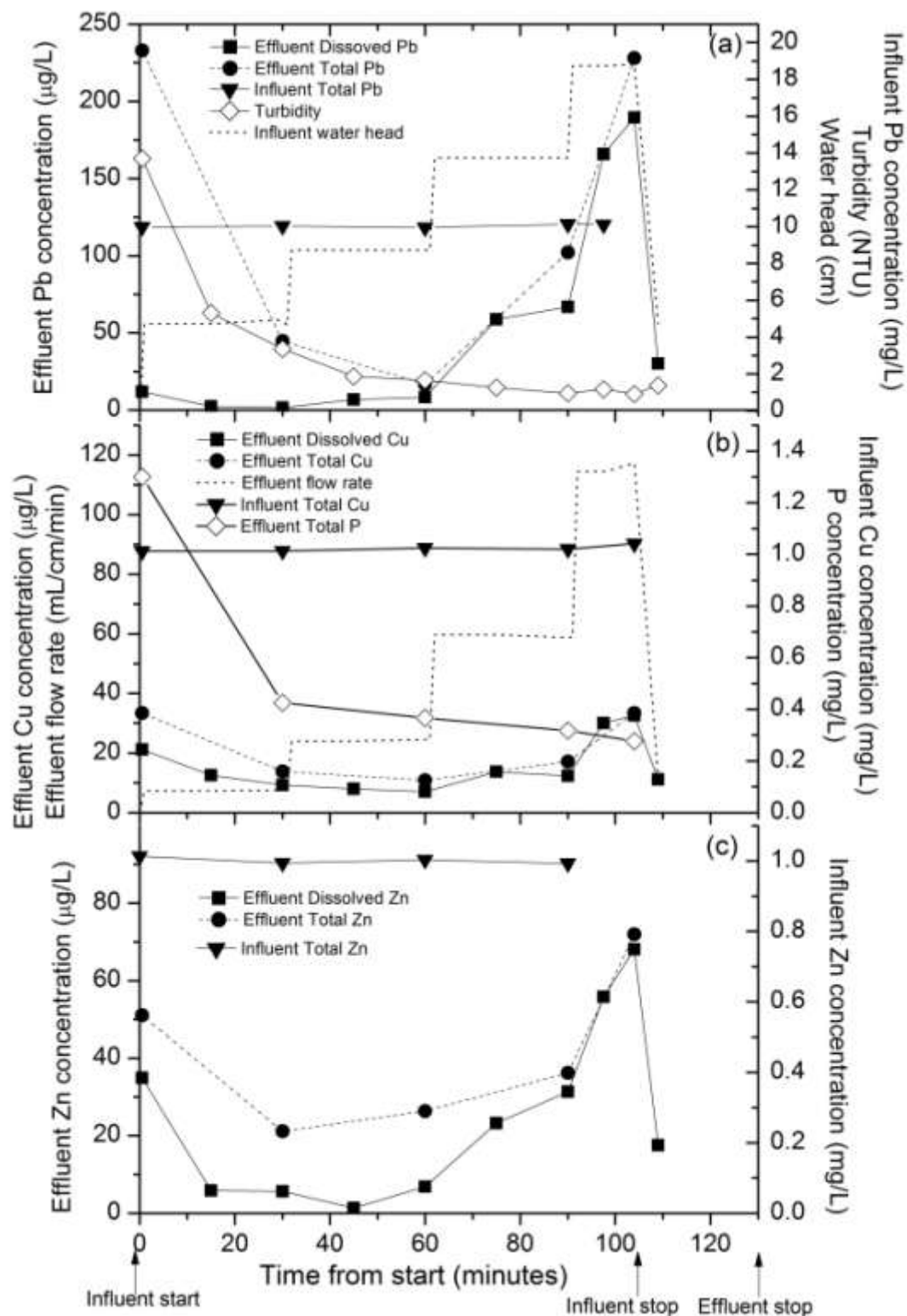


Figure 7-10. Water quality parameters for Experiment 7 during bench scale experiments. (a) Pb concentrations, water head, and turbidity; (b) Cu concentrations, P concentrations, and effluent flow rate; (c) Zn concentrations.

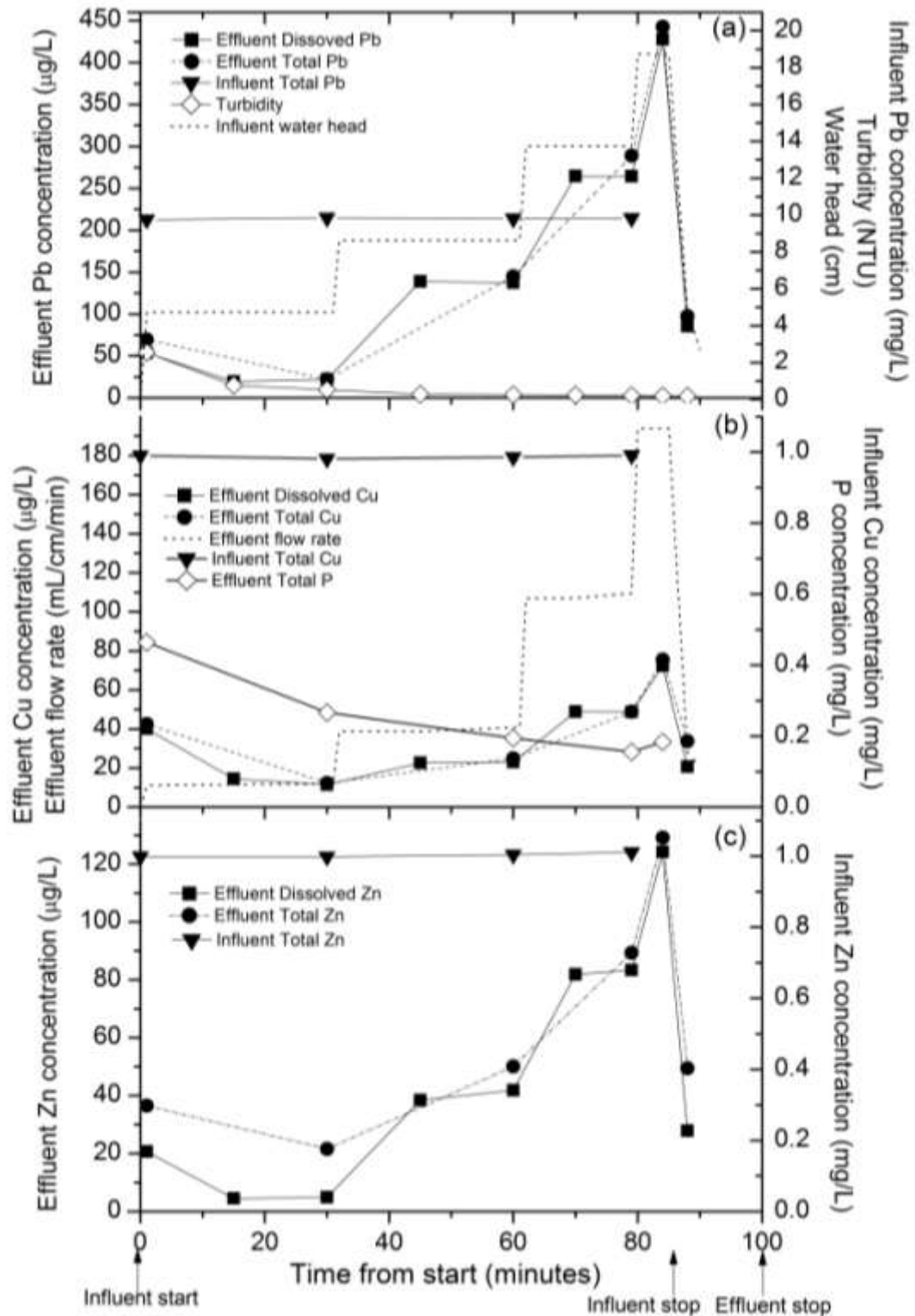


Figure 7-11. Water quality parameters for Experiment 8 during bench scale experiments. (a) Pb concentrations, water head, and turbidity; (b) Cu concentrations, P concentrations, and effluent flow rate; (c) Zn concentrations.

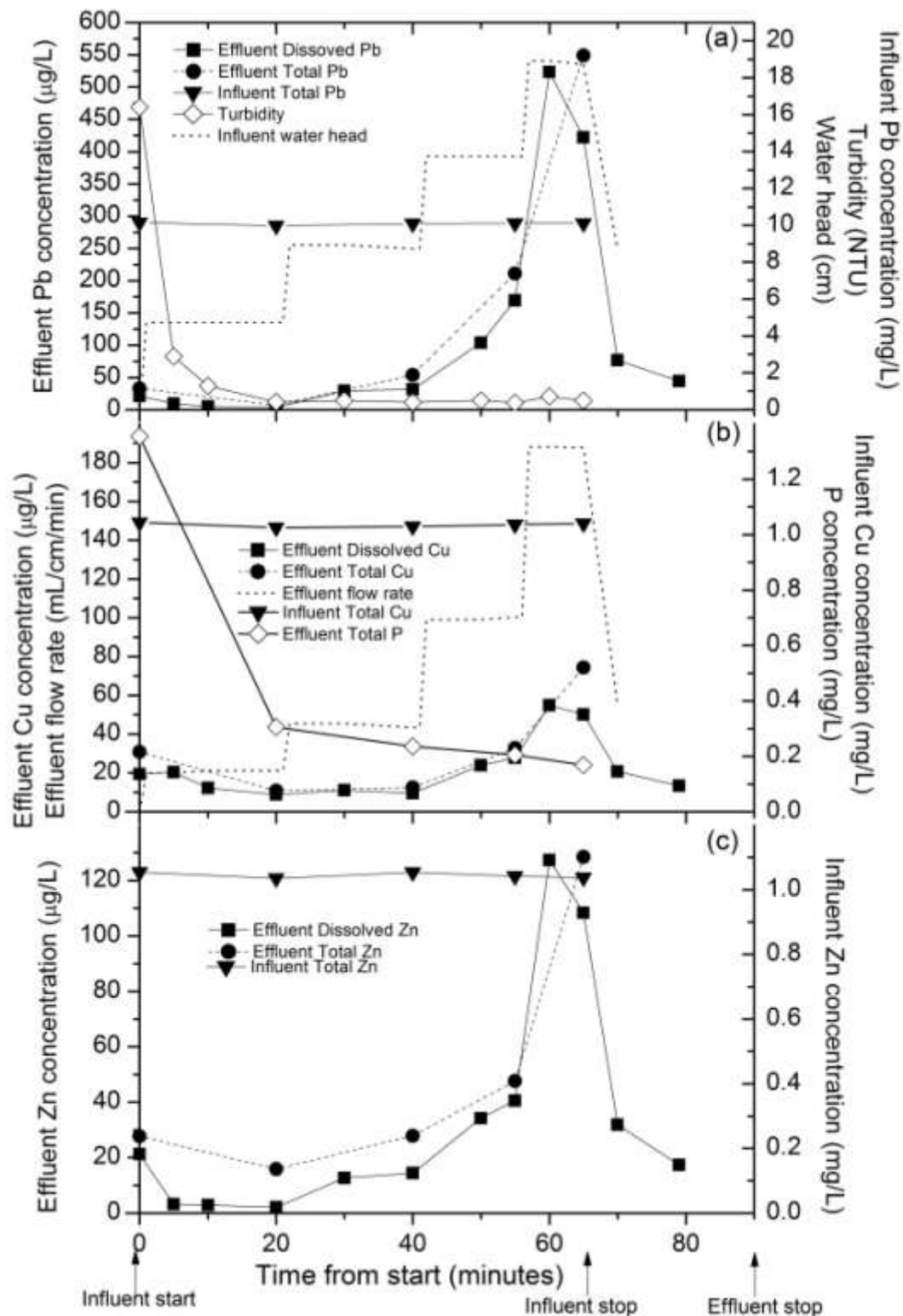


Figure 7-12. Water quality parameters for Experiment 9 during bench scale experiments. (a) Pb concentrations, water head, and turbidity; (b) Cu concentrations, P concentrations, and effluent flow rate; (c) Zn concentrations.

Table 7-5. Hydraulic conductivity of Biomat media for each experiment during bench scale study.

Experiment ID	Average hydraulic conductivity, k (cm/min)*	Accumulative days from Experiment 1
Experiment 1	6.6	0
Experiment 2	6.6	10
Experiment 3	6.3	40
Experiment 4	6.7	45
Experiment 5	6.2	73
Experiment 7	11.5	263
Experiment 8	19.9	389
Experiment 9	19.5	393
Experiment 10	20.4	401
Experiment 11	20.5	415

\* The hydraulic conductivity data at the lowest water head of each experiment was not used to calculate the average conductivity during each experiment due to the high deviation compared to the hydraulic conductivity data for the rest of water head studied (~8.7, 13.7 and 18.8 cm).

#### **7-3-4. Biomat performance for low influent concentration during bench scale (Experiment 10).**

The Biomat performance for lower influent metal concentrations (about 200 µg/L for each metal) was investigated in Experiment 10 and the results are presented in Figure 7-12. The expected influent metal concentrations from roof/wall runoff from Building-580 (APHIS building) are relatively higher (see Table 5-1 in Chapter 5) compared to typical storm water runoff (see Table 3-6 in Chapter 3) and roof runoff (see Table 3-7a and b in Chapter 3). Specifically, various levels of heavy metals in highway and urban runoff are Zn 20-500 µg/L, Cu and Pb 5-200 µg/L, and Cd <12 µg/L (Davis et al., 2001).



Boller (1997) reported average roof runoff metal concentrations of 90 µg/L Pb, 200 µg/L Cu, 400 µg/L Zn, and 0.6 µg/L Cd, based on his literature surveys, although significantly different metal concentrations were observed from different roof material types (e.g., tile roof, polyester roof, and flat gravel roof) in various roof runoff studies (see Tables 3-7a and 3-7b in Chapter 3). Therefore, quantifying Biomat performance for low metal concentrations is important to evaluate its applicability for treating wide ranges of storm water runoff as a possible Best Management Practice (BMP) technology. Furthermore, possible impacts on effluent water quality change including metal and phosphorus leaching under low influent metal concentrations was investigated to evaluate the feasibility of the Biomat media with low ranges of influent metal concentrations.

Effluent dissolved Pb and Cu concentrations were less than 5 µg/L for all samples except a sample from first flush (19 µg/L dissolved and 30 µg/L total Pb; 6 µg/L dissolved and 8 µg/L total Cu ) and samples from highest water head (around 11 µg/L dissolved and 12 µg/L total Pb; 13 µg/L for both dissolved and total Cu) (Figure 7-13a and b) . The 11 µg/L dissolved Pb (13 µg/L dissolved Cu) at the highest water head during Experiment 10 were very low compared to 428 µg/L dissolved Pb (72 µg/L dissolved Cu: Figure 7-11) for Experiment 8 and 523 µg/L dissolved Pb (55 µg/L dissolved Cu: Figure 7-12) for Experiment 9 at the similar influent water head of about 18.7 cm with very close flow rate (i.e., similar hydraulic conductivity between Experiments 8 and 9 and Experiment 10: see Table 7-5). This suggests that the effluent metal concentrations from Biomat media are related not only to flow rate, but also to influent concentration. Therefore, metal loading rate, a combined parameter of the flow

rate and influent concentration, was introduced to systematically evaluate Biomat performance, which is further discussed in Section 7-3-7.

Effluent dissolved Zn was less than the instrumentation detection limit of 25 µg/L for all samples except the first flush sample (27 µg/L dissolved and 33 µg/L total Zn) (Figure 7-13c). Furthermore, significant differences in phosphorus (see Figure 7-13b) or total chromium release (all  $\leq 1$  µg/L) between Experiment 10 and other experiments were not noted. This excellent Biomat performance with the lower influent metal concentration suggests the feasibility of employing a Biomat for treating water contaminated with heavy metals at lower concentrations. Specifically, the results show the effluent heavy metal concentrations at or near instrumentation detection limits even at the high flow rate; broadening the possible applicability of the Biomat as a BMP technology for treating stormwater runoff.

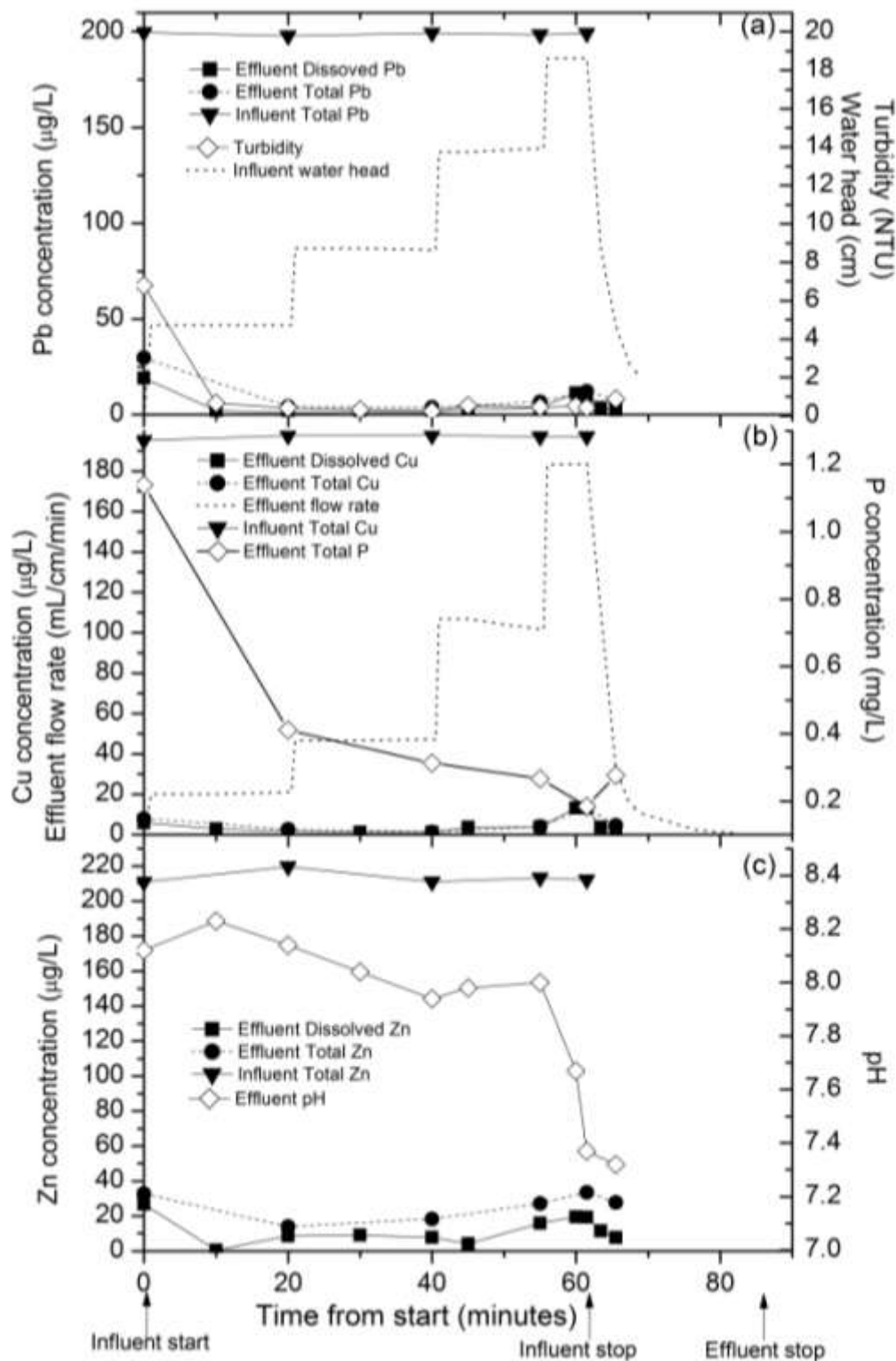


Figure 7-13. Water quality parameters for Experiment 10 during bench scale experiments. (a) Pb concentrations, water head, and turbidity; (b) Cu concentrations, P concentrations, and effluent flow rate; (c) Zn concentrations and pH.

### **7-3-5. Metal leaching study in bench scale Experiments 5 and 11.**

Heavy metal leaching from Biomat media was investigated in Experiments 5 and 11 and the results are presented in Figures 7-14 and 7-15, respectively. Both experiments demonstrated very low dissolved concentrations for all three metals (Pb, Cu, and Zn), suggesting minimal heavy metal leaching from the Biomat media. For all the samples from Experiment 5 at all water heads studied, dissolved effluent Pb and Cu concentrations were less than 5 µg/L for Pb and 2 µg/L for Cu (instrumentation detection limits) except the first two initial samples (12 and 6 µg/L, respectively for Pb and 5 and 3 µg/L for Cu) during the lowest water head. Dissolved effluent Zn concentrations for the all samples were also lower than the instrumentation detection limit of 25 µg/L except for a sample (29 µg/L) at the highest flow rate. Essentially, all samples at all water heads studied during Experiment 11 showed dissolved effluent metal concentrations lower than the instrumentation for the all three metals (Pb, Cu and Zn).

In spite of no metals in influent and low dissolved effluent metal concentrations, moderately high effluent total metal concentrations were observed from the samples during Experiment 5, showing 288 µg/L Pb, 37 µg/L Cu, and 53 µg/L Zn from its first flush sample, which decreased gradually (e.g., down to 9 µg/L for Pb) during the experiment (Figure 7-14). This suggests that the total effluent metals during Experiments 5 were originated from adsorbed or precipitated metal during previous experiments (i.e., no metal in influent). Therefore, it can be also postulated that the high total metal in the first flushes during other experiments originated from loss of fine media on which metals were captured by adsorption and/or precipitation from previous experiments, rather than leaching of precipitated solid metal species during the

operational experiments. Experiments 6 and 7, especially, along with Experiment 5 showed the highest total effluent metal concentrations compared to those from the other Experiments. The reason is unclear but this metal release can be attributed to the changes in the Biomat media packing or compost material decomposition during the relatively longer period of time between experiments, which produced fine particles with high metal concentrations which were washed out, therefore, increasing the total effluent metal concentration.

Interestingly, the total metal concentrations throughout Experiment 8 decreased dramatically compared the previous Experiment 7. Since low total metal concentrations were observed, including the first flushes throughout the rest of bench-scale experiments, it appears that decomposition of compost organic materials slowed and became stabilized after readily decomposable organic matter decreased from previous experiments.

Consequently, low total effluent metal concentrations were observed from all samples at all water heads studied during Experiment 11, showing most samples at less than instrumentation detection limits, except for the first flush sample (21 µg/L Pb, 6 µg/L Cu and 31 µg/L Zn), suggesting minimal loss of solid phase metals along with essentially no leaching of dissolved metals (Figure 7-15).

No significant difference were found in effluent P concentration between an adjacent sorption experiment and a leaching experiment (Figure 7-14b and 7-15b), suggesting that influent metal concentrations is minimally related to P release. Like phosphorus, no significant difference in effluent chromium concentration during the leaching experiments (ranged 0.5 to 2.4 µg/L for Experiment 5, and less than instrumentation detection limit of 0.5 µg/L to 1.2 µg/L for Experiment 11) was observed.

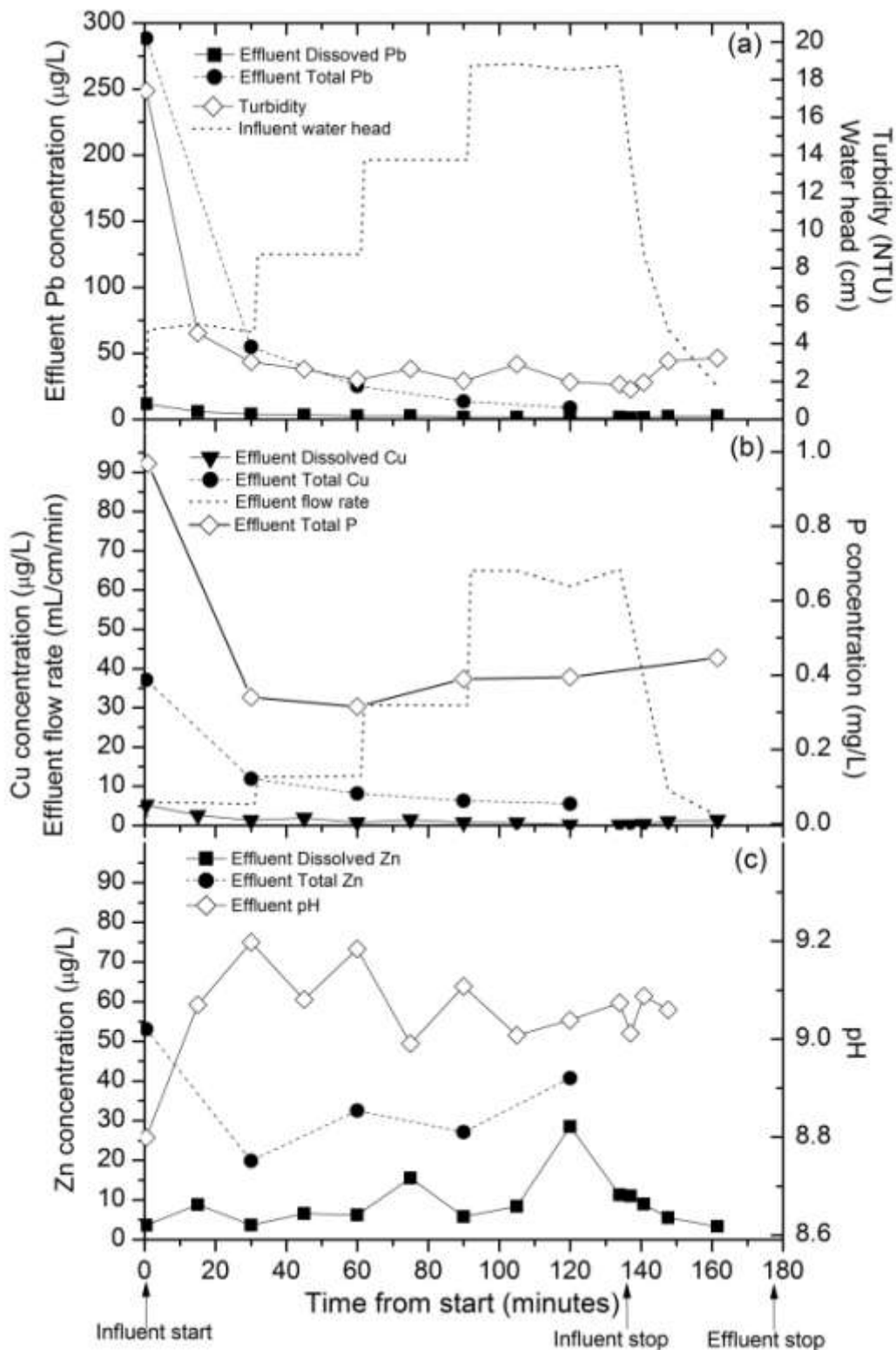


Figure 7-14. Water quality parameters for Experiment 5 during bench scale experiments. (a) Pb concentrations, water head, and turbidity; (b) Cu concentrations, P concentrations, and effluent flow rate; (c) Zn concentrations and pH.

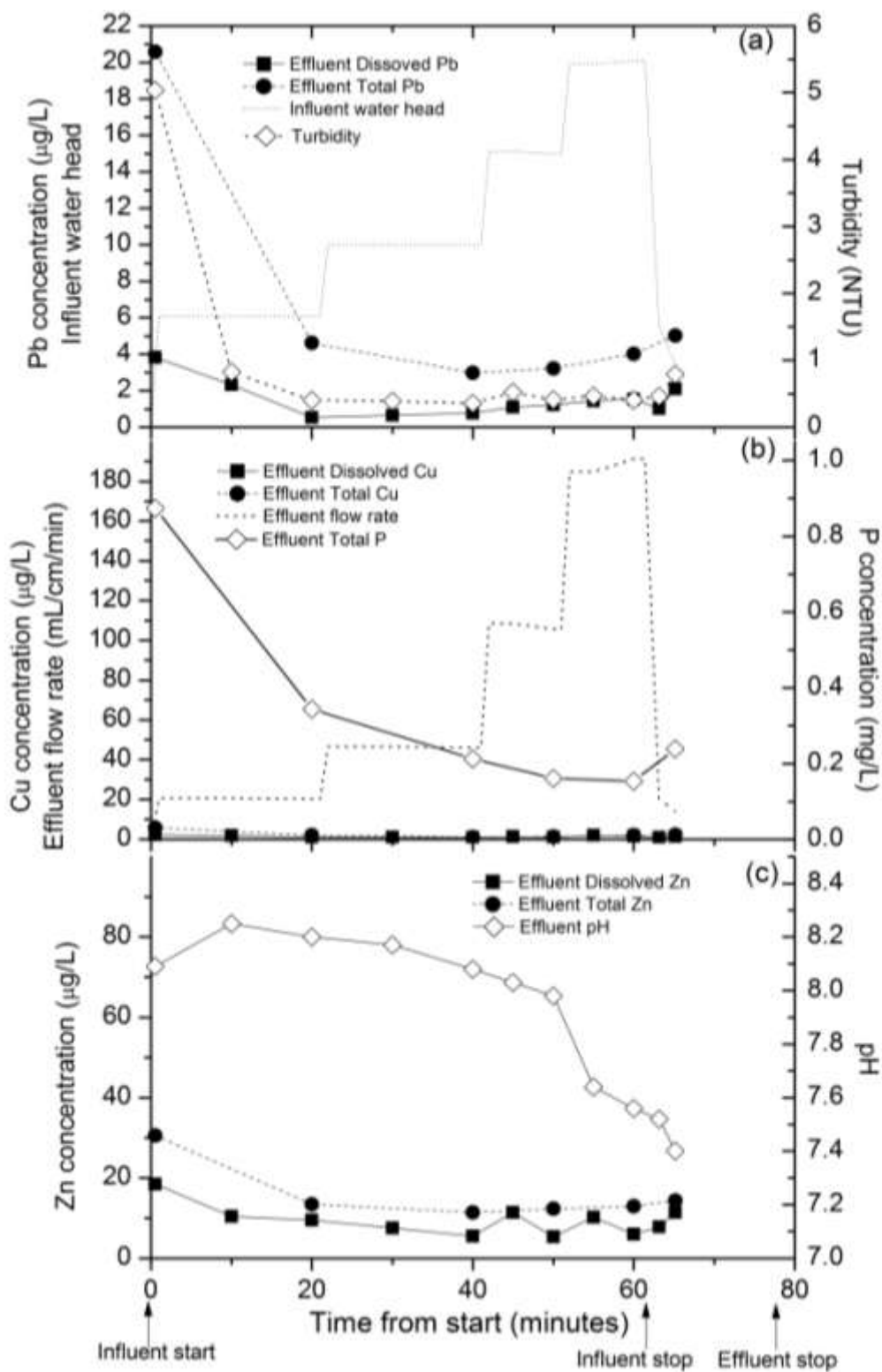


Figure 7-15. Water quality parameters for Experiment 11 during bench scale experiments. (a) Pb concentrations, water head, and turbidity; (b) Cu concentrations, P concentrations, and effluent flow rate; (c) Zn concentrations and pH.

#### **7-3-6. Other water quality parameters:**

Effluent total chromium concentrations during Experiment 5 to 11 were measured to investigate possible chromium leaching from steel slag in the Biomat media. Most samples tested during Experiment 5 through 11 demonstrated less than instrumentation detection limit (0.5 µg/L) for dissolved and total Cr. The highest effluent total Cr concentration was observed from the first flush samples during the experiments, showing as high as 3 mg/L total Cr, which is however considered as low concentration with minimal environmental risk based on State of Maryland Toxic metal criteria for Ambient Surface Waters (16 and 11 µg/L for acute and chronic Cr(VI) level, respectively; 570 and 74 µg/L for acute and chronic Cr(III) level; Code of Maryland Regulations (COMAR) 26.08.02.03-2) (See Table 6-5).

As mentioned partially in the previous sections, relatively high turbidity first flush was noted throughout the bench-scale experiments, but with significant drop as subsequent flow was further treated through media. More importantly, the turbidity generally decreased as more experiments were performed with more cumulative treated flow (Figures 7-5 through 7-12). Moderate effluent turbidity was observed during the first two experiments (Experiments 1 and 2) ranging from 5.1 to 17.9 NTU although a portion of the turbidity probably originated from leaching of particulate metal precipitates in the influent. In spite of high first flush turbidity (18.7 NTU) for Experiment 3, turbidity decreased rapidly as more flow was treated during the experiment and therefore, most samples were less than 2.0 NTU during the experiment. Turbidity generally decreased as more experiments were performed and, therefore, most of samples



demonstrated less than 0.5 NTU during Experiment 8 through Experiment 11, except the first flush samples and some initial samples.

High effluent pH was observed during Experiment 1, showing pH around 9.7 after initial pH of 10.2, and decreased with flow (Figure 7-6c) simply due to high initial alkalinity leached from CaO and MgO in the steel slag. However, this high effluent pH decreased as more experiments were performed. Specifically, gradual decrease of effluent pH was noted from Experiment 1 to Experiment 5, showing effluent pH for Experiment 2 ranged from 9.3 to 9.6 (Figure 7-7c), Experiment 3 from 9.1 to 9.4 (Figure 7-8c), Experiment 4 from 9.0 to 9.4 (Figure 7-9c), and Experiment 5 (Figure 7-14c) from 8.8 to 9.2. This indicates the gradual decrease of alkalinity leaching from steel slag as more experiments were performed with increased cumulative treated flow.

However, relatively significant decrease of effluent pH was observed for Experiment 7 ranging pH 7.8 to 8.4, compared to pH during Experiment 5 (8.8 to 9.2). Further effluent pH decrease was also observed for Experiment 8 ranging from 7.4 to 8.2, but the rest of experiments (Experiments 9, 10 and 11) showed relatively similar effluent pH with the Experiment 8, ranging effluent pH of 7.5 to 8.2 for Experiment 9, 7.3 to 8.2 for Experiment 10, and 7.4 to 8.3 for Experiment 11. The significant decrease of effluent pH between Experiments 5 and 7 and further decrease for Experiment 8 can be explained by increase of hydraulic conductivity. As discussed in the previous section (7-3-3) and Table 7-5, hydraulic conductivity increased significantly from Experiment 5 to Experiment 7 and further increase was observed from Experiment 7 to Experiment 8. This increased hydraulic conductivity caused high flow rate during the experiment and, therefore, less retention time of the flow, which caused less leached alkalinity and

therefore lower effluent pH. Interestingly, the highest pH was observed during the lowest water head (lowest flow rate) of each experiment. Again, this is because the higher retention time of the flow caused the higher alkalinity leaching from steel slag.

#### **7-3-7. Discussion on hydraulic conductivity and metal loading rate of Biomat media during the bench scale experiments**

Hydraulic characteristics of the Biomat media were evaluated throughout the bench-scale experiments based on measured influent water head and effluent flow rate. The estimated hydraulic conductivities are presented in Table 7-5. The hydraulic conductivity for the first 5 Experiments was relatively constant at around 6.5 cm/min, which is considered as excellent for porous media (Wanielista, 1990). The hydraulic conductivity significantly increased from 6.2 to 11.5 cm/min for Experiment 7. Another significant increase of the hydraulic conductivity was also noted, from 11.5 cm/min for Experiment 7 to 19.9 cm/min for Experiment 8; hydraulic conductivity remained relatively constant for the rest of the bench scale experiments.

It is speculated that the hydraulic conductivity change of the Biomat media is affected by structural changes within the media via physical, chemical, and biological changes. This includes drying processes between storm events, decomposition and mineralization of mat media between storm events, media packing, media composition change by washing or erosion of media during storm event. Specifically, medium-term changes in mat media between storm events (e.g., structural changes through decomposition or mineralization of mat media) are likely to be more important than short-term impact during a storm event (e.g., washing or erosion of media during storm event) because the hydraulic conductivity change was observed when the time lags

between two experiments were long. Specifically, there was an extended time lag between Experiment 5 and 7 (64 days lag between Experiments 5 and 6 and 126 days lag between Experiments 6 and 7), which is relatively long compared to the time lag between any of two adjacent experiments from Experiments 1 to 5 (Table 7-4).

High hydraulic conductivity of the mat media is required to enable the treatment of high intensity storm events with limited space and media. However, the high hydraulic conductivity of media can lead to poor contaminant removal due to high contaminant loading rates (i.e., high flow rates and low retention times).

The heavy metal removal performances through the Biomat can be affected by influent metal concentration and effluent flow rate (i.e., heavy metal loading rate) as well as adsorption/precipitation rates on Biomat media. The effluent flow rate is controlled by both influent water head and Biomat media hydraulic conductivity. Low hydraulic conductivity of the Biomat can ensure good heavy metal removal performance with low effluent concentration, by moderating flow rate through media. However, low Biomat flows limit the amount of contaminated water treating capacity and therefore can cause increase of influent water head and eventually flooding over the mat. The net results is bypass of the contaminated water and, therefore, overall poor performance of heavy metal removal. Therefore, Biomat design must be optimized for both water quantity and quality. In other words, the optimum design for the Biomat should consider maximum conductivity which can treat the maximum contaminated water flow, but still can produce good metal removal with low effluent metal concentrations to ensure meeting water quality criteria. This is especially important when the Biomat is applied to systems

where the water flow rate is not controlled and in extreme events where very high water flow is expected, which is usually the case for most diffuse pollution sources.

The hydraulic conductivity of the Biomat media can be controlled by the use of different sizes of sand or compost. The hydraulic conductivity can be also adjusted by the degree of media packing, although adjustment is somewhat limited. Therefore, it is important to investigate optimum hydraulic conductivity, at which maximum flow rate can be treated while still meeting environmental criteria.

Effluent concentrations based on various mass loading rates (in  $\text{mg}/\text{m}^3/\text{min}$ ) of each metal to the Biomat media during the bench scale experiments are plotted in Figure 7-16. Effluent metal concentration as a function of influent loading rate of three metal combined was also plotted in Figure 7-17. Data from Experiments 1 and 2 are not included in Figure 7-16, due to the much higher effluent metal concentration from influent precipitated metals. The leaching experiments, Experiments 5 and 11 were also not included due to 0 metal loading (no metal in influent). The first flush metal data from the other experiments were not used due to inaccurate and low flow rates, as well as high particulate metal concentrations. During Experiments 3 and 4, high total Zn levels were also observed due to exceptionally high particulate Zn loss (points in the dotted square in Figure 7-16c) and therefore, these points were not used (although they are plotted).

A trend line for each metal was added for visual aid only and has no scientific basis. Each solid arrow on each graph plot indicates ‘the critical metal loading rate’ at which the effluent metal concentration is expected to be equal to the Maryland acute metal concentration for aquatic life ( $65 \mu\text{g}/\text{L}$  for Pb,  $13 \mu\text{g}/\text{L}$  for Cu, and  $120 \mu\text{g}/\text{L}$  for Zn; see Table 6-5 in Chapter 6). Therefore, it is recommended to keep each metal

loading rate less than the critical metal loading rate. Based on each plot on Figure 7-16, critical metal loading rates of about 2.25 and 0.225 g/m<sup>3</sup>/min were estimated for Pb and Cu, respectively, while approximately 0.55 g/m<sup>3</sup>/min was estimated for Zn.

Metal loading rate (volumetric) was calculated as shown in Equation 7-4, where Q = flow rate per unit mat length (mL/cm/min), h = water head (cm), C = influent metal concentration (mg/L; 10 mg/L for Pb), and l = Biomat length parallel to water flow (constant of 18 cm).

$$\text{Metal loading rate} \left( \frac{\text{g}}{\text{m}^3 \cdot \text{min}} \right) = \frac{Q \cdot C}{h \cdot l} \quad \text{Eq. 7-4}$$

Based on Eq. 7-4, the ratio of flow rate to water head (Q/h) can be calculated through Eq. 7-5 and the calculated Q/h values for Pb, Cu, and Zn are shown in Eq. 7-6-1, 7-6-2, and 7-6-3, respectively. For example, the critical Pb loading rate of  $2.25 \frac{\text{g}}{\text{m}^3 \cdot \text{min}}$  was employed in the Eq. 7.5 in order to calculate the critical ratio of Q/h, which was found to be 4.1 cm/min as calculated in Equation 7-6-1.

$$\frac{Q}{h} = \text{Metal loading rate} \times \frac{l}{C} \quad \text{Eq. 7-5}$$

$$\text{For Pb } \frac{Q}{h} = \frac{2.25 \text{ g}}{\text{m}^3 \cdot \text{min}} \times 18 \text{ cm} \times \frac{L}{10 \text{ mg}} = 4.1 \frac{\text{cm}}{\text{min}} \quad \text{Eq. 7-6-1}$$

$$\text{For Cu } \frac{Q}{h} = \frac{0.225 \text{ g}}{\text{m}^3 \cdot \text{min}} \times 18 \text{ cm} \times \frac{L}{1 \text{ mg}} = 4.1 \frac{\text{cm}}{\text{min}} \quad \text{Eq. 7-6-2}$$

$$\text{For Zn } \frac{Q}{h} = \frac{0.55 \text{ g}}{\text{m}^3 \cdot \text{min}} \times 18 \text{ cm} \times \frac{L}{1 \text{ mg}} = 9.9 \frac{\text{cm}}{\text{min}} \quad \text{Eq. 7-6-3}$$

The lowest Q/h values among three metals should be used as critical Q/h value so that all effluent concentrations for all three metals are below the Maryland acute metal criteria for aquatic life. This calculated critical value of Q/h was plotted (as thick dark solid line) on Figure 7-18 with theoretical flow rate versus influent water head at different hydraulic conductivities of Biomat media (at Biomat media length parallel to the flow = 18 cm) based on Equation 7-3. Flow rate less than the critical line at the specific water head indicates that the effluent metal concentration is predicted to be less than the Maryland acute metal criteria for aquatic life. Therefore the lowest Q/h value among three metals should be picked to have the effluent concentrations from all three metals are lower than the Maryland acute metal criteria.

Assuming that the hydraulic conductivity is known, critical water head can be also predicted from Figure 7-18; for example, at Biomat hydraulic conductivity of 11.5 cm/min, influent water head should not be over ~ 12.5 cm to not exceed the Maryland acute metal criteria. Different value of Q/h can be applied as Biomat operation goals based on target percent removals or effluent metal concentrations of a specific metal. As shown with a dashed arrow in Figure 7-16, the Pb loading rate for 500 µg/L effluent Pb concentration (95% Pb removal from 10 mg/L influent) was around  $5.5 \frac{g}{m^3 \cdot min}$ . It should be noted that influent Pb, Cu and Zn concentrations of 10, 1, and 1 mg/L, respectively (10:1:1 in mg/l) were used for all experiments employed for Figure 7-16 except Experiment 10. Therefore, the corresponding Cu and Zn loading rate at  $5.5 \frac{g}{m^3 \cdot min}$  Pb loading rate is  $0.55 \frac{g}{m^3 \cdot min}$  at which effluent Cu and Zn concentration is estimated around 65 and 120 µg/L, respectively (total metal loading of  $43.6 \frac{mmol}{m^3 \cdot min}$ ). At this loading rate, only 93.5% Cu and 88% Zn removals are expected (based on 1 mg/L influent), while 95

% Pb is estimated to be removed. Based on Equation 7-5 and  $5.5 \frac{g}{m^3 \cdot min}$ , Pb loading rate, Q/h of 9.9 cm/min was calculated and plotted in the thin brighter solid line on Figure 7-16 as a example. Based on Figure 7-16, 95% or great Pb removal (or less than 500 µg/L effluent Pb concentration) is expected if flow rate is less than the thin solid line at the selected water head.

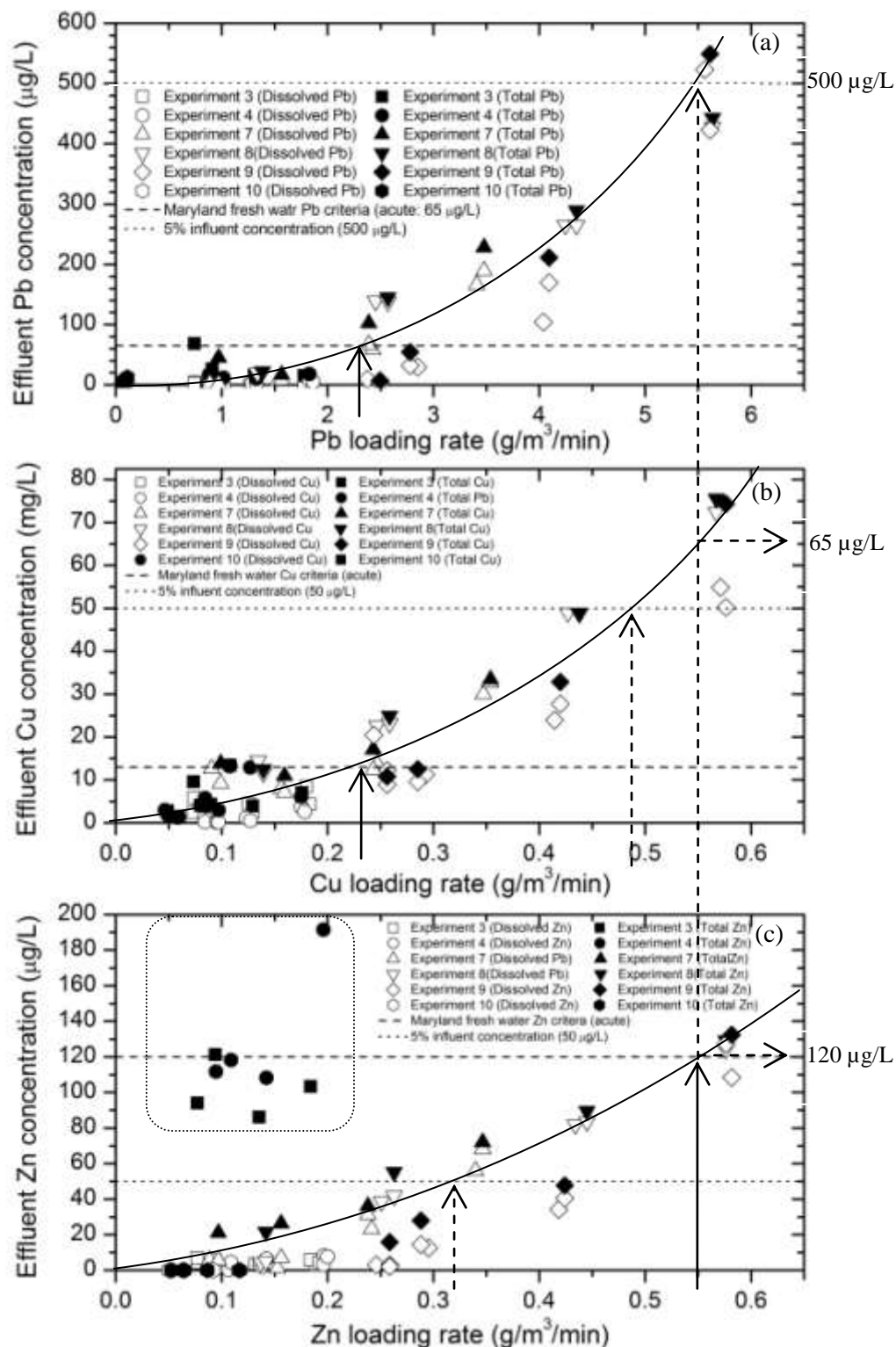


Figure 7-16. Effluent metal concentration based on influent loading rate of each metal (in  $\text{mg/m}^3/\text{min}$ ) for: (a) Pb, (b) Cu, and (c) Zn. Solid line is trend line. Solid arrows are indicating the loading rate at Maryland fresh water acute criteria for each metal. Dashed lines are indicating the loading rate at 5% of influent (95% removal) for each metal.



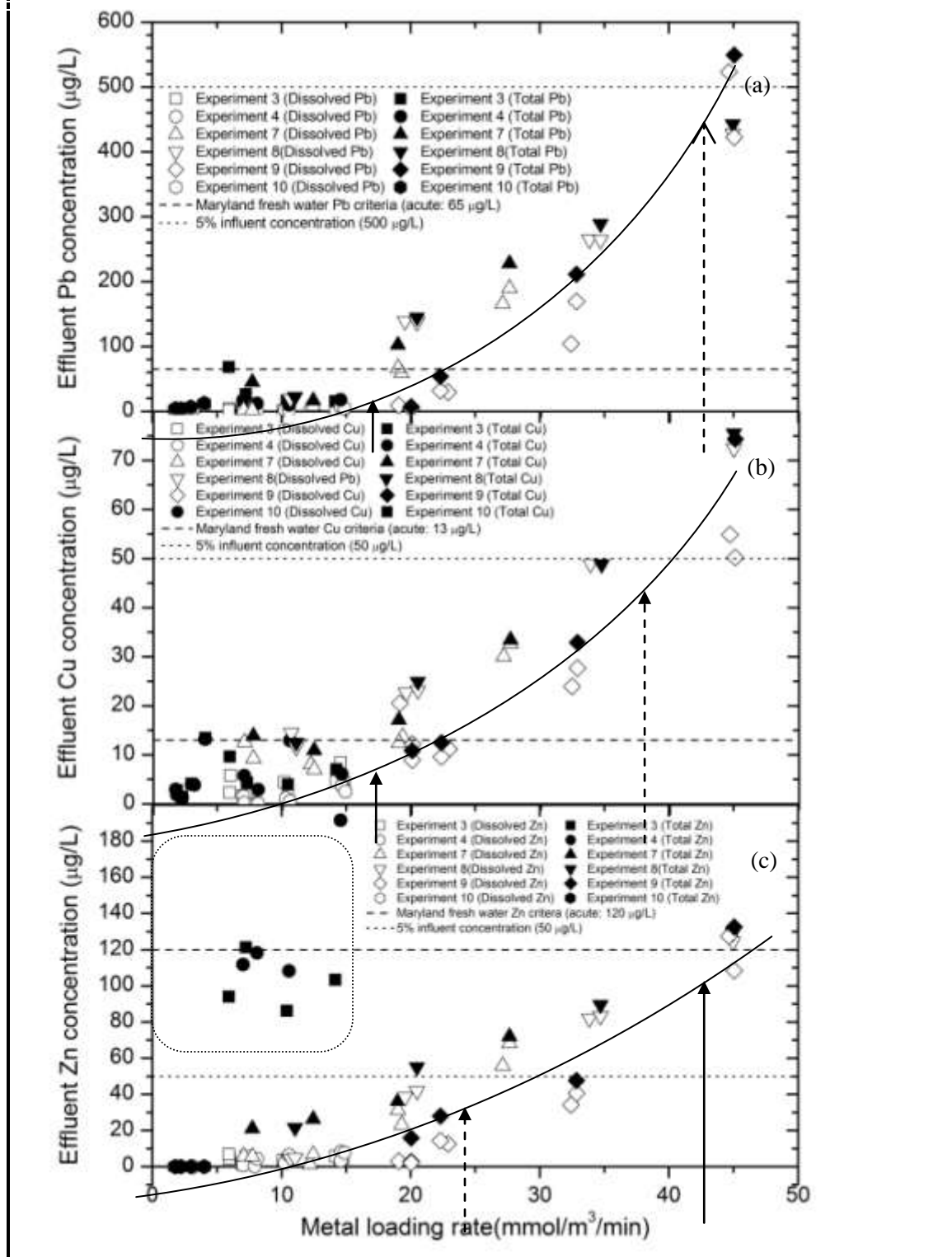


Figure 7-17. Effluent metal concentration based on influent loading rate of three metal combined (mmol/m<sup>3</sup>/min) for: (a) Pb, (b) Cu, and (c) Zn. \* Solid line is trend line. Solid arrows are indicating the loading rate at Maryland fresh water acute criteria for each metal. Dashed lines are indicating the loading rate at 5% of influent (95% removal) for each metal.

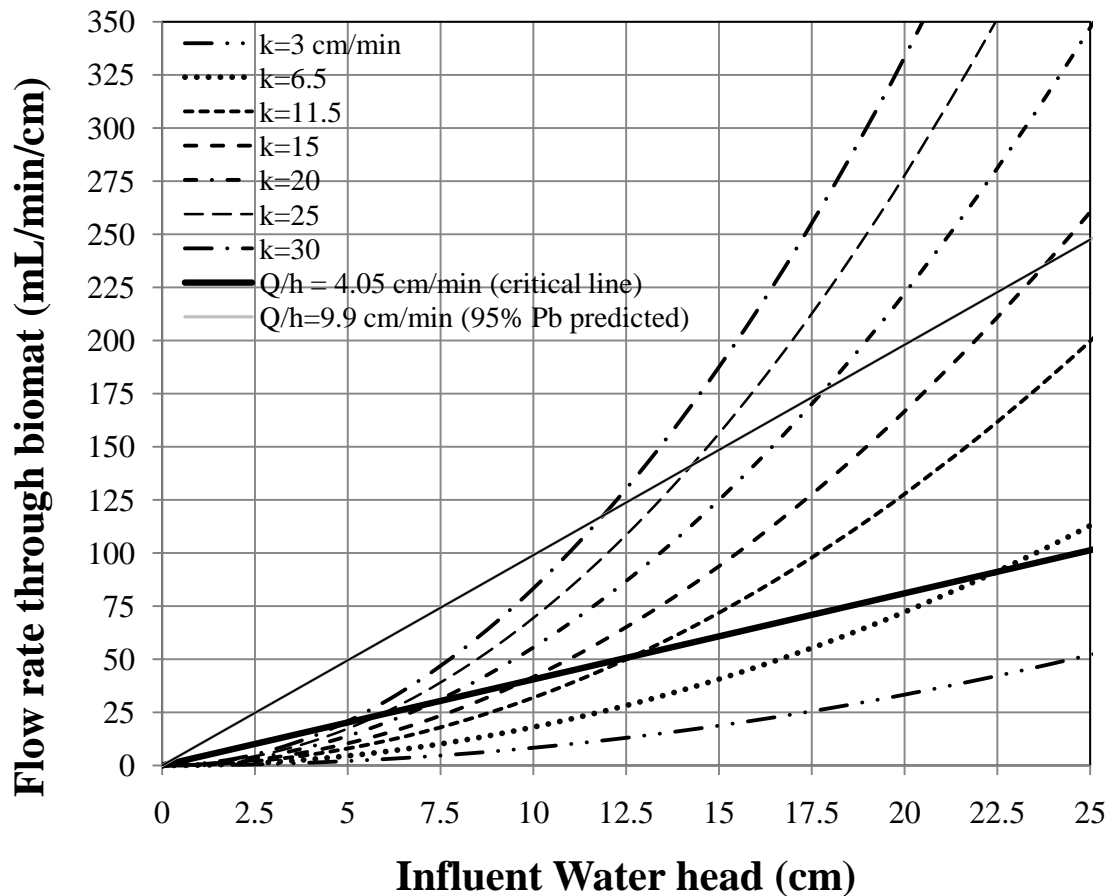


Figure 7-18. Flow rate through Biomat based on an influent water head at different hydraulic conductivities of Biomat media (Biomat media length parallel to the flow = 18 cm).

One of the biggest challenges for Biomat operation occurs during an extreme rainfall event due to extremely high flow rate to treat. Therefore, evaluating Biomat performance during a extreme rainfall intensity can be important. Based on the point precipitation frequency estimates for the area of Beltsville, MD, as shown in Table 7-6a, and the Bldg-580 total roof area (approximately 300 m<sup>2</sup> each side), the flow rate to the Biomat for each precipitation intensity of each average occurrence was estimated assuming the Biomat is installed along the same length of roof next to each wall; results

are shown in Table 7-6b. The building roof consists of two metal roofs (one on each side of the front and rear wall) and part of a concrete roof between the metal roofs (see Appendix B-5). Actual roof area for each metal roof is  $193 \text{ m}^2$  (10.06 m (33ft) width and 19.2 m (63ft) length). Therefore, actual total metal roof area is  $386 \text{ m}^2$ . However, the concrete roof should be also included due to difficulty in separating two different roof runoff flows. If Biomat is installed on each side of the wall, the precipitation area that one Biomat will treat is approximately  $300 \text{ m}^2$ , half of the total area of  $597 \text{ m}^2$ . If 20 cm of influent water head is assumed to be the highest head for the Biomat, the effluent flow rate should be less than  $81 \frac{\text{mL}}{\text{min} \cdot \text{cm}}$  (i.e., critical flow rate at 20 cm water head) to expect an effluent Pb concentration less than the Maryland acute criterion for fresh water (Figure 7-18). The flow rate and the corresponding precipitation intensity lower than the critical flow rate ( $81 \frac{\text{mL}}{\text{min} \cdot \text{cm}}$ ) and critical precipitation intensity (1.23 in/hr) are shown in large font in Table 7-6, where the effluent metal concentrations are lower than Maryland acute criterion for fresh water.

Furthermore, 95% Pb removal (with ~10 mg/L influent concentration) is at least expected when the effluent flow rate is no more than  $198 \frac{\text{mL}}{\text{min} \cdot \text{cm}}$  (Figure 7-18). The flow rate and corresponding precipitation intensity greater than  $198 \frac{\text{mL}}{\text{min} \cdot \text{cm}}$  and 3.01 in/hr, respectively, are marked in italics in Table 7-6, which are predicted to produce less than 95 % Pb removal. Therefore, the values marked in bold in Table 7-6, indicates the effluent concentrations for each metal at these values are estimated greater than Maryland acute criteria but less than 5% of influent concentration.

Table. 7-6. (a) Point precipitation frequency estimates of Beltsville, MD From NOAA ATLAS 14 (adapted from <http://hdsc.nws.noaa.gov/cgi-bin/hdsc/buildout.perl?type=idf&units=us&series=pd&statename=MARYLAND&stateabv=md&study=orb&season=All&intype=1&plat=&plon=&liststation=BELTSVILLE++++++MD+%2C+18-0700&slat=lat&slon=lon&mLat=40.816&mLon=-76.150&elev=1397>), (b) Flow rate to Biomat estimates.

(a) Precipitation Intensity Estimates (in/hr)													
ARI <sup>a</sup> (years)	<u>5</u> <u>min</u>	<u>10</u> <u>min</u>	<u>15</u> <u>min</u>	<u>30</u> <u>min</u>	<u>60</u> <u>min</u>	<u>120</u> <u>min</u>	<u>3 hr</u>	<u>6 hr</u>	<u>12</u> <u>hr</u>	<u>24</u> <u>hr</u>	<u>48</u> <u>hr</u>	<u>4</u> <u>day</u>	<u>7</u> <u>day</u>
1	4.15 <sup>b</sup>	3.32	<b>2.76<sup>c</sup></b>	<b>1.90</b>	1.18 <sup>d</sup>	0.7	0.51	0.31	0.19	0.11	0.06	0.04	0.02
2	4.97	3.97	3.33	<b>2.30</b>	<b>1.44</b>	0.86	0.62	0.38	0.23	0.13	0.08	0.04	0.03
5	5.92	4.74	4.00	<b>2.84</b>	<b>1.82</b>	1.09	0.78	0.48	0.29	0.17	0.1	0.05	0.04
10	6.61	5.29	4.46	3.23	<b>2.10</b>	<b>1.26</b>	0.91	0.56	0.35	0.21	0.12	0.07	0.04
25	7.49	5.96	5.04	3.73	<b>2.49</b>	<b>1.51</b>	1.1	0.69	0.43	0.26	0.15	0.08	0.05

(b) Flow rates to Biomat Estimates (mL/min/cm)													
ARI <sup>a</sup> (years)	5 min	10 min	15 min	30 min	60 min	120 min	3 hr	6 hr	12 hr	24 hr	48 hr	4 day	7 day
1	273 <sup>b</sup>	218	<b>182<sup>c</sup></b>	<b>125</b>	78 <sup>d</sup>	46	34	20	13	7	4	3	1
2	328	261	219	<b>151</b>	<b>95</b>	57	41	25	15	9	5	3	2
5	390	312	263	<b>187</b>	<b>120</b>	72	51	32	19	11	7	3	3
10	435	348	293	213	<b>138</b>	<b>83</b>	60	37	23	14	8	5	3
25	493	392	332	245	<b>164</b>	<b>99</b>	72	45	28	17	10	5	3

<sup>a</sup> These precipitation frequency estimates are based on a partial duration series. **ARI** is the Average Recurrence Interval.

<sup>b</sup> Numbers in *italic* refer to the precipitation intensity(a) and flow rates to Biomat(b), at which the expected metal concentrations are higher than 5% of influent Pb concentration (>500 µg/L for Pb), 6.5% influent Cu (>65 µg/L), and 12% influent Zn (>120 µg/L for Zn).

<sup>c</sup> Numbers in *italic* refer to the precipitation intensity(a) and flow rates to Biomat(b), at which the expected effluent metal concentrations are lower than 5% of influent Pb concentration (<500 µg/L for Pb), 6.5% influent Cu (<65 µg/L), and 12% influent Zn (<120 µg/L for Zn; Maryland fresh water acute criteria for Zn), but higher than Maryland fresh water acute criteria for Pb (>65 µg/L) and Cu (>13 µg/L).

<sup>d</sup> Numbers in the larger font refer to the precipitation intensity(a) and flow rates to Biomat(b), at which the expected effluent metal concentrations are lower than Maryland fresh water acute criteria for all three metals.

Based on Table 7-6, the effluent Pb concentrations above the Maryland fresh water acute criteria of 65 µg/L are expected to occur only at extreme precipitation intensities with very low frequency.

If a Biomat is installed for metal removal for typical roof/wall runoff from typical buildings or is used as a BMP for typical storm water runoff (i.e., much lower influent Pb

concentrations than B-580 roof/wall runoff) (see Tables 3-6 and 3-7 in Chapter 3 for typical runoff values), the effluent metal concentrations at most of precipitation intensities and flows shown in Table 7-6, should satisfy Maryland freshwater acute metal criteria for aquatic life (COMAR 26.08.02.03-2: see Table 6-6). This would be an excellent application of the Biomat, with excellent expected metal removal performance from typical runoff even at extreme rainfall intensities.

#### **7-3-8. Biomat media total metal extraction**

Total metal concentrations (Pb, Cu and Zn) from each sampling segment of the Biomat media are presented in Figure 7-19 on the Biomat cross sectional side view (see Figure 7-5 for detailed dimensions for each sampling segment). Based on mass estimation of removed heavy metals by the Biomat media and the total metal concentration of the media shown in Figure 7-19, 92% of the captured Pb by Biomat media was recovered through the aqua regia digestion, while 95 and 97% was recovered for Cu and Zn, respectively.

As expected, the higher metal concentration in the media was observed from the layer closer to the influent side and the lowest sampling segment. Specifically, the first 2.5 cm layer (IN layer; IN1-IN4) showed the highest metal concentration compared to the other layers with the same segment height. Furthermore, the bottom layer IN1 showed the highest metal concentrations for all three metals because greater water flow was treated through the lower segment. It is estimated that 82% of total removed Pb was captured by the first 2.5 cm layer (IN layer; IN1 to IN4) in terms of Biomat length parallel to the water flow. In addition, more than 98% of total removed Pb was found in

the first quarter (4.5 cm) layer of Biomat. Very similar to Pb, Cu also demonstrated 81% and 97% total Pb removal from the first 2.5 and 4.5 cm layer, respectively. This significant metal removal within a relatively shallow layer length of Biomat media strongly supports the treatment feasibility of Biomat media at variable flow, suggesting fast process for metal removal via adsorption/precipitation, which enabled low effluent metal concentrations even at high metal loading rates.

Although the majority of Zn was also removed by the first two layers (IN and IO layers), showing 67 and 87% total Zn removal by the first 2.5 and 4.5 cm layer, respectively, relatively high Zn was also observed in layer MI, suggesting that Zn was the least favored among the three metals in adsorption/precipitation by Biomat media. Similarly, Jang et al. (2005) found that the order of initial metal removal rates using hardwood bark mulch was  $\text{Pb(II)} > \text{Cu(II)} > \text{Zn(II)}$  with possible explanation based on differences in electronegativity and ionic radius of the metal ions. Therefore, the weaker metal removal rates of Zn by the Biomat media required the deeper layer to remove Zn from the influent and, therefore, more metals were found further down to the deeper layer.

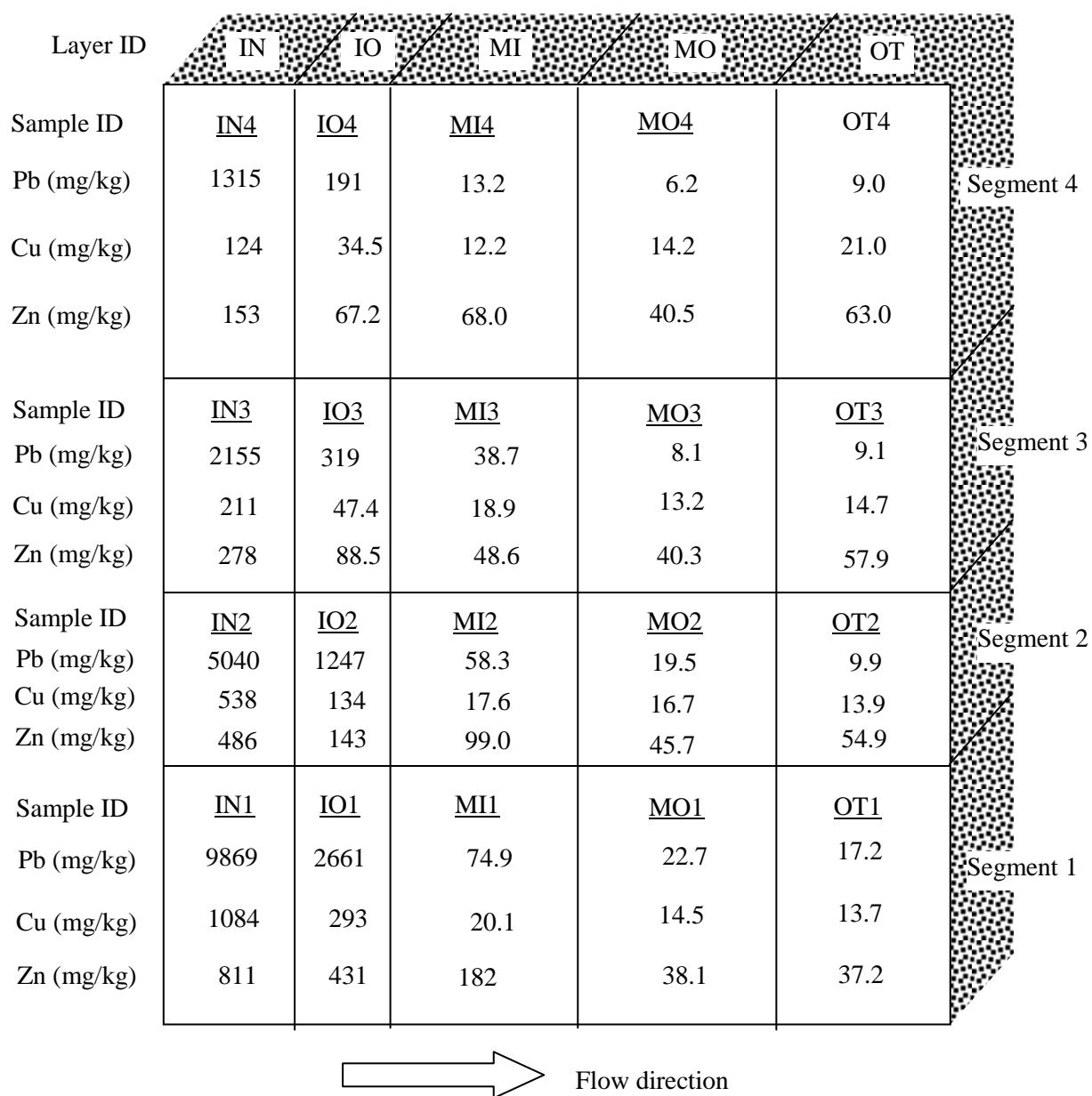


Figure 7-19. Total Metal (Pb, Cu, and Zn) concentrations extracted from Biomat media (see Figure 7-5 for dimensions)

Based on the total metal concentrations in the Biomat media shown in Figure 7-19, the metal concentrations in the upper segments and effluent side Biomat layer remained unchanged (i.e., background metal concentration), suggesting that this portion

of the Biomat media has not been used to remove heavy metals from influent. This is simply due to the hydrologic characteristic of the Biomat media design and operation of perpendicular water flow through the mat media; most of water flow will be treated through the lower part of the Biomat media even at high influent water head due to much faster flow rate through the lower part of the Biomat compared to the top part. This results in unused Biomat media and therefore decreases metal removal capacity per unit mat media used. Furthermore, considering the rain intensity and frequency in the Maryland area, the majority of rainfall events will be relatively low in intensity and therefore, the lower part of mat will be mostly used and significant portion of Biomat media (specifically the upper part and the effluent side of media) will mostly remain unused.

Therefore, design modification may be needed to enhance the Biomat media use efficiency (i.e., ideally, the water flow would go through the entire Biomat media and the metal is removed and saturated throughout the Biomat media) including modification of water flow (e.g., installation of baffles or different sizes of orifices inside or on the surface of the Biomat) or media dimensional configuration (e.g., longer media length in the lower part of media and gradual decrease in media length in the upper part of the media).

It is, however, expected that the Biomat metal removal capacity will decrease before it starts breakthrough, compared to the capacity expected in the previous column study (Chapter 6) if the modification of mat media is not possible due to various economical or technical reasons. Therefore, further bench scale experiments under realistic conditions of various rainfall intensity and duration around Maryland may be



needed until significant effluent concentrations are detected to evaluate the Biomat media capacity for metal removal and frequency of media replacement based on the capacity.

#### **7-3-9. Other metal extractions from Biomat media**

Three additional extractions: the Relative Bioavailability Leaching Procedure (RBALP) for the bioaccessible fraction of heavy metals (at pH 1.5 and 37 °C); acid ammonium oxalate extraction in darkness (at pH 3); and  $\text{Sr}(\text{NO}_3)_2$  extraction for phyto-available metals were performed for the first two layers (IN and IO layers). Extracted metal concentration results are presented in Table 7-7 as percent of metal extraction to total metal concentration.

RBALP extraction, which represents the bioavailable metals under simulated gastric conditions, was validated for only lead and arsenic in good correlation with in vivo results (Drexler and Brattin, 2007). Therefore, Cu and Zn RBALP data do not have scientific underpinnings. However, RBALP extracted Cu and Zn results were also analyzed and included in Table 7-7 to compare the extracted metal concentration with the other metal extractions. First, 78.0% total Pb from the first 4.5 cm layer (IN and IO layers) was extracted through RBALP extraction, while 49.5 and 86.9% of total Cu and Zn were extracted, respectively. The high extractability of the captured Pb by Biomat through RBALP extraction suggests that the majority of removed Pb by Biomat is bioavailable. This is usually the greatest risk for children when they ingest the soil/media materials by playing on and contacting them (Ryan et al., 2004). Fortunately, the APHIS building, a research facility, is far from residential areas and usually accessible only to APHIS employees. Therefore, risks from the mat media with high Pb concentration are

minimal for people in the neighborhood including children if the mat media is properly treated/disposed after its exhaustion. Furthermore, it is suggested by some studies (Ryan et al., 2004; Scheckel and Ryan, 2005; Scheckel et al., 2009) that the RBALP extraction at pH 1.5 does not represent remediation effectiveness for highly effective soil remediation treatments, supported by low bioavailability to swine, rats and humans. The RBALP extraction represents a smaller reduction in soil Pb bioavailability (15%) than found with human volunteers fed Joplin soil (MO) on fasting (69%) (Chaney et al., unpublished paper). The same RBALP extraction procedure but at pH 2.5 was suggested in order to provide better representation of soil remediation effectiveness, as well as Pb bioavailability.

Much lower Pb concentrations were extracted from the first 4.5 cm layer mat media by acid ammonium oxalate extraction at pH 3 (oxalate extraction) compared to that by RBALP extraction, only 9.6% of total Pb. This relatively low Pb extractability by the oxalate extraction indicates that Pb is strongly bound on the Biomat media. As discussed earlier, possible lead removal mechanisms by Biomat media are surface complexation processes and/or simple surface precipitation. If the Pb was removed mostly through the latter mechanism, simple surface precipitation, the removed Pb is expected to be readily leached out to the environment through re-dissolution at the acidic condition and resulting in increased environmental risks. Therefore, the low Pb extractability by the oxalate extraction confirms the limited mobility of removed Pb and the feasibility of Biomat media for Pb removal from the roof/wall runoff, demonstrating little risk of Pb release from the media to environment.

Unlike Pb, Cu and Zn were highly extracted by the oxalate extraction, showing that 73.7% and 75.1% of total Cu and Zn was extracted from the first 4.5 cm layer, respectively. Interestingly, more Cu was extracted by oxalate (73.7%) than by the RBALP (49.5%) in spite of the lower buffered pH (1.5) of RBALP extraction solution than that of oxalate extraction solution (pH 3.0). This is apparently due to the greater formation of Cu complexes with organic chelation compounds such as oxalate, compared to Pb and Zn (Hsu and Lo, 2000a; Zhou and Wong, 2001). High Zn extractability by both RBALP extraction (87.1%) and oxalate extraction (76.6%) are probably due to the higher pH dependence of Zn adsorption and precipitation on the Biomat media. Both RBALP and oxalate extraction was capable of extracting relatively weakly bound and pH-dependent adsorbed Zn on the mat media. Only 9.7% total Pb was extracted by the oxalate extraction, suggesting that Pb is less pH dependent than Zn and less organic complexation dependent than Cu, resulting in the lower oxalate extracted Pb concentration.

The phyto-available metal concentration was determined through 0.01M  $\text{Sr}(\text{NO}_3)_2$  extraction and the results are also presented in Table 7-7. Low extracted metal concentrations for all three metals (Pb, Cu, and Zn) were detected, suggesting that the removed heavy metals are minimally phyto-available, and therefore, little risk is derived for heavy metal accumulation in plants grown on the media. Although no vegetation or plants are expected on the mat media in this project research, plants (such as those favoring sandy soils) or hyperaccumulators can be established on the Biomat media for aesthetic or technical (i.e., phytoextraction) reasons, based on the environmental

condition and media configuration. The low metal extraction by  $\text{Sr}(\text{NO}_3)_2$  also confirms the minimal leachability of heavy metals by the media during storm events.

Table 7-7. Extracted metal concentrations in the Biomat media; Relative Bioavailability Leaching Procedure (RBALP), acid ammonium oxalate extraction in darkness, and  $\text{Sr}(\text{NO}_3)_2$  (0.01M) extraction; numbers in parenthesis represents percent of total metal concentration.

	<u>Pb (mg/kg)</u>			<u>Cu (mg/kg)</u>			<u>Zn (mg/kg)</u>		
	RBALP	Oxalate	$\text{Sr}(\text{NO}_3)_2$	RBALP	Oxalate	$\text{Sr}(\text{NO}_3)_2$	RBALP	Oxalate	$\text{Sr}(\text{NO}_3)_2$
IN1	7987 (80.9) <sup>a</sup>	858 (8.7)	0.793 (0.008)	607 (56.0)	771 (71.2)	0.465 (0.043)	767 (94.5)	633 (78.0)	1.06 (0.124)
IN2	3732 (74.0)	543 (10.8)	0.513 (0.010)	241 (44.9)	440 (81.9)	0.417 (0.078)	440 (90.5)	358 (73.6)	0.382 (0.078)
IN3	1589 (73.7)	226 (10.5)	0.209 (0.010)	87.9 (41.7)	146 (69.4)	0.245 (0.116)	196 (70.4)	208 (74.8)	0.198 (0.071)
IN4	968 (73.6)	102 (8.2)	0.140 (0.011)	51.7 (41.6)	85.5 (68.7)	0.207 (0.166)	114 (66.8)	119 (77.3)	0.099 (0.064)
IO1	2200 (82.6)	328 (12.3)	0.227 (0.009)	161 (54.9)	239 (81.6)	0.266 (0.091)	372 (86.2)	316 (73.2)	0.161 (0.037)
IO2	999 (80.2)	103 (8.3)	0.127 (0.010)	60.7 (45.5)	87.9 (65.9)	0.199 (0.149)	126 (88.3)	123 (86.4)	0.070 (0.049)
IO3	198 (62.2)	25.9 (8.1)	0.050 (0.016)	7.0 (14.7)	32.1 (67.6)	0.090 (0.191)	62.2 (70.3)	63.9 (72.2)	0.042 (0.048)
IO4	107 (56.4)	21.0 (11.0)	0.017 (0.009)	3.8 (10.9)	27.4 (79.6)	0.055 (0.159)	61.1 (90.9)	60 (89.3)	0.022 (0.033)

<sup>a</sup> Percent of total metal concentration

#### **7-4. Heavy metal removal mechanisms by Biomat media used in Bench-scale Experiments**

Ion exchange has been mostly suggested as a major heavy metal removal mechanism for bio/cellulose/agricultural material and by-product sorbents including composts, sawdust, peat, mulches, and tree fern (Yu et al., 2000; Ho et al., 2002; Jang et al., 2004). While most of these studies were performed below pH 7, the effluent pH throughout the bench scale experiments, however, ranged from around 7 to 10. Furthermore, the steel slag added in Biomat media contained high amorphous Fe and Mn contents. Therefore, the pH-dependent metal adsorption on organic matter and Fe/Mn (oxy)hydroxides (Bradl, 2004), precipitation of metal oxy/hydroxides and metal carbonates (Liu and Liu, 2003; Gibert et al., 2005), and co-precipitation of heavy metals with Fe (oxy)hydroxides (Martinez and McBride, 1998; Gibert et al., 2005) may also be possible as heavy metal removal mechanisms for Biomat media used for the bench-scale experiments.

Based on the previous column studies, it is found that the heavy metal removal capacities of each media were very pH dependent. In addition, amendments with hubcutter heavies did not improve the heavy metal capacity of Biomat media, suggesting minimal contribution of heavy metal removal by increase of amorphous Fe content. It is stated by Bradl (2004) that heavy metal adsorption on humic constituents and oxides of soil generally increases with pH as a primary variable, following the “metal-like adsorption” as the basic trend. Therefore, metal adsorption on compost humic constituents is considered as a major mechanism for heavy metal removal through Biomat media. Based on solubility products (based on solubility products,  $K_{sp}$  of metal

precipitates), precipitation of metal oxy/hydroxides and metal carbonates can be another potential retention mechanism at high pH (Harter, 1983).

Ho et al. (2004) suggested through their Pb sorption study on tree fern that surface cation exchange is the initial rapid sorption mechanism of lead and a gradual uptake of cation exchange at the inner surface was suggested as the later slow sorption of lead. This can also be the case when the Biomat is operated at lower pH, where the majority of Pb species are  $\text{Pb}(\text{OH})^+$  or  $\text{Pb}^{2+}$ . It is important to note that the solution never reached an equilibrium during the Biomat bench scale experiments due to its relatively short retention time. Therefore, solution pH may be lower at the time of sorption in Biomat media (i.e., the influent side layer), compared to the effluent pH.

Based on the results of 0.01M  $\text{Sr}(\text{NO}_3)_2$  extraction of the used mat media (Chapter 7-3-9), very low extracted metal concentrations for all three metals (Pb, Cu, and Zn) were detected, suggesting that the removed heavy metals by Biomat were not exchanged and extracted by the  $\text{Sr}^{2+}$  ion. This also suggests that the removed heavy metals are likely to be bound at the inner surface. Based on the column study, approximately 17% and 20% of previously adsorbed Zn in MC10 (10% manure compost column) and GF10 (10% grass/food waste compost column), respectively, still remained in the column media after desorption by simultaneous sorption by Pb and Cu at the end of the adsorption study, suggesting possible inner sphere (specific) adsorption on inorganic constituents of the compost media or occlusion of the previously adsorbed Zn with organic constituents (Goto and Suyama, 2000). It was noted by Fontes et al. (2000) that Zn and Cd are more often immobilized by nonspecific sorption (i.e., electrostatic interactions with exchange sites), while Pb and Cu are more involved with specific sorption (i.e., covalent

interactions). Therefore, specific sorption of Pb and Cu on Biomat media was more likely and can be a major sorption mechanism, compared to Zn.

Possible complex or chelate formation between metal and dissolved organic matter may affect metal retention in the Biomat. Increase of heavy metal mobility is usually expected at higher pH as anionic forms of organic acids increase in solution, while decrease of the metal mobility is expected as significant amount of organic acids adsorb to positively charged soil mineral surfaces and, therefore, the humic-coated mineral surfaces can adsorb metal ions (Bradl, 2004). However, this increase of heavy metal mobility at higher pH was not observed, suggesting minimal effect of dissolved organic matter on metal retention on Biomat media.



## 7-5. Summary and conclusions

A total of 11 bench-scale experiments were performed during a 13 month period and four different metal extractions for the Biomat media were performed based on five different experimental objectives: (1) evaluating Biomat performance at different water heads (flow rates); (2) investigating Biomat hydraulic characteristics; (3) evaluating Biomat performance with the lower influent concentrations; (4) investigating metal leachability during Biomat operation through leaching studies; (5) evaluating metal extractability and mobility through media extraction.

Approximately 92 to 96% total Pb removal throughout various Pb loading rates were observed for Experiment 1, while Experiment 2 demonstrated similar results, but slightly lower percent removal, showing 89 to 92% total Pb removal. However, it was found that most of the dissolved Pb was efficiently removed by the mat media from the influent during the experiments while some of precipitated solids from the influent (i.e., small particle sizes) were not removed and became the majority form of Pb in the effluent.

This is because large particle sand used in the Biomat media for good hydraulic characteristics likely did not trap/filter out the freshly precipitated fine amorphous solid Pb species in the influent, while dissolved metals were effectively removed by the media by adsorption/precipitation.

Dissolved effluent Pb concentrations for Experiments 3 and 4 were mostly lower than 5  $\mu\text{g/L}$ , demonstrating very efficient influent Pb removal and minimal release of dissolved Pb to effluent. Compared to Experiments 1 and 2, much lower effluent total Pb concentrations were observed for Experiment 3 (15-83  $\mu\text{g/L}$ ) and Experiment 4 (10 to 29

µg/L) demonstrating much greater than 99% Pb removal, mainly because only dissolved Pb was introduced to the media, which is more efficiently removed by Biomat media.

No significant Biomat performance change (i.e., effluent concentration increase) for heavy metal removal was noted for influent water head increase (i.e., effluent flow rate increase) for all heavy metal loadings (by changing influent water head). This suggests that the heavy metal removal rate by the mat was fast enough not to be limited even at the highest water head studied during Experiments 1 to 4. However, effluent heavy metal concentration increases were observed as water head increased during Experiments 7 to 9 because the hydraulic conductivity significantly increased from Experiments 1-4 (around 6.5 cm/min) to Experiments 7 (11.5 cm/min) and further to Experiments 8 to 9 (around 20 cm/min). This increase caused significantly increased effluent flow rates during the experiments compared to Experiments 1 to 4 at the same water head. Relatively high effluent heavy metal concentrations were noted from Experiment 8 and 9, showing up to 443 µg/L total Pb ( 428 µg/L dissolved Pb) for Experiment 8 and 549 µg/L total Pb (523 µg/L dissolved Pb) for Experiment 9 at the highest water head studied (~18.7 cm). In spite of still good percent removal of Pb (~95% Pb removal), these effluent Pb concentration well exceeded the Maryland fresh water acute criteria of 65 µg/L. Nonetheless, these high metal concentrations are expected to occur only at extreme precipitation intensities with very low frequency.

The Biomat performance for lower influent metal concentrations (about 200 µg/L for each metal) was investigated through Experiment 10 and the results suggests excellent Biomat performance and excellent feasibility of the Biomat for treating moderately contaminated waters. Effluent dissolved Pb and Cu concentrations were less than 5 µg/L

for all samples except samples from the first flush and samples from the highest water head.

Heavy metal leaching from Biomat media through Experiments 5 and 11 demonstrated very low dissolved concentrations for all three metals (Pb, Cu, and Zn), suggesting minimal heavy metal leaching from Biomat media, in spite of some particulate metal leaching from the first flush in Experiment 5, possibly due to loss of media particles.

Four different Biomat media metal extractions were performed after completion of the bench scale experiments. Results indicate that the removed Pb is strongly bound with the media, showing low extractability by both oxalate and strontium nitrate extractions. However, high bioavailable portion of the Pb in the media through RBALP was noted, suggesting possible human Pb risk by ingesting media materials. Concern about high Pb in the Biomat is moderated because the media are enclosed during use and thus not available for children to ingest, and the disposal of used media will be into landfills for non-hazardous wastes (based on reported TCLP extractions of high Pb biosolids and composts).

The bench scale experimental results clearly demonstrate that the Biomat media with grass/food waste and steel slag is a promising technology, with excellent performance for heavy metal removal, coupled with excellent hydraulic characteristics of the media for treating high intensity storms. Stability of adsorbed metals on the mat media confirms the feasibility of mat utilization. Nonetheless, a few drawbacks are apparent including relatively high P release from first flush and risks from high bioavailable portions of removed metals in the media. Therefore, further investigation

may be needed to investigate possible modifications of mat media configuration and design parameters for minimizing these drawbacks and risks.

## CHAPTER 8. CONCLUSIONS AND RECOMMENDATIONS

Beneficial use of by-products/waste materials from industrial or agricultural activities as amendments or media/barriers to treat pollutants from diffuse sources can provide cost-effective solutions over various ranges of pollutants and flows. This is because diffuse source pollution is difficult to address due to the dispersed and often dynamic nature of the flows, which often lead to economic impracticality of traditional approaches which attempt to collect and treat runoff/infiltration in centralized facilities.

Therefore, two different research were studied to practice two different in-situ approaches for sequestering heavy metals (e.g., Pb, Cu, and Zn) or nutrients (e.g., phosphorus and nitrogen) which were released from diffuse sources: 1) Immobilization of phosphorus using Fe/Mn inorganic materials and an anaerobic incubation process: A direct application as amendments through direct diffuse source sequestration or stabilization; (2) Heavy metal removal from roof/wall runoff using a Biomat with compost and inorganic by-products; An barrier approach as its media constituents. The overall objective of the two research studies was to evaluate beneficial use of industrial and agricultural by-product materials in order to decrease environmental risks from heavy metals and nutrients released from diffuse sources by urban and agricultural runoff. Throughout the two research studies for beneficial use of different types of industrial or/and agricultural by-products, the overall objective was well accomplished by evaluating the feasibility of the by-products studied including investigating possible risks of the beneficial by-product. Specific summary, conclusions and suggestion were made from each study as follows.

### **8-1. Conclusions and recommendations on immobilization of phosphorus using Fe/Mn inorganic materials and an anaerobic incubation process**

Land application of manure and biosolids is limited by environmental risks resulting from highly soluble phosphorus species. Through the first research, three different low cost Fe/Mn rich materials (iron ore, steel slag and Mn tailings) were evaluated as amendments to decrease phosphorus from manure and use of the anaerobic incubation of fresh dairy manure with three different low cost Fe/Mn rich materials (iron ore, steel slag and Mn tailings). Steel slag addition significantly decreased water soluble phosphorus by 93% and Mehlich III extracted phosphorus by 80%, compared to manure only control. An anaerobic incubation of manure with Fe ore decreased 62% water extractable P (WEP) compared to fresh manure and a 76% compared to incubated manure due to oxalate extractable Fe (considered as amorphous Fe) increase by iron ore addition through anaerobic incubation, suggesting possible anaerobic incubation use for non-active byproduct to decrease P loss from manure.

However, the greatest increase of oxalate extractable Fe was observed in IOM, but it is estimated that only 9.2 % of the crystalline iron ore added was converted into active amorphous Fe during the 127 days of anaerobic incubation. This slow conversion of iron ore to more active Fe material through anaerobic incubation forced us to go toward using already highly active byproduct materials like steel slag for immobilizing phosphorus from manure and biosolids rather than going through anaerobic incubation.

However, any optimization or modification of anaerobic incubation to improve the synthesis of amorphous Fe was not attempted in this study. Therefore, further study is necessary to increase both the rate and percent conversion of crystalline iron ore to active amorphous iron material. In fact, the importance of well-mixed conditions for increasing

diffusional flux (thermodynamic driving force) of Fe(II) to enhance Fe(III) reduction was noted in a recent study (Royer et al., 2004), demonstrating that higher mixing intensity increased hematite reduction. In particular, for field application, biosolids is usually needed to go through stabilization process, such as anaerobic digestion which operates with mechanical mixing in a typical digester and this may enhance the synthesis of active amorphous Fe/Mn oxides from nonactive Fe/Mn materials. Therefore, studies for optimization and modification of typical manure digesting processes may be needed to enhance the bacterial Fe reductive dissolution and therefore increase the synthesis of amorphous Fe in bio solids and manure if low cost iron ore byproducts are to be used to reduce phosphate risks from manures.

## **8-2. Conclusions on Heavy metals removal using industrial by-products.**

Through the second research study, feasibility of Biomat, a mixture of sand, compost and inorganic by-products was evaluated through column and bench-scale experiments to remove heavy metals from roof/wall runoff. As a 1<sup>st</sup> phase of the research experiment, feasibility of varied Biomat media for removing three different heavy metals (Zn, Pb, and Cu) using 5 different media columns was evaluated: 10% manure compost + sand (MC10), 10% grass/food waste compost + sand (GF10), A 25% grass/food waste compost + sand (GF25), 25% grass/food waste compost + 5% steel slag + sand (GFS25), and 25% grass/food waste compost + 5% hubcutter heavies + sand (GFH25). 25% grass/food waste compost + steel slag + sand column was the best tester as Biomat media, not only demonstrating the best metal removal of heavy metals from diffuse sources but also exhibiting the greatest immobility of sorbed metal on the media.

Throughout the second phase bench scale experiments, hydraulic characteristics and heavy metal removal performance of the mat media was evaluated and mat configuration and installation recommendation was made from bench scale experiments.

### **8-3. Discussion and recommendations on Biomat configuration, installation and operation.**

Based on the bench-scale experiment, about 20 cm high and 20 cm long (parallel to the flow) Biomat media is recommended for installation if the Biomat media is installed with same length (perpendicular to the flow) as the wall length and same media configuration and properties as used in the bench scale experiment (Figure 7-17a). The length of Biomat media can be adjusted based on the expected Biomat longevity, but the length should be no less than 9 cm to maintain high metal removal based on media extraction results.

It is also recommended to install the Biomat about 10 to 20 cm distant from the wall to minimize untreated water from influent overflow (when it is installed by contacting with the wall) or splashed water from the wall structure and to have space for influent water head and flow buffer. A plastic liner should be installed from the wall to Biomat effluent side on slanted and leveled ground on which Biomat is installed (Figure 7-17a). Slight slope toward the flow and well evened ground will assist the water drainage of the Biomat which can prevent excessive decomposition of compost media. The wall height (20 cm) submerged in water should be water-proof treated or covered by a plastic liner sealed to the wall.

The Biomat media should be installed between two relatively fine screens (40 mesh, 0.38 mm opening size) (Figure 7-17a). The screen supporting structures should be



installed to support Biomat media at every certain length based on the screen thickness and rigidity (Figure 7-17c). An alternative to metal screen is media installation inside of a filter sock. Various kinds of filter socks are commercially available with variable opening sizes and sock diameters, as shown in Figure 7-18. However, it is recommended to install the Biomat inside of the sock a couple of centimeters below the ground to prevent water flow from bypassing underneath the mat media or from less detention time than it is designed for (Figure 7-17b). In fact, it will be also beneficial if screened Biomat media is also installed a few cm below grade. Biomat media packed in filter sock can be also supported by some frames installed every fixed length to fix the Biomat media in the designed shape.

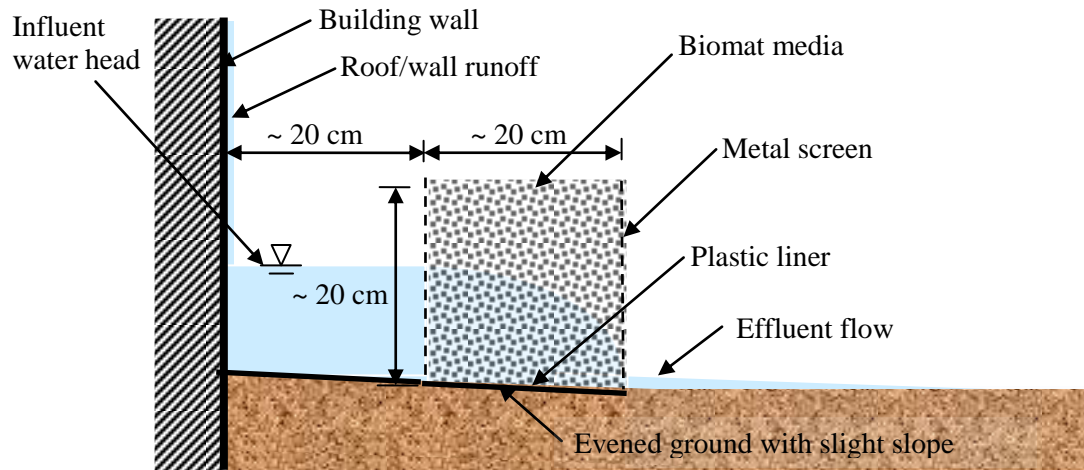
An extra sand layer can be added to minimize possible loss of small compost media particles during storm events and, therefore, to limit possible leaching of phosphorus and adsorbed/precipitated metals from the media (mainly from the first flush through the media). As a further aggressive approach, some phosphorus removal amendment such as Al/Fe based water treatment residual (WTR) can be applied to limit phosphorus leaching from compost media. Metal leaching tests for the WTR should be carefully performed and evaluated before the application.

It is speculated that the metal saturation of the media is expected to start from the influent side and bottom segment of the media layer and the degree of saturation of metal binding capacity is strongly related to rain frequency of different storm intensities, as shown in Figure 7-19. As an example, the bottom segment of the media will be more quickly saturated when most of rainfalls are of low intensity, which may cause earlier

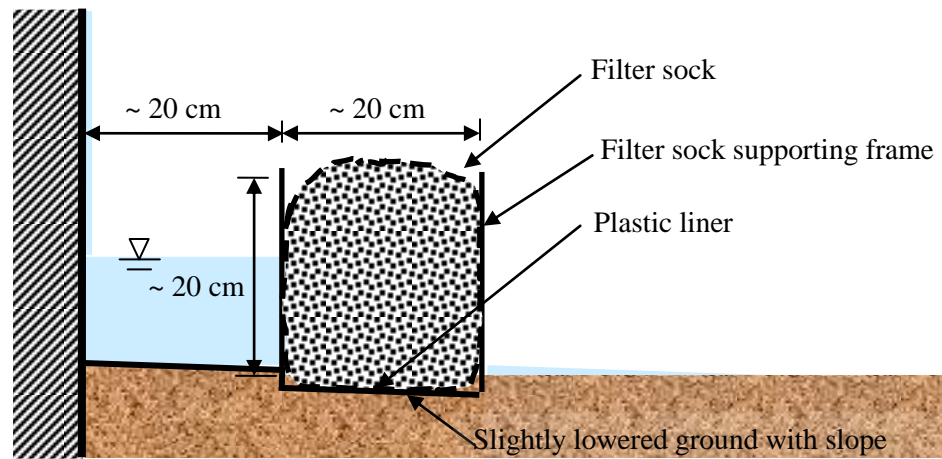
breakthrough compared to the previously estimated longevity of Biomat media (Chapter 6).

As shown in Figure 7-18, the top-effluent side of Biomat will not be efficiently used due to the hydraulic characteristics of the perpendicular flow system. As briefly discussed earlier, hydraulic modification of Biomat, including installation baffles or different size of orifices inside or on the surface of the mat may better distribute the flow. If filter socks are used for Biomat packing, the socks can be periodically rotated to efficiently use the mat media.

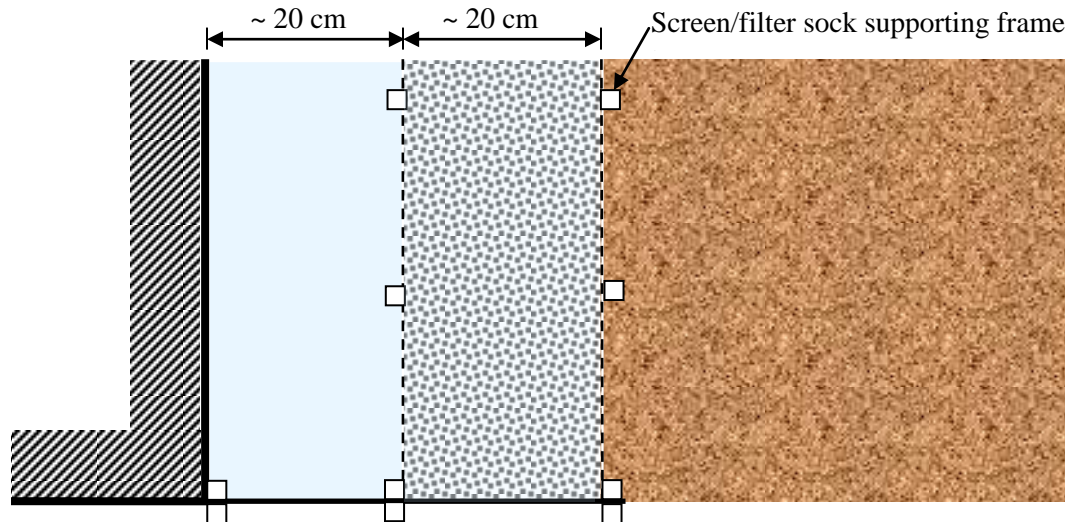
In spite of long expected life time of the Biomat, it will eventually be necessary to replace the mat media when the metal removal performance of the Biomat drops (i.e., when effluent metal concentrations are persistently greater than Maryland metal criteria). At that time, spent media should be analyzed using the Toxicity Characteristic Leaching Procedure (TCLP: EPA test method 1311) (EPA, 1992). If the extracted solution via TCLP shows 5 mg/L Pb or greater (based on Code of Federal Regulations, 40 CFR 261.24), the mat media should be treated as a hazardous waste. If the mat media meet the regulatory level of TCLP (<5 mg/L Pb), it can be disposed in standard landfills. Experience with TCLP extraction of biosolids rich in Pb, and Pb contaminated soils other than mine wastes suggests that the TCLP for spent Biomats will not be exceeded (Scheckel et al, 2009).



(a) Side view of recommended Biomat field design (metal screen)



(b) Side view of recommended Biomat field design (metal screen)



(c) Topview of recommended Biomat field design (metal screen or filter sock)

Figure 8-1. Recommended field design for Biomat media installation.

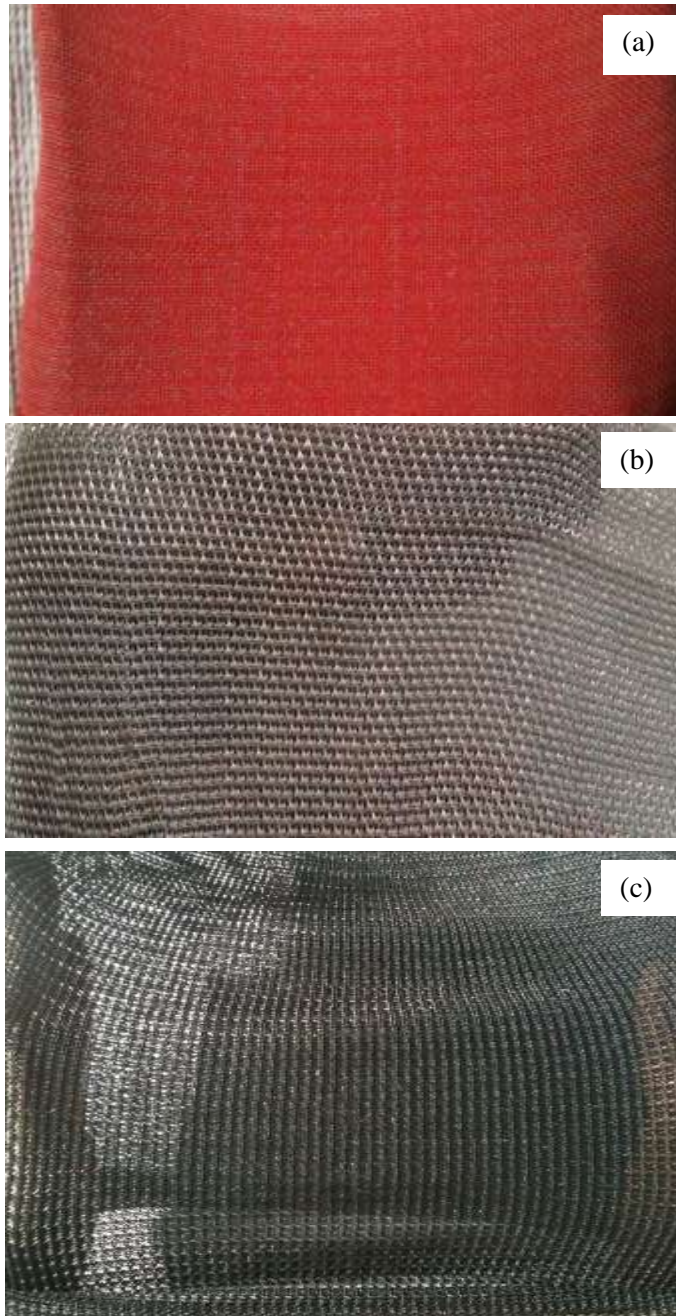
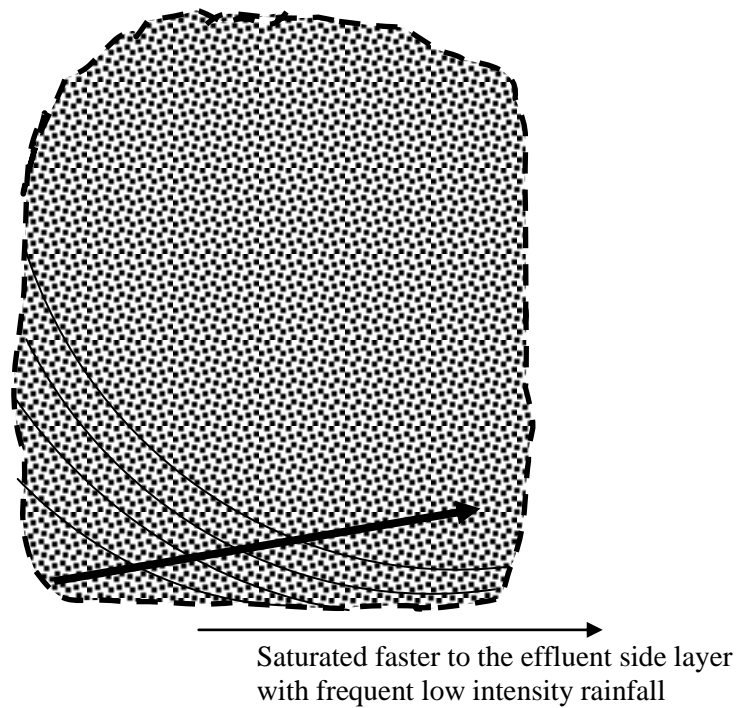
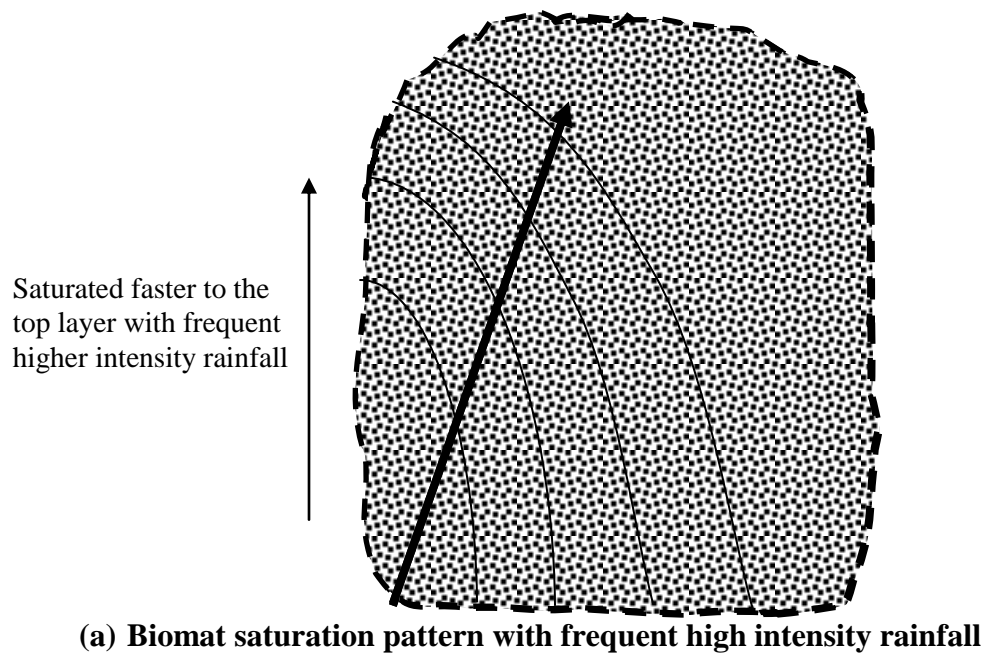


Figure 8-2. Filter socks with different opening size. (a) fine opening size filter sock, (2) medium opening size filter sock, (3) large opening size filter sock.



**Figure 8-3. Biomat saturation patterns.**

#### **8-4. Consequences of work: Strength and weakness of the study, and necessary future work.**

Overall, both researches projects demonstrate the effectiveness of beneficial use of by-products/waste materials from industrial and agricultural activities as amendments or media/barriers to treat heavy metal and phosphorus from diffuse sources.

The first study, immobilization of phosphorus using Fe/Mn inorganic materials and an anaerobic incubation process, newly introduced and evaluated the use of an anaerobic incubation process as a possible process to transform inactive byproducts (i.e., low in amorphous Fe/Mn content) to active amendments for phosphorus immobilization through adsorption/precipitation. This is specifically unique due to its aggressive approach for beneficial use of byproducts, which attempted to alter the physicochemical characteristics of the by-products and therefore to enhance/maximize the beneficial characteristics of the byproducts as amendments by decreasing environmental risk from diffuse source contamination, while traditional beneficial use of byproducts exploits only the existing characteristics of the byproducts. In particular, this aggressive approach of beneficial use of byproducts can become more useful when byproducts with necessary physicochemical characteristics or quantity supply are not available or limited.

The study demonstrated the effectiveness of anaerobic incubation showing increase in amorphous Fe content (oxalate extractable Fe increase by about  $4740 \text{ mg kg}^{-1}$ ), and decrease of P mobility (62% reduction of WEP compared to fresh manure before digestion and a 76% reduction compared to the control) in a manure mixture with Fe ore (with 5% total Fe content) throughout the 127 days of anaerobic incubation.

Nonetheless, in spite of the unique approach to beneficial byproduct use and the effectiveness of the study, some weaknesses of the study are also postulated. First, it is

estimated that only 9.2 % of the crystalline iron ore added in the manure mixture with iron ore (IOM) was converted into active amorphous Fe during the 127 days of anaerobic incubation. This low percent yield of amorphous Fe will limit the applicability of anaerobic incubation unless technical improvements are made for higher amorphous Fe synthesis. However, it should be noted that any application of mechanical mixing or adjustment of environmental condition (e.g., operation temperature) were not attempted during anaerobic incubation to improve the synthesis of amorphous Fe. A typical anaerobic digestion process operates with mechanical mixing condition at high temperature. Therefore, future study is needed to evaluate synthesis of amorphous Fe using a typical anaerobic digestion process and its operation conditions because more harsh environmental conditions (e.g., higher temperature) and mechanical mixing may provide significant improvement of amorphous Fe yield from non-active Fe byproducts (e.g., iron ore). Furthermore, the importance of well-mixed conditions for increasing diffusional flux (thermodynamic driving force) of Fe(II) to enhance Fe(III) reduction was noted in a recent study (Royer et al., 2004), demonstrating that higher mixing intensity increased hematite reduction. Therefore, mechanical mixing in a typical manure digester should enhance the synthesis of active amorphous Fe/Mn oxides from non-active Fe/Mn materials.

Another weakness of the study is the possibility of methane yield decrease during anaerobic digestion of manure/biosolids due to competition between methane producing bacteria and Fe reducing bacteria as noted in paddy soil (Achtnich et al., 1995) and fresh water sediments (Roden and Wetzel, 2003). If addition of non-active Fe/Mn byproduct limits the biogas production during anaerobic digestion of manure due to inhibition of

methane producing bacteria by Fe reducing bacteria, applicability of anaerobic digestion of manure mixtures with Fe/Mn by products will be significantly limited because anaerobic digestion of manure is optimally used for biogas production (i.e., stabilization of manure is not required for manure land application). If stabilization is the main purpose of anaerobic digestion like biosolids, decrease of biogas production caused by addition of Fe/Mn byproduct materials is of lesser concern.

The second study, heavy metal removal from roof/wall runoff using a Biomat with compost and inorganic by-products, newly introduced and developed the Biomat media. Metal removal performance and hydraulic characteristics of the mat media were evaluated and demonstrated during both the column and bench scale studies.

One of the strengths of this study was to systematically develop the technical approaches on a site with diffuse source pollution through four specific experimental phases starting from (1) monitoring and characterizing the contamination on the site (Phase 1: monitoring and characterizing roof/wall runoff from the building) and (2) developing the heavy metal removal Biomat media barrier technology (Phase 2: screening, selecting and evaluating the mat media employing long-term column studies; and Phase 3: investigating hydraulic characteristics and demonstrating heavy metal removal capacity of the mat media with a bench-scale mat), and finally (4) establishing design parameters for the Biomat technology (Phase 4: establishing design parameters, implementations, and recommendations for future full scale Biomat application in the field).

Furthermore, this study evaluated not only the performance of the Biomat media (the sorbent materials), but also the possible adverse environmental impact of the media



materials by monitoring not only target contaminants, but also other water quality parameters (e.g., phosphorus, turbidity, and Cr) which can be potentially produced and/or released. This is again the unique strength of the study because the majority of heavy metal sorption studies using these bio sorbents fail to examine the potential risk of various water quality parameters other than their target metal contaminants.

Furthermore, most of the studies only evaluate dissolved metal concentrations by filtering samples without either evaluating possible total metal release to the environment or providing possible separation techniques of the sorbents slurries.

In spite of the strengths of this unique study, weaknesses of the study were also postulated. Firstly, column studies with more variable Biomat media column configurations would have given more complete information for better screening and evaluation of the media configuration for optimized heavy metal removal. Furthermore, lack of hydraulic characteristic information based on different compost contents during the column study leaves the selection/evaluation of Biomat media less optimized. Therefore, further study for evaluating hydraulic characteristics for different compost types and contents may be necessary for finding better Biomat media configurations, resulting in better media performance in terms of heavy metal removal as well as hydraulic characteristics.

Secondly, studying more variable influent metal loading rates through varying metal concentrations (different ratio of each influent metal concentration) and flow rates during column and bench scale experiments would allow one to better understand and predict the heavy metal removal performance, capacity and lifetime of the Biomat media.

Competitive sorption/desorption behavior of each metal can be strongly affected by the influent metal concentration of coexisting metals.

Finally, the column study was performed by simulating the Biomat operation with saturated flows. However, perpendicular flow was studied during bench-scale experiments, which was a unique study but also demonstrated some weakness in terms of hydraulic/hydrologic characteristics and heavy metal removal performance, showing unsaturated flows as described in the previous sections (Sections 7-3-7, 7-3-8 and 8-3). Therefore, further bench scale experiments under realistic conditions of various rainfall intensity and duration around the Maryland area may be needed until significant effluent concentrations are detected in order to evaluate the Biomat media capacity for metal removal and frequency of media replacement based on the capacity. Another Biomat bench scale experiment with down flow may be also studied to compare the heavy metal removal performance and capacity and hydraulic/hydrologic characteristics with those of perpendicular flow.

Overall, the research studies demonstrated the beneficial use of by-products/waste materials for diffuse source pollution by satisfying the overall goals of the studies. With completion of suggested further studies as mentioned above, these two unique studies can strongly contribute to minimizing environmental risks from diffuse source pollutions, through implementing beneficial use of byproducts from agricultural/industrial activities

## APPENDIX

### Appendix A. Information for Chapter 4

#### Appendix A-1. Water P (Figure 4-3a)

--	Iron ore	--	Steel Slag	--	Mn Tailings	--	Manure only	--
Time (Day)	Average (mg P/kg)	stdev	Average (mg P/kg)	stdev	Average (mg P/kg)	stdev	Average (mg P/kg)	stdev
0	309.3	16.1	19.81	2.174	216.8	18.35	299.9	9.14
3	440.7	30.0	5.40	0.117	120.4	1.92	489.0	3.69
10	294.6	17.1	2.75	0.061	50.88	5.18	460.3	11.1
33	305.1	16.8	2.18	0.284	67.23	1.23	910.3	12.9
68	240.5	11.3	1.85	0.096	71.71	3.21	603.8	22.1
127	114.6	9.64	1.82	0.205	182.6	6.57	470.7	22.1

#### Appendix A-2. Mehlich III (Figure 4-3c)

--	Iron ore	--	Steel slag	--	Mn Tailings	--	Manure only	--
Time (Day)	Average (mg P/kg)	stdev	Average (mg P/kg)	stdev	Average (mg P/kg)	stdev	Average (mg P/kg)	stdev
0	2454.5	63.9	536.3	61.7	2089.2	69.8	2677.4	46.5
3	1935.5	101.6	805.6	12.0	1752.9	11.8	2223.5	67.1
10	1837.3	33.2	709.0	51.8	2224.3	13.1	2724.8	143.7
33	1901.6	88.8	834.9	30.5	2165.7	29.4	3036.5	28.7
68	2142.2	94.9	904.1	123.9	2167.7	62.4	3192.4	172.5
127	2409.8	51.2	1056.6	29.7	2604.4	15.1	3815.7	95.8

#### Appendix A-3. Oxalate Fe (Figure 4-3d)

Day	average Fe, mg/kg	stdev	average Fe, mg/kg	stdev	average Fe, mg/kg	stdev	average Fe, mg/kg	stdev
	Iron ore		Steel slag		Mn tailings		Control	
0	1254.6	36.5	17559	2866	1634.0	100.2	1338.2	117.3
3	1767.6	40.9	19320	2756	1684.0	60.5	1442.5	2.5
10	3182.7	35.9	17726	1450	1705.6	85.4	1665.0	31.3
33	4385.7	106.8	18900	1782	1787.7	167.4	1815.3	20.8
68	5004.9	68.8	16741	2594	1914.2	140.2	1932.7	24.9
127	5988.2	48.0	17930	2802	2283.7	55.6	2078.3	79.4

Appendix A-4. pH of wet sample (Figure 4-5a)

day	Iron ore	Steel slag	Mn tailings	Manure only
0	7.96	10.38	7.81	7.94
3	6.88	10.37	7.41	6.90
10	6.49	10.23	6.99	6.71
33	7.72	10.31	6.72	6.70
68	7.63	10.17	7.19	7.31
127	7.82	9.49	7.74	7.65

Appendix A-5. pH of dry sample (Figure 4-5b)

dry sample	pH	--	--	--
day	Iron ore	Steel Slag + Manure	Mn tailings + Manure	Manure only
0	7.93	8.49	7.79	7.92
3	7.71	8.62	7.69	7.71
10	7.31	8.80	7.09	7.49
33	7.48	8.69	6.69	6.70
68	7.74	8.71	6.70	7.06
127	8.45	8.55	7.61	7.27

Appendix A-6.  $\text{Sr}(\text{NO}_3)_2$  extractable Zn (Figure 4-6a)

	Iron ore + Manure		Steel Slag + Manure		Mn tailing + Manure		Manure only (Controls)	
Day	average Zn (mg/kg)	stdev Zn (mg/kg)	average Zn (mg/kg)	stdev Zn (mg/kg)	average Zn (mg/kg)	stdev Zn (mg/kg)	average Zn (mg/kg)	stdev Zn (mg/kg)
0	7.94	0.28	2.54	0.096	5.53	0.238	9.118	0.301
3	7.17	0.31	3.09	0.122	5.23	0.115	8.392	0.141
10	7.36	0.16	3.23	0.167	5.79	0.216	8.192	0.057
33	4.76	0.27	3.77	0.477	5.38	0.113	7.596	0.085
68	5.70	0.69	3.72	0.010	4.97	0.693	6.747	0.056
127	8.09	0.61	2.77	0.283	3.62	0.166	5.092	0.025

Appendix A-6.  $\text{Sr}(\text{NO}_3)_2$  extractable Zn (Figure 4-6b)

	Iron ore +Manure		Steel Slag + Manure		Mn tailing + Manure		Manure only (Controls)	
Day	average Cu (mg/kg)	stdev Cu (mg/kg)	average Cu (mg/kg)	stdev Cu (mg/kg)	average Cu (mg/kg)	stdev Cu (mg/kg)	average Cu (mg/kg)	stdev Cu (mg/kg)
0	48.94	0.46	41.69	2.32	46.5	0.98	54.16	0.81
3	32.41	1.07	39.39	0.86	23.3	0.02	38.01	0.24
10	16.94	5.09	47.93	0.15	26.4	2.49	20.54	0.28
33	21.94	0.59	43.75	2.30	22.0	0.17	24.08	0.27
68	26.07	2.08	44.78	2.38	21.1	0.40	20.56	0.52
127	36.07	1.14	30.10	2.17	26.7	0.87	27.19	0.18

Appendix A-7 pH of  $\text{Sr}(\text{NO}_3)_2$  extraction solution Zn (Figure 4-6c)

--	Iron ore +Manure	Steel Slag + Manure	Mn tailing + Manure	Manure only (Controls)
Day	pH average	pH average	pH average	pH average
0	8.01	8.56	7.78	7.98
3	7.53	8.83	7.50	7.52
10	7.20	9.02	7.18	7.68
33	7.40	8.90	6.92	7.35
68	7.71	8.91	6.98	6.73
127	8.29	8.71	7.56	7.28

Appendix A-8 Oxalate extractable Zn (Figure 4-7a)

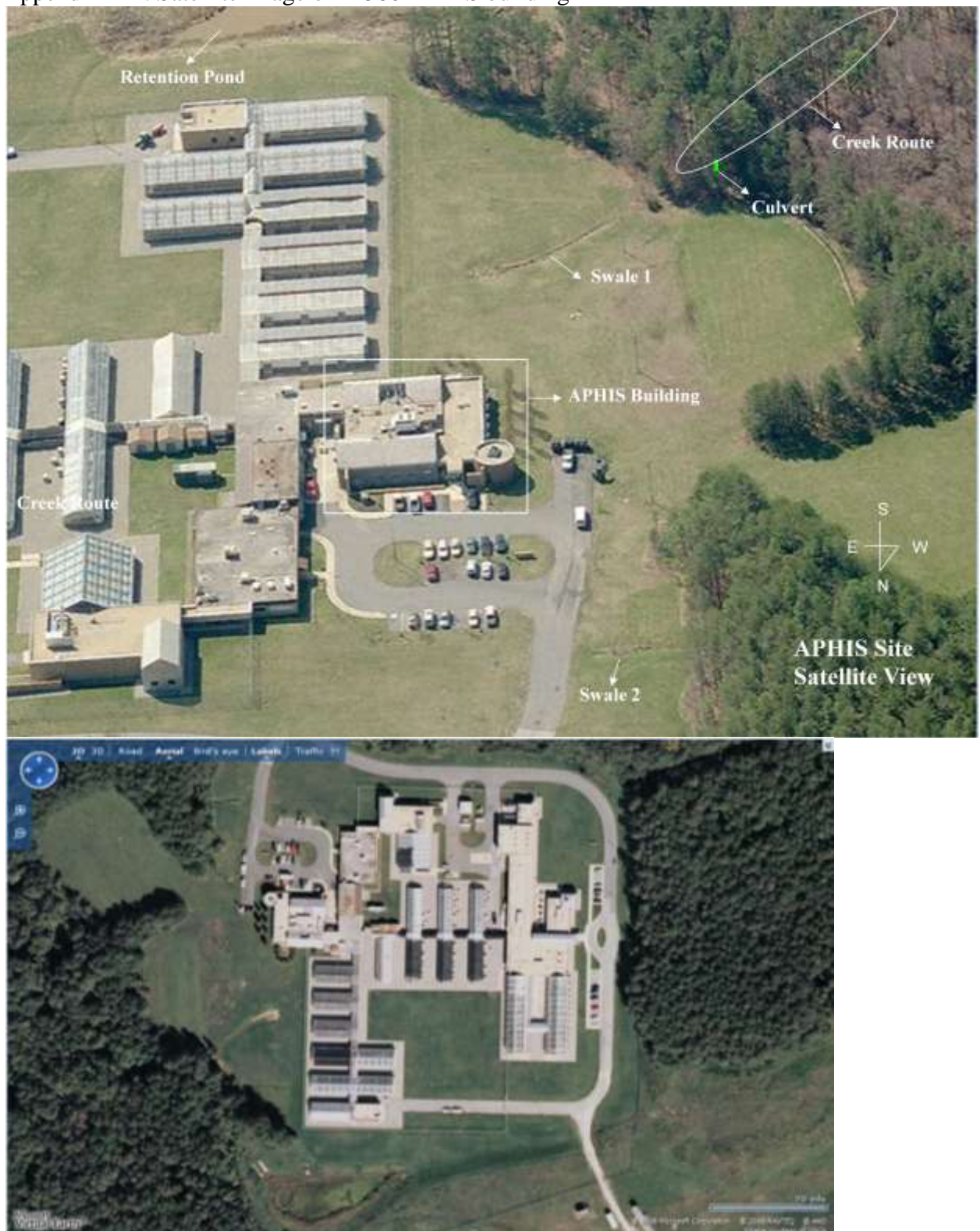
--	Iron ore	--	Steel Slag	--	Mn Tailing	--	control	--
day	average Zn (mg/kg)	stdev Zn	average Zn (mg/kg)	stdev Zn	average Zn (mg/kg)	stdev Zn	average Zn (mg/kg)	stdev Zn
0	263.0	6.2	65.1	12.7	224.3	43.9	296.8	9.9
3	258.5	6.3	75.7	4.6	240.3	11.2	289.3	2.7
10	262.7	5.9	67.9	7.0	199.6	6.9	290.7	4.6
33	271.2	1.1	71.0	5.2	164.9	2.1	286.5	10.4
68	281.9	1.6	77.3	9.2	164.7	7.8	292.8	3.7
127	315.6	3.5	54.6	0.72	176.9	2.1	319.6	6.9

Appendix A-9 Oxalate extractable Cu (Figure 4-7b)

--	Iron ore	--	Steel Slag	--	Mn Tailing	--	control	--
day	average Cu (mg/kg)	Stdev Cu	average Cu (mg/kg)	Stdev Cu	average Cu (mg/kg)	Stdev Cu	average Cu (mg/kg)	Stdev Cu
0	260.7	3.70	177.0	15.3	292	8.95	293.1	9.41
3	232.3	4.71	180.0	4.53	276	6.11	254.3	5.60
10	205.6	1.66	165.2	1.07	251	3.13	235.4	4.35
33	210.4	10.4	158.6	14.3	237	2.41	216.8	6.22
68	224.6	3.91	162.8	6.11	228	3.51	232.8	7.16
127	270.6	1.89	148.3	2.12	263	6.05	254.0	4.02

## Appendix B. Information for Chapter 5.

### Appendix B-1. Satellite image of B-580 APHIS building





Appendix B-2. Corroded wall of B-580 APHIS building.

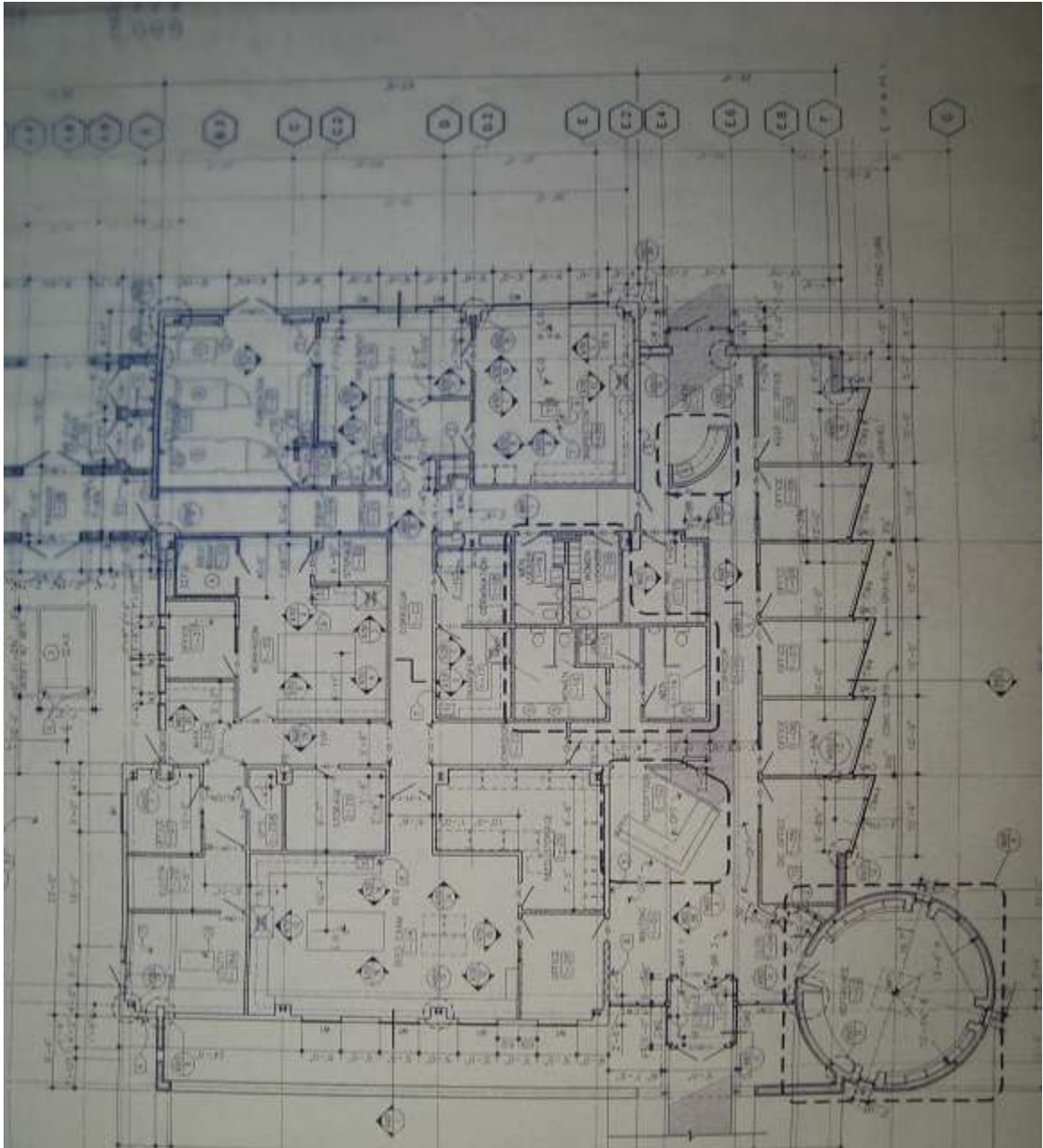




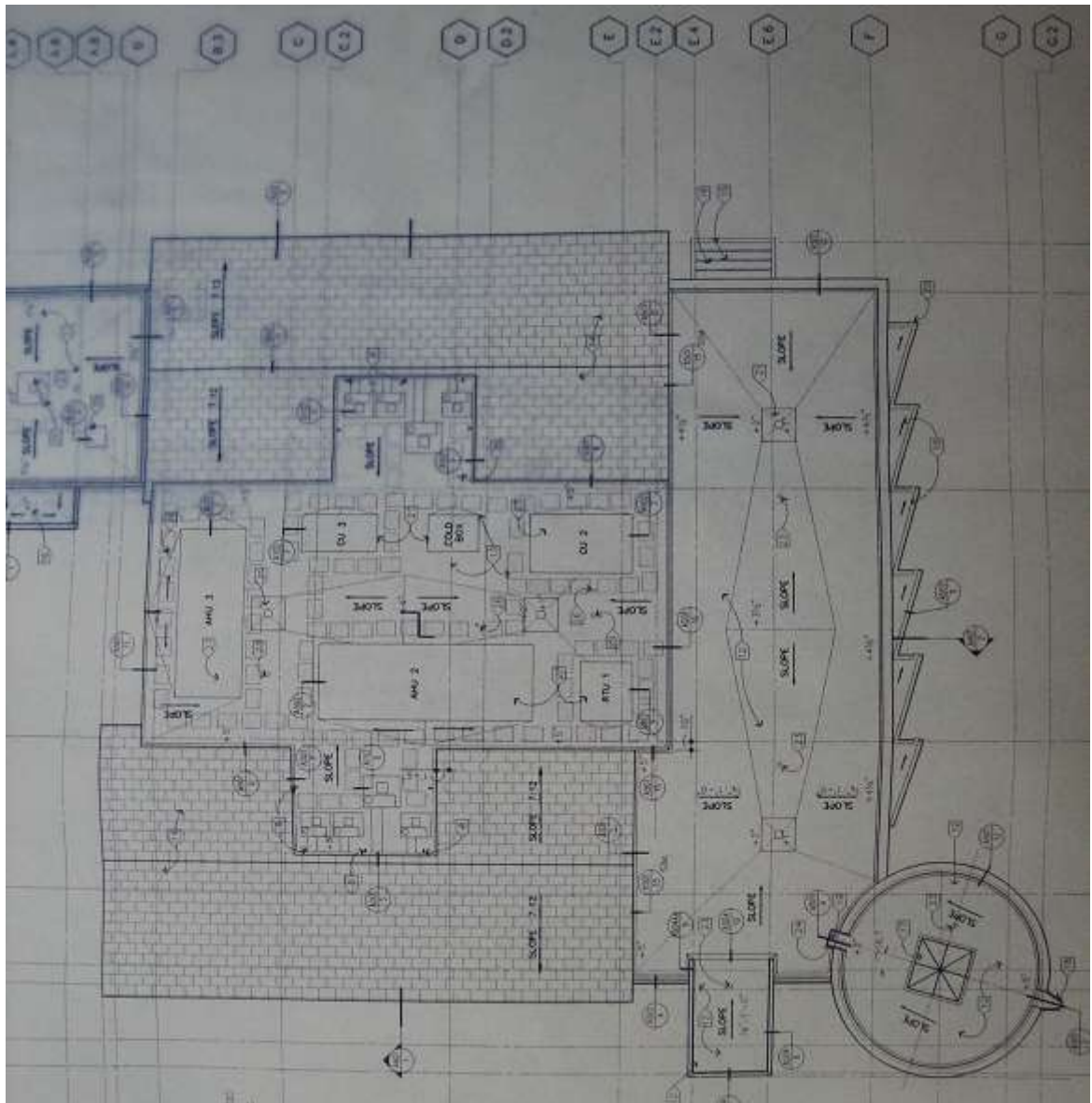
Appendix B-3. Gravel layer adjacent to wall of B-580 APHIS building.



Appendix B-4. Design (top view) of B-580 APHIS building.

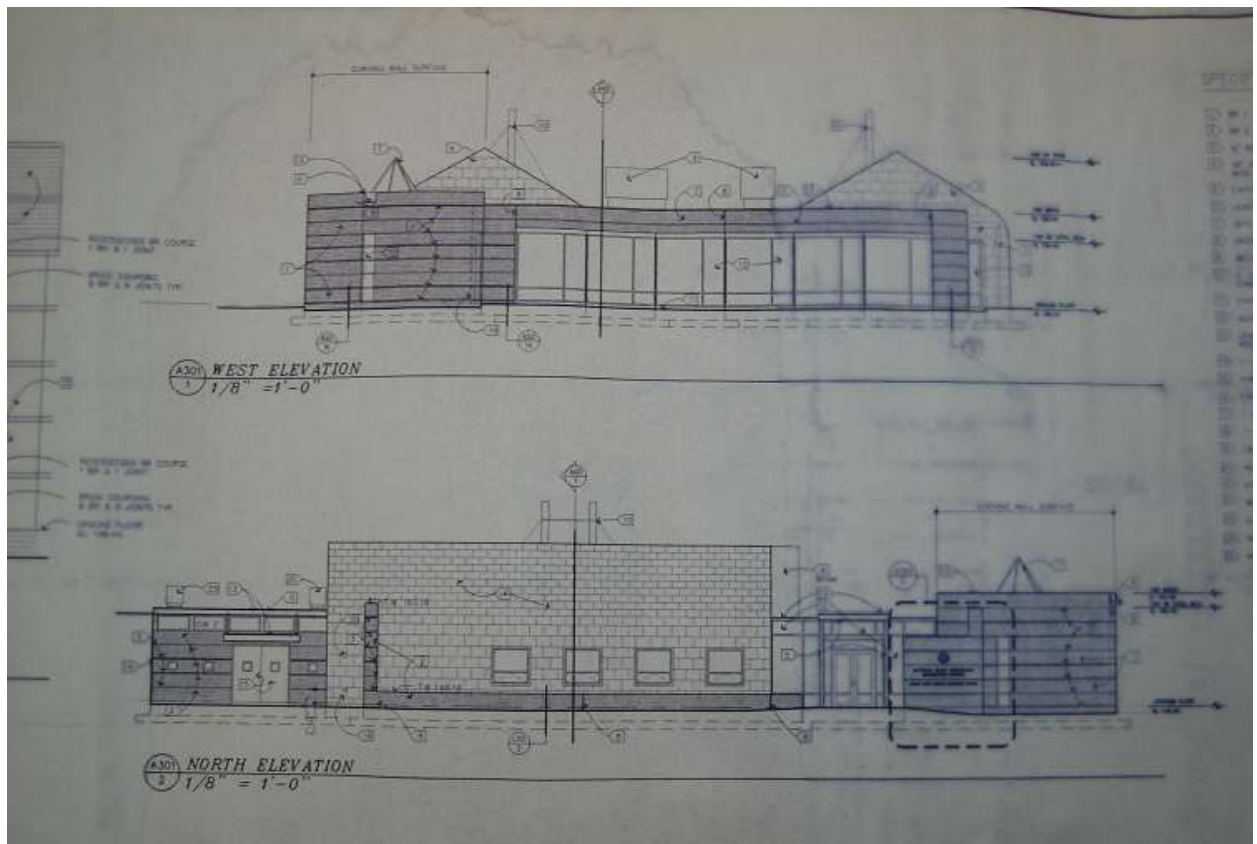
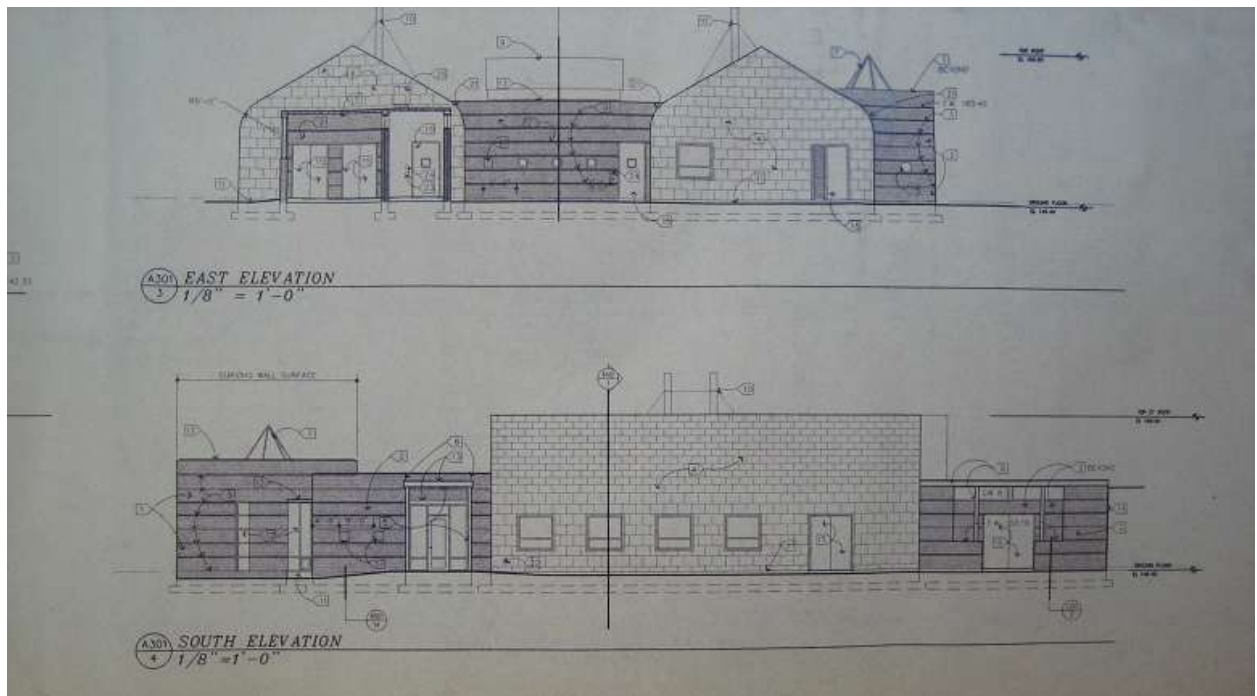


Appendix B-5. Design (roof) of B-580 APHIS building.





Appendix B-6 Design (Side) of B-580 APHIS building.

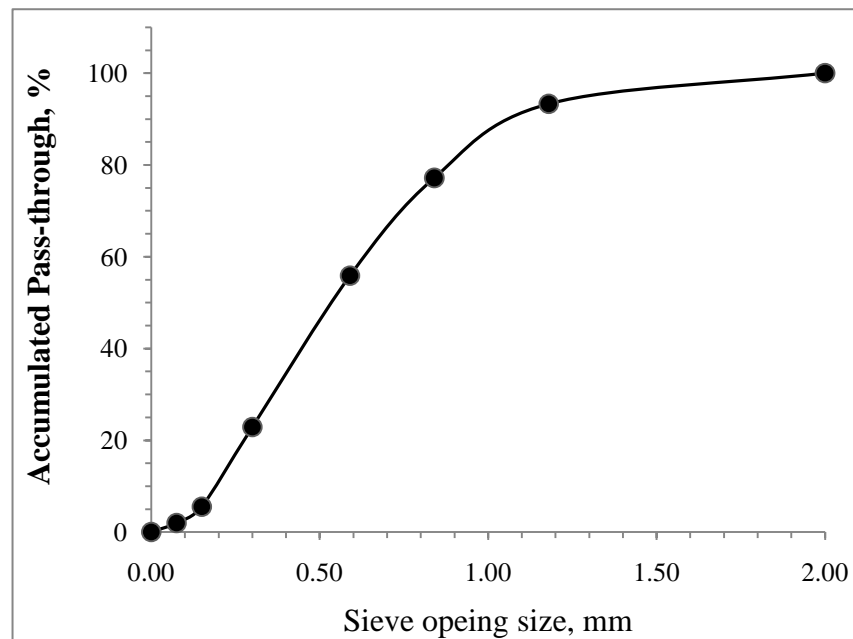


## Appendix C. Information for Chapter 6

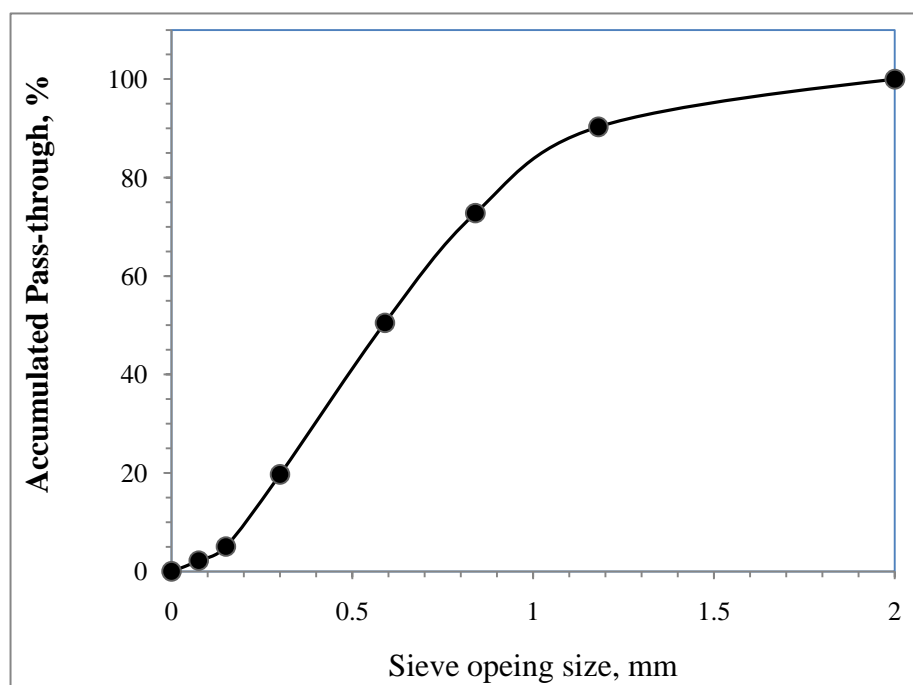
Appendix C-1. Sieve analysis for manure compost, grass/food waste compost, and steel slag used for the Column sorption study.

Sieve opening size, mm	Accumulated Pass-through %	
	Manure compost	Grass/Food waste compost
2.00	100	100
1.18	93.31	90.31
0.84	77.17	72.76
0.59	55.88	50.50
0.30	22.88	19.70
0.15	5.55	5.03
0.075	1.98	2.18
0	0	0

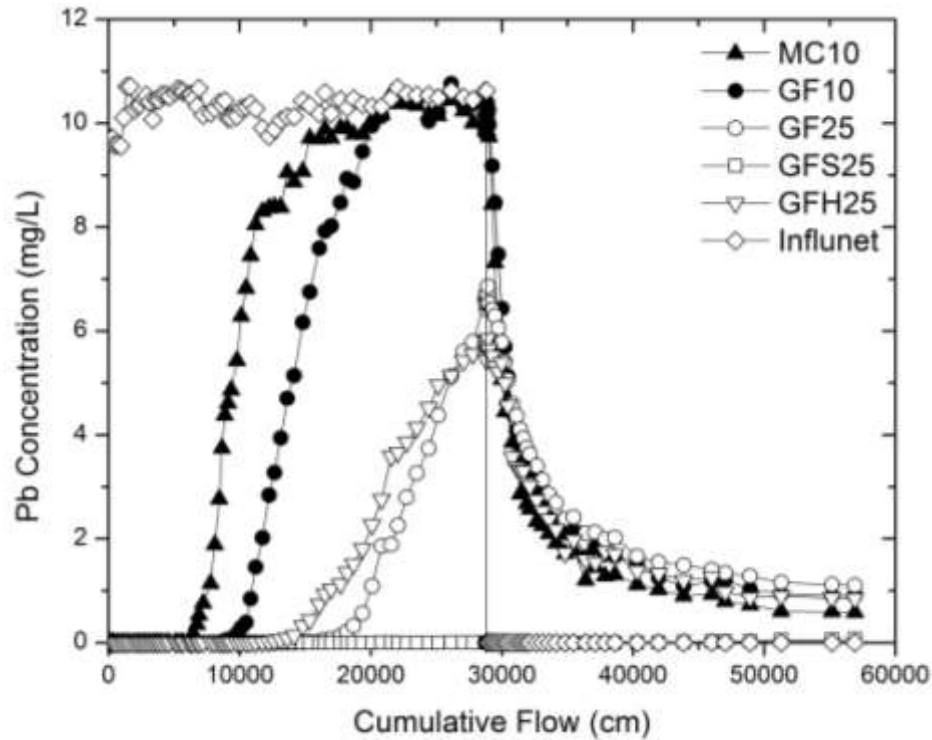
Appendix C-2. Sieve analysis for Manure compost used for the Column sorption study.



Appendix C-3. Sieve analysis for Grass/food waste compost used for the Column sorption study



Appendix C-4. Figure: Pb influent and effluent concentration during sorption/leaching column study



Appendix C-5. Data: Pb influent and effluent concentration during sorption/leaching column study.

flow	Pb Conc. ( $\mu\text{g/L}$ )	Pb Conc. ( $\mu\text{g/L}$ )	Pb Conc. ( $\mu\text{g/L}$ )	Pb Conc. ( $\mu\text{g/L}$ )	Pb Conc. ( $\mu\text{g/L}$ )	Pb Conc. ( $\mu\text{g/L}$ )
cm	MC10	GF10	GF25	GFS25	GFH25	Influent
15	22.8	3.7	6.4	7.3	11.1	9715
50	7.3	1.8	1.6	0.6	3.4	9715
80	3.1	1.1	0.9	0.8	2.4	9715
115	2.4	0.7	0.6	0.7	1.9	9715
175	1.7	1.5	1.4	1.5	1.7	9715
265	1.2	1.2	0.8	0.3	1.7	9715
415	1.1	1.5	1.6	1.2	2.3	9583
665	0.3	0.2	0.2	0.3	0.4	9588
925	0.2	1.6	0.4	0.4	0.4	9563
1165	0.0	0.4	0.6	0.9	0.5	10110

1405	0.9	1.0	0.7	0.4	1.0	10710
1645	0.6	1.0	0.6	0.5	0.9	10710
1955	0.6	0.2	1.0	0.7	0.9	10260
2195	0.2	0.1	0.4	0.5	0.9	10330
2405	0.7	0.7	0.9	0.3	0.8	10360
2645	0.5	0.6	0.3	0.0	0.0	10480
2875	0.3	0.5	0.6	0.2	0.2	10540
3125	0.5	0.7	0.1	0.5	0.2	10410
3365	0.6	1.4	0.5	0.2	0.3	10070
3605	0.1	0.1	0.3	0.6	0.2	10450
3815	0.1	0.1	0.1	0.9	0.2	10450
4055	0.1	0.1	0.1	0.3	0.3	10550
4355	0.2	0.1	0.4	1.3	0.1	10550
4615	0.1	0.2	0.2	0.1	0.0	10510
5075	0.1	0.2	0.1	0.1	0.5	10600
5275	0.3	0.3	0.7	0.1	0.2	10660
5535	0.2	0.1	0.0	0.0	0.0	10640
5695	2.5	0.2	0.1	1.2	0.1	10600
6085	32	1.6	1.2	0.0	3.5	10550
6285	86	1.5	1.0	1.2	1.4	10550
6435	171	0.8	2.4	1.6	1.3	10470
6735	354	1.2	1.4	1.5	1.7	10330
6895	531	1.3	1.6	1.6	1.1	10670
7205	762	0.3	0.7	0.9	0.9	10160
7765	1142	1.7	0.9	0.6	0.6	10200
8100	1890	3.4	0.7	0.9	0.5	10280
8435	2771	7.3	0.7	0.9	0.9	10400
8635	3749	15	0.5	0.9	0.7	10350
8855	4385	42	12	2	2	10430
9105	4612	69	1.6	1.1	0.9	10100
9345	4865	75	1.1	1.1	2.2	10100

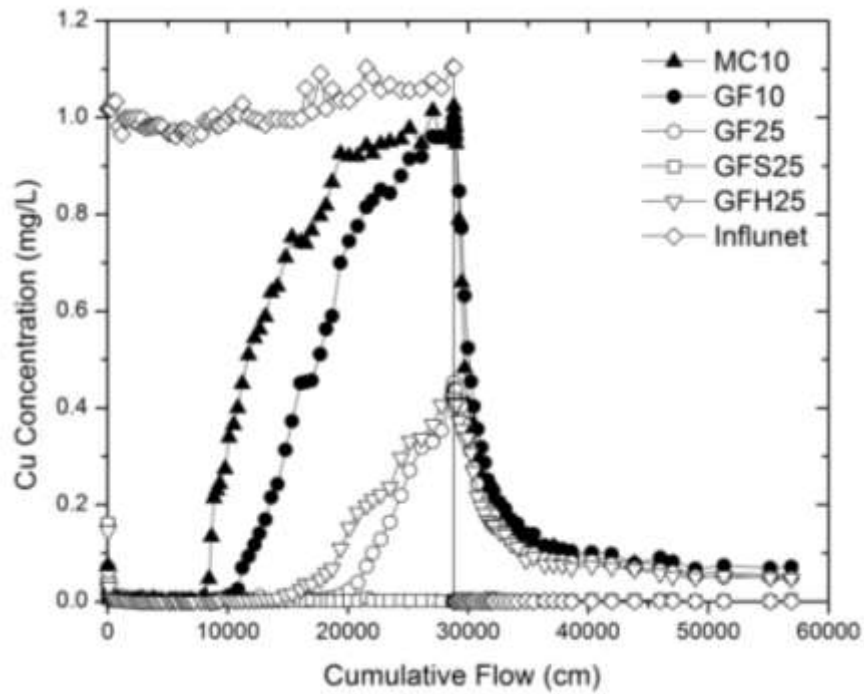


9775	5434	173	8.5	2.4	4.0	10140
10105	6287	293	1.6	1.5	1.7	10290
10485	6825	392	1.3	1.2	1.2	10310
10830	7454	848	1.7	1.4	2.3	10380
11205	8051	1459	1.6	2.1	3.3	10280
11735	8304	2019	1.6	0.7	7.1	9909
12225	8369	2842	0.9	1.3	17	9750
12640	8398	3278	2.7	0.9	31	9885
13125	8385	3942	1.9	0.5	59	10060
13615	9057	4705	1.5	0.5	85	10130
14145	8872	5143	1.6	0.5	137	10130
14805	9076	6167	6.4	0.4	322	10430
15345	9718	6752	16	2.7	443	10340
16065	9702	7592	26	2.5	740	10190
16495	9887	7924	55	2.9	938	10590
16980	9715	8024	67	0.4	1034	10190
17685	9916	8475	128	0.1	1125	10450
18185	9902	8936	215	0.2	1351	10300
18685	9789	8871	326	0.8	1517	10470
19365	9787	9455	567	0.5	1813	10360
20095	10070	9957	1090	2.3	2272	10320
20815	10170	10140	1862	6.6	2759	10320
21545	10560	10420	1889	4.2	3590	10480
22055	10380	10470	2257	1.2	3663	10680
22725	10380	10440	2801	1.4	3863	10570
23495	10350	10460	3265	2.6	4142	10540
24415	10170	10040	3743	1.1	4521	10540
25135	10150	10210	4380	1.6	4959	10490
26135	10450	10760	5132	4.7	5145	10630
27065	10240	10330	5609	4.1	5426	10500
27775	10010	10370	5792	4.3	5556	10450

28725	10230	9826	6614	6.8	5807	10630
28813	10050	10060	6555	4.7	5474	10630
28818	10090	10180	6429	3.6	5447	5.649
28823	9838	10100	6693	2.6	5670	5.649
28828	9983	9999	6510	2.3	5498	5.649
28833	9870	9978	6537	2.5	5447	5.649
28838	9983	10220	6733	2.1	5775	5.649
28849	10250	10150	6677	2.0	5647	5.649
28873	10010	10390	6710	1.9	5702	5.649
28928	10340	10290	6862	2.3	5856	5.649
29000	9742	9980	6540	4.7	5648	5.649
29255	8440	9181	6408	1.8	5526	7.513
29455	7318	8475	6292	2.2	5308	1.476
29705	5716	7474	6051	5.5	5215	1.053
29980	5069	6436	5790	5.3	5389	3.690
30235	4450	5699	5406	2.5	4995	1.460
30450	4670	5127	5062	1.6	4565	2.583
30790	3858	4419	4595	2.5	3574	2.753
31115	3524	4083	4373	2.1	3381	2.012
31390	2864	3831	4107	1.9	3328	2.606
31640	2970	3450	3935	2.2	3313	2.359
31900	2681	3237	3754	1.8	3071	1.802
32125	2576	3181	3632	2.1	3017	2.07
32640	2338	2884	3404	1.7	2746	1.758
33100	2255	2628	3136	2.0	2534	1.789
33585	2104	2394	2861	2.0	2375	2.001
34120	1925	2246	2695	2.4	2182	1.844
34815	1718	2119	2381	2.6	1729	1.788
35455	1775	2133	2418	2.3	1978	1.786
36390	1208	1645	2109	2.1	1599	1.445
37115	1463	1840	2121	2.4	1550	1.882

37855	1289	1700	1991	2.4	1761	1.713
38610	1310	1667	2025	1.9	1702	1.767
40305	1121	1556	1667	3.7	1386	1.312
41945	1026	1254	1552	4.1	1335	1.388
43855	905	1088	1494	14	1201	1.435
46000	935	1189	1407	25	1259	2.988
47025	799	1215	1345	26	979	1.489
48915	735	1029	1283	32	868	1.355
51295	604	943	1161	51	900	2.436
55165	599	907	1123	59	862	0.983
56915	584	910	1105	73	851	1.205

Appendix C-6. Figure: Cu influent and effluent concentration during sorption/leaching column study



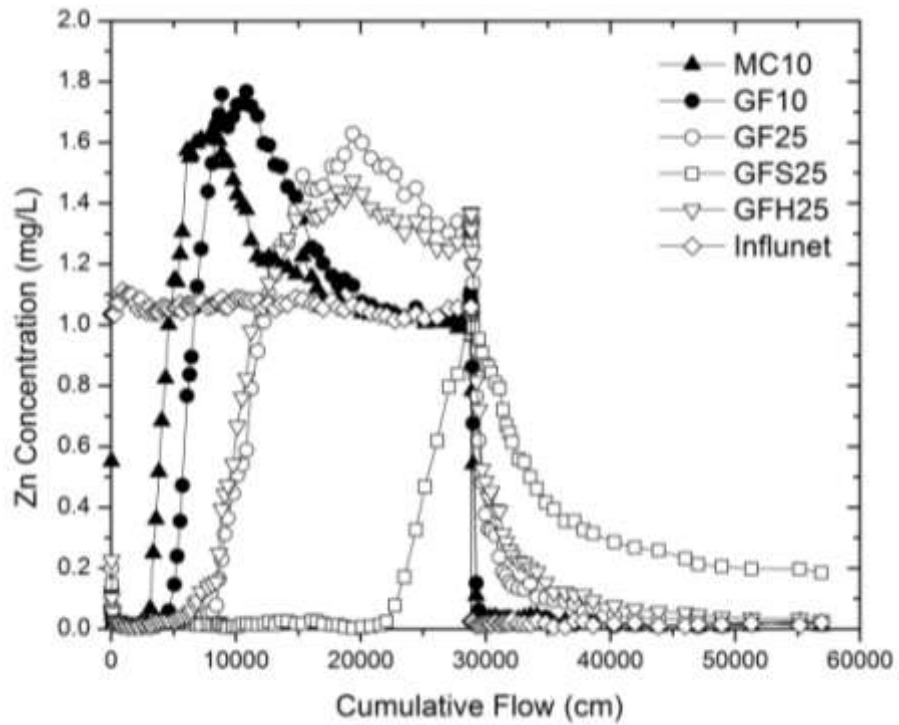
Appendix C-7. Data: Cu influent and effluent concentration during sorption/leaching column study

Flow cm	Cu Conc. (ppb) MC10	Cu Conc. (ppb) GF10	Cu Conc. (ppb) GF25	Cu Conc. (ppb) GFS25	Cu Conc. (ppb) GFH25	Cu Conc. (ppb) Influent
15	75	70	159	162	146	1,018
50	44	23	42	38	55	1,018
80	25	13	21	20	40	1,018
115	14	10	13	13	30	1,018
175	3.6	5.2	5.7	8.4	7.4	1,018
265	4.8	7.9	3.5	5.9	7.7	1,018
415	7.9	5.2	6.2	8.6	8.5	1,033
665	5.1	3.7	4.4	3.8	5.7	1,033
925	8.1	3.4	6.0	5.6	6.5	982
1165	5.0	4.5	9.9	6.7	6.5	966
1405	4.0	3.6	3.5	3.5	4.9	997
1645	3.6	3.2	3.2	2.9	4.1	997
1955	3.0	3.1	3.0	2.8	3.7	999
2195	2.7	2.7	4.9	3.4	4.6	992
2405	3.1	3.4	3.0	2.9	3.1	999
2645	5.1	6.3	2.5	3.0	2.5	986
2875	5.9	1.7	1.5	1.5	1.1	998
3125	1.2	1.0	2.0	5.0	2.5	980

3365	2.4	3.5	2.5	2.4	2.0	981
3605	1.7	1.9	2.3	1.9	2.9	982
3815	6.0	1.8	2.2	2.1	1.8	982
4055	1.6	1.8	1.5	1.6	1.5	984
4355	2.3	1.6	1.8	2.3	1.8	984
4615	0.7	1.2	0.8	1.1	1.5	980
5075	1.2	1.1	0.9	1.9	0.9	967
5275	1.9	2.6	1.5	1.2	2.5	968
5535	1.7	2.4	1.9	1.6	1.7	973
5695	3.0	4.4	2.2	1.9	1.9	961
6085	1.6	1.8	1.8	1.5	1.9	972
6285	1.8	4.7	2.2	3.6	2.2	972
6435	0.6	1.6	2.5	2.4	1.8	975
6735	1.1	0.7	1.4	0.9	0.9	971
6895	2.8	2.1	2.1	0.9	1.5	957
7205	1.6	2.3	1.4	0.7	0.6	965
7765	5.2	0.8	0.9	1.2	1.2	967
8100	12.0	1.2	0.8	1.0	3.3	993
8435	47	0.8	0.9	0.8	0.8	991
8635	134	3.1	0.4	2.0	0.5	995
8855	214	4.4	4.0	3.4	2.7	1,004
9105	230	4.8	3.0	2.5	2.5	984
9345	243	4.9	2.7	2.2	3.3	984
9775	274	8.0	3.2	4.6	7.3	990
10105	339	13	4.5	3.4	5.0	1,002
10485	366	15	3.6	3.0	3.0	1,009
10830	400	26	2.9	3.1	3.1	1,005
11205	450	70	4.7	3.2	3.7	1,029
11735	510	93	4.7	1.3	3.4	1,002
12225	544	117	2.3	1.1	3.3	996
12640	563	141	11	2.0	4.4	993
13125	589	170	1.7	0.9	5.4	985
13615	639	216	2.1	1.1	5.7	997
14145	651	243	1.4	1.1	6.5	997
14805	711	314	2.1	1.4	14	996
15345	753	373	3.4	1.4	16	995
16065	743	451	3.2	1.5	25	998
16495	740	454	8.0	1.3	37	1,061
16980	767	457	3.7	2.8	36	1,012
17685	797	511	4.4	1.5	46	1,091
18185	818	563	6.3	1.5	58	1,019
18685	866	590	7.9	1.1	68	1,058
19365	925	700	14.0	1.3	110	1,036
20095	920	745	24.0	1.5	152	1,035
20815	920	776	39.8	1.5	185	1,052
21545	942	815	73.2	7.4	198	1,103
22055	925	829	100	2.6	211	1,083
22725	945	851	129	2.1	221	1,057

23495	950	844	164	1.7	236	1,068
24415	955	880	219	2.5	298	1,057
25135	978	915	271	1.7	332	1,056
26135	946	919	318	2.2	338	1,059
27065	1014	962	331	2.6	366	1,077
27775	956	961	354	0.9	407	1,062
28725	988	969	436	1.6	417	1,104
28813	1007	995	453	1.2	411	1,104
28818	1024	990	431	0.6	413	0.6
28823	1008	998	439	0.9	422	0.6
28828	995	983	438	1.1	412	0.6
28833	1007	972	434	0.5	409	0.6
28838	988	972	432	0.6	411	0.6
28849	985	975	440	0.9	402	0.6
28873	980	956	438	1.8	400	0.6
28928	983	973	440	1.1	409	0.6
29000	946	957	438	1.7	408	0.6
29255	789	848	414	2.1	374	0.9
29455	660	772	404	2.1	356	0.3
29705	483	632	367	5.1	337	0.3
29980	407	524	337	5.3	339	0.7
30235	360	455	311	1.0	307	0.9
30450	367	403	277	0.8	269	0.5
30790	299	356	244	0.7	217	0.8
31115	258	319	218	0.8	198	0.4
31390	219	287	200	0.7	182	0.7
31640	220	252	192	1.4	168	0.4
31900	194	237	186	7.2	160	0.9
32125	189	229	179	1.8	158	0.4
32640	169	205	159	3.8	144	0.9
33100	166	191	144	2.1	139	0.4
33585	141	170	125	2.0	121	0.6
34120	144	161	113	0.9	113	0.3
34815	135	141	100	1.7	86	1.1
35455	125	139	99	1.4	93	0.2
36390	113	116	89	0.9	76	1.1
37115	113	113	85	0.6	77	1.5
37855	101	108	84	1.3	76	0.3
38610	100.	104	82	2.4	70	0.2
40305	92.5	102	83	4.3	74	0.6
41945	85.9	98.2	78	3.3	71	0.4
43855	78.5	79.1	69	3.2	66	0.5
46000	80.8	90.6	65	3.4	58	1.0
47025	68.2	82.8	61	3.9	53	0.7
48915	59.4	67.9	53	0.9	50	0.4
51295	60.8	74.4	51	1.5	54	0.5
55165	54.5	69.5	50	1.1	49	0.4
56915	56.2	71.6	49	3.9	48	0.5

Appendix C-6. Figure: Zn influent and effluent concentration during sorption/leaching column study



Appendix C-8, Data: Zn influent and effluent concentration during sorption/leaching column study

Flow cm	MC10 Zn Conc. (ppm)	GF10 Zn Conc. (ppm)	GF25 Zn Conc. (ppm)	GFS25 Zn Conc. (ppm)	GFH25 Zn Conc. (ppm)	Influent Influent Zn (ppm)
15	552	131	200	148	226	1036
50	87	63	76	56	103	1036
80	68	44	62	36	62	1036
115	47	48	47	30	54	1036
175	26	25	28	20	30	1036
265	22	26	23	19	25	1036
415	20	15	22	17	23	1074
665	13	16	16	16	17	1074
925	13	18	12	14	17	1113
1165	15	14	11	10	6	1096
1405	10	12	16	8	11	1098
1645	9	9	8	8	8	1098
1955	7	7	12	6	10	1073
2195	9	8	12	5	7	1052
2405	20	15	15	18	18	1084
2645	15	16	13	12	15	1052
2875	20	14	15	11	20	1044
3125	67	15	12	10	11	1058

3365	251	14	12	9	17	1041
3605	362	22	24	17	23	1043
3815	517	23	25	18	26	1043
4055	685	30	28	25	30	1059
4355	825	38	25	23	31	1059
4615	1002	60	27	27	30	1054
5075	1150	146	24	22	26	1056
5275	1142	240	30	19	33	1057
5535	1233	355	29	24	36	1069
5695	1307	472	27	28	43	1045
6085	1574	768	24	21	43	1067
6285	1552	837	21	24	50	1067
6435	1562	895	25	19	60	1059
6735	1598	1060	27	17	80	1068
6895	1597	1127	27	15	91	1079
7205	1611	1250	36	14	123	1078
7765	1614	1439	54	16	139	1059
8100	1629	1532	58	15	149	1065
8435	1663	1658	79	11	156	1073
8635	1607	1692	164	19	249	1073
8855	1564	1759	230	17	394	1088
9105	1533	1657	313	10	443	1060
9345	1535	1651	365	7	474	1060
9775	1477	1686	446	9	542	1081
10105	1429	1724	507	9	668	1089
10485	1399	1728	542	18	762	1086
10830	1380	1768	589	18	824	1079
11205	1278	1720	791	16	981	1078
11735	1225	1688	914	15	1056	1080
12225	1210	1597	1011	17	1081	1059
12640	1224	1591	1104	24	1138	1068
13125	1216	1527	1166	16	1173	1053
13615	1193	1520	1261	27	1244	1069
14145	1189	1454	1270	26	1284	1069
14805	1168	1422	1377	19	1346	1090
15345	1226	1353	1491	18	1386	1084
16065	1157	1256	1447	28	1358	1070
16495	1121	1243	1445	27	1354	1068
16980	1088	1203	1456	18	1367	1055
17685	1070	1163	1522	14	1393	1080
18185	1089	1134	1522	14	1440	1059
18685	1056	1151	1560	8	1414	1052
19365	1068	1131	1629	4	1473	1066
20095	1040	1076	1599	7	1432	1056
20815	1035	1065	1548	10	1384	1041
21545	1041	1041	1520	15	1363	1034
22055	1042	1048	1524	25	1366	1030
22725	1036	1036	1496	78	1344	1016



23495	1022	1025	1427	172	1304	1022
24415	1036	1057	1450	327	1343	1037
25135	1007	1015	1372	468	1292	1022
26135	1021	1015	1330	620	1251	1027
27065	1009	1019	1303	797	1246	1054
27775	990	1010	1340	839	1273	1056
28725	1035	1096	1293	1056	1314	1059
28813	1083	1089	1304	1058	1342	1059
28818	1081	1110	1328	1049	1370	25
28823	1080	1079	1309	968	1331	25
28828	1043	1066	1294	968	1325	25
28833	1069	1064	1294	977	1366	25
28838	1057	1054	1290	971	1366	25
28849	1052	1062	1275	990	1316	25
28873	1015	1022	1271	1007	1314	25
28928	784	863	1200	997	1244	25
29000	543	676	1138	993	1196	25
29255	110	151	766	920	815	15
29455	55	63	621	954	720	12
29705	29	38	482	909	526	16
29980	39	33	378	870	486	18
30235	35	24	329	863	433	19
30450	37	28	324	843	452	17
30790	40	24	309	811	392	22
31115	33	19	238	792	390	17
31390	32	16	189	722	313	22
31640	33	19	176	672	286	21
31900	34	18	155	646	259	21
32125	30	21	144	615	242	30
32640	33	16	135	560	223	20
33100	38	18	131	550	217	20
33585	44	28	150	500	200	18
34120	44	21	106	462	189	27
34815	21	39	103	417	153	20
35455	18	17	95	395	122	9
36390	28	16	90	356	121	9
37115	20	16	82	355	112	27
37855	19	37	58	327	113	26
38610	22	23	70	315	93	14
40305	22	11	46	286	77	18
41945	11	16	39	269	66	20
43855	9	11	34	259	57	10
46000	17	17	32	233	53	12
47025	10	9	30	213	46	16
48915	10	11	23	207	39	15
51295	12	17	23	199	36	19
55165	24	16	25	198	33	13
56915	12	16	21	186	29	22

Appendix C-9, Data: Effluent pH data during sorption/leaching study.

pH	Column 1	Column 5	Column 6	Column 7	Column 8
Cumulative effluent flow (cm)	MC10	GF10	GF25	GFS25	GFH25
80	8.99	8.15	8.50	10.88	8.50
115	8.07	7.70	8.35	10.56	8.42
175	7.45	7.54	7.60	10.54	7.81
265	7.68	7.73	7.58	10.55	7.65
415	7.99	7.50	7.49	10.47	7.80
665	7.61	7.62	7.67	10.48	7.99
925	7.54	7.77	7.60	10.50	7.63
1165	7.46	7.44	7.56	9.97	7.61
1955	7.53	7.54	7.44	10.11	7.46
2405	7.41	7.39	7.64	9.89	7.47
2645	7.24	7.09	7.11	9.70	7.23
2875	7.10	7.09	7.05	9.79	6.85
3125	7.23	7.14	7.33	9.53	7.26
3605	7.01	7.12	7.14	9.33	7.03
3815	6.87	7.06	7.02	9.59	6.81
4355	6.78	7.00	7.10	9.60	6.72
4615	6.77	7.03	7.03	9.47	6.86
5075	7.17	7.19	7.25	9.38	7.01
6085	6.75	6.98	6.94	8.95	6.69
6285	6.60	6.68	6.96	9.03	6.91
6435	6.62	6.72	6.92	9.13	6.87
6735	6.30	6.62	6.88	9.26	6.72
7205	6.33	6.70	6.97	8.78	6.88
8100	6.24	6.72	7.03	7.75	6.99
8435	6.11	6.65	6.93	7.70	6.83
8635	5.97	6.54	6.84	7.67	6.74
8855	5.95	6.52	6.88	7.72	6.75
9105	5.91	6.51	6.86	7.95	6.79
9345	6.04	6.52	6.98	7.66	6.80
9775	5.91	6.47	6.98	7.62	6.71
10105	5.94	6.45	6.98	7.51	6.73
10485	5.87	6.33	6.80	7.93	6.72
10830	5.84	6.24	6.78	7.85	6.63
11735	5.75	6.08	6.75	7.54	6.58
12225	5.81	6.08	6.70	7.55	6.53
12640	5.87	6.15	6.87	7.49	6.59
13125	5.82	6.02	6.78	7.45	6.50
13615	5.79	6.00	6.71	7.37	6.37
14805	5.81	5.86	6.54	7.52	6.30
15345	5.79	5.85	6.39	7.35	6.25
16065	5.75	5.76	6.48	7.37	6.06
16980	5.79	5.74	6.58	7.33	6.14
17685	5.71	5.66	6.18	7.28	5.85
18685	5.74	5.66	6.08	7.13	5.84

19365	5.76	5.66	6.08	7.14	5.91
20095	5.73	5.63	6.05	7.12	5.74
21545	5.71	5.62	6.04	7.07	5.62
22055	5.66	5.57	5.89	7.05	5.51
22725	5.66	5.57	5.80	7.07	5.68
24415	5.66	5.59	5.85	7.06	5.50
26135	5.66	5.62	5.79	6.80	5.44
27775	5.71	5.57	5.78	6.85	5.54
28725	5.67	5.61	5.82	6.83	5.56
29000	5.42	5.52	5.60	6.78	5.52
29255	5.73	5.63	5.75	6.83	5.66
29455	5.79	5.65	5.78	6.87	5.64
29705	5.80	5.63	5.65	6.85	5.53
30235	5.97	5.76	5.72	6.83	5.34
30450	5.94	5.78	5.76	6.86	5.31
30790	5.90	5.73	5.71	6.87	5.48
31115	5.96	5.77	5.74	6.79	5.50
31390	6.09	5.84	5.76	6.81	5.48
31640	5.94	5.79	5.73	6.77	5.38
31900	5.93	5.77	5.76	6.73	5.32
32125	6.13	5.87	5.83	6.78	5.39
32640	5.80	5.97	5.76	6.72	5.40
33100	5.96	5.87	5.83	6.82	5.48
33585	6.04	5.93	5.84	6.86	5.50
34120	6.06	5.89	5.87	6.70	5.35
34815	6.05	5.92	5.85	6.65	5.47
35455	6.04	5.96	5.89	6.70	5.64
37115	6.01	5.93	5.88	6.71	5.79
37855	5.97	5.89	5.89	6.74	5.60
38610	5.87	5.89	5.81	6.60	5.64
39515	5.98	5.93	5.93	6.64	5.73
40305	5.91	6.00	5.89	6.58	5.63
41945	5.96	5.91	5.85	6.64	5.68
43855	5.93	5.91	5.84	6.59	5.66
46000	6.00	6.01	5.87	6.69	5.77
47025	6.00	6.02	5.88	6.62	5.75
48915	5.90	5.99	5.89	6.69	5.69
51295	6.01	6.01	5.80	6.55	5.80
55165	6.02	6.00	5.79	6.59	5.78
56915	6.10	6.03	5.74	6.52	5.80

Appendix C-10, Data: Effluent initial total Pb data during sorption/leaching study.  
(Figure 6-8)

Flow	MC10	GF10	GF25	GFS25	GFH25
Cm	Pb Conc. (ppb)	Pb Conc. (ppb)	Pb Conc. (ppb)	Pb Conc. (ppb)	Pb Conc. (ppb)
15	35.4	20.4	17.6	2.7	17.6
80	3.1	1.3	2.0	1.0	2.4
175	2.9	2.5	13.8	1.9	2.6
415	2.9	2.4	2.3	1.5	2.6
925	6.0	4.7	2.8	2.4	6.0
2405	1.9	1.6	1.8	0.5	1.6
3125	2.9	2.6	2.1	0.7	0.4
3605	0.6	0.7	0.4	0.7	1.5
5075	1.7	1.5	0.3	0.1	0.5

Appendix C-11, Data: Effluent initial total Cu data during sorption/leaching study.  
(Figure 6-8)

flow	Column 1	Column 5	Column 6	Column 7	Column 8
cm	Cu Conc. (ppb)	Cu Conc. (ppb)	Cu Conc. (ppb)	Cu Conc. (ppb)	Cu Conc. (ppb)
15	260.8	99.3	130.3	177.4	186.6
80	21.4	8.1	13.3	9.9	19.6
175	9.1	8.2	14.3	11.7	10.4
415	8.5	6.4	9.4	8.9	9.1
925	8.4	6.3	10.5	8.6	8.5
2405	5.1	3.4	3.8	7.5	4.5
3125	3.4	2.6	2.3	3.0	2.6
3605	3.3	5.2	1.7	1.9	2.4
5075	2.5	2.1	1.9	2.3	3.0

Appendix C-12, Data: Effluent initial total Zn data during sorption/leaching study.  
(Figure 6-8)

Flow	Column 1	Column 5	Column 6	Column 7	Column 8
Cm	Zn Conc. (ppb)	Zn Conc. (ppb)	Zn Conc. (ppb)	Zn Conc. (ppb)	Zn Conc. (ppb)
15	989	185	380	157	392
80	293	200	350	168	204
175	94	124	135	105	125
415	74	29	80	110	70
925	74	26	73	118	56
2405	280	183	90	136	157
3125	254	94	111	136	136
3605	516	86	182	155	123
5075	1231	233	60	100	30

Appendix C-13, Data: Effluent Turbidity during sorption/leaching study. (Figure 6-9)

Flow	MC10	GF10	GF25	GFS25	GFH25
cm	Turbidity (NTU)	Turbidity (NTU)	Turbidity (NTU)	Turbidity (NTU)	Turbidity (NTU)
15	177	280	583	45	437
50	54	54	45	12	102
115	18.20	6.05	31.80	4.01	41.80
265	2.37	1.73	3.81	2.28	4.54
415	2.09	1.82	4.54	2.42	4.29
665	2.02	1.72	6.27	2.99	5.88
1165	2.68	6.31	8.82	2.82	9.55
1645	6.2	2.82	4.94	2.46	3.39
2195	5.57	1.48	3.78	2.14	1.97
2645	0.874	2.227	0.337	0.909	0.412
4615	0.612	0.228	0.239	0.445	0.203
7205	0.086	0.13	0.219	0.144	0.114
10485	0.063	0.087	0.112	0.167	0.142
15345	0.110	0.104	0.125	0.133	0.082
21545	0.113	0.107	0.119	0.182	0.137
24415	0.106	0.108	0.128	0.158	0.136

Appendix C-14, Data: Effluent total P data during sorption/leaching study. (Figure 6-10)

	Column 1	Column 5	Column 6	Column 7	Column 8
flow	P (mg/L)	P (mg/L)	P (mg/L)	P (mg/L)	P (mg/L)
cm	MC10	GF10	GF25	GFS25	GFH25
15	78.8	33.0	53.0	1.1	54.0
50	13.5	8.3	19.8	0.5	21.4
80	3.98	2.69	10.9	0.24	12.9
115	2.50	1.92	5.01	0.17	6.53
265	2.44	1.81	4.08	0.14	4.38
415	1.45	1.73	2.70	0.13	2.75
1165	1.39	1.18	1.80	0.10	1.81
2195	1.20	0.77	1.26	0.08	1.28
2875	1.05	0.43	0.65	0.13	0.66
3605	0.64	0.41	0.79	0.14	0.68
5075	0.31	0.39	0.72	0.17	0.65
6285	0.08	0.20	0.50	0.19	0.47
7765	0.05	0.16	0.46	0.23	0.42
9105	0.01	0.07	0.28	0.24	0.27
10830	0.00	0.05	0.24	0.27	0.23
13125	0.00	0.04	0.18	0.23	0.12
18685	0.00	0.03	0.02	0.20	0.05
19195	0.00	0.00	0.00	0.18	0.00
26135	-0.02	0.03	0.05	0.19	0.03

Appendix C-14, Data: Effluent total Cr data during sorption/leaching study. (Figure 6-9)

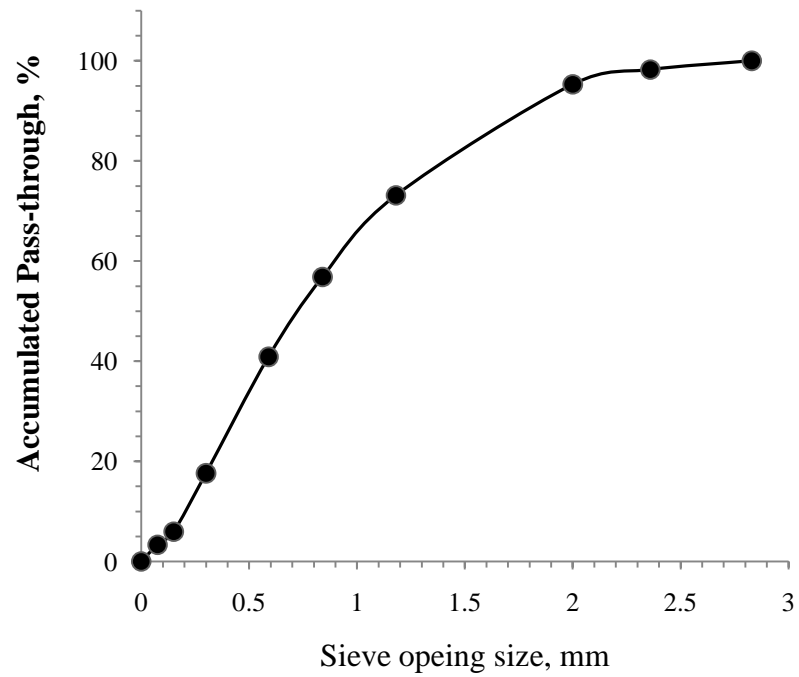
	Column 1	Column 5	Column 6	Column 7	Column 8
flow	Cr Conc. (ppb)	Cr Conc. (ppb)	Cr Conc. (ppb)	Cr Conc. (ppb)	Cr Conc. (ppb)
cm					
15	19.1	18.2	23.9	5.5	20.4
80	3.1	0.4	1.9	2.0	1.7
175	1.0	1.0	1.0	2.3	1.1
415	0.1	0.9	1.0	2.0	1.1
925	0.7	1.4	0.9	2.1	1.0
2405	0.1	0.1	0.7	0.1	0.2
3125	0.0	0.1	0.2	0.7	0.0
3605	0.3	0.0	0.0	0.8	0.0
5075	0.2	0.1	0.0	0.8	0.0
6085	0.1	0.1	0.1	0.5	0.0
6895	0.2	0.1	0.1	0.4	0.1
8855	0.0	0.0	0.1	0.2	0.0
11205	0.1	0.1	0.2	0.4	0.1
13615	0.1	0.0	0.1	0.4	0.2
16495	0.1	0.1	0.2	0.3	0.1
19365	0.1	0.2	0.2	0.1	0.2
22725	0.0	0.1	0.1	0.0	0.1

## Appendix D. Information for Chapter 7.

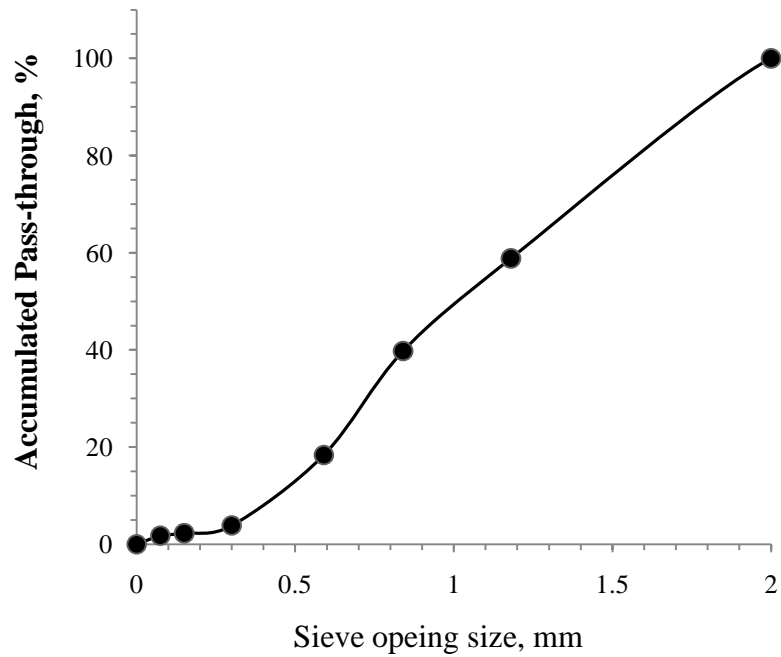
Appendix D1. Sieve analysis for the Grass/food waste compost, Steel slag, and Sand used for the Bench scale study.

Sieve opening size, mm	Accumulated Pass through %		
	Grass/Food waste compost	Steel Slag	Sand
2.83	100	-	-
2.36	98.23	-	-
2.00	95.28	100	-
1.18	73.10	58.84	100
0.84	56.81	39.77	99.11
0.59	40.89	18.36	2.30
0.30	17.60	3.85	0.134
0.15	5.97	2.27	0.012
0.075	3.33	1.76	0.007
0	0	0	0

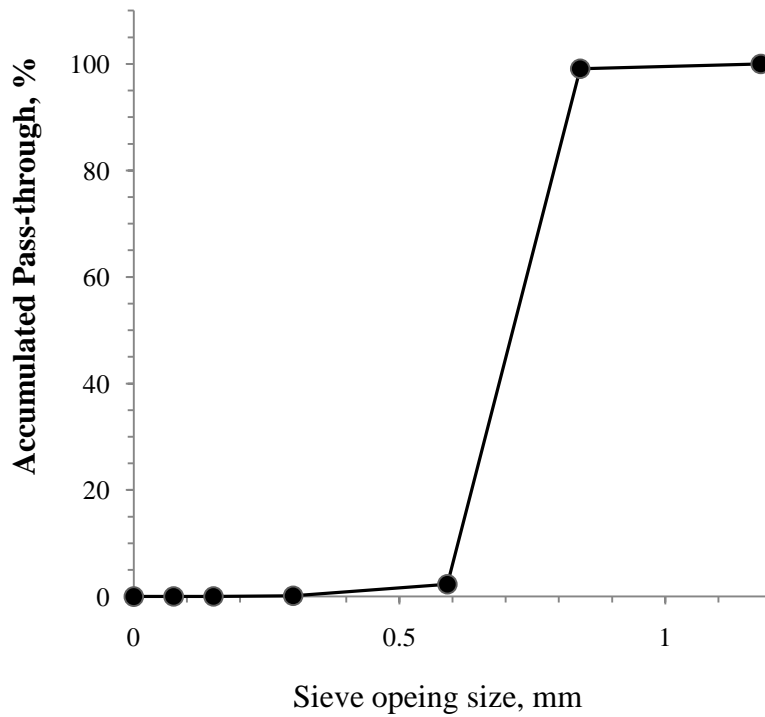
AppendixD2. Sieve analysis graph for the Grass/food waste compost used for the Bench scale study



Appendix D3. Sieve analysis graph for the Steel slag used for the Bench scale study.



AppendixD4. Sieve analysis for the Sand used for the Bench scale study.





Appendix D5. Sand information from the company (US Silica)



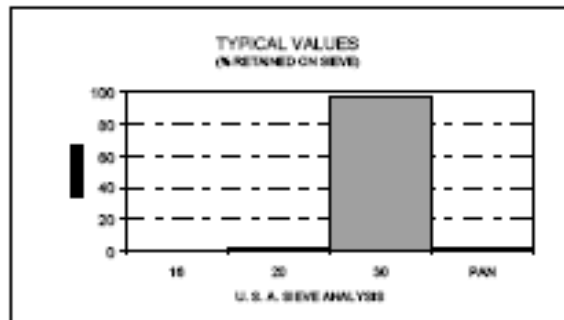
**ASTM<sup>(1)</sup> 20/30**

**UNGROUND SILICA**

**PLANT: OTTAWA, ILLINOIS**

(1) AMERICAN SOCIETY FOR TESTING AND MATERIALS

**PRODUCT DATA**



USA STD SIEVE SIZE		TYPICAL VALUES		
		% RETAINED		% PASSING
MESH	MILLIMETERS	INDIVIDUAL	CUMULATIVE	CUMULATIVE
16	1.180	0.0	0.0	100.0
20	0.850	1.0	1.0	99.0
30	0.600	97.0	98.0	2.0
PAN		2.0	100.0	0.0

**TYPICAL PROPERTIES**

COLOR ..... WHITE      MINERAL ..... QUARTZ  
 GRAIN SHAPE ..... ROUND      pH ..... 7  
 HARDNESS (Mohs) ..... 7      SPECIFIC GRAVITY ..... 2.65  
 MELTING POINT (Degrees F) ..... 3100

**TYPICAL CHEMICAL ANALYSIS, %**

SiO<sub>2</sub> (Silicon Dioxide) ..... 99.8      MgO (Magnesium Oxide) ..... <0.01  
 Fe<sub>2</sub>O<sub>3</sub> (Iron Oxide) ..... 0.020      Na<sub>2</sub>O (Sodium Oxide) ..... <0.01  
 Al<sub>2</sub>O<sub>3</sub> (Aluminum Oxide) ..... 0.06      K<sub>2</sub>O (Potassium Oxide) ..... <0.01  
 TiO<sub>2</sub> (Titanium Dioxide) ..... 0.01      LOI (Loss On Ignition) ..... 0.1  
 CaO (Calcium Oxide) ..... <0.01

**CONFORMS TO ASTM C778**

December 15, 1997

**DISCLAIMER:** The information set forth in this Product Data Sheet represents typical properties of the product described; the information and the typical values are not specifications. U.S. Silica Company makes no representation or warranty concerning the Products, expressed or implied, by this Product Data Sheet.

**WARNING:** The product contains crystalline silica - quartz, which can cause silicosis (an occupational lung disease) and lung cancer. For detailed information on the potential health effect of crystalline silica - quartz, see the U.S. Silica Company Material Safety Data Sheet.

U.S. Silica Company

P.O. Box 187, Berkeley Springs, WV 25411-0187

(304) 258-2500

Appendix D6. Average total metal concentration of the silica sand

Element*	Silica Sand
Al	<215**
B	<12.8
Ba	<2.82
Be	<0.54
Cd	<0.54
Co	<0.33
Cr	<1.31
Cu	<10.1
Fe	<126
Mg	<1693
Mn	<3.95
Mo	<1.69
Ni	<2.63
Pb	<16.4
V	<1.27
Zn	<5.48

\* Analyzed by Environmental management and by-product utilization laboratory in USDA ARS

\*\* <, less than the limit of quantitation

## Appendix D7. Stainless screen information

(Source: [http://www.twpinc.com/twpinc/control/product/~category\\_id=TWPCAT\\_12/~product\\_id=040X040T0100W36T](http://www.twpinc.com/twpinc/control/product/~category_id=TWPCAT_12/~product_id=040X040T0100W36T))

 <b>TWP</b> PRODUCT DATA SHEET		TWP Inc 2831 Tenth St. Berkeley, CA 94710 USA phone 510-548-4434 800-227-1570 fax 510-548-3073 website <a href="http://www.twpinc.com">www.twpinc.com</a>	
<b>40 Mesh T316 Stainless .010" Wire Dia. 36 Inch Wide</b>			
	<b>Name:</b> 40 Mesh T316 Stainless .010" Wire Dia. 36 Inch Wide		
	<b>Part Number:</b> 040X040T0100W36T		
	<b>Material:</b> Stainless Steel		
<b>Mesh:</b> 40 x 40 per Inch (per 2.54 cm)		<b>Wire Diameter:</b> 0.0100 Inch Wire Diameter: 0.2540 mm	
<b>Opening Size:</b> 0.0150 Inch 0.38 mm 381 microns		<b>Open Area Percentage:</b> 36 %	
<b>Overall Thickness:</b> 0.020 Inch 0.5080 mm		<b>Weight per Square Foot:</b> 0.28 pounds <b>Weight per Sq. Meter:</b> 1.37 Kg.	
<b>Full Roll Length:</b> 100 feet 30.49 meters		<b>Standard Widths:</b> 36 or 48 Inches	
<b>Weave Type:</b> PSW		<b>Finish (Coating):</b> Mill Finish	
<b>Common Name:</b> 40 Mesh T316 Stainless .010		<b>Link to Product Page:</b> <a href="#">Click Here</a>	
<b>Purchasing Units of Measure:</b> Full rolls or by the square foot.			
<b>Typical Uses:</b>			
<b>Comments:</b>			
YOUR ONE SOURCE FOR MESH MATERIALS AND PRECISION CUTTING TWP Inc. is a California corporation, founded in 1969, with its principal office at 2831 Tenth Street, Berkeley, California.			

### Specification

Part Number	Mesh / Inch	Wire Dia. Inches	Opening Inches	% Open	Roll Width Inches	Weight / SFT
040X040T0100W36T	40	0.0100	0.015	36	36	0.28

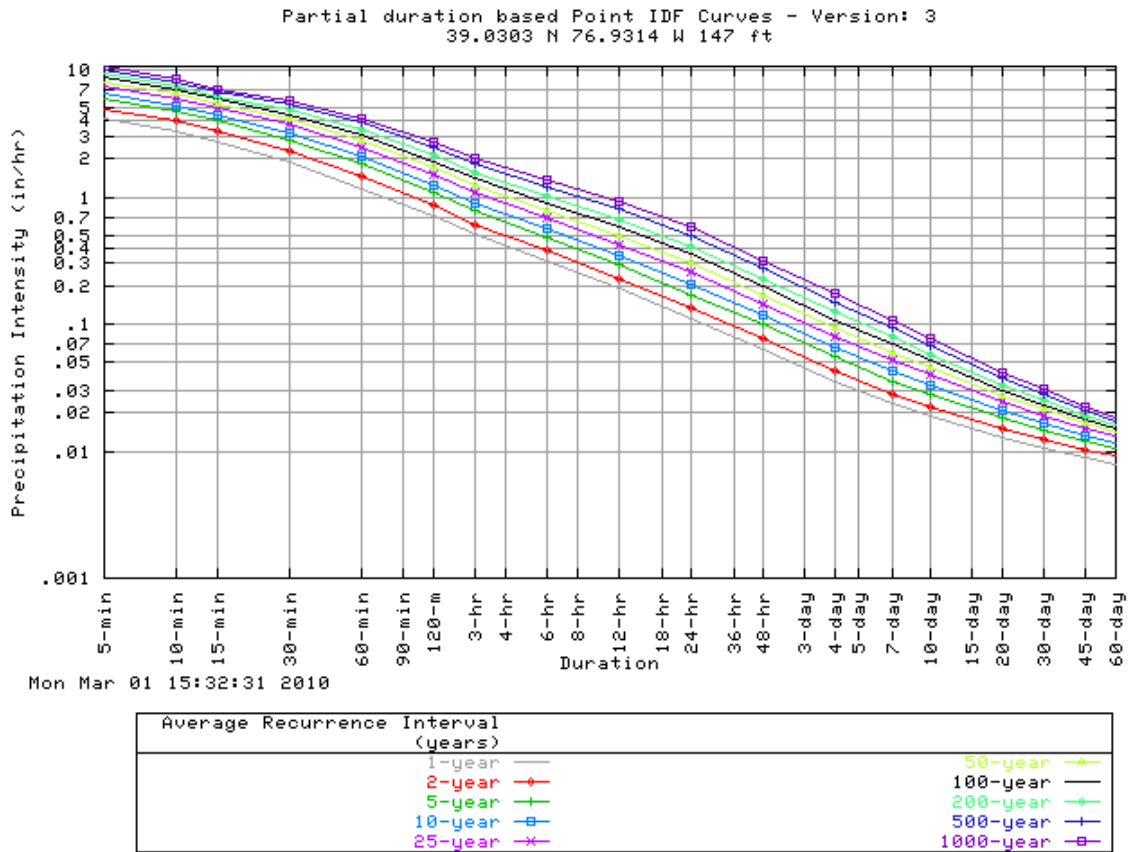
### Metric Specification

Part Number	Mesh / 2.54 cm	Wire Dia. mm	Opening mm	Opening microns	% Open	Roll Width cm
040X040T0100W36T	40	0.2540	0.38	381	36	36

### Pricing

<u>1 - 24 SFT</u>	<u>25 - 99 SFT</u>	<u>100 or More SFT</u>	<u>Swatch</u>	<u>Full Roll</u>
\$6.50	\$4.94	\$4.36	\$8.00	\$562.00

# Appendix D-8. Partial duration based point IDF curves for Beltsville, MD



# Appendix D-9-1. Data for Experiment 1 (Figure 7-6a):

\*Appendix D-9-1 to Appendix D-18-3: Any values below instrumentation detection limit (Pb = 5 µg/L, Cu = 2 µg/L, and Zn = 25 µg/L) were used for plotting the figures only. A half of detection limit (e.g. 2.5 µg/L for any value less than the Pb detection limit) was instead used for data analysis for any Pb concentration less than Pb detection limit.

Time (min)	Effluent Dissolved Pb	Time (min)	Effluent Total Pb	Time (min)	Influent Dissolved Pb	Influent Total Pb	Time from start (min)	Turbidity	Time from start (min)	Influent water head
minutes	mg/L	minutes	mg/L	minutes	mg/L	mg/L	minutes	NTU	minutes	cm
0		60	0.761	0	6.335	10.01	0		0	0
30	0.122	90	0.752	60	6.443	9.896	30	17.9	2	8.7
60	0.070	120	0.782	120	6.352	10.24	60	9.82	30	8.7
75	0.064	180	0.556	180	6.395	10.30	75	10.6	60	8.7
90	0.058	240	0.439	240	6.295	10.13	90	9.93	63	8.7
105	0.060						105	13.4	65	13.7
120	0.055						120	11.2	75	13.5
150	0.039						150	9.88	90	13.5
180	0.027						180	6.87	92	13.5
210	0.024						210	5.94	95	18.7
240	0.022						240	5.14	105	18.6
270	0.011						270		120	18.7
									122	18.6
									140	3.7
									150	3.7
									180	3.7
									210	3.6
									240	3.2
									270	0.6

Appendix D-9-2. Data for Experiment 1 (Figure 7-6b)

Time (min)	Effluent Dissolved Cu	Time (min)	Effluent Total Cu	Time (min)	Influent Dissolved Cu	Influent Total Cu	Time from start (min)	Effluent Dissolved P	Time from start (min)	Flow rate	Time from start (min)	Effluent Total P
minutes	mg/L	minutes	mg/L	minutes	mg/L	mg/L		mg/L		mL/min /cm		mg/L
0		60	0.015	0	0.949	1.009	0		0	0	0	
30	0.014	90	0.019	60	0.943	1.008	30	0.960	2	15.07	60	0.56
60	0.006	120	0.022	120	0.947	1.003	60	0.540	30	15.07	90	0.69
75	0.013	180	0.013	180	0.944	1.001	75	0.524	60	15.01	120	1.00
90	0.010	240	0.011	240	0.944	1.006	90	0.588	63	15.01	210	0.60
105	0.021						105	1.018	65	32.69	240	0.54
120	0.013						120	0.980	75	32.69		
150	0.007						150	0.629	90	32.07		
180	0.006						180	0.621	92	32.07		
210	0.005						210	0.580	95	59.81		
240	0.006						240	0.524	105	59.81		
270	0.004						270	0.475	120	61.56		
									122	61.56		
									140	6.91		
									150	6.69		
									180	6.11		
									210	5.80		
									240	5.58		
									270	1.85		

Appendix D-9-3. Data for Experiment 1 (Figure 7-6c)

Time from start (min)	Effluent Dissolved Zn	Time (min)	Effluent Total Zn	Time (min)	Influent Dissolved Zn	Influent Total Zn	Time from start (min)	Effluent pH
minutes	mg/L	minutes	mg/L	minutes	mg/L	mg/L	minutes	pH
0		60	0.116	0	1.026	1.029	0	
30	0.014	90	0.120	60	1.02	1.028	30	10.22
60	0.007	120	0.151	120	1.025	1.023	60	9.99
75	0.010	180	0.122	180	1.035	1.043	75	9.78
90	0.005	240	0.080	240	1.039	1.041	90	9.73
105	0.020						105	9.72
120	0.022						120	9.74
150	0.021						150	9.66
180	0.009						180	9.72
210	0.009						210	9.71
240	0.015						240	9.71
270	0.013						270	

Appendix D-10-1. Data for Experiment 2 (Figure 7-7a)

Time (min)	Effluent Dissolved Pb	Time (min)	Effluent Total Pb	Time (min)	Influent Dissolved Pb	Influent Total Pb	Time from start (min)	Turbidity	Time from start (min)	Influent water head (cm)
minutes	mg/L	minutes	mg/L	minutes	mg/L	mg/L	minutes	NTU	minutes	cm
5	0.0159	5	0.8067	0	6.427	10.64	5	17.4	0	0
30	0.08093	60	1.04	60	6.26	10.57	30	9.06	2	8.73
60	0.07971	90	1.045	120	6.302	10.41	60	8.54	30	8.73
75	0.0812	120	1.109	180	6.314	10.52	75	10.7	60	8.83
90	0.07067	150	1.137				90	9.98	63	8.83
105	0.07883	180	1.113				105	15.9	65	13.73
120	0.07058						120	12.5	75	13.73
135	0.07213						135	11.9	90	13.73
150	0.07359						150	11.2	93	13.73
165	0.07199						165	11.3	96	18.73
180	0.05665						180	10.8	105	18.73
200	0.05335						200	10.6	120	18.83
210	0.05615								122	18.73
									127	8.73
									135	8.73
									150	8.73
									152	8.73
									165	3.73
									180	3.73
									200	3.23
									210	1.73



Appendix D-10-2. Data for Experiment 2 (Figure 7-7b)

Time (min)	Effluent Dissolved Cu	Time (min)	Effluent Total Cu	Time (min)	Influent Dissolved Cu	Influent Total Cu	Time from start (min)	Effluent Dissolved P	Time from start (min)	Effluent flow rate	Time from start (min)	Effluent Total P
minutes	mg/L	minutes	mg/L	minutes	mg/L	mg/L	minute	mg/L	minutes	mL/min/s	minutes	mg/L
5	0.0126	5	0.1342	0	0.9696	1.022	5	0.723	0	0	5	1.11422
30	0.00381	60	0.01675	60	0.9658	1.027	30	0.544	2	16.2228	60	0.18346
60	0.00851	90	0.01408	120	0.972	1.034	60	0.157	30	16.2228	90	0.316
75	0.00569	120	0.01651	180	0.9704	1.007	75	0.234	60	17.07566	120	0.541
90	0.005	150	0.01344				90	0.283	63	17.07566	150	0.498
105	0.01057	180	0.01301				105	0.521	65	31.71403	180	0.434
120	0.00748						120	0.507	75	31.71403	210	0.7291
135	0.00591						135	0.458	90	31.58028		
150	0.00499						150	0.472	93	31.58028		
165	0.00396						165	0.409	96	57.84616		
180	0.00402						180	0.409	105	57.84616		
200	0.00374						200	0.374	120	59.20944		
210	0.00387						210	0.374	122	59.20944		
									127	20.63043		
									135	20.63043		
									150	20.26572		
									152	20.26572		
									165	6.81354		
									180	6.42834		
									200	4.63873		
									210	1.57737		

Appendix D-10-3. Data for Experiment 2 (Figure 7-7c)

Time from start (min)	Effluent Dissolved Zn	Time (min)	Effluent Total Zn	Time (min)	Influent Dissolved Zn	Influent Total Zn	Time from start (min)	Effluent pH
minutes	mg/L	minutes	mg/L	minutes	mg/L	mg/L	minutes	pH
5	0.004	5	0.085	0	1.028	1.031	5	9.37
30	0.002	60	0.136	60	1.025	1.031	30	9.57
60	0.002	90	0.089	120	1.03	1.024	60	9.59
75	0.009	120	0.116	180	1.022	1.014	75	9.45
90	0.005	150	0.119				90	9.48
105	0.006	180	0.116				105	9.36
120	0.005						120	9.34
135	0.009						135	9.32
150	0.000						150	9.38
165	0.002						165	9.41
180	0.001						180	9.43
200	0.000						200	9.39
210	0.001							

Appendix D-11-1 Data for Experiment 3 (Figure 7-8a)

Time (minutes)	Effluent Dissolved Pb	Time (min)	Effluent Total Pb	Time (min)	Influent Total Pb	Time from start (min)	Turbidity	Time from start (min)	Influent water head
minutes	mg/L	minutes	mg/L	minutes	mg/L	minutes	NTU	minutes	cm
1	0.005	0.5	0.083	0	10.09	1	18.7	0	0
15	0.004	30	0.068	30	10.03	15	6.28	2	4.73
30	0.002	60	0.026	60	10.18	30	3.34	15	4.93
45	0.001	90	0.016	90	10.11	45	2.2	30	4.73
60	0.001	120	0.015	120	10.13	60	1.58	31	4.73
75	0.001	160.5	0.026			75	1.98	33	8.73
90	0.001					90	1.35	45	8.73
105	0.005					105	2.9	60	8.73
120	0.003					120	1.85	61	8.73
134	0.003					134	1.42	63	13.73
141	0.001					141	1.61	75	13.73
147	0.001					147	2.22	90	13.63
161	0.001					161	2.49	91	13.63
								93	18.73
								105	18.83
								120	18.73
								134	18.93
								140.5	8.73
								147.1667	3.73
								160.5	1.73

Appendix D-11-2 Data for Experiment 2 (Figure 7-8b)

Time (min)	Effluent Dissolve d Cu	Time (min)	Effluent Total Cu	Time (min)	Influent Total Cu	Time from start (min)	Effluent Dissolve d P	Time from start (min)	Effluent flow rate	Time from start (min)	Effluent Total P
minutes	mg/L	minutes	mg/L	minutes	mg/L	minutes	mg/L	minutes	mg/L	minutes	mg/L
0.5	0.003	0.5	0.006	0	1.002	0.5	1.217	1	4.95	0.5	1.260
15	0.006	30	0.010	30	1.000	15	0.192	2	6.26	30	0.281
30	0.002	60	0.004	60	0.997	30	0.178	15	6.57	60	0.184
45	0.002	90	0.004	90	0.996	45	0.135	30	6.26	90	0.214
60	0.002	120	0.007	120	0.998	60	0.142	31	6.26	120	0.302
75	0.004	160.5	0.006			75	0.199	33	13.57	140.5	0.245
90	0.002					90	0.185	45	13.57		
105	0.008					105	0.284	60	14.14		
120	0.005					120	0.255	61	14.14		
134	0.004					134	0.255	63	31.10		
140.5	0.003					140.5	0.241	75	31.10		
147.2	0.002					147.2	0.227	90	31.75		
160.5	0.002					160.5	0.199	91	31.75		
								93	61.10		
								105	61.10		
								120	59.35		
								134	62.53		
								147	9.26		
								161	2.45		

Appendix D-11-3 Data for Experiment 3 (Figure 7-8b)

Time from start (min)	Effluent Dissolved Zn	Time (min)	Effluent Total Zn	Time (min)	Influent Total Zn	Time from start (min)	Effluent pH
minutes	mg/L	minutes	mg/L	minutes	mg/L	minutes	pH
1	0.013	0.5	0.110	0	1.047	0.5	9.07
15	0.004	30	0.094	30	1.032	15	9.39
30	0.007	60	0.121	60	1.044	30	9.41
45	0.002	90	0.086	90	1.045	45	9.37
60	0.006	120	0.103	120	1.06	60	9.38
75	0.004	160.5	0.116			75	9.22
90	0.003					90	9.32
105	0.003					105	9.18
120	0.006					120	9.29
134	0.004					134	9.25
141	0.009					141	9.37
147	0.000					147	9.37
161	0.002					160.5	9.18

Appendix D-12-1 Data for Experiment 4 (Figure 7-9a)

Time (minutes)	Effluent Dissolved Pb	Time (min)	Effluent Total Pb	Time (min)	Influent Total Pb	Time from start (min)	Turbidity	Time from start (min)	Influent water head
minutes	mg/L	minutes	mg/L	minutes	mg/L	minutes	NTU	minutes	cm
0.5	0.002	0.5	0.029	0	9.865	1	9.30	0	0
15	0.001	30	0.017	30	9.886	15	2.09	1	4.73
30	0.001	60	0.012	60	9.952	30	1.02	15	4.83
45	0.001	90	0.010	90	9.948	45	0.85	30	4.73
60	0.001	120	0.018	120	9.8	60	0.64	31	4.73
75	0.002	155	0.016			75	1.07	32	8.73
90	0.002					90	0.91	45	8.73
105	0.007					105	1.98	60	8.73
120	0.008					120	1.33	61	8.73
129.1	0.005					129.1	1.19	63	13.73
134.6	0.002					134.6	1.40	75	13.73
140.6	0.001					140.6	1.91	90	13.83
155.1	0.001					155.1	2.02	91	13.83
								93	18.73
								105	18.73
								120	18.73
								129.1	18.83
								131.1	13.73
								134.6	8.73
								140.6	4.43
								155.1	1.73

Appendix D-12-2 Data for Experiment 4 (Figure 7-9b)

Time (min)	Effluent Dissolve d Cu	Time (min)	Effluent Total Cu	Time (min)	Influent Total Cu	Time from start (min)	Effluent Dissolve d P	Time from start (min)	Effluent flow rate	Time from start (min)	Effluent Total P
minutes	mg/L	minutes	mg/L	minutes	mg/L	minutes	mg/L	minutes	mL/min/cm	minutes	mg/L
0.5	0.002	0.5	0.008	0	0.942	0.5	0.369	0	0	0	0.60
15	0.002	30	0.006	30	0.950	15	0.255	1	7.58	30	0.23
30	0.000	60	0.003	60	0.947	30	0.199	15	7.69	60	0.15
45	0.000	90	0.013	90	0.950	45	0.156	30	7.58	90	0.22
60	0.000	120	0.006	120	0.941	60	0.142	31	7.58	120	0.26
75	0.001	155.1	0.004			75	0.213	32	15.82	134.6	0.23
90	0.001					90	0.199	45	15.82	--	--
105	0.004					105	0.248	60	16.14	--	--
120	0.004					120	0.227	61	16.14	--	--
129.1	0.003					129.1	0.234	63	32.15	--	--
134.6	0.001					134.6	0.220	75	32.15	--	--
140.6	0.000					140.6	0.255	90	33.42		
155.1	0.000					155.1	0.213	91	33.42		
								93	62.54		
								105	62.54		
								120	62.37		
								129.1	63.89		
								140.6	9.09		
								155.1	2.48		

Appendix D-12-3 Data for Experiment 4 (Figure 7-9c)

Time from start (min)	Effluent Dissolved Zn	Time (min)	Effluent Total Zn	Time (min)	Influent Total Zn	Time from start (min)	Effluent pH
minutes	mg/L	minutes	mg/L	minutes	mg/L	minutes	pH
1	0.001	0.5	0.097	0	1.05	0.5	9.05
15	0.003	30	0.112	30	1.07	15	9.30
30	0.001	60	0.118	60	1.07	30	9.37
45	0.000	90	0.108	90	1.05	45	9.37
60	0.004	120	0.192	120	1.07	60	9.37
75	0.002	155.1	0.154			75	9.19
90	0.006					90	9.27
105	0.008					105	9.18
120	0.003					120	9.20
129.1	0.008					129.1	9.21
134.6	0.003					134.6	9.16
140.6	0.005					140.6	9.32
155.1	0.001					155.1	9.14



Appendix D-13-1 Data for Experiment 5 (Figure 7-10a)

Time (minutes)	Effluent Dissolved Pb	Time (min)	Effluent Total Pb	Time (min)	Influent Total Pb	Time from start (min)	Turbidity	Time from start (min)	Influent water head
minutes	$\mu\text{g/L}$	minutes	$\mu\text{g/L}$	minutes	$\mu\text{g/L}$	minutes	NTU	minutes	cm
5	11.9	0.5	288	0	0.8	0.5	17.4	0	0
15	5.9	30	55	30	0.8	15	4.55	1	4.73
30	4.1	60	25	60	0.6	30	3.03	15	5.03
45	3.5	90	14	90	0.9	45	2.65	30	4.63
60	2.8	120	9	120	1.0	60	2.08	31	4.63
75	2.8					75	2.66	32	8.73
90	1.7					90	2.03	45	8.73
105	1.7					105	2.91	60	8.73
120	1.3					120	1.96	61	8.73
134	1.6					134	1.84	62	13.73
137.1	1.2					137.1	1.58	75	13.73
140.8	1.5					140.8	1.93	90	13.73
147.7	2.4					147.7	3.08	91	13.73
161.5	2.7					161.5	3.24	92	18.73
								105	18.83
								120	18.53
								134	18.73
								137.1	13.73
								140.8	8.73
								147.7	4.73
								161.5	1.73

Appendix D-13-2Data for Experiment 5(Figure 7-10b)

Time (min)	Effluent Dissolved Cu	Time (min)	Effluent Total Cu	Time (min)	Influent Total Cu	Time from start (min)	Effluent flow rate	Time from start (min)	Effluent Total P
minutes	$\mu\text{g/L}$	minutes	$\mu\text{g/L}$	minutes	$\mu\text{g/L}$	minutes	mL/min/cm	minutes	mg/L
0.5	5.3	0.5	37	1	0.2	0.5	0	1	0.97
15	2.6	30	12	30	0.2	1	5.83	30	0.34
30	1.4	60	8	60	0.1	15	5.83	60	0.31
45	1.9	90	6	90	0.2	30	5.40	90	0.39
60	0.8	120	6	120	0.0	31	5.40	120	0.39
75	1.5					32	12.34	161.5	0.45
90	0.8					45	12.34		
105	0.7					60	12.67		
120	0.2					61	12.67		
134	0.2					62	30.64		
137.1	0.2					75	30.64		
140.8	0.4					90	30.60		
147.7	1.1					91	30.60		
161.5	1.4					92	64.93		
						105	64.93		
						120	60.98		
						134	65.37		
						147.7	9.09		
						161.5	2.42		

Appendix D-13-3Data for Experiment 5(Figure 7-10c)

Time from start (min)	Effluent Dissolved Zn	Time (min)	Effluent Total Zn	Time (min)	Influent Total Zn	Time from start (min)	Effluent pH
minutes	$\mu\text{g/L}$	minutes	$\mu\text{g/L}$	minutes	$\mu\text{g/L}$	minutes	pH
0.5	4	0.5	53	0	1	0.5	8.80
15	9	30	20	30	1	15	9.07
30	4	60	33	60	0	30	9.20
45	7	90	27	90	1	45	9.08
60	6	120	41	120	1	60	9.18
75	16					75	8.99
90	6					90	9.11
105	8					105	9.01
120	29					120	9.04
134	11					134	9.07
137.1	11					137.1	9.01
140.8	9					140.8	9.09
147.7	6					147.7	9.06
161.5	3						

Appendix D-14-1 Data for Experiment 7(Figure 7-11a)

Time (minutes)	Effluent Dissolved Pb	Time (min)	Effluent Total Pb	Time (min)	Influent Total Pb	Time from start (min)	Turbidity	Time from start (min)	Influent water head
minutes	$\mu\text{g/L}$	minutes	$\mu\text{g/L}$	minutes	mg/L	minutes	NTU	minutes	cm
0.5	12.0	0.5	233.0	0.5	10.0	0.5	13.70	0	0
15	2.4	30	44.9	30	10.0	15	5.32	1	4.73
30	1.7	60	16.8	60	10.0	30	3.36	15	4.73
45	6.7	90	102.2	90	10.1	45	1.86	30	4.93
60	8.4	104	228.0	97.5	10.1	60	1.65	31	4.63
75	58.7					75	1.26	32	8.73
90	66.8					90	0.94	45	8.73
97.5	165.8					97.5	1.16	60	8.73
104	189.6					104	0.91	61	8.73
109	30.1					109	1.38	62	13.73
								75	13.73
								90	13.73
								91	18.73
								92	18.73
								98	18.73
								104	18.83
								109	4.73

Appendix D-14-2 Data for Experiment 7(Figure 7-11b)

Time (min)	Effluent Dissolved Cu	Time (min)	Effluent Total Cu	Time (min)	Influent Total Cu	Time from start (min)	Effluent flow rate	Time from start (min)	Effluent Total P
minutes	$\mu\text{g/L}$	minutes	$\mu\text{g/L}$	minutes	mg/L	minutes	mL/min/cm	minutes	mg/L
0.5	21.2	0.5	33.4	0.5	1.012	0	0.0	0.5	1.30
15	12.6	30	13.9	30	1.013	1	7.3	30	0.43
30	9.2	60	10.9	60	1.025	15	7.3	60	0.37
45	8.0	90	17.1	90	1.02	30	7.5	90	0.32
60	7.0	104	33.5	104	1.042	31	7.5	104	0.28
75	13.7					32	24.0		
90	12.4					45	24.0		
97.5	30.1					60	24.5		
104	32.6					61	24.5		
109	11.2					62	59.7		
						75	59.7		
						90	58.8		
						91	58.8		
						92	114.5		
						98	114.5		
						104	117.4		
						109	12.1		

Appendix D-14-3 Data for Experiment 7 (Figure 7-11c)

Time from start (min)	Effluent Dissolved Zn	Time (min)	Effluent Total Zn	Time (min)	Influent Total Zn	Time from start (min)	Effluent pH
minutes	$\mu\text{g/L}$	minutes	$\mu\text{g/L}$	minutes	mg/L	minutes	pH
0.5	35	0.5	51	0	1.013	0	8.11
15	6	30	21	30	0.994	15	8.36
30	6	60	26	60	1.003	30	8.32
45	1	90	36	90	0.993	45	8.06
60	7	104	72			60	7.83
75	23					75	8.03
90	31					90	7.81
97.5	56					97.5	8.28
104	68					104	8.08
109	18					109	7.82

Appendix D-15-1 Data for Experiment 8(Figure 7-12a)

Time (minutes)	Effluent Dissolved Pb	Time (min)	Effluent Total Pb	Time (min)	Influent Total Pb	Time from start (min)	Turbidity	Time from start (min)	Influent water head
minutes	$\mu\text{g/L}$	minutes	$\mu\text{g/L}$	minutes	mg/L	minutes	NTU	minutes	cm
1	54	1	70	1	9.757	1	2.54	0	0
15	19	30	22	30	9.846	15	0.751	1	4.73
30	22	60	145	60	9.803	30	0.518	15	4.73
45	139	79	289	79	9.833	45	0.274	30	4.73
60	138	84	443			60	0.248	31	4.73
70	265	88	97			70	0.234	32	8.63
79	264					79	0.204	45	8.63
84	428					84	0.194	60	8.63
88	86					88	0.168	61	8.63
								62	13.73
								70	13.73
								79	13.73
								80	18.73
								84	18.73
								85	18.73
								88	4.73
								90	2.73

Appendix D-15-2 Data for Experiment 8(Figure 7-12b)

Time (min)	Effluent Dissolved Cu	Time (min)	Effluent Total Cu	Time (min)	Influent Total Cu	Time from start (min)	Effluent flow rate	Time from start (min)	Effluent Total P
minutes	$\mu\text{g/L}$	minutes	$\mu\text{g/L}$	minutes	$\mu\text{g/L}$	minutes	mL/min/cm	minutes	mg/L
1	40	1	43	0	0.990	0	0.0	1	0.464
15	14	30	12	30	0.981	1	11.1	30	0.266
30	12	60	25	60	0.985	15	11.6	60	0.194
45	23	79	49	79	0.991	30	12.0	79	0.156
60	23	84	76			31	12.0	84	0.184
70	49	88	34			32	38.8		
79	49					45	38.8		
84	72					60	40.7		
88	21					61	40.7		
						62	106.9		
						70	106.9		
						79	109.6		
						80	193.8		
						84	193.8		
						85	193.8		
						88	27.9		
						90	20.6		



Appendix D-15-3 Data for Experiment 8(Figure 7-12c)

Time from start (min)	Effluent Dissolved Zn	Time (min)	Effluent Total Zn	Time (min)	Influent Total Zn	Time from start (min)	Effluent pH	Time from start (min)	Effluent dissolved Cr	Time from start (min)	Effluent total Cr
minutes	$\mu\text{g/L}$	minutes	$\mu\text{g/L}$	minutes	mg/L	minutes	pH	minutes	$\mu\text{g/L}$	minutes	$\mu\text{g/L}$
1	21	1	37	0	0.999	1	8.19	1	1.0	1	1.9
15	4	30	22	30	0.999	15	8.21	15	0.4	30	0.9
30	5	60	50	60	1.004	30	8.09	30	0.2	60	0.5
45	38	79	89	79	1.011	45	7.97	45	0.1	79	0.4
60	42	84	129			60	7.93	60	0.2	84	0.4
70	82	88	49			70	7.88	70	0.2	88	0.3
79	83					79	7.50	79	0.2		
84	124					84	7.59	84	0.1		
88	28					88	7.40	88	0.3		
						90	7.44				

Appendix D-16-1 Data for Experiment 9(Figure 7-13a)

Time (minutes)	Effluent Dissolved Pb	Time (min)	Effluent Total Pb	Time (min)	Influent Total Pb	Time from start (min)	Turbidity	Time from start (min)	Influent water head
minutes	$\mu\text{g/L}$	minutes	$\mu\text{g/L}$	minutes	$\mu\text{g/L}$	minutes	NTU	minutes	cm
0	22	0	33	0	10.15	0	16.4	0	0
5	9	20	7	20	9.97	5	2.89	1	4.73
10	5	40	54	40	10.09	10	1.28	5	4.73
20	4	55	211	55	10.10	20	0.415	10	4.73
30	29	65	549	65	10.10	30	0.485	20	4.73
40	32					40	0.395	21	4.73
50	104					50	0.503	22	8.93
55	169					55	0.358	30	8.93
60	523					60	0.71	40	8.73
65	422					65	0.49	41	8.73
70	77							42	13.73
79	44							50	13.73
								55	13.73
								56	13.73
								57	18.93
								60	18.93
								65	18.73
								70	8.73

Appendix D-16-2 Data for Experiment 9(Figure 7-13b)

Time (min)	Effluent Dissolved Cu	Time (min)	Effluent Total Cu	Time (min)	Influent Total Cu	Time from start (min)	Effluent flow rate	Time from start (min)	Effluent Total P
minutes	$\mu\text{g/L}$	minutes	$\mu\text{g/L}$	minutes	$\mu\text{g/L}$	minutes	mL/min/cm	minutes	mg/L
0	19	0	31	0	1.04	0	0.0	0	1.355
5	20	20	11	20	1.03	1	20.1	20	0.305
10	12	40	12	40	1.03	5	20.1	40	0.236
20	9	55	33	55	1.04	10	21.1	55	0.205
30	11	65	74	65	1.04	20	21.1	65	0.169
40	10					21	21.1		
50	24					22	45.5		
55	28					30	45.5		
60	55					40	43.3		
65	50					41	43.3		
70	21					42	99.0		
79	13					50	99.0		
						55	100.3		
						56	100.3		
						57	188.0		
						60	188.0		
						65	187.7		
						70	55.3		

Appendix D-16-3 Data for Experiment 9(Figure 7-13c)

Time from start (min)	Effluent Dissolved Zn	Time (min)	Effluent Total Zn	Time (min)	Influent Total Zn	Time from start (min)	Effluent pH	Time from start (min)	Effluent dissolved Cr	Time from start (min)	Effluent total Cr
minutes	$\mu\text{g/L}$	minutes	$\mu\text{g/L}$	minutes	mg/L	minutes	pH	minutes	$\mu\text{g/L}$	minutes	$\mu\text{g/L}$
0	21.29	0	27.68	0	1.055	0	7.97	0	0.5	0	0.3
5	3.14	20	15.84	20	1.035	5	8.1	5	0.0	20	0.2
10	2.86	40	27.95	40	1.054	10	8.2	10	0.1	40	0.4
20	2.11	55	47.66	55	1.042	20	8	20	0.1	55	0.6
30	12.62	65	128.52	65	1.038	30	8.02	30	0.1	65	0.2
40	14.39					40	8.05	40	0.0	70	
50	34.19					50	7.94	50	0.0	79	
55	40.56					55	7.82	55	0.0		
60	127.4					60	7.66	60	0.0		
65	108.4					65	7.52	65	0.1		
70	31.89							70	0.1		
79	17.37							79	0.1		

Appendix D-17-1 Data for Experiment 10 (Figure 7-14a)

Time (minutes)	Effluent Dissolved Pb	Time (min)	Effluent Total Pb	Time (min)	Influent Total Pb	Time from start (min)	Turbidity	Time from start (min)	Influent water head
minutes	$\mu\text{g/L}$	minutes	$\mu\text{g/L}$	minutes	$\mu\text{g/L}$	minutes	NTU	minutes	cm
0	19	0	30	0	200	0	6.800	0	0
10	2	20	4	20	198	10	0.655	1	4.73
20	1	40	4	40	199	20	0.403	10	4.73
30	1	55	7	55	199	30	0.325	20	4.73
40	1	61.5	12	61.5	199	40	0.248	20.5	4.73
45	3	65.5	8			45	0.542	21	8.73
55	4					55	0.461	30	8.73
60	11					60	0.507	40	8.63
61.5	10					61.5	0.443	40.5	8.63
63.4	4					63.4		41	13.73
65.5	3					65.5	0.882	45	13.73
								55	13.93
								55.5	13.93
								56	18.63
								60	18.63
								61.5	18.63
								63.4	8.73
								65.5	4.73
								67.4	2.73
								69.0	1.93

Appendix D-17-2 Data for Experiment 10 (Figure 7-14b)

Time (min)	Effluent Dissolved Cu	Time (min)	Effluent Total Cu	Time (min)	Influent Total Cu	Time from start (min)	Effluent flow rate	Time from start (min)	Effluent Total P
minutes	$\mu\text{g/L}$	minutes	$\mu\text{g/L}$	minutes	$\mu\text{g/L}$	minutes	mL/min/cm	minutes	mg/L
0	6	0	8	0	195	0	0.0	0	1.138
10	3	20	3	20	198	1	20.1	20	0.411
20	2	40	1	40	198	10	20.1	40	0.313
30	1	55	4	55	197	20	21.1	55	0.267
40	1	61.5	13	61.5	197	20.5	21.1	61.5	0.184
45	4	65.5	5			21	46.6	65.5	0.277
55	4					30	46.6		
60	13					40	47.2		
61.5	13					40.5	47.2		
63.4	4					41	106.7		
65.5	3					45	106.7		
						55	101.6		
						55.5	101.6		
						56	183.3		
						60	183.3		
						61.5	183.8		
						65.5	32.9		
						67.4	15.6		
						69.0	10.6		
						76.5	2.5		
						82	0.7		

Appendix D-17-3 Data for Experiment 10 (Figure 7-14c)

Time from start (min)	Effluent Dissolved Zn	Time (min)	Effluent Total Zn	Time (min)	Influent Total Zn	Time from start (min)	Effluent pH	Time from start (min)	Effluent dissolved Cr	Time from start (min)	Effluent total Cr
minutes	$\mu\text{g/L}$	minutes	$\mu\text{g/L}$	minutes	$\mu\text{g/L}$	minutes	pH	minutes	$\mu\text{g/L}$	minutes	$\mu\text{g/L}$
0	27	0	33	0	211	0	8.12	0	0.2	0	1.1
10	1	20	14	20	220	10	8.23	10	0.0	20	0.1
20	9	40	18	40	211	20	8.14	20	0.0	40	0.1
30	9	55	27	55	213	30	8.04	30	0.0	55	0.0
40	8	61.5	33	61.5	212	40	7.94	40	0.0	61.5	0.1
45	4	65.5	28			45	7.98	45	0.0	65.5	0.5
55	16					55	8.00	55	0.0		
60	20					60	7.67	60	0.0		
61.5	19					61.5	7.37	61.5	0.0		
63.4	12					65.5	7.32	63.4	0.0		
65.5	8							65.5	0.6		

Appendix D-18-1 Data for Experiment 11 (Figure 7-15a)

Time (minutes)	Effluent Dissolved Pb	Time (min)	Effluent Total Pb	Time (min)	Influent Total Pb	Time from start (min)	Turbidity	Time from start (min)	Influent water head
minutes	$\mu\text{g/L}$	minutes	$\mu\text{g/L}$	minutes	$\mu\text{g/L}$	minutes	NTU	minutes	cm
0.5	3.8	0.5	20.6	0	0.7	0.5	5.04	0	0.0
10	2.3	20	4.6	20	0.8	10	0.824	1	6.1
20	0.5	40	3.0	40	1.0	20	0.403	10	6.1
30	0.7	50	3.2	50	0.8	30	0.39	20	6.1
40	0.8	60	4.0			40	0.354	21	6.1
45	1.1	65.17	5.0			45	0.522	22	10.0
50	1.2					50	0.411	30	10.0
55	1.4					55	0.466	40	10.0
60	1.5					60	0.404	41	10.0
63.2	1.0					63.2	0.459	42	15.1
65.2	2.1					65.2	0.788	45	15.1
								50	15.0
								51	15.0
								52	19.9
								55	19.9
								60	20.1
								61.4	20.1
								63.2	5.5
								65.2	3.5



Appendix D-18-2 Data for Experiment 11 (Figure 7-15b)

Time (min)	Effluent Dissolved Cu	Time (min)	Effluent Total Cu	Time (min)	Influent Total Cu	Time from start (min)	Effluent flow rate	Time from start (min)	Effluent Total P
minutes	$\mu\text{g/L}$	minutes	$\mu\text{g/L}$	minutes	$\mu\text{g/L}$	minutes	mL/min/cm	minutes	mg/L
0.5	2.2	0.5	5.6	0.5	0.7	0	0	0.5	0.874
10	1.9	20	2.0	20	0.8	1	20.7	20	0.344
20	1.0	40	1.0	40	1.0	10	20.7	40	0.213
30	1.0	50	1.3	50	0.8	20	20.2	50	0.161
40	0.8	60	2.0			21	20.2	60	0.153
45	1.2	65.16667	2.3			22	46.5	65.2	0.238
50	1.0					30	46.5		
55	2.0					40	46.0		
60	1.5					41	46.0		
63.2	0.9					42	108.5		
65.2	1.4					45	108.5		
						50	105.6		
						51	105.6		
						52	184.7		
						55	184.7		
						60	191.3		
						61.4	191.3		
						63.2	20.2		
						65.2	13.9		

Appendix D-18-3 Data for Experiment 11 (Figure 7-15c)

Time from start (min)	Effluent Dissolved Zn	Time (min)	Effluent Total Zn	Time (min)	Influent Total Zn	Time from start (min)	Effluent pH
minutes	$\mu\text{g/L}$	minutes	$\mu\text{g/L}$	minutes	$\mu\text{g/L}$	minutes	pH
0.5	18.4	1	30.6	0.5	5.4	0.5	8.09
10	10.4	20	13.4	20	6.5	10	8.25
20	9.5	40	11.4	40	2.1	20	8.20
30	7.6	50	12.3	60	3.4	30	8.17
40	5.5	60	13.0			40	8.08
45	11.4	65.2	14.4			45	8.03
50	5.4					50	7.98
55	10.2					55	7.64
60	6.0					60	7.56
63.2	7.9					63.2	7.52
65.2	11.4					65.2	7.40

## REFERENCES

- AASHTO. 2003. *Standard Specifications for Transportation Materials and Methods of Sampling and Testing, Designation MP-9, Compost for Erosion/Sediment Control (Filter Berms), Provisional*, American Association of State Highway Officials, Washington, D.C.
- Achtnich, C., F. Bak, and R. Conrad. 1995. Competition for electron donors among nitrate reducers, ferric iron reducers, sulfate reducers, and methanogens in anoxic paddy soil. *Biol. Fertil. Soils.*, 19:65-72.
- Alexander, R. 2001. *Compost Use on State Highway Applications*, Composting Council Research and Education Fund and U.S. Composting Council, Harrisburg, Pennsylvania.
- Alexander, R. 2003. *Standard Specifications for Compost for Erosion/Sediment Control*, developed for the Recycled Materials Resource Center, University of New Hampshire, Durham, New Hampshire. Available at <www.alexassoc.net>.
- Athanasiadis, K., B. Helmreich, H. Horn. 2007. On-site infiltration of a copper roof runoff: role of clinoptilolite as an artificial barrier material, *Wat. Res.* 41: 3251-3258.
- American Public Health Association (APHA); American Water Works Association; Water Environment Federation. 1995. "Standard Methods for the Examination of Water and Wastewater", 19th ed.; Washington, D.C.
- Antoniadis, V., J. D. McKinley, and W. Y. W. Zuhairi. 2007. Single-element and Competitive metal mobility measured with column infiltration and batch tests, *J. Environ. Qual.*, 36: 63-60.
- Arnold, R.G., T.J. DiChristina, and M.R. Hoffmann. 1988. Reductive dissolution of Fe(III) oxides by *Pseudomonas* sp. 200. *Biotechnol. Bioeng.*, 32:1081-1096.
- Boesch, D.F., R.B. Brinsfield, and R.E. Magnien. 2001. Chesapeake Bay Eutrophication: Scientific Understanding, Ecosystem Restoration, and Challenges for Agriculture. *J. Environ. Qual.* 30:303–320.
- Boller, M. 1997. Tracking heavy metals reveals sustainability deficits of urban drainage systems, *Wat Sci Tech*, 35(9):77-87.
- Boruvka, L. and J.E. Rechcigl. 2003. Phosphorus retention by the Ap horizon of a spodosol as influenced by calcium amendments. *Soil Sci.*, 168:699-706.
- Bousserhine, N., U.G. Gasser, E. Jeanroy, and J. Berthelin. 1999. Bacterial and chemical reductive dissolution of Mn-, Co-, Cr-, and Al-substituted *Goethites*. *Geomicrobiol. J.* 16:245-258.

- Boynton, W.R., J.H. Garber, R. Summers, and W.M. Kemp. 1995. Input, transformations, and transport of nitrogen and phosphorus in Chesapeake Bay and selected tributaries. *Estuaries* 18: 285-314
- Bradl, H.B. 2004. Adsorption of heavy metals ions on soils and soil constituents. *J. Colloid Interf. Sci.*, 277:1-18.
- Brady, N. C., and R. R. Weil. 2002. "Elements of the nature and properties of soil", 2<sup>nd</sup> Ed., Pearson Prentice Hall, Upper Saddle River, NJ, USA.
- Brock, T.D., J. Gustafson. 1976. Ferric iron reduction by sulfur- and iron-oxidizing bacteria. *Appl. Environ. Microbiol.*, 32:567-571.
- Brown S., Angle, J. S., Chaney, R. L. 1997a. Correction of limed-biosolid induced manganese deficiency on a long-term field experiment. *J. Environ. Qual.*, 26:1375-1384.
- Brown, S.L., Xue, Q., Chaney, R.L., Hallfrishch, J.G., 1997b. Effect of biosolids processing on the bioavailability of Pb in urban soils, In "Biosolids management innovative treatment technologies and processes.", Proc. Water Environmental Research Foundation Workshop #104, 43-54, Oct 4, 1997 Chicago, IL.
- Brown, S.L., Chaney, R.L., Angle, J.S., and Ryan, J.A., 1998. The phytoavailability of Cadmium to Lettuce in Long-Term Biosolids-Amended Soils, *J. Environ. Qual.*, 27, 1071-1078.
- Bunzl, K., W. Schmidt, and B. Sansoni, 1976, Kinetics of ion exchange in soil organic matter. IV. Adsorption and desorption of Pb<sup>2+</sup>, Cu<sup>2+</sup>, Cd<sup>2+</sup>, Zn<sup>2+</sup> and Ca<sup>2+</sup> by peat, *J. Soil Sci.* 27: 32-41.
- Carpenter S.R., N.F. Caraco, D.L. Correll, R.W. Howarth, A.N. Sharpley, and V.H. Smith. 1998. Nonpoint pollution of surface waters with phosphorus and nitrogen. *Ecol. Appl.*, 8:559-568.
- Chaney, R.L., J.A. Ryan, S.L. Brown. 1999. Environmentally acceptable endpoints for soil metals, In W.C. Anderson, R.C. Loehr and B.P. Smith (eds.) "Environmental availability in soils: Chlorinated organics, Explosives, Metals" Am. Acad. Environ. Eng., Annapolis, MD.
- Chang, M., M.W. McBroom, R.S. Beasley. 2004. Roofing as a source of nonpoint water pollution, *J. Environ. Manage.*, 73: 307-315.
- Codling, E.E., R.L. Chaney, C.L. Mulchi. 2000. Use of aluminum- and iron-rich residues to immobilize phosphorus in poultry litter and litter-amended soils. *J. Environ. Qual.*, 29:1924-1931.

- Correll, D.L.. 1998. The role of phosphorus in the eutrophication of receiving waters: A review. *J. Environ. Qual.*, 27:261-266.
- D'Angelo, E.M., M.V. Vandiviero, W.O. Thom, and F. Sikora. 2003. Estimating soil phosphorus requirements and limits from oxalate extract data. *J. Environ. Qual.*, 32:1082-1088.
- Daniel, T.C., A.N. Sharpley, and J.L. Lemunyon. 1998. Agricultural phosphorus and eutrophication: a symposium overview. *J. Environ. Qual.*, 27:251-257.
- Dao, T. H. 1999. Coamendments to modify phosphorus extractability and nitrogen/phosphorus ratio in feedlot manure and composted manure. *J. Environ. Qual.*, 28:1114-1121.
- Dao, T.H., L.J. Sikora, A. Hamasaki, and R.L. Chaney. 2001. Manure phosphorus extractability as affected by aluminum- and iron by-products and aerobic composting. *J. Environ. Qual.*, 30:1693-1698.
- Dassonville, F. and P. Renault. 2002. Interactions between microbial processes and geochemical transformations under anaerobic conditions: a review. *Agronomie.*, 22:51-68.
- Davis, A.P., and M. Burns. 1999. Evaluation of lead concentration in runoff from painted structures, *Wat Res*, 33: 2949-2958.
- Davis, A.P., M. Shokouhian, and S. Ni. 2001a. Loading estimates of lead, copper, cadmium, and zinc in urban runoff from specific sources. *Chemosphere*, 44(5): 997-1009.
- Davis, A. P., M. Shokouhian, H. Sharma, C. Minami. 2001b. Laboratory study of biological retention for urban stormwater management, *Water Environ. Res.*, 73, 5-14.
- Dayton, E.A. and N.T. Basta. 2005. A method for determining the phosphorus sorption capacity and amorphous aluminum or aluminum based drinking water treatment residuals. *J. Environ. Qual.*, 34:1112-1118.
- Dou, Z., G.Y. Zhang, W.L. Stout, J. D. Toth, and J. D. Ferguson. 2003. Efficacy of alum and coal combustion by-products in stabilizing manure phosphorus. *J. Environ. Qual.*, 32:14990-1497.
- Drexler, J.W., and W. Brattin. 2007. An *In Vitro* Procedure for Estimation of Lead Relative Bioavailability: With Validation. *Hum. Ecol. Risk Assess.* 13(2): 383-401.
- Elliott, H.A., G.A. O'Conner, P. Lu, and S. Brinton. 2002. Influence of water treatment residuals on phosphorus solubility and leaching. *J. Environ. Qual.*, 31:1362-1369.

Elliott, H.A., M. R. Liberati and C. P. Huang. 1986. Competitive Adsorption of Heavy Metals by Soils. *J. Environ. Qual.*, 15:214-219

EPA (Environmental Protection Agency). 1992. *Toxicity Characteristic Leaching Procedure, Method 1311* in "Test methods for evaluating solid waste, Physical/Chemical Method", EPA publication SW-846.  
<http://www.epa.gov/osw/hazard/testmethods/sw846/pdfs/1311.pdf> (for Method 1311)  
<http://www.epa.gov/osw/hazard/testmethods/sw846/online/index.htm> (for SW-846 online)

Faucette L. B., C.F. Jordan, L.M. Risse, M. Cabrera, D.C. Coleman, L.T. West. 2005. Evaluation of Stormwater from Compost and Conventional Erosion Control Practices in Construction Activities, *J. Soil Water Conserv.* 60:6, 288-297.

FitzGerald, K.P., J. Nairn, G. Skennerton, A. Atrens. 2006. Atmospheric corrosion of copper and the colour, structure and composition of natural patinas on copper. *Corrosion Science*, 48:2480-2509.

Fontes, M.P.F., A.T. de Matos, L.M. da Costa, and J.C.L. Neves, 2000. Competitive adsorption of Zinc, Cadmium, Copper, and Lead in three highly weathered Brazilian soils, *Commun Soil Sci Plan*, 31(18): 2939-2958.

Francis, A.J., C.J. Dodge, A.W. Rose, and A.J. Ramirez. 1989. Aerobic and anaerobic microbial dissolution of toxic metals from Coal Waste: Mechanisms of Action. *Environ. Sci. Technol.*, 23:435-441.

Francis, A.J., and C.J. Dodge. 1990. Anaerobic microbial remobilization of toxic metal coprecipitated with iron oxide. *Environ. Sci. Technol.*, 24:373-378.

Gallimore, L.E., N.T. Basta, D.E. Storm, M.E. Payton, R.H. Huhnke, and M.D. Smolen. 1999. Water treatment residual to reduce nutrients in surface runoff from agricultural land. *J. Environ. Qual.*, 28:1474-1478.

Gerardi, M. 2003. *The microbiology of anaerobic digesters*, John Wiley & Sons, Inc. Hoboken, New Jersey.

Gibert, O., J. de Pablo, J. L. Cortina, and C. Ayora. 2005. Municipal compost-based mixture for acid mine drainage bioremediation: Metal retention mechanisms. *Appl. Geochem.*, 20:1648-1657.

Glanville et al. 2003. *Impacts of Compost Blankets on Erosion Control, Revegetation, and Water Quality at Highway Construction Sites in Iowa*, T. Glanville, T. Richard, and R. Persyn, Agricultural and Biosystems Engineering Department, Iowa State University of Science and Technology, Ames, Iowa.

- Goto, M., and K. Suyama. 2000. Occlusion of transition metal ions by new adsorbents synthesized from plant polyphenols and animal fibrous proteins, *Appl. Biol. Biotechnol.*, 84:1021-1038.
- Graedel, T.E. 1994. Chemical mechanisms for the atmospheric corrosion of lead. *J. Electrochem. Soc.*, 141(4), 922-927.
- Gromaire, M.C., G. Chebbo, and A. Constant. 2002. Impact of zinc roofing on urban runoff pollutant loads: the case of Paris, *Wat. Sci. Technol.*, 45(7):113-122.
- Gruneberg, B., and J. Kern, 2001. Phosphorus retention capacity of iron-ore and blast furnace slag in subsurface flow constructed wetlands, *Wat. Sci. Technol.*, 44(11-12):69-75.
- Hamon, R.E., M.J. McLaughlin, and G. Cozens. 2002. Mechanisms of Attenuation of metal availability in in-situ remediation treatment, *Environ. Sci. Technol.*, 36:3991-3996.
- Han, N. and M.L. Thompson. 1999. Copper-binding ability of dissolved organic matter derived from anaerobically digested biosolids. *J. Environ. Qual.* 28:939-944.
- Harter, R.D. 1983. Effect of soil pH on adsorption of lead, copper, zinc, and nickel. *Soil Sci. Soc. Am. J.* 47:47-51.
- Haustein, G.K., T.C. Daniel, D.M. Miller, P.A. Moor, Jr., and R.W. McNew. 2000. Aluminum-containing residuals influence high-phosphorus soils and runoff water quality. *J. Environ. Qual.* 29:1954-1959.
- Henry, C. and S. Brown. 1997. Restoring a superfund site with biosolids and fly ash, *Biocycle*, 38 (11):79-83.
- Heron, G. and T.H. Christensen. 1995. Impact of sediment-bound iron on redox buffering in a landfill leachate polluted aquifer (Vejen, Denmark). *Environ. Sci. Technol.* 29:187-192.
- Ho, Y.S., C.T. Huang, H.W. Husang. 2002. Equilibrium sorption isotherm for metal ions on three fern, *Process Biochem.*, 37:1421-1430.
- Ho, Y., W. Chiu, C. Hsu, and C. Huang. 2003. Sorption of lead ions from aqueous solution using tree fern as sorbent, *Hydrometallurgy*, 73:55-61.
- Hsu, J.-H. and S.-L. Lo. 2000a. Effect of dissolved organic carbon on leaching of copper and zinc from swine manure compost. *Wat. Sci. Technol.* 42:247-252.
- Hsu, J.-H. and S.-L. Lo. 2000b. Characterization and extractability of copper, manganese, and zinc in swine manure composts. *J. Environ. Qual.* 29:447-453.

Jang, A. Y. Seo, and P.L. Bishop. 2005. The removal of heavy metals in urban runoff by sorption on mulch. *Environ. Pollut.*, 133:117-127.

Juries, D. 2004. *Environmental Protection and Enhancement with Compost*, Oregon Department of Environmental Quality, Northwest Region.

Kalbasi, M. and K.G. Karthikeyan. 2004. Phosphorus dynamics in soils receiving chemically treated dairy manure. *J. Environ. Qual.*, 33:2296-2305.

Kirchmann, H. and E. Witter. 1989. Ammonia volatilization during aerobic and anaerobic manure decomposition. *Plant Soil*. 115:35-41.

Knox, A.S., J.C. Seaman, M.J. Mench, and J. Vangronsveld. 2001. Remediation of metal and radionuclides contaminated sils by in situ stabilization techniques, In Iskandar, I.K. (Ed.), *Environmental restoration of metals contaminated soils*, Lewis publishers, New York.

Kostka, J.E. and K.H. Nealson. 1995. Dissolution and reduction of magnetite by bacteria. *Enviorn. Sci. Technol.*, 29:2535-2540.

Krishnamurti, G.S.R. and Naidu, R., 2002, Solid-solution speciation and phytoavailability of copper and zinc in soil, *Environ. Sci. Technol.*, 36:2645-2651.

Li, Y., R.L. Chaney, G. Siebielec, and B.A. Kerschner. 2000. Response of Four Turfgrass cultivars to limestone and biosolids-comopost amendment of a zinc and cadmium contaminated soil at Palmerton, Pennsylvanic, *J. Environ. Qual.*, 29:1440-1447.

Li, Z., J.A. Ryan, J. Chen, and S.R. Al-Abed. 2001. Adsorption of Cadmium on Biosolids-amended soils, *J. Environ. Qual.*, 30:930-911.

Line, D. E., J.A. Arnold, G.D. Jennings, J. Wu. 1996. Water Quality of Stormwater Runoff from Ten Industrial Sites. *Water Resour. Bull.*, 32:807-816.

Liu, Q. and Y. Liu. 2003. Distribution of Pb(II) species in aqueous solutions. *J. Colloid Interf. Sci.* 268:266–269

Loeppert, R.H., and W.P. Inskeep. 1996. Iron. 639–664. In D.L. Sparks (ed.) “Methods of soil analysis” Part 3. SSSA Book Ser. no. 5. SSSA, Madison, WI.

Lombi, E., R.E. Hamon, S.P. McGrath, and M.J. McLaughlin. 2003. Lability of Cd, Cu, and Zn in polluted soil treated with lime, beringite, and red mud and identification of a non-labile colloidal fraction of metals using isotopic techniques, *Environ Sci. Technol.*, 37:979-984.

Lovely, D.R. and E.J.P. Phillips. 1986a. Organic matter mineralization with reduction of ferric iron in anaerobic sediments. *Appl. Environ. Microbiol.*, 51: 683-689.



- Lovely, D.R. and E.J.P. Phillips. 1986b. Availability of ferric iron for Microbial reduction in bottom sediments of the freshwater tidal Potomac River. *Appl. Environ. Microbiol.*, 52:751-757.
- Lovely, D.R. and E.J.P. Phillips. 1987. Competitive mechanisms for inhibition of sulfate reduction and methane production in the zone of ferric iron reduction in sediments. *Appl. Environ. Microbiol.*, 53:2636-2641.
- Lovely, D.R. and E.J.P. Phillips. 1988. Novel mode of microbial energy metabolism: Organic carbon oxidation coupled to dissimilatory reduction of iron or manganese. *Appl. Environ. Microbiol.*, 54:1472-1480.
- Lovely, D.R. 1991. Dissimilatory Fe(III) and Mn(IV) reduction. *Microbiol. Rev.*, 55:259-287.
- Lovely, D.R., E.J.P. Philips, and D.J. Lonergan. 1991. Enzymatic versus nonenzymatic mechanisms for Fe(III) reduction in aquatic sediments. *Environ. Sci. Technol.*, 25:1062-1067.
- Lovely, D.R., J.D. Coates, E.L. Blunt-Harris, E.J.P. Phillips, and J.C. Woodward. 1996a. Humic substances as electron acceptors for microbial respiration. *Nature*, 382:445-448.
- Lovely, D.R., J.C. Woodward, and F.H. Chapelle. 1996b. Rapid anaerobic benzene oxidation with a variety of chelated Fe(III) forms. *Appl. Environ. Microbiol.*, 62:288-291.
- Lovely, D.R. 2000. Fe(III) and Mn(IV) reduction. p.3-30. In D. R. Lovely (ed.) "Environmental microbe-Metal interactions". ASM Press, Washington, D.C.
- Lye, D.J. 2009. Rooftop runoff as a source of contamination: A review, *Science of Total Environment*, 407: 5429-5434.
- Madden, M.S. 1988. "Adapting the  $\text{Sr}(\text{NO}_3)_2$  methods for determining available cations to a routine soil procedure". MS thesis. University of Wisconsin. Madison, WI.
- Makris, K.C., W.G. Harris, G.A. O'connor, and T.A. Obreza. 2004. Phosphorus immobilization in micropores of drinking-water treatment residuals: Implications for long-term stability. *Environ. Sci. Technol.*, 38:6590-6596.
- Marani D., G. Macchi, and M. Pagano. 1995. Lead precipitation in the presence of sulfate and carbonate: Testing of thermodynamic prediction. *Wat Res.*, 29 (4):1085-1092.
- Martinez, C. E., and M. B. McBride. 1998. Solubility of  $\text{Cd}^{2+}$ ,  $\text{Cu}^{2+}$ ,  $\text{Pb}^{2+}$ , and  $\text{Zn}^{2+}$  in aged coprecipitates with amorphous iron hydroxides. *Environ. Sci. Technol.*, 32:743-748.

Matthes, S.A., S.D. Cramer, B.S. Covino, Jr., S.J. Bullard, and G.R. Holcomb. 2002. Precipitation runoff from lead. In *Outdoor atmospheric Corrosion*, ASTM STP1421, H.E. Townsend, Ed., American society for testing and materials international, West Conshohocken, PA.

Maxwell, C., and Mahn S., 1987, "Spatial and Temporal distribution of Precipitation chemistry across Maryland" vol 2, p D7. Versar, Inc, Columbia, Maryland.

McBride, M.B. 1998. Soluble trace metals in alkaline stabilized sludge products. *J. Environ. Qual.*, 27:578-584.

McCoy, S. 2005. Filter Sock Presentation provided at *Erosion, Sediment Control and Stormwater Management with Compost BMPs Workshop*, U.S. Composting Council 13th Annual Conference and Trade Show, January 2005, San Antonio, Texas.

McGrath, S.P., and C.H. Cunliffe. 1985. Simplified Method for the Extraction of the Metals Fe, Zn, Cu, Ni, Cd, Pb, Cr, Co and Mn from Soils and Sewage Sludges. *J. Sci. Food Agric.*, 36:794-798.

McLaughlin, J.R., J.C. Ryden, and J.K. Syers. 1981. Sorption of inorganic phosphate by iron- and aluminum- containing components. *J. Soil Sci.*, 32:365-377.

McLean EO. Soil pH and lime requirement.. In: A.L. Page et al. (ed.) "Methods of soil analysis". Part 2. Agron. Monogr. 9. 2<sup>nd</sup> ed. ASA and SSSA, Madison, WI., 1982, pp. 199-224

MnDOT. 2005. *Storm Drain Inlet Protection Provisions, S-5.5 Materials, B. Compost Log*, Minnesota Department of Transportation, Engineering Services Division, Technical Memorandum No. 05-05-ENV-03, January 18, 2005.

Moffett, B.F., F.A. Nicholson, N.C. Uwankwe, B.J. Chambers, J.A. Harris, and T.C.J. Hill. 2003. Zinc contamination decreases the bacterial diversity of agricultural soil, *FEMA Microbiol. Ecol.*, 43: 13-19.

Moore, Jr., P.A., and D.M. Miller. 1994. Decreasing phosphorus solubility in poultry litter with aluminum, calcium, and iron amendments. *J. Environ. Qual.*, 23:325-330.

Moreno, A.M., J. R. Quintana, L. Perez, J.G. Parra. 2006. Factors influencing lead sorption-desorption at variable added metal concentration in Rhodoxeralfs. *Chemosphere*, 64:758-763.

Nealson, K.H. and C.R. Myers. 1992. Microbial reduction of manganese and iron: New approaches to carbon cycling. *Appl. Environ. Microbiol.*, 58:439-443.

Ni, J. 1999. Mechanistic models of ammonia release from liquid manure: a review. *J. Agric. Eng. Res.*, 72:1-17.

Nolan, A.L., M.J. McLaughlin, and S.D. Mason. 2003. Chemical speciation of Zn, Cd, Cu, and Pb in pore water of Agricultural and Contaminated soils using Donnan Dialysis, *Environ. Sci. Technol.*, 37, 90-98.

Novak, J.M., D.W. Watts, P.G. Hunt, and K.C. Stone. 2000. Phosphorus movement through a coastal plain soil after a decade of intensive swine manure application. *J. Environ. Qual.*, 29:1310-1315

Novak, J.M., and D.W. Watts. 2004. Increasing the phosphorus sorption capacity of southeastern coastal plain soils using water treatment residuals. *Soil Sci.*, 169:206-214.

Novak, J.M., and D.W. Watts. 2005. Water treatment residuals aggregate size influences phosphorus sorption kinetics and  $P_{\max}$  values. *Soil Sci.*, 170:425-432.

ODEQ. 2004. *Best Management Practices for Stormwater Discharges Associated with Construction Activity, Guidance for Eliminating or Reducing Pollutants in Stormwater Discharges*, Oregon Department of Environmental Quality, Northwest Region.

Oyler, J.A., 1993, Use of power plant fly ash/municipal sludge admixture to reclaim land near a smelter, Proceedings:Tenth International Ash Use Symposium: Volume 1 High-volume uses/concrete applications.

Pacific Environmental Services, Inc., Background report AP-42 Section 12.7, Primary Zinc smelting, <<http://www.epa.gov/ttn/chief/ap42/ch12/bgdocs/b12s07.pdf>>

Pacific Environmental Services, Inc., Background report AP-42 Section 12.14, Secondary Zinc Industry, <<http://www.epa.gov/ttn/chief/ap42/ch12/bgdocs/b12s14.pdf>>

Pandey, A.K., S.D. Pandey, and V. Misra. 2000. Stability constants of metal-humic acid complexes and its role in environmental detoxification. *Ecotoxicol. Environ. Saf.*, 47:195-200.

Patterson, J.W., H.E. Allen, and J.J. Scala. 1977. Carbonate precipitation for heavy metals pollutants, *J. Wat. Poll. Cont. Fed.*, 49(12):2397-2410.

Peacock, S. and D.L. Rimmer. 2000. The suitability of an iron oxide-rich gypsum by-product as a soil amendment. *J. Environ. Qual.*, 29:1969-1975.

Personal communications, 2005. Industry representatives were interviewed regarding the particle size and composition of composts currently used in vegetated and unvegetated filter socks. These representatives included Britt Faucette and Rod Tyler of Filtrexx, International, LLC; Nora Goldstein of BioCycle, Journal of Composting & Organics Recycling; and Ron Alexander of R. Alexander Associates, Inc.

- Peters, L.M., and N.T. Basta. 1996. Reduction of excessive bioavailable phosphorus in soils by using municipal and industrial waste. *J. Environ. Qual.*, 25:1236-1241.
- Petersen, E., A. Jennings, and J. Ma. 2006. Screening level risk assessment of heavy metal contamination in cleveland area commons. *J. Environ. Eng.*, 132(3): 392-404.
- Phillips, E.J.P., D.R. Lovely, and E.E. Roden. 1993. Composition of non-microbially reducible Fe(III) in aquatic sediments. *Appl. Environ. Microbiol.*, 59:2727-1729.
- Pierzynski, G.M, J.T. Sims, and G.F. Vance. 2000. Soils and environmental quality. CRC Press LLC. Boca Raton, FL.
- Ponizovsky, A.A., C.C. Tsadilas, 2003, Lead(II) retention by alfisol and clinoptilolite: cation balance and pH effect. *Geoderma*, 115:303-312.
- Proctor D. M., K.A. Fehling, E.C. Shay, J.L. Wittenborn, J.J. Green, C. Avent, R.D. Bigham, M. Connolly, B. Lee, T.O. Shepker, and M.A. Zak. 2000. Physical and chemical characteristics of blast furnace, basic oxygen furnace, and electric arc furnace steel industry slags. *Environ Sci Technol.*, 34:1576-1582.
- Wolf, A.M. and J.T. Sims (eds.). 1991. Recommended soil Testing Procedures for the Northeastern United States. 2<sup>nd</sup> ed. Northeast Regional Publication no.493, Agric. Exp. Stn., Univ. of Delaware, Newark.
- Roberts, D.R., A.C. Scheinost, D.L. Sparks. 2002. Zinc speciation in a smelter-contaminated soil profile using bulk and microspectroscopic techniques, *Environ. Sci. Technol.*, 36:1742-1750.
- Roden, E. E. and J.M. Zachara. 1996. Microbial reduction of crystalline iron(III) oxides: Influence of oxide surface area and potential for cell growth. *Environ. Sci. Technol.*, 30:1619-1628.
- Roden, E. E., M. M. Urrutia. 1999. Ferrous iron removal promotes microbial reduction of crystalline iron(III) oxides. *Environ. Sci. Technol.*, 33:1847-1853.
- Roden, E. E., M.M. Urrutia and C.J. Mann. 2000. Bacterial reductive dissolution of crystalline Fe(III) oxide in continuous-flow column reactors. *Appl. Environ. Microbiol.*, 66:1062-1065.
- Roden, E.E. 2003. Fe(III) oxide reactivity toward biological versus chemical reduction. *Environ. Sci. Technol.*, 37:1319-1324.
- Roden, E.E., and R.G. Wetzal. 2003. Competition between Fe(III)-reducing and methanogenic bacteria for acetate in iron-rich freshwater sediments. *Microbiol. Ecol.*, 45(3):252-258.

- Roden, E. E. 2004. Analysis of long-term bacteria vs. chemical Fe(III) oxide reduction kinetics. *Environ. Sci. Technol.*, 68:3205-3216.
- Royer, R.A., W.D. Burgos, A.S. Fisher, R.F. Unz, and B.A. Dempsey. 2002a. Enhancement of biological reduction of hematite by electron shuttling and Fe(II) complexation. *Environ. Sci. Technol.*, 36:1939-1946.
- Royer, R.A., W.D. Burgos, A.S. Fisher, B-H. Jeon, R.F. Unz, and B.A. Dempsey. 2002b. Enhancement of hematite reduction by natural organic matter. *Environ. Sci. Technol.*, 36:2897-2904.
- Royer, R.A., B.A. Dempsey, B-H. Jeon, and W.D. Burgos. 2004. Inhibition of biological reductive dissolution of hematite by ferrous iron. *Environ. Sci. Technol.*, 38:187-193.
- Ryan, J.A., K.G. Scheckel, W.R. Berti, S.L. Brown, S.W. Casteel, R.L. Chaney, J. Hallfrisch, M. Doolan, P. Grevatt, M. Maddaloni, D. Mosby, 2004. Reducing children's risk from lead in soil, *Environ. Sci. Technol.*, 38(1):18A-24A.
- Sakadevan, K., and H.J. Bavor. 1998. Phosphate adsorption characteristics of soils, slags and zeolite to be used as substrates in constructed wetland systems. *Wat. Res.*, 32:393-399.
- Sanchez, E., R. Borja, P. Weiland, L. Travieso, A. Martin. 2000. Effect of temperature and pH on the kinetics of methane production, organic nitrogen and phosphorus removal in the batch anaerobic digestion process of cattle manure. *Bioprocess Eng.*, 22:247-252.
- Scheckel, K.G., R.L. Chaney, N.T. Basta, and J.A. Ryan. 2009. Advances in assessing bioavailability of metal(loid)s in contaminated soils. In *Advances in Agronomy*. Ed. Donald L. Sparks, Vol. 104, Burlington: Academic Press, pp 1-52.
- Scheckel, K.G., and A.R. James, 2004. Spectroscopic speciation and quantification of lead in phosphate-amended soils. *J. Environ. Qual.*, 33:1288-1295.
- Seelsaen, N., R. McLaughlan, S. Moore, and R.M. Stuetz. 2007. Influence of compost characteristics on heavy metal sorption from synthetic stormwater. *Wat Sci Technol*, 55(4):219-226.
- Sharpley, A.N., S.C. Chapra, R. Wedepohl, J.T. Sims, T.C. Daniel, and K.R. Reddy. 1994. Managing agricultural phosphorus for protection of surface waters: Issues and options. *J. Environ. Qual.*, 23:437-451.
- Sharpley, A.N., T. Daniel, T. Sims, J. Lemunyon, R. Stevens, and R. Parry. 2003. *Agricultural Phosphorus and Eutrophication*, 2<sup>nd</sup> ed., USDA Agricultural research service, ARS-149.

Shreve, B.R., P.A. Moore, Jr., T.C. Daniel, D.R. Edwards, and D.M. Miller. 1995. Reduction of phosphorus in runoff from field-applied poultry litter using chemical amendments. *J. Environ. Qual.*, 24:106-111.

Smidt, E., K. Meissl, M. Schmutzer, and B. Hinterstoisser, 2008. Co-composting of lignin to build up humic substances-Strategies in waste management to improve compost quality, *Ind Crop Prod*, 27:196-201.

Smith, D.R., P.A. Moore, Jr., C.L. Griffis, T.C. Daniel, D.R. Edwards, and D.L. Boothe. 2001. Effects of alum and aluminum chloride on phosphorus runoff from swine manure. *J. Environ. Qual.*, 30:992-998.

Sommer, S.G. and B.T. Christensen. 1992. Ammonia volatilization after injection of anhydrous ammonia into aerable soils of different moisture levels. *Plant Soil.*, 142:143-146.

Sparks, D.L. 1996. Phosphorus. P. 869-919. In D.L. Sparks (ed.) "Methods of soil analysis. Part 3". SSSA Book Ser. no. 5. SSSA, Madison, WI.

Stout, W.L., A.N. Sharpley, and H.B. Pionke. 1998. Reducing soil phosphorus solubility with coal combustion by-products. *J. Environ. Qual.*, 27:111-118.

Stronach, S.M., T. Rudd, and J.N. Lester. 1986. Anaerobic digestion processes in industrial wastewater treatment. Spring-Verlag Berling Heidelberg, Germany.

Stüben, D., Z. Berner, B. Kappes, and H. Puchelt. 2001. Environmental monitoring of heavy metals and arsenic from Ag-Pb-Zn mining: A Case study over two millennia, *Environ. Monitoring and Assessment*, 70:181-200.

Torbert, H.A., K.W.K. King, and R.D. Harmel. 2005. Impact of soil amendments on reducing phosphorus losses from runoff in Sod. *J. Environ. Qual.*, 34:1415-1421.

Tyler, R. and B. Faucette. 2005. *Organic BMPs used for Stormwater Management—Filter Media Test Results from Private Certification Program Yield Predictable Performance*, U.S. Composting Council 13 th Annual Conference and Trade Show, January 2005, San Antonio, Texas.

Urrutia, M.M., E.E. Roden, J.K. Fredrickson, and J.M. Zacharra. 1998. Microbial and surface chemistry controls on reduction of synthetic Fe(III)-oxide minerals by the dissimilatory iron-reducing bacterium *Shewanella alga*. *Geomicrobiol. J.*, 15: 269-291.

Urrutia, M.M., E.E. Roden, and J.M. Zacharra. 1999. Influence of aqueous and solid phase Fe(II) complexants on microbial reduction of iron(III) oxides. *Environ. Sci. Technol.* 33:4022-4028.

US Geological Survey. 1999. Maryland and the District of Columbia: Surface-water, U.S. Geological Survey Water Supply Paper 2300, Maryland and District of Columbia resources, <<http://pubs.usgs.gov/wsp/wsp2300/>>.

USCC. 2001. *Compost Use on State Highway Applications*, U.S. Composting Council, Washington, D.C.

USEPA. 1998. *An Analysis of Composting as an Environmental Remediation Technology*. U.S. Environmental Protection Agency, Solid Waste and Emergency Response (5305W), EPA530-R-98-008, April 1998.

Veeresh, H., S. Tripathy, D. Chaudhuri, B.R. Hart, M.A. Powell. 2003. Competitive adsorption behavior of selected heavy metals in three soil types of india amended with fly ash and sewage sludge, *Environ. Geol.*, 44:363-370.

W&H Pacific. 1993. *Demonstration Project Using Yard Debris Compost for Erosion Control, Final Report*, presented to Metropolitan Service District, Portland, Oregon.

Wanielista, M.P. 1990. *Hydrology and Water Quantity Control*. John Wiley and Sons,. New York, N.Y.

Weng, L., E.J.M. Temminghoff, S. Lofts, E. Tipping, and W.H. Van Riemsdijk. 2002. Complexation with dissolved organic matter and solubility control on heavy metals in a sandy soil. *Environ. Sci. Technol.*, 36:4804-4810.

Wild, D., A. Kisliakova, and H. Siegrist. 1997. Prediction of recycle phosphorus loads from anaerobic digestion. *Wat. Res.* 31:2300-2308.

Wolf, A., and D.B. Beegle. 1995. Recommended Soil Tests for Macronutrients: phosphorus, potassium, calcium and magnesium. p. 30–39. *In* J.T Sims and A. Wolf (ed.).

Wu, J. S., C.J. Allen, W.L. Saunders, J.B. Evett. 1998. Characterization and Pollutant Loading Estimation for Highway Runoff. *J. Environ.Eng.* (Reston, Virginia), 124: 584-592.

Yousfi, I. and A. Bermond. 2001. Physical-Chemical Approach to Assess the Effectiveness of several amendments used for in situ remediation of trace metals-contaminated soils by adding solid phases, *In* Iskandar, I.K. (Ed.), “Environmental restration of metals contaminated soils”, Lewis publishers, New York.

Yu, B., Y. Zhang, A. Shukla, S.S. Shukla, K.L. Dorris. 2000. The removal of heavy metal from aqueous solutions by sawdust adsorption - removal of copper, *J. Hazard Mater.*, B80: 33-42.

Zhou, L. X., and J. W.C. Wong. 2001. Effect of dissolved organic matter from sludge and sludge compost on soil copper sorption, *J. Environ. Qual.*, 30:878-883.

Zimmermann, J., C. Dierkes, P. Gobel, C. Klinger, H. Stubbe, and W.G. Coldewey. 2005. Metal concentrations in soil and seepage water due to infiltration of roof runoff by long term numerical modeling. *Wat. Sci. Tech.*, 51(2): 11–19.